



An increased high-mobility group A2 expression level is associated with malignant phenotype in pancreatic exocrine tissue.

Abe N, Watanabe T, Suzuki Y, Matsumoto N, Masaki T, Mori T, Sugiyama M, Chiappetta G, Fusco A, Atomi Y.

First Department of Surgery, Kyorin University School of Medicine, 6-20-2, Shinkawa, Mitaka, Tokyo 181-8611, Japan. abenbtg@kyorin-u.ac.jp

The altered form of the high-mobility group A2 (HMGA2) gene is somehow related to the generation of human benign and malignant tumours of mesenchymal origin. However, only a few data on the expression of HMGA2 in malignant tumour originating from epithelial tissue are available. In this study, we examined the HMGA2 expression level in pancreatic carcinoma, and investigated whether alterations in the HMGA2 expression level are associated with a malignant phenotype in pancreatic tissue. High-mobility group A2 mRNA and protein expression was determined in eight surgically resected specimens of non-neoplastic tissue (six specimens of normal pancreatic tissue and two of chronic pancreatitis tissue) and 27 pancreatic carcinomas by highly sensitive reverse transcriptase-polymerase chain reaction (RT-PCR) techniques and immunohistochemical staining, respectively. Reverse transcriptase-polymerase chain reaction analysis revealed the expression of the HMGA2 gene in non-neoplastic pancreatic tissue, although its expression level was significantly lower than that in carcinoma. Immunohistochemical analysis indicated that the presence of the HMGA2 gene in non-neoplastic pancreatic tissue observed in RT-PCR reflects its abundant expression in islet cells, together with its focal expression in duct epithelial cells. Intense and multifocal or diffuse HMGA2 immunoreactivity was noted in all the pancreatic carcinoma examined. A strong correlation between HMGA2 overexpression and the diagnosis of carcinoma was statistically verified. Based on these findings, we propose that an increased expression level of the HMGA2 protein is closely associated with the malignant phenotype in the pancreatic exocrine system, and accordingly, HMGA2 could serve as a potential diagnostic molecular marker for distinguishing pancreatic malignant cells from non-neoplastic pancreatic exocrine cells.

PMID: 14647145 [PubMed - indexed for MEDLINE]



Selective apoptosis of natural killer-cell tumours by l-asparaginase.

Ando M, Sugimoto K, Kito T, Sasaki M, Mukai K, Ando J, Egashira M, Schuster SM, Oshimi K.

Department of Haematology, Juntendo University School of Medicine, Tokyo, Japan.

We examined the effectiveness of various anti-tumour agents to natural killer (NK)-cell tumour cell lines and samples, which are generally resistant to chemotherapy, using flow cytometric terminal deoxynucleotidyl transferase-mediated dUTP-biotin nick end-labelling (TUNEL) assay. Although NK-YS and NK-92 were highly resistant to various anti-tumour agents, l-asparaginase induced apoptosis in these two NK-cell lines. NK-cell leukaemia/lymphoma and acute lymphoblastic leukaemia (ALL) samples were selectively sensitive to l-asparaginase and to doxorubicin (DXR) respectively. Samples of chronic NK lymphocytosis, an NK-cell disorder with an indolent clinical course, were resistant to both drugs. Our study clearly separated two major categories of NK-cell disorders and ALL according to the sensitivity to DXR and l-asparaginase. We examined asparagine synthetase levels by real-time quantitative polymerase chain reaction (RQ-PCR) and immunostaining in these samples. At least in nasal-type NK-cell lymphoma, there was a good correlation among asparagine synthetase expression, in vitro sensitivity and clinical response to l-asparaginase. In aggressive NK-cell leukaemia, although asparagine synthetase expression was high at both mRNA and protein levels, l-asparaginase induced considerable apoptosis. Furthermore, samples of each disease entity occupied a distinct area in two-dimensional plotting with asparagine synthetase mRNA level (RQ-PCR) and in vitro l-asparaginase sensitivity (TUNEL assay). We confirmed rather specific anti-tumour activity of l-asparaginase against NK-cell tumours in vitro, which provides an experimental background to the clinical use of l-asparaginase for NK-cell tumours.

PMID: 16156856 [PubMed - in process]

Comment in:

- [Cancer Res. 2002 Jan 15;62\(2\):618-9.](#)

FREE full text article at
cancerres.aacrjournals.org

BMI-1 gene amplification and overexpression in hematological malignancies occur mainly in mantle cell lymphomas.

Bea S, Tort F, Pinyol M, Puig X, Hernandez L, Hernandez S, Fernandez PL, van Lohuizen M, Colomer D, Campo E.

The Hematopathology Section, Laboratory of Anatomic Pathology, Hospital Clinic, Institut d'Investigacions Biomediques August Pi i Sunyer (IDIBAPS), University of Barcelona, Spain.

The BMI-1 gene is a putative oncogene belonging to the Polycomb group family that cooperates with c-myc in the generation of mouse lymphomas and seems to participate in cell cycle regulation and senescence by acting as a transcriptional repressor of the INK4a/ARF locus. The BMI-1 gene has been located on chromosome 10p13, a region involved in chromosomal translocations in infant leukemias, and amplified in occasional non-Hodgkin's lymphomas (NHLs) and solid tumors. To determine the possible alterations of this gene in human malignancies, we have examined 160 lymphoproliferative disorders, 13 myeloid leukemias, and 89 carcinomas by Southern blot analysis and detected BMI-1 gene amplification (3- to 7-fold) in 4 of 36 (11%) mantle cell lymphomas (MCLs) with no alterations in the INK4a/ARF locus. BMI-1 and p16INK4a mRNA and protein expression were also studied by real-time quantitative reverse transcription-PCR and Western blot, respectively, in a subset of NHLs. BMI-1 expression was significantly higher in chronic lymphocytic leukemia and MCL than in follicular lymphoma and large B cell lymphoma. The four tumors with gene amplification showed significantly higher mRNA levels than other MCLs and NHLs with the BMI-1 gene in germline configuration. Five additional MCLs also showed very high mRNA levels without gene amplification. A good correlation between BMI-1 mRNA levels and protein expression was observed in all types of lymphomas. No relationship was detected between BMI-1 and p16INK4a mRNA levels. These findings suggest that BMI-1 gene alterations in human neoplasms are uncommon, but they may contribute to the pathogenesis in a subset of malignant lymphomas, particularly of mantle cell type.

PMID: 11289106 [PubMed - indexed for MEDLINE]

BMI-1 Gene Amplification and Overexpression in Hematological Malignancies Occur Mainly in Mantle Cell Lymphomas¹

Silvia Beà, Frederic Tort, Magda Pinyol, Xavier Puig, Luis Hernández, Silvia Hernández, Pedro L. Fernández, Maarten van Lohuizen, Dolores Colomer,² and Elias Campo²

The Hematopathology Section, Laboratory of Anatomic Pathology, Hospital Clinic, Institut d'Investigacions Biomèdiques "August Pi i Sunyer" (IDIBAPS), University of Barcelona, 08036 Barcelona, Spain [S. B., F. T., M. P., X. P., L. H., S. H., P. L. F., D. C., E. C.], and Division of Molecular Carcinogenesis, The Netherlands Cancer Institute, 1066 CX Amsterdam, Netherlands [M. v. L.]

Abstract

The *BMI-1* gene is a putative oncogene belonging to the Polycomb group family that cooperates with *c-myc* in the generation of mouse lymphomas and seems to participate in cell cycle regulation and senescence by acting as a transcriptional repressor of the *INK4a/ARF* locus. The *BMI-1* gene has been located on chromosome 10p13, a region involved in chromosomal translocations in infant leukemias, and amplified in occasional non-Hodgkin's lymphomas (NHLs) and solid tumors. To determine the possible alterations of this gene in human malignancies, we have examined 160 lymphoproliferative disorders, 13 myeloid leukemias, and 89 carcinomas by Southern blot analysis and detected *BMI-1* gene amplification (3- to 7-fold) in 4 of 36 (11%) mantle cell lymphomas (MCLs) with no alterations in the *INK4a/ARF* locus. *BMI-1* and *p16^{INK4a}* mRNA and protein expression were also studied by real-time quantitative reverse transcription-PCR and Western blot, respectively, in a subset of NHLs. *BMI-1* expression was significantly higher in chronic lymphocytic leukemia and MCL than in follicular lymphoma and large B cell lymphoma. The four tumors with gene amplification showed significantly higher mRNA levels than other MCLs and NHLs with the *BMI-1* gene in germline configuration. Five additional MCLs also showed very high mRNA levels without gene amplification. A good correlation between *BMI-1* mRNA levels and protein expression was observed in all types of lymphomas. No relationship was detected between *BMI-1* and *p16^{INK4a}* mRNA levels. These findings suggest that *BMI-1* gene alterations in human neoplasms are uncommon, but they may contribute to the pathogenesis in a subset of malignant lymphomas, particularly of mantle cell type.

Introduction

The *BMI-1*³ gene is a putative oncogene of the Polycomb group originally identified by retroviral insertional mutagenesis in Eμ-*c-myc* transgenic mice infected with the Moloney murine leukemia virus (1, 2). These animals had a rapid development of pre-B cell lymphomas showing frequent proviral insertions near the *BMI-1* gene. This integration resulted in *BMI-1* overexpression suggesting a cooperative effect between *C-MYC* and *BMI-1* genes in the development of these tumors (3, 4). Recent studies have indicated that the *BMI-1* gene may also participate in cell cycle control and senescence through the

INK4a/ARF locus by acting as an upstream negative regulator of *p16^{INK4a}* and *p14/p19^{ARF}* gene expression (5). The human *BMI-1* gene has been mapped to chromosome 10p13 (6), a region involved in chromosomal translocations in infant leukemias (7) and rearrangements in malignant T cell lymphomas (8, 9). More recently, high-level DNA amplifications of this region have been found by comparative genomic hybridization in NHLs and solid tumors (10, 11). However, the possible implication of the *BMI-1* gene in these alterations and its role in the pathogenesis of human tumors is not known. The aim of this study was to analyze the possible *BMI-1* gene alterations and expression in a large series of human neoplasms and to determine the relationship with *INK4a/ARF* locus aberrations.

Materials and Methods

Case Selection. A series of 262 human tumors, including 173 hematological malignancies and 89 carcinomas (Table 1), matched normal tissues from all carcinomas, 11 samples of normal peripheral mononuclear cells, and 5 reactive lymph nodes and tonsils, were selected based on the availability of frozen samples for molecular analysis.

DNA Extraction and Southern Blot Analysis. Genomic DNA was obtained using Proteinase K/RNase treatment. 15 μg were digested with *EcoRI* and *HindIII* restriction enzymes (Life Technologies, Inc., Gaithersburg, MD), for Southern blot analysis and hybridized with a 1.5-kb *PstI* fragment of the partial *BMI-1* cDNA (6).

RNA Extraction and Real-time Quantitative RT-PCR. Total RNA was obtained from 67 lymphoid neoplasms (10 CLLs, 27 MCLs, 8 FLs, and 22 LCLs) using guanidine/isothiocyanate extraction and cesium/chloride gradient centrifugation. One μg of total RNA was transcribed into cDNA using MMLV-reverse transcriptase (Life Technologies, Inc.) and random hexamers, following manufacturer's directions. Sequences of the *BMI-1* and the *p16* detection probes and primers were designed using the Primer Express program (Applied Biosystems, Foster City) as follows: *BMI-1* sense, 5'-CTGGTTGCCATTGACAGC-3'; *BMI-1* antisense, 5'-CAGAAATGAATGCGAGCCA-3'; *p16* sense, 5'-CAACGCACCGAATAGTTACGG-3'; *p16* antisense, 5'-AACTTCGTCCTCCAGAGTCGC-3'. The probes *BMI-1*, 5'-CAGCTCGCTTCAAGATGGCCGC-3', and *p16*, 5'-CGGAGCCGATCCAGGTGGTA-3', were labeled with 6-carboxy-fluorescein as the reporter dye. The TaqMan-GAPDH Control Reagents (Applied Biosystems) were used to amplify and detect the *GAPDH* gene, as recommended by the manufacturer. The quantitative assay amplified 1 μl of cDNA in two to four replicates using the primers and probes described above and the standard master mix (Applied Biosystems). All reactions were performed in an ABI PRISM 7700 Sequence Detector System (Applied Biosystems). *GAPDH*, *BMI-1*, and *p16^{INK4a}* expression was related to a standard curve derived from serial dilutions of Raji cDNA. The RUs of *BMI-1* and *p16^{INK4a}* expression were defined as the mRNA levels of these genes normalized to the *GAPDH* expression level in each case.

Protein Analysis. Whole-cell protein extracts were obtained from additional frozen tissue available in 31 cases (7 CLLs, 12 MCLs, 8 FLs, and 4 LCLs), loaded onto a 10% SDS-polyacrylamide gel, and electroblotted to a nitrocellulose membrane (Amersham). Blocked membranes were incubated sequentially with the monoclonal antibody BMI-F6 (12), antimouse conju-

Received 10/16/00; accepted 1/29/01.

The costs of publication of this article were defrayed in part by the payment of page charges. This article must therefore be hereby marked advertisement in accordance with 18 U.S.C. Section 1734 solely to indicate this fact.

¹ Supported by Grant SAF 99/20 from Comisión Interministerial de Ciencia y Tecnología, European Union Contract QLGI-CT-2000-689, the Asociación Española contra el Cáncer, and Generalitat de Catalunya 98SGR21. S. B. and F. T. were fellows supported by Spanish Ministerio de Educación y Cultura, and S. H. was supported by the Asociación Española contra el Cáncer and the Fundació Rius i Virgili.

² To whom requests for reprints should be addressed, at the Department of Pathology, Hospital Clinic, University of Barcelona, Villarroel 170, 08036-Barcelona, Spain. Phone: 34 93 227 5450; Fax: 34 93 227 5572; E-mail: campo@medicina.ub.es.

³ The abbreviations used are: *BMI-1*, B cell-specific Moloney murine leukemia virus integration site 1; NHL, non-Hodgkin's lymphoma; CLL, chronic lymphocytic leukemia; FL, follicular lymphoma; LCL, large B cell lymphoma; MCL, mantle cell lymphoma; RT-PCR, reverse-transcription-PCR; RU, relative units.

Table 1 Hematological malignancies and solid tumor samples analyzed for BMI-1 gene alterations

Tissue samples	No. of cases
Hematological malignancies	
Hodgkin's disease	2
B cell lymphoproliferative disorders	
B-Acute lymphoblastic leukemia	14
CLL	29
Hairy cell leukemia	4
FL	15
MCL	36
LCL	40
T cell lymphoproliferative disorders	
T-Acute lymphoblastic leukemia	8
Large granular cell leukemia	4
Peripheral T-cell lymphoma	8
Myceloproliferative disorders	
Acute myeloid leukemia	7
Chronic myeloid leukemia	6
Solid tumors	
Colon carcinoma	26
Breast carcinoma	29
Laryngeal squamous cell carcinoma	34
Total	262

gated to horseradish peroxidase (Amersham), and detected by enhanced chemiluminescence (Amersham) according to the manufacturer's recommendations.

Statistical Analysis. Because of the non-normal distribution of the samples and the small size of some subsets of tumors, the statistical evaluation was performed using nonparametric tests (SPSS, version 9.0). Comparison between mRNA expression levels in the different groups of NHLs was performed using the Kruskal-Wallis Test, with a *P* for significance set at 0.05. For differences between particular groups, the conservative Bonferroni procedure was performed, and the *P* was set at 0.005. The remaining statistical analyses were carried out using the Mann-Whitney nonparametric *U* test (significance, *P* < 0.05). The comparison between BMI-1 and p16^{INK4a} quantitative mRNA levels was also performed using the Pearson's correlation coefficient.

Results

BMI-1 Gene Amplification. The BMI-1 gene was examined by Southern blot in a large series of human tumors and normal samples (Table 1). The cDNA probe used in the study detected three *Eco*RI fragments of 7.3, 3.8, and 2.6 kb and three *Hind*III fragments of 6.2, 4, and 3.5 kb. BMI-1 gene amplification (3- to 7-fold) was detected in 4 of 36 (11%) MCLs (Fig. 1). The amplifications were confirmed with both restriction enzymes. The amplified MCLs were two blastoid and two typical variants. No amplifications were observed in any of the solid tumors when compared with their respective matched non-neoplastic mucosa. No BMI-1 gene rearrangements were observed in any of the samples examined.

BMI-1 mRNA Expression. To determine the BMI-1 expression pattern in NHL we analyzed BMI-1 mRNA levels by real-time quantitative RT-PCR in 67 lymphomas (10 CLLs, 27 MCLs, 8 FLs, and 22 LCLs), including the four tumors with gene amplification. A distinct BMI-1 mRNA expression pattern was observed in the different types of lymphomas (Fig. 2; Kruskal-Wallis Test; *P* < 0.001). The BMI-1 mRNA levels in CLLs (mean, 2.2 RU; SD, 1.3) and MCLs with no BMI-1 gene amplification (mean, 2.5 RU; SD, 2.3) were significantly higher than in FLs (mean, 0.9 RU; SD, 0.8) and LCLs (mean, 0.6 RU; SD, 0.4; Mann-Whitney nonparametric *U* test; *P* < 0.01). The 4 MCLs with BMI-1 gene amplification showed significantly higher levels of expression than all other groups of tumors (mean, 5.1 RU; SD, 1.6; *P* < 0.005). In addition, five typical MCLs with no structural alterations of the gene also showed very high levels of BMI-1 mRNA expression ranging from 4 to 9.8 RU, similar to cases with gene amplification (Fig. 2A).

BMI-1 Protein Expression. BMI-1 protein expression was examined by Western blot in 31 tumors (7 CLLs; 12 MCLs, including two

cases with BMI-1 gene amplification and 4 cases with mRNA overexpression and no structural alteration of the gene; 8 FLs, and 4 LCLs) in which additional frozen tissue was available. The monoclonal antibody against BMI-1 detected three closely migrating proteins of *M_r* 45,000–48,000 (2). The two more slowly migrating bands probably represent phosphorylated isoforms of the protein (12). The two MCLs with gene amplification and three of four cases with mRNA overexpression without amplification of the gene showed very high levels of protein expression. The remaining MCLs and CLLs showed intermediate levels of protein expression, whereas low- or no-expression signals were detected in the LCLs and FLs included in the study (Fig. 3). These results indicate that BMI-1 protein expression in NHL is concordant with the mRNA levels observed by real-time quantitative RT-PCR.

Relationship between BMI-1 and p16^{INK4a} Gene Alterations. The *INK4a/ARF* locus has been recently identified as a downstream target of the transcriptional repressing activity of the BMI-1 gene, suggesting that this gene may contribute to human neoplasias with wild type *INK4a/ARF* (5). Most of the lymphoproliferative disorders analyzed in the present study, including the four cases with BMI-1 gene amplification, had been previously examined for *p53* gene mutations and *INK4a/ARF* locus alterations, including gene deletions, mutations, hypermethylation, and expression (13, 14). The four MCLs with BMI-1 gene amplification and mRNA overexpression and the five tumors with BMI-1 mRNA overexpression with no structural alterations of the gene showed a wild-type configuration of the *INK4a/ARF* locus (13). However, one case with BMI-1 gene amplification and one case with mRNA overexpression with no alteration of the gene showed *p53* gene mutations associated with allelic deletions.

To determine the possible relationship between BMI-1 and p16^{INK4a} mRNA expression, p16^{INK4a} mRNA levels were evaluated by real-time quantitative RT-PCR in 50 tumors (10 CLLs, 27 MCLs, and 13 LCLs), including 6 cases with alterations in the *INK4a/ARF* locus (2 MCLs and 1 LCL with p16^{INK4a} gene deletion, 2 LCLs with p16 promoter hypermethylation, and 1 CLL with p16^{INK4a} gene mutation), and the 4 lymphomas with BMI-1 amplification. Negative or negligible levels of p16^{INK4a} were observed in the 6 tumors with *INK4a/ARF* locus alterations. These cases were not included in the comparisons between BMI-1 and p16^{INK4a} mRNA expression. The p16^{INK4a} expression levels were relatively similar in the different types of tumors. Only LCLs tended to have lower levels of expression, but the differences did not reach statistical significance (Fig. 2B). No differences were observed in the p16^{INK4a} mRNA levels between tumors with BMI-1 gene amplification and overexpression and lymphomas with germline configuration of the gene.

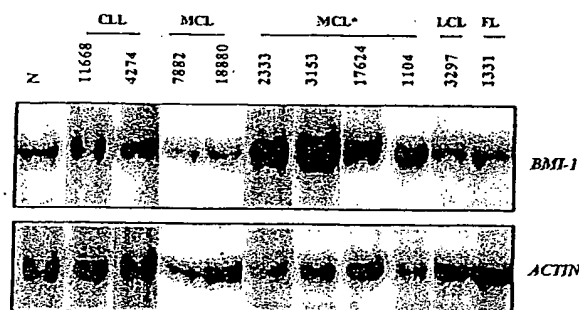


Fig. 1. Southern blot analysis of BMI-1 gene. Four MCLs (MCL*) showed BMI-1 gene amplification (3- to 7-fold) compared with non-neoplastic tissues (N) and other NHLs. No amplifications or gene rearrangements were detected in the remaining NHLs and carcinomas included in the study.

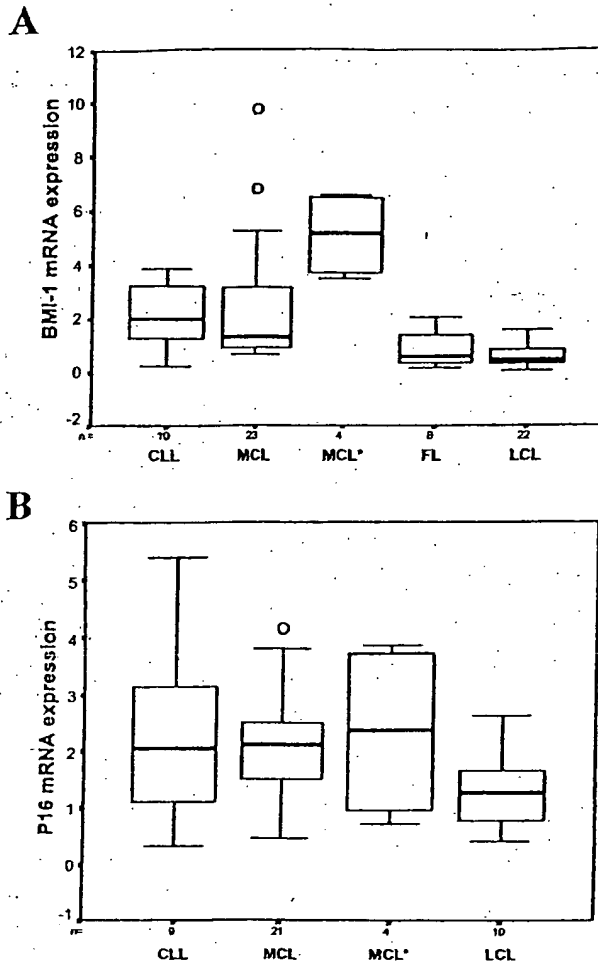


Fig. 2. A, quantitative BMI-1 mRNA transcript analysis (median and range) using real-time RT-PCR in a series of NHLs. MCLs with *BMI-1* gene amplification (MCL*) revealed significantly higher overall BMI-1 mRNA levels than all other types of NHLs, including MCLs with no structural alterations of the gene ($P < 0.005$). MCLs and CLLs expressed significantly higher levels than FLs and LCLs ($P < 0.001$). Results are depicted as the ratio of absolute BMI-1:GADPH mRNA transcript numbers (RU). Bars, SD. B, quantitative p16^{INK4a} mRNA transcript analysis (median and range) using real-time RT-PCR in a series of NHLs. Expression levels were relatively similar in the different types of tumors. Results are depicted as the ratio of absolute p16^{INK4a}:GADPH mRNA transcript numbers (RU). Bars, SD.

Discussion

In the present study, we have examined a large series of human tumors for the presence of gene alterations and mRNA expression of the *BMI-1* gene. Gene amplification was identified in four MCLs. These tumors showed significantly higher levels of mRNA and protein expression compared with other lymphomas with *BMI-1* in germline configuration. BMI-1 expression levels were also highly up-regulated in a subset of MCLs with no apparent structural alterations of the gene. No alterations were detected in any of the different types of carcinomas included in the study. *BMI-1* is considered an oncogene belonging to the Polycomb group family of genes. These proteins mainly act as transcriptional regulators, controlling specific target genes involved in development, cell differentiation, proliferation, and senescence. Different studies have shown the implication of BMI-1 overexpression in the development of lymphomas in murine and feline animal models (3, 4). The findings of the present study indicate

for the first time that *BMI-1* gene alterations in human neoplasms are an uncommon phenomenon, but they seem to occur mainly in a subset of NHLs, particularly of mantle cell type.

The human *BMI-1* gene has been mapped to chromosome 10p13. High-level DNA amplifications and gains in this region have been identified by comparative genomic hybridization in occasional solid tumors and NHLs (10, 11). Different chromosomal translocations involving the 10p13 region have also been identified in infant leukemias and T cell lymphoproliferative disorders (7, 8, 15). Most acute leukemias with this chromosomal alteration occur in children <12 months of age, whereas it seems to be extremely rare in adults. 10p translocations in T-cell lymphoproliferative disorders have been observed mainly in adult T cell leukemia/lymphomas and occasional cutaneous T cell lymphomas. In our study, we did not observe *BMI-1* rearrangements or amplifications in any of the acute leukemias or T cell lymphomas. However, all of the acute leukemias in this study were diagnosed in patients over 16 years, and no adult T cell leukemia/lymphomas or cutaneous lymphomas could be included in the series. Similarly, high-level DNA amplifications at the 10p13 region have been detected in head and neck carcinomas and other solid tumors. Although we found no evidence for *BMI-1* gene rearrangements or amplifications in a substantial set of carcinomas, this does not exclude the possibility of increased gene expression or protein levels in these tumors. Additional studies are required to elucidate the possible involvement of *BMI-1* in these particular groups of human neoplasms.

In human hematopoietic cells, BMI-1 is preferentially expressed in primitive CD34+ bone marrow cells, whereas it is negative or very low in more mature CD34- cells (16). In peripheral lymphocytes, and particularly in follicular B cells, BMI-1 protein expression has been detected in resting cells of the mantle zone, whereas it is down-regulated in proliferating germinal center cells (17, 18). These observations indicate that BMI-1 expression in normal hematopoietic cells is tightly regulated in relation with cell differentiation in bone marrow and antigen-specific response in peripheral lymphocytes. BMI-1 expression in human tumors has not been examined previously. In this study, we have demonstrated that BMI-1 mRNA and protein expression show a distinct pattern in different types of lymphomas. Thus, BMI-1 levels were low in LCLs and FLs and significantly higher in MCLs and CLLs. These findings suggest that BMI-1 expression patterns in B cell lymphomas maintain in part the expression profile of their normal cell counterparts; because FLs and at least a subgroup of LCLs are considered lymphomas derived from follicular germinal center cells, whereas MCLs and CLLs are tumors mainly derived from naive pregerminal center cells. However, the four MCLs with *BMI-1* gene amplification expressed significantly higher mRNA levels than all other tumors. In addition, five MCLs with no structural alterations of the gene showed high mRNA levels similar to those observed in tumors with *BMI-1* gene amplification, suggesting that other mechanisms may be involved in up-regulation of the gene in these lymphomas. Different studies using animal models have shown a dose-dependent effect of *BMI-1* gene expression on skeleton development

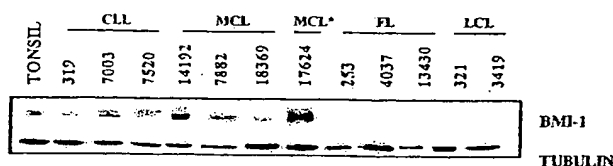


Fig. 3. Western blot analysis of BMI-1 protein in NHLs. The amplified MCL (17624) showed the highest BMI-1 protein levels, whereas other MCLs and CLLs had intermediate levels of expression. Very low or negative signal was observed in FLs and LCLs.

and lymphomagenesis (1, 3). These observations suggest that the high mRNA and protein levels detected in a subset of MCLs may play a role in the pathogenesis of these neoplasms.

Recent studies have identified the *INK4a/ARF* locus as a downstream target of the BMI-1 transcriptional repressor activity, suggesting that BMI-1 overexpression may contribute to human neoplasias that retain the wild-type *INK4a/ARF* locus (5). Interestingly, in our study, BMI-1 amplification and overexpression appeared in tumors with no alterations in *p16^{INK4a}* and *p14^{ARF}* genes. However, we could not detect differences in the expression levels of *p16^{INK4a}* in tumors with and without BMI-1 gene alterations. The reasons for this apparent discrepancy with experimental observations are not clear. One possibility may be that genes other than *INK4a/ARF* are the main targets of BMI-1 repressor activity in these tumors. Particularly, different genes of the HOX family are regulated by BMI-1 and may also be involved in lymphomagenesis (19, 20).

In conclusion, the findings of this study indicate that BMI-1 gene expression is differentially regulated in B cell lymphomas. Alterations of the gene seem to be an uncommon phenomenon in human neoplasms, but they may contribute to the pathogenesis in a subset of MCLs. Although, BMI-1 gene alterations occurred in tumors with wild-type *INK4a/ARF* locus, the possible cooperation between these genes and the oncogenic mechanisms of BMI-1 in human neoplasms require additional analysis.

Acknowledgments

The authors thank Iracema Nayach for her excellent technical assistance.

References

- Haupt, Y., Alexander, W. S., Barri, G., Klinken, S. P., and Adams, J. M. Novel zinc finger gene implicated as myc collaborator by retrovirally accelerated lymphomagenesis in E μ -myc transgenic mice. *Cell*, 65: 753-763, 1991.
- van Lohuizen, M., Verbeek, S., Scheijen, B., Wientjens, E., van der Gulden, H., and Ems, A. Identification of cooperating oncogenes in E μ -myc transgenic mice by provirus tagging. *Cell*, 65: 737-752, 1991.
- Alkema, M. J., Jacobs, H., van Lohuizen, M., and Berns, A. Perturbation of B and T cell development and predisposition to lymphomagenesis in E μ Bmi1 transgenic mice require the Bmi1 RING finger. *Oncogene*, 15: 899-910, 1997.
- Haupt, Y., Bath, M. L., Harris, A. W., and Adams, J. M. Bmi-1 transgene induces lymphomas and collaborates with myc in tumorigenesis. *Oncogene*, 8: 3161-3164, 1993.
- Jacobs, J. J., Kieboom, K., Marino, S., DePinho, R. A., and van Lohuizen, M. The oncogene and Polycomb-group gene *bmi-1* regulates cell proliferation and senescence through the *ink4a* locus. *Nature (Lond.)*, 397: 164-168, 1999.
- Alkema, M. J., Wiegant, J., Raap, A. K., Berns, A., and van Lohuizen, M. Characterization and chromosomal localization of the human proto-oncogene *BMI-1*. *Hum. Mol. Genet.*, 2: 1597-1603, 1993.
- Pui, C. H., Raimondi, S. C., Murphy, S. B., Ribeiro, R. C., Kalwinsky, D. K., Dahl, G. V., Crist, W. M., and Williams, D. L. An analysis of leukemic cell chromosomal features in infants. *Blood*, 69: 1289-1293, 1987.
- Berger, R., Baranger, L., Bernheim, A., Valensi, F., Flandrin, G., and Berheim, A. T. Cytogenetics of T-cell malignant lymphoma. Report of 17 cases and review of the chromosomal breakpoints. *Cancer Genet. Cytogenet.*, 36: 123-130, 1988.
- D'Alessandro, E., Paterlini, P., Lo Re, M. L., Di Cola, M., Ligas, C., Quagliano, D., and Del Porto, G. Cytogenetic follow-up in a case of Sezary syndrome. *Cancer Genet. Cytogenet.*, 45: 231-236, 1990.
- Bea, S., Ribas, M., Hernandez, J. M., Bosch, F., Pinyol, M., Hernandez, L., Garcia, J. L., Flores, T., Gonzalez, M., Lopez-Guillermo, A., Piris, M. A., Cardesa, A., Montserrat, E., Miro, R., and Campo, E. Increased number of chromosomal imbalances and high-level DNA amplifications in mantle cell lymphoma are associated with blastoid variants. *Blood*, 93: 4365-4374, 1999.
- Knuutila, S., Bjorkqvist, A. M., Autio, K., Tarkkanen, M., Wolf, M., Monni, O., Szymanska, J., Larramendy, M. L., Tapper, J., Pere, H., el-Rifai, W., Hemmer, S., Wasenius, V. M., Vidgren, V., and Zhu, Y. DNA copy number amplifications in human neoplasms: review of comparative genomic hybridization studies. *Am. J. Pathol.*, 152: 1107-1123, 1998.
- Alkema, M. J., Bronk, M., Verhoeven, E., Ote, A., van't Veer, L. J., Berns, A., and van Lohuizen, M. Identification of Bmi1-interacting proteins as constituents of a multimeric mammalian polycomb complex. *Genes Dev.*, 11: 226-240, 1997.
- Pinyol, M., Hernandez, L., Martinez, A., Cobo, F., Hernandez, S., Bea, S., Lopez-Guillermo, A., Nayach, I., Palacin, A., Nadal, A., Fernandez, P., Montserrat, E., Cardesa, A., and Campo, E. *INK4a/ARF* locus alterations in human non-Hodgkin's lymphomas mainly occur in tumors with wild type *p53* gene. *Am. J. Pathol.*, 156: 1987-1996, 2000.
- Pinyol, M., Cobo, F., Bea, S., Jares, P., Nayach, I., Fernandez, P. L., Montserrat, E., Cardesa, A., and Campo, E. *p16/INK4a* gene inactivation by deletions, mutations, and hypermethylation is associated with transformed and aggressive variants of non-Hodgkin's lymphomas. *Blood*, 91: 2977-2984, 1998.
- Foot, A. B., Onkhill, A., and Kitchen, C. Acute monoblastic leukemia of infancy in Klinefelter's syndrome. *Cancer Genet. Cytogenet.*, 61: 99-100, 1992.
- Lessard, J., Baban, S., and Sauvageau, G. Stage-specific expression of polycomb group genes in human bone marrow cells. *Blood*, 91: 1216-1224, 1998.
- Raaphorst, F. M., van Kemenade, F. J., Fieret, E., Hamer, K. M., Satijn, D. P., Ote, A. P., and Meijer, C. J. Cutting edge: polycomb gene expression patterns reflect distinct B cell differentiation stages in human germinal centers. *J. Immunol.*, 164: 1-4, 2000.
- Raaphorst, F. M., van Kemenade, F. J., Blokzijl, T., Fieret, E., Hamer, K. M., Satijn, D. P., Ote, A. P., and Meijer, C. J. Coexpression of *BMI-1* and *EZH2* polycomb group genes in Reed-Sternberg cells of Hodgkin's disease. *Am. J. Pathol.*, 157: 709-715, 2000.
- Gould, A. Functions of mammalian Polycomb group and trithorax group related genes. *Curr. Opin. Genet. Dev.*, 7: 488-494, 1997.
- van Oostveen, J., Bijl, J., Raaphorst, F., Walboomers, J., and Meijer, C. The role of homeobox genes in normal hematopoiesis and hematological malignancies. *Leukemia*, 13: 1675-1690, 1999.

Human thyroid carcinoma cell lines and normal thyrocytes: expression and regulation of matrix metalloproteinase-1 and tissue matrix metalloproteinase inhibitor-1 messenger-RNA and protein.

Aust G, Hofmann A, Laue S, Rost A, Kohler T, Scherbaum WA.

Institut of Anatomy, University of Leipzig, Germany.

Matrix metalloproteinase-1 (MMP-1) and tissue matrix metalloproteinase inhibitor 1 (TIMP-1) play an important role in remodeling the extracellular matrix in normal and pathological processes. The effect of phorbol-myristate acetate (PMA), interleukin-1 (IL-1), and tumor necrosis factor-alpha (TNF-alpha) on MMP-1 and TIMP-1 expression was studied on highly purified thyrocytes and undifferentiated 8505 C, C 643, HTh 74, SW 1736 thyroid carcinoma cells compared with thyroid-derived fibroblasts. Messenger RNA (mRNA) levels were monitored by competitive semiquantitative reverse transcriptase polymerase chain reaction (RT-PCR) after 24 hours. Culture supernatants were assayed for free and/or complexed MMP-1 and TIMP-1 after 48 hours using enzyme-linked immunosorbent assay (ELISA) systems (detection limit: <2 ng/mL). MMP-1 and TIMP-1 mRNA were present in all cell types, although thyrocytes showed MMP-1 mRNA levels near the detection limit. 8505 C expressed MMP-1 mRNA levels of up to 10(6) times those of the other cells analyzed. PMA and IL-1 increased MMP-1 mRNA in most cell types. TIMP-1 mRNA increased after treatment with PMA in all cells except 8505 C, whereas only slight effects were shown after IL-1 stimulation. MMP-1 protein was undetectable in normal thyrocyte cultures, but was secreted spontaneously by all cell lines ([ng/mL]; C 643: 15+/-7; HTh 74: 81+/-1; SW 1736: 13+/-2; 8505 C: 2097+/-320). There was a strong correlation between levels of MMP-1 mRNA and protein ($r = 0.99$, $p < .0001$). PMA and IL-1 increased MMP-1 secretion in all cell types after 48 hours. Fibroblasts ([ng/mL] 517+/-55) and the cell lines (C 643: 142+/-48; HTh 74: 115+/-13; SW 1736: 202+/-14; 8505C: 120+/-19) secreted TIMP-1 in unstimulated cultures, whereas only a trace amount was detected in thyrocyte cultures, even after PMA treatment. IL-1 upregulated TIMP-1 secretion after 48 hours in SW 1736, HTh 74, and C 643 cells. Our data suggest that in contrast to normal thyrocytes, dedifferentiated thyroid carcinoma cell lines are potential producers of MMP-1 as well as TIMP-1. High MMP-1 or MMP-1/TIMP-1 expression may play a role in tissue invasion of undifferentiated thyroid cancer cells.

PMID: 9349574 [PubMed - indexed for MEDLINE]



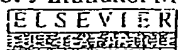
Expression of embryonic fibronectin isoform EIIIA parallels alpha-smooth muscle actin in maturing and diseased kidney.

Barnes VL, Musa J, Mitchell RJ, Barnes JL.

Department of Medicine, Division of Nephrology, University of Texas Health Science Center, San Antonio, Texas, USA.

In this study we examined if an association exists between expression of an alternatively spliced "embryonic" fibronectin isoform EIIIA (Fn-EIIIA) and alpha-smooth muscle actin (alpha-SMA) in the maturing and adult rat kidney and in two unrelated models of glomerular disease, passive accelerated anti-glomerular basement membrane (GBM) nephritis and Habu venom (HV)-induced proliferative glomerulonephritis, using immunohistochemistry and in situ hybridization. Fn-EIIIA and alpha-SMA proteins were abundantly expressed in mesangium and in periglomerular and peritubular interstitium of 20-day embryonic and 7-day (D-7) postnatal kidneys in regions of tubule and glomerular development. Staining was markedly reduced in these structures in maturing juvenile (D-14) kidney and was largely lost in adult kidney. Expression of Fn-EIIIA and alpha-SMA was reinitiated in the mesangium and the periglomerular and peritubular interstitium in both models and was also observed in glomerular crescents in anti-GBM nephritis. Increased expression of Fn-EIIIA mRNA by in situ hybridization corresponded to the localization of protein staining. Dual labeling experiments verified co-localization of Fn-EIIIA and alpha-SMA, showing a strong correlation of staining between location and staining intensity during kidney development, maturation, and disease. Expression of EIIIA mRNA corresponded to protein expression in developing and diseased kidneys and was lost in adult kidney. These studies show a recapitulation of the co-expression of Fn-EIIIA and alpha-SMA in anti-GBM disease and suggest a functional link for these two proteins.

PMID: 10330455 [PubMed - indexed for MEDLINE]



Rapid quantitation of proinflammatory and chemoattractant cytokine expression in small tissue samples and monocyte-derived dendritic cells: validation of a new real-time RT-PCR technology.

Blaschke V, Reich K, Blaschke S, Zipprich S, Neumann C.

Department of Dermatology, von-Siebold-Str. 3, D-37075, Goettingen, Germany.
vblasch@gwdg.de

The analysis of cytokine profiles plays a central part in the characterization of disease-related inflammatory pathways and the identification of functional properties of immune cell subpopulations. Because tissue biopsy samples are too small to allow the detection of cytokine protein, the detection of mRNA by RT-PCR analysis is often used to investigate the cytokine milieu in inflammatory lesions. RT-PCR itself is a qualitative method, indicating the presence or absence of specific transcripts. With the use of internal or external standards it may also serve as a quantitative method. The most widely accepted method is quantitative competitive RT-PCR, based on internal shortened standards. Recently, online real-time PCR has been introduced (LightCycler), which allows quantitation in less than 30 min. Here, we have tested its use for the analysis of cytokine gene expression in different experimental in vitro and ex vivo settings. First, we compared quantitative competitive RT-PCR with real-time RT-PCR in the quantitation of transcription levels of the CD4(+) cell-specific chemoattractant Interleukin-16 during the maturation of monocyte-derived dendritic cells, and found a good correlation between both methods. Second, differences in the amounts of IL-16 mRNA in synovial tissue from patients with rheumatoid arthritis and osteoarthritis as assessed by real-time RT-PCR paralleled differences in the level of IL-16 protein in the synovial fluid. Finally, we employed real-time RT-PCR to study the cutaneous expression of several cytokines during experimental immunomodulatory therapy of psoriasis by Interleukin-10, and demonstrate that the technique is suitable for pharmacogenomic monitoring. In summary, real-time RT-PCR is a sensitive and rapid tool for quantifying mRNA expression even with small quantities of tissue. The results obtained do not differ from those generated by quantitative competitive RT-PCR.

Publication Types:

- Evaluation Studies

PMID: 11121549 [PubMed - indexed for MEDLINE]

74: Apoptosis. 1997;2(6):518-28.

Related Articles, Links

 SpringerLink
Full Text Available

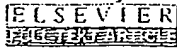
Butyrate-induced reversal of dexamethasone resistance in autonomous rat Nb2 lymphoma cells.

Buckley AR, Krumenacker JS, Buckley DJ, Leff MA, Magnuson NS, Reed JC, Miyashita T, de Jong G, Gout PW.

Department of Pharmacology and Toxicology, University of North Dakota School of Medicine and Health Sciences, Grand Forks 58202-9037, USA.
abuckley@mail.med.und.nodak.edu

The parental rat Nb2 lymphoma is a prolactin (PRL)-dependent T cell line. Exposure of a PRL-independent subline, Nb2-SFJCD1, to sodium butyrate (NaBT) causes transient reversal of their growth factor-independent proliferation in association with constitutive expression of protooncogenes pim-1 and c-myc. In the present study, we investigated the effect of NaBT treatment on the sensitivity of Nb2-SFJCD1 cells to dexamethasone (DEX)-induced apoptosis. Pretreatment with NaBT (2 mM, 72 h) partially reversed resistance to apoptosis in Nb2-SFJCD1 cells exposed to DEX (100 nM) for 12 h, assessed by flow cytometric analyses of DNA fragmentation. However, the cytolytic effect of DEX was abrogated by PRL in a time- and concentration-dependent manner. Evaluation of apoptosis-associated gene expression in NaBT-pre-treated cultures incubated with DEX or DEX+PRL indicated that the apoptosis resistance did not stem from altered bcl-2 or bax expression. However, there was a strong correlation between the resistance to DEX-activated apoptosis and their enhanced expression of pim-1 mRNA and protein. The results show that it is possible to reverse DEX-induced apoptosis of Nb2 pre-T cells and suggest the pim-1 gene product has an important role as a suppressor of this process, perhaps functioning as a mediator of PRL action.

PMID: 14646523 [PubMed]



Characterization of cyclin D2 expression in human endometrium.

Choi D, Yoon S, Lee E, Hwang S, Song S, Kim J, Yoon BK, Lee JH.

Department of Obstetrics and Gynecology, Samsung Medical Center, Sungkyunkwan University School of Medicine, Seoul, South Korea. dschoi@smc.samsung.co.kr

OBJECTIVE: This study was undertaken to investigate cyclin D2 mRNA and protein expression in human endometrium during the menstrual cycle. **METHODS:** Endometrial samples were obtained from 15 premenopausal nonpregnant women who had hysterectomies for benign gynecologic reasons. They were divided into the following five groups according to histologic dating: early proliferative ($n = 3$), mid to late proliferative ($n = 3$), early secretory ($n = 3$), mid secretory ($n = 3$), and late secretory ($n = 3$). Cyclin D2 mRNA and protein expression were analyzed using reverse transcriptase-polymerase chain reaction, Western blotting, and immunohistochemistry. **RESULTS:** Cyclin D2 mRNA and protein were expressed in human endometrial tissue throughout the menstrual cycle. Cyclin D2 mRNA and protein expression of proliferative phase endometrium were significantly higher than those of secretory phase endometrium ($P < .05$). The staining intensity of cyclin D2 in proliferative phase endometrium was higher than that in secretory phase ($P < .05$). Cyclin D2 mRNA level showed good correlation with cyclin D2 protein level ($R = 0.579$, $P < .03$), and cyclin D2 protein also showed good correlation with immunohistochemical staining intensity ($R = 0.562$, $P < .03$). **CONCLUSION:** Cyclin D2 was expressed in human endometrium throughout the menstrual cycle. Cyclin D2 mRNA and protein were expressed at high levels in proliferative phase endometrium, especially in the early proliferative phase, and then decreased in the secretory phase.

PMID: 11839508 [PubMed - indexed for MEDLINE]

86: Am J Physiol Lung Cell Mol Physiol. 2004 Feb;286(2):L301-11.
Epub 2003 Sep 26.

Related Articles,
Links

FREE full-text article at
ajplung.physiology.org

Downregulation of ENaC activity and expression by TNF-alpha in alveolar epithelial cells.

Dagenais A, Frechette R, Yamagata Y, Yamagata T, Carmel JF, Clermont ME, Brochiero E, Masse C, Berthiaume Y.

Centre de recherche, CHUM-Hotel-Dieu, 3850 St-Urbain, Montréal, Quebec, Canada H2W 1T7. andre.dagenais.chum@ssss.gouv.qc.ca

Sodium absorption by an amiloride-sensitive channel is the main driving force of lung liquid clearance at birth and lung edema clearance in adulthood. In this study, we tested whether tumor necrosis factor-alpha (TNF-alpha), a proinflammatory cytokine involved in several lung pathologies, could modulate sodium absorption in cultured alveolar epithelial cells. We found that TNF-alpha decreased the expression of the alpha-, beta-, and gamma-subunits of epithelial sodium channel (ENaC) mRNA to 36, 43, and 16% of the controls after 24-h treatment and reduced to 50% the amount of alpha-ENaC protein in these cells. There was no impact, however, on alpha(1) and beta(1) Na(+)-K(+)-ATPase mRNA expression. Amiloride-sensitive current and ouabain-sensitive Rb(+) uptake were reduced, respectively, to 28 and 39% of the controls. A strong correlation was found at different TNF-alpha concentrations between the decrease of amiloride-sensitive current and alpha-ENaC mRNA expression. All these data show that TNF-alpha, a proinflammatory cytokine present during lung infection, has a profound influence on the capacity of alveolar epithelial cells to transport sodium.

PMID: 14514522 [PubMed - indexed for MEDLINE]



Inhibin and activin production and subunit expression in human placental cells cultured in vitro.

Debieve F, Pampfer S, Thomas K

Department of Obstetrics and Gynecological Endocrinology, Université Catholique de Louvain, 1200 Brussels, Belgium.

Inhibins and activins are dimeric proteins, with each subunit being one of three related protein subunits (alpha, betaA or betaB). The mRNA levels of these subunits were studied quantitatively during in-vitro differentiation of human cytotrophoblast cells into syncytium, using Northern blot analysis and semi-quantitative reverse transcription-polymerase chain reaction (RT-PCR) analysis. The corresponding protein concentrations were determined by specific enzyme-linked immunosorbent assays for inhibin A, B, pro alphaC and activin A in cellular protein extracts and culture medium (n = 5). Immunofluorescence studies showed syncytium formation after 48 h. The alpha subunit was present before plating and increased at 48 h ($P < 0.001$) while the betaA subunit was weak before plating and increased at 24 h. The betaB subunit was not detected. With respect to corresponding protein synthesis, inhibin A (alpha + betaA) had risen after 48 h in cellular protein extract and after 72 h in culture medium, while activin A (betaA + betaB) was detected after 24 h, with no significant variations in culture medium. There was a good correlation between inhibin A and alpha subunit expression ($r = 0.736$, $P < 0.001$), as well as between activin A and betaA subunit expression ($r = 0.755$, $P < 0.001$). This study showed that mRNA expression parallels protein synthesis of inhibin and activin in trophoblast cells. Inhibin A synthesis appears to be dependent on alpha subunit mRNA expression, rather than on the betaA subunit which controls activin A synthesis. This study has also shown that isolated cytotrophoblast cells do not produce dimeric inhibin. However, during the transformation of cytotrophoblast cells into syncytium, betaA subunit mRNA expression may be an indicator of cell aggregation, while alpha subunit mRNA expression may be an indicator of cell fusion.

PMID: 10908285 [PubMed - indexed for MEDLINE]

Involvement of the CCND1 gene in hairy cell leukemia.

de Boer CJ, Kluin-Nelemans JC, Dreef E, Kester MG, Kluin PM, Schuurung E, van Krieken JH.

Department of Pathology, University of Leiden, The Netherlands.

BACKGROUND: Previous results suggested increased mRNA expression of CCND1 in hairy cell leukemia (HCL). The CCND1 gene is involved in the t(11;14)(q13;q32) chromosomal rearrangement, a characteristic abnormality in mantle cell lymphoma (MCL). We and others reported that, in contrast to other B-cell lymphomas, almost all MCL have over-expression of the CCND1 gene with a good correlation between RNA and protein analysis. Recent studies showed that overexpression of the cyclin D1 protein can be easily detected by immunohistochemistry (IHC) on formalin-fixed, paraffin embedded tissues. **PATIENTS AND METHODS:** To investigate whether the CCND1 gene is involved in HCL, we performed IHC on a series of 22 cases using formalin-fixed paraffin embedded splenectomy specimens. For IHC the sections were boiled in citrate buffer. The presence of rearrangements within the BCL-1 locus and the CCND1 gene was analyzed in 13 of 22 cases by Southern blot analysis using all available break-point probes. Expression of CCND1 was analyzed at the mRNA level (Northern blot) and protein level (IHC). **RESULTS:** Overexpression of the cyclin D1 protein using IHC was observed in all cases, with strong expression in 5 cases. Pre-existing B- and T-cell areas of the spleen did not express significant levels of the cyclin D1 protein. Seven of 9 cases analyzed by both IHC and Northern blotting showed overexpression of the CCND1 gene with both methods. No genomic abnormalities were observed in any of the 13 cases studied by Southern blot analysis. Additionally, no 11q13 abnormalities were detected by banding analysis of 19 of 22 cases. **CONCLUSIONS:** The elevated levels of CCND1 mRNA and protein in conjunction with the absence of overt rearrangements within the BCL-1 locus distinguish HCL from MCL and other B-cell malignancies. This suggests that activation of the CCND1 gene in HCL is due to mechanisms other than chromosomal rearrangement.

PMID: 8740788 [PubMed - indexed for MEDLINE]



Expression of membrane-type matrix metalloproteinases 4, 5, and 6 in mouse corneas infected with *P. aeruginosa*.

Dong Z, Katar M, Alousi S, Berk RS.

Department of Immunology and Microbiology, Wayne State University School of Medicine, 540 E. Canfield, Detroit, MI 48201, USA.

PURPOSE: To investigate the expression and regulation of membrane-type matrix metalloproteinases (MT-MMPs) 4, 5, and 6 in the mouse corneas infected with *Pseudomonas aeruginosa*. **METHODS:** C57BL/6J mice were intracorneally infected with *P. aeruginosa*. The expression of MT4-, MT5-, and MT6-MMP was detected at both the mRNA and protein levels by RT-PCR and immunoblot analysis. Immunohistochemical staining was performed to localize the expression of MT4- and MT5-MMP in the mouse corneas. **RESULTS:** Expression of MT4- and MT5-MMP was detected in the normal (uninfected) cornea by RT-PCR and immunoblot analysis. When infected with *P. aeruginosa*, the corneas showed significant induction of each MT-MMP. Localization of MT4- and MT5-MMP revealed that the expression of MT5-MMP was restricted to the epithelial tissue in the normal cornea, whereas the induced expression of MT4- and MT5-MMP was predominantly in the substantia propria, which contained most of the infiltrating cells. MT6-MMP expression was not detected in the uninfected cornea but was upregulated in the infected corneas. **CONCLUSIONS:** Expression of MT4-, MT5-, and MT6-MMP was induced in corneas infected with *P. aeruginosa*. Immunohistochemistry showed predominant immunoreactivity of MT4- and MT5-MMP in the substantia propria. Previous histologic studies have revealed different patterns of inflammatory cell infiltration with an increased number of polymorphonuclear neutrophils (PMNs) during the early stage of inflammation and increased macrophages during the late stage. These results indicate a good correlation between the overexpression of the MT-MMPs in the infected corneas and the inflammatory response—that is, leukocyte infiltration—indicating that inflammatory cells such as macrophages and PMNs may play a role in the upregulation of MT-MMPs during corneal infection, which in turn can cause the destruction of corneal tissue.

PMID: 11726626 [PubMed - indexed for MEDLINE]

FREE full text article at
www.jimmunol.org

Suppressors of cytokine signaling proteins are differentially expressed in Th1 and Th2 cells: implications for Th cell lineage commitment and maintenance.

Egwuagu CE, Yu CR, Zhang M, Mahdi RM, Kim SJ, Gery I.

Laboratory of Immunology, National Eye Institute, National Institutes of Health, Bethesda, MD 20892, USA. emeka@helix.nih.gov

Positive regulatory factors induced by IL-12/STAT4 and IL-4/STAT6 signaling during T cell development contribute to polarized patterns of cytokine expression manifested by differentiated Th cells. These two critical and antagonistic signaling pathways are under negative feedback regulation by a multimember family of intracellular proteins called suppressor of cytokine signaling (SOCS). However, it is not known whether these negative regulatory factors also modulate Th1/Th2 lineage commitment and maintenance. We show here that CD4(+) naive T cells constitutively express low levels of SOCS1, SOCS2, and SOCS3 mRNAs. These mRNAs and their proteins increase significantly in nonpolarized Th cells after activation by TCR signaling. We further show that differentiation into Th1 or Th2 phenotype is accompanied by preferential expression of distinct SOCS mRNA transcripts and proteins. SOCS1 expression is 5-fold higher in Th1 than in Th2 cells, whereas Th2 cells contain 23-fold higher levels of SOCS3. We also demonstrate that IL-12-induced STAT4 activation is inhibited in Th2 cells that express high levels of SOCS3 whereas IL-4/STAT6 signaling is constitutively activated in Th2 cells, but not Th1 cells, with high SOCS1 expression. These results suggest that mutually exclusive use of STAT4 and STAT6 signaling pathways by differentiated Th cells may derive in part, from SOCS3- or SOCS1-mediated repression of IL-12/STAT4- or IL-4/STAT6 signaling in Th2 and Th1 cells, respectively. Given the strong correlation between distinct patterns of SOCS expression and differentiation into the Th1 or Th2 phenotype, SOCS1 and SOCS3 proteins are therefore Th lineage markers that can serve as therapeutic targets for immune modulation therapy.

PMID: 11907070 [PubMed - indexed for MEDLINE]

Altered levels of scavenging enzymes in embryos subjected to a diabetic environment.

Forsberg H, Borg LA, Cagliero E, Eriksson UJ.

Department of Medical Cell Biology, University of Uppsala, Sweden.

Maternal diabetes during pregnancy is associated with an increased rate of congenital malformations in the offspring. The exact molecular etiology of the disturbed embryogenesis is unknown, but an involvement of radical oxygen species in the teratological process has been suggested. Oxidative damage presupposes an imbalance between the activity of the free oxygen radicals and the antioxidant defence mechanisms on the cellular level. The aim of the present study was to investigate if maternal diabetes *in vivo*, or high glucose *in vitro* alters the expression of the free oxygen radical scavenging enzymes superoxide dismutase (CuZnSOD and MnSOD), catalase and glutathione peroxidase in rat embryos during late organogenesis. We studied offspring of normal and diabetic rats on gestational days 11 and 12, and also evaluated day-11 embryos after a 48 hour culture period in 10 mM or 50 mM glucose concentration. Both maternal diabetes and high glucose culture caused growth retardation and increased rate of congenital malformations in the embryos. The CuZnSOD and MnSOD enzymes were expressed on gestational day 11 and both CuZnSOD, MnSOD and catalase were expressed on day 12 with increased concentrations of MnSOD transcripts when challenged by a diabetic milieu. There was a good correlation between mRNA, protein, and activity levels, suggesting that the regulation of these enzymes occurs primarily at the pretranslational level. Maternal diabetes *in vivo* and high glucose concentration *in vitro* induced increased MnSOD expression, concomitant with increased total SOD activity, and a tentative decrease in catalase expression and activity in the embryos. These findings support the notion of enhanced oxidative stress in the embryo as an etiologic agent in diabetic teratogenesis.

PMID: 8804988 [PubMed - indexed for MEDLINE]

Induction of the estrogen receptor by growth hormone and glucocorticoid substitution in primary cultures of rat hepatocytes.

Freyschuss B, Stavreus-Evers A, Sahlin L, Eriksson H.

Department of Reproductive Endocrinology, Karolinska Hospital, Stockholm, Sweden.

Hepatic estrogen receptors (ER) mediate estrogenic effects on mammalian liver metabolism and are thereby involved in the regulation of important physiological/pathological processes, such as coagulation, atherosclerosis, and hypertension. The regulation of the formation of the ER in primary cultures of rat hepatocytes was studied by assaying ER and ER mRNA under different endocrine conditions. The ER concentration was measured using two different methods, a ligand-binding technique and an ER enzyme immunoassay. The results obtained by the two methods showed good correlation, and linear regression analysis gave a correlation coefficient of 0.95. ER concentrations fell to low steady state levels within 16 h after establishing the cell culture and remained low in the absence of hormonal substitution. Upon medium supplementation with pituitary GH and the glucocorticoid dexamethasone (DEX) in combination, the ER concentration increased 6-fold from 4.2 ± 1.0 to 25.8 ± 7.0 fmol/mg cytosolic protein. ER mRNA was measured by solution hybridization. Substitution with GH and DEX in combination increased ER mRNA to $210 \pm 14\%$ of control levels. No effect on ER mRNA stability was seen after hormone treatment. It is concluded that the regulatory effects of GH and DEX on the hepatic ER in this in vitro system are very similar to the effects of these hormones under in vivo conditions. The inducible expression of the ER has never before, to our knowledge, been demonstrated in any mammalian liver cell culture system.

PMID: 8404593 [PubMed - indexed for MEDLINE]



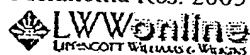
Oxytocin receptors in bovine cervix: distribution and gene expression during the estrous cycle.

Fuchs AR, Ivell R, Fields PA, Chang SM, Fields MJ.

Department of Obstetrics and Gynecology, Cornell University Medical College, New York, New York 10021, USA.

Oxytocin (OT) receptor (OTR) concentrations were determined in the cervix of nonpregnant cows on cycle Days 0, 3, 7-8, 17, and 19 (n = 3-4 cows each day); [3H]OT was used as the labeled ligand. Mucosal and muscle layers of the cervix were also analyzed separately for both ligand binding and expression of the OTR gene using a newly developed RNase protection assay (RAP). Cellular localization of OTR protein was determined by immunohistochemistry. All regions of cervix from cows at estrus had high concentrations of OTR; in the luteal phase, all were sharply down-regulated. At estrus the mucosal layer had about 30-fold higher concentrations than the muscle layer. OTR mRNA was readily detected by RAP in the mucosa from estrous cows, while much weaker signals were found in the muscle. On Days 7-17, the OTR mRNA signals in both mucosa and muscle were very faint or nondetectable. Thus, there was a good correlation between ligand binding and mRNA expression, which suggests that OTR concentrations are mainly regulated at the transcriptional level. The epithelial cells at the luminal surface of the mucosa were the principal site of immunoreactive OTR; muscle cells showed significantly weaker signals. Previously, OT was found to stimulate prostaglandin (PG) E₂ output in vitro in bovine cervical tissues. Since PGE₂ is capable of softening the cervix, our findings suggest that OT may have a novel physiological function to cause softening of the bovine cervix mediated by the release of PGE₂.

PMID: 8835394 [PubMed - indexed for MEDLINE]



Silencing of the thrombomodulin gene in human malignant melanoma.

Furuta J, Kaneda A, Umebayashi Y, Otsuka F, Sugimura T, Ushijima T.

Carcinogenesis Division, National Cancer Center Research Institute, Tokyo, Japan.

The loss of thrombomodulin (TM) expression is associated with tumour growth, infiltration and lymph node metastasis in human tumours. In melanoma cell lines, TM is reported to mediate cell adhesion, and its introduction into TM-negative melanoma cell lines suppresses their growth. In this study, we analysed TM expression in surgical melanoma specimens and the role of its promoter methylation in the loss of its expression. In 15 (75%) of the 20 specimens (five from a primary site and 15 from metastatic sites), melanoma cells lacked TM immunoreactivity. Methylation of the TM promoter region was detected in 10 (67%) of the 15 TM-negative specimens by methylation-specific polymerase chain reaction, whereas methylation was detected in two (40%) of the five TM-positive specimens. In cell lines, complete methylation of the TM promoter CpG island was detected in six (46%) of 13 melanoma cell lines, whereas no methylation was detected in two cultured normal melanocytes. There was a good correlation between the methylated status of the CpG island and the loss of TM messenger RNA (mRNA) expression. Treatment of melanoma cell lines with a demethylating agent, 5-aza-2'-deoxycytidine, induced demethylation of the promoter CpG island and the restoration of mRNA and protein expression. These findings suggest that most human melanomas lack TM expression, and that methylation of the promoter CpG island is one of the mechanisms responsible.

PMID: 15714116 [PubMed - indexed for MEDLINE]

FREE full text article at
www.jimmunol.org

Cyclooxygenase-2 expression in macrophages: modulation by protein kinase C-alpha.

Giroux M, Descoteaux A.

Institut National de la Recherche Scientifique-Institut Armand-Frappier, Universite du Quebec, Laval, Canada.

Cyclooxygenase-2 (COX-2) is an inducible enzyme responsible for high levels of PG production during inflammation and immune responses. Previous studies with pharmacological inhibitors suggested a role for protein kinase C (PKC) in PG production possibly by regulating COX-2 expression. In this study, we addressed the role of PKC-alpha in the modulation of COX-2 expression and PGE2 synthesis by the overexpressing of a dominant-negative (DN) mutant of this isoenzyme in the mouse macrophage cell line RAW 264.7. We investigated the effect of various stimuli on COX-2 expression, namely, LPS, IFN-gamma, and the intracellular parasite *Leishmania donovani*. Whereas LPS-induced COX-2 mRNA and protein expression were down-regulated in DN PKC-alpha-overexpressing clones, IFN-gamma-induced COX-2 expression was up-regulated in DN PKC-alpha-overexpressing clones with respect to normal RAW 264.7 cells. Measurements of PGE2 levels revealed a strong correlation between PGE2 secretion and IFN-gamma-induced COX-2 mRNA and protein levels in DN PKC-alpha-overexpressing clones. Taken together, these results suggest a role for PKC-alpha in the modulation of LPS- and IFN-gamma-induced COX-2 expression, as well as in IFN-gamma-induced PGE2 secretion.

PMID: 11034408 [PubMed - indexed for MEDLINE]

Society for Endocrinology
FREE FULL TEXT

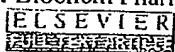
Modulation of gap junction mediated intercellular communication in TM3 Leydig cells.

Goldenberg RC, Fortes FS, Cristancho JM, Morales MM, Franci CR, Varanda WA, Campos de Carvalho AC.

Institute of Biophysics Carlos Chagas Filho, UFRJ, Brazil.

Long-term modulation of intercellular communication via gap junctions was investigated in TM3 Leydig cells, under low and high confluence states, and upon treatment of the cells for different times with activators of protein kinase A (PKA) and protein kinase C (PKC). Cells in low confluence were readily coupled, as determined by transfer of the dye Lucifer Yellow; on reaching confluence, the cells uncoupled. Western blots and RT-PCR revealed that connexin 43 (Cx43) was abundantly expressed in TM3 Leydig cells and its expression was decreased after the cells achieved confluence. Stimulation of PKA or PKC induced a decrease in cell-cell communication. Staurosporin, an inhibitor of protein kinases, increased coupling and was able to prevent and reverse the uncoupling actions of dibutyryl cAMP and 12-O-tetradecanoyl-phorbol-13-acetate (TPA). Under modulation by confluence, Cx43 was localized to the appositional membranes when cells were coupled and was mainly in the cytoplasm when they were uncoupled. In addition, cAMP and TPA reduced the surface membrane labeling for Cx43, whereas staurosporin increased it. These data show a strong correlation between functional coupling and the membrane distribution of Cx43, implying that this connexin has an important role in intercellular communication between TM3 cells. Furthermore, increased testosterone secretion in response to luteinizing hormone was accompanied by a decrease in intercellular communication, suggesting that gap junction mediated coupling may be a modulator of hormone secretion in TM3 cells.

PMID: 12740021 [PubMed - indexed for MEDLINE]



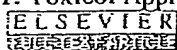
Restored expression and activity of organic ion transporters rOAT1, rOAT3 and rOCT2 after hyperuricemia in the rat kidney.

Habu Y, Yano I, Okuda M, Fukatsu A, Inui K.

Department of Pharmacy, Kyoto University Hospital, Faculty of Medicine, Kyoto University, Sakyo-ku, Kyoto 606-8507, Japan.

We previously reported that in hyperuricemic rats, renal impairment occurred and organic ion transport activity decreased, accompanied with a specific decrease in the expression of rat organic anion transporters, rOAT1 and rOAT3, and organic cation transporter, rOCT2. In the present study, we investigated the reversibility of the organic ion transport activity and expression of organic ion transporters (slc22a) during recovery from hyperuricemia. Hyperuricemia was induced by the administration of a chow containing uric acid and oxonic acid, an inhibitor of uric acid metabolism. Four days after discontinuance of the chow, the plasma uric acid concentration returned to the normal level, and renal functions such as creatinine clearance and BUN levels were restored, although the recovery of tubulointerstitial injury was varied in sites of the kidney. Basolateral uptake of p-aminohippurate (PAH) and tetraethylammonium (TEA), and both protein and mRNA levels of rOAT1, rOAT3 and rOCT2 in the kidney gradually improved during 14 days of recovery from hyperuricemia. Basolateral PAH transport showed a higher correlation with the protein level of rOAT1 ($r(2)=0.80$) than rOAT3 ($r(2)=0.34$), whereas basolateral TEA transport showed a strong correlation with rOCT2 protein ($r(2)=0.91$). The plasma testosterone concentration, which is a dominant factor in the regulation of rOCT2, was gradually restored during the recovery from hyperuricemia, but the correlation between the plasma testosterone level and rOCT2 protein expression in the kidney was not significant. These results suggest that the regulation of organic ion transporters, rOAT1, rOAT3 and rOCT2, by hyperuricemia is reversible, and the organic ion transport activity restores according to the expression levels of these transporters.

PMID: 15748710 [PubMed - indexed for MEDLINE]



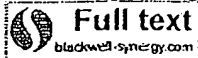
Regulation of cytochrome P4501A1 in teleosts: sustained induction of CYP1A1 mRNA, protein, and catalytic activity by 2,3,7,8-tetrachlorodibenzofuran in the marine fish *Stenotomus chrysops*.

Hahn ME, Stegeman JJ.

Biology Department, Woods Hole Oceanographic Institution, Massachusetts 02543.

Cytochrome P4501A1 (CYP1A1) is known to play important roles in the activation and detoxification of carcinogens and other toxicants in vertebrate animals, including fish. Although extensively studied in mammalian systems, the regulation of CYP1A forms in other vertebrates is less well understood. We examined the time course and dose-response relationships for induction of CYP1A1 mRNA, protein, and catalytic activity by 2,3,7,8-tetrachlorodibenzofuran (TCDF) in the marine fish *Stenotomus chrysops* (scup). The time course of CYP1A1 induction was determined following a single ip dose (10 nmol/kg) of 2,3,7,8-TCDF. Hepatic ethoxyresorufin O-deethylase activity was increased after 1 day, reached a maximum by 8 days, and was still elevated 14 days after treatment. The content of immunodetectable CYP1A1 protein in liver was elevated on Day 1 and continued to increase through 14 days. CYP1A1 protein content was also strongly induced in heart and gill beginning at 2 days after treatment and extending through Day 14. Hepatic CYP1A1 mRNA was strongly induced by 1 day after dosing and remained elevated through 14 days. The sustained induction of CYP1A1 mRNA by 2,3,7,8-TCDF contrasts with the transient induction seen previously in fish treated with nonhalogenated inducers and most likely reflects differences in persistence of the inducers. Dose-response studies indicated that induction of CYP1A1 mRNA, protein, and catalytic activity occurred following doses of 2,3,7,8-TCDF as low as 0.4 nmol/kg (120 ng/kg), within the range of whole-body contents of this congener measured in fish from contaminated environments. The estimated dose producing half-maximal CYP1A1 induction in scup was approximately 2-10 nmol/kg, suggesting that the sensitivity of these fish to induction may be as great as or greater than that of rats. In contrast to previous results obtained with 3,3',4,4'-tetrachlorobiphenyl (TCB) and beta-naphthoflavone, which appear to inhibit or inactivate CYP1A1 in fish and other vertebrates, there was a good correlation among levels of CYP1A1 mRNA, protein, and catalytic activity in individual fish following various doses of 2,3,7,8-TCDF. The difference in response to 2,3,7,8-TCDF versus 3,3',4,4'-TCB may reflect differences in the inducing potencies of the two compounds relative to their similar potencies as inhibitors of CYP1A1 catalytic activity. In additional studies to evaluate structure-activity relationships for CYP1A1 induction by chlorinated dibenzofurans in fish, scup were treated with 2,3,6,8-tetrachlorodibenzofuran (2,3,6,8-TCDF). At 10 or 50 nmol/kg, 2,3,6,8-TCDF was inactive as an inducer of CYP1A1 mRNA, protein, or catalytic activity. (ABSTRACT TRUNCATED AT 400 WORDS)

PMID: 8048062 [PubMed - indexed for MEDLINE]



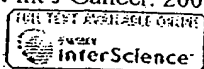
The role of the epidermal growth factor receptor in sustaining neutrophil inflammation in severe asthma.

Hamilton LM, Torres-Lozano C, Puddicombe SM, Richter A, Kimber I, Dearman RJ, Vrugt B, Aalbers R, Holgate ST, Djukanovic R, Wilson SJ, Davies DE.

Division of Infection, Inflammation & Repair, School of Medicine, University of Southampton, UK.

BACKGROUND: The extent of epithelial injury in asthma is reflected by expression of the epidermal growth factor receptor (EGFR), which is increased in proportion to disease severity and is corticosteroid refractory. Although the EGFR is involved in epithelial growth and differentiation, it is unknown whether it also contributes to the inflammatory response in asthma. **OBJECTIVES:** Because severe asthma is characterized by neutrophilic inflammation, we investigated the relationship between EGFR activation and production of IL-8 and macrophage inhibitory protein-1 alpha (MIP-1alpha) using in vitro culture models and examined the association between epithelial expression of IL-8 and EGFR in bronchial biopsies from asthmatic subjects. **METHODS:** H292 or primary bronchial epithelial cells were exposed to EGF or H2O2 to achieve ligand-dependent and ligand-independent EGFR activation; IL-8 mRNA was measured by real-time PCR and IL-8 and MIP-1alpha protein measured by enzyme-linked immunosorbent assay (ELISA). Epithelial IL-8 and EGFR expression in bronchial biopsies from asthmatic subjects was examined by immunohistochemistry and quantified by image analysis. **RESULTS:** Using H292 cells, EGF and H2O2 increased IL-8 gene expression and release and this was completely suppressed by the EGFR-selective tyrosine kinase inhibitor, AG1478, but only partially by dexamethasone. MIP-1alpha release was not stimulated by EGF, whereas H2O2 caused a 1.8-fold increase and this was insensitive to AG1478. EGF also significantly stimulated IL-8 release from asthmatic or normal primary epithelial cell cultures established from bronchial brushings. In bronchial biopsies, epithelial IL-8, MIP-1alpha, EGFR and submucosal neutrophils were all significantly increased in severe compared to mild disease and there was a strong correlation between EGFR and IL-8 expression ($r = 0.70$, $P < 0.001$). **CONCLUSIONS:** These results suggest that in severe asthma, epithelial damage has the potential to contribute to neutrophilic inflammation through enhanced production of IL-8 via EGFR-dependent mechanisms.

PMID: 12580917 [PubMed - indexed for MEDLINE]



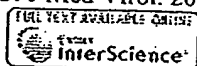
Localization of tissue inhibitor of metalloproteinases 1 (TIMP-1) in human colorectal adenoma and adenocarcinoma.

Holten-Andersen MN, Hansen U, Brunner N, Nielsen HJ, Illemann M, Nielsen BS.

The Finsen Laboratory, Rigshospitalet, Denmark.

Tissue inhibitor of matrix metalloproteinases 1 (TIMP-1) inhibits the proteolytic activity of matrix metalloproteinases and hereby prevents cancer invasion. However, TIMP-1 also possesses other functions such as inhibition of apoptosis, induction of malignant transformation and stimulation of cell-growth. We have previously demonstrated that TIMP-1 is elevated in blood from colorectal cancer patients and that high TIMP-1 levels predict poor prognosis. To clarify the role of TIMP-1 in colorectal tumorigenesis, the expression pattern of TIMP-1 in benign and malignant colorectal tumors was studied. In all of 24 cases of colorectal adenocarcinoma TIMP-1 mRNA was detected by in situ hybridization. In all cases TIMP-1 expression was found in fibroblast-like cells located at the invasive front but was seen only sporadically in normal mucosa. No TIMP-1 mRNA was seen in any of the cases in benign or malignant epithelial cells, in vascular cells or smooth muscle cells. Comparison of sections processed for TIMP-1 in situ hybridization with sections immunohistochemically stained with antibodies against TIMP-1 showed good correlation between TIMP-1 mRNA and immunoreactivity. Combining TIMP-1 in situ hybridization with immunohistochemical staining for alpha-smooth muscle actin or CD68 showed TIMP-1 mRNA in myofibroblasts but not in macrophages. TIMP-1 mRNA was detected in 2 of 7 adenomatous polyps in the adenoma area: in both cases associated with focal stromal inflammation at the epithelial-stromal interface. In conclusion, TIMP-1 expression is a rare event in benign human colon tissue but is highly expressed by myofibroblasts in association with invading colon cancer cells.

PMID: 15386409 [PubMed - indexed for MEDLINE]



Tissue plasminogen activator induced by dengue virus infection of human endothelial cells.

Huang YH, Lei HY, Liu HS, Lin YS, Chen SH, Liu CC, Yeh TM.

Department of Microbiology and Immunology, College of Medicine, National Cheng Kung University, Tainan, Taiwan, ROC.

Dengue hemorrhagic fever and dengue shock syndrome (DHF/DSS) are severe complications of dengue virus (DV) infection. However, the pathogenesis of hemorrhage induced by dengue virus infection is poorly understood. Since endothelial cells play a pivotal role in the regulation of hemostasis, we studied the effect of DV infection on the production of tissue plasminogen activator (tPA) and plasminogen activator inhibitor 1 (PAI-1) in vitro using both primary isolated endothelial cells; human umbilical cord veins cells, and a human microvascular endothelial cell line. DV infection significantly induced the secretion of tPA but not PAI-1 of human endothelial cells. In addition, tPA mRNA of endothelial cells was induced by DV as demonstrated by RT-PCR. Antibody against IL-6 but not control antibody inhibited DV-induced tPA production of endothelial cells. Furthermore, a good correlation between sera levels of IL-6 and tPA was found in DHF but not DF patients. These results suggest that IL-6 can regulate DV-induced tPA production of endothelial cells, which may play important roles in the pathogenic development of DHF/DSS. Copyright 2003 Wiley-Liss, Inc.

PMID: 12794725 [PubMed - indexed for MEDLINE]

Neu oncogene expression in ovarian tumors: a quantitative study.

Huettner PC, Carney WP, Naber SP, DeLellis RA, Membrino W, Wolfe HJ.

Department of Pathology, Tufts University School of Medicine, Massachusetts.

We studied neu mRNA expression by slot blot analysis and protein product expression by capture ELISA and immunohistochemistry in 57 primary and metastatic ovarian neoplasms, two paraovarian leiomyosarcomas, and eight normal ovaries. Some 61% of ovarian tumors but none of the paraovarian neoplasms or normal ovaries overexpressed neu mRNA. A total of 96% of the ovarian tumors that overexpressed neu were of epithelial type. Epithelial ovarian tumors had significantly higher amounts of the neu oncogene product as determined by capture ELISA than either germ cell and stromal tumors or normal ovaries (p less than 0.025). Different subtypes of ovarian carcinomas had significantly different amounts of neu oncogene product as measured by capture ELISA; endometrioid tumors had the highest, and poorly differentiated carcinomas not otherwise specified had the lowest (p less than 0.025). ELISA values, mRNA overexpression, and immunohistochemical staining intensity did not correlate with stage at diagnosis or architectural or nuclear grade in ovarian tumors. We conclude that capture ELISA is a simple, effective way to measure the neu oncogene protein product and that there is a good correlation between ELISA levels and immunohistochemical staining intensity. However, ELISA values did not correlate with stage or histologic prognostic factors in ovarian neoplasms.

PMID: 1353878 [PubMed - indexed for MEDLINE]

Elevation of topoisomerase I messenger RNA, protein, and catalytic activity in human tumors: demonstration of tumor-type specificity and implications for cancer chemotherapy.

Husain I, Mohler JL, Seigler HF, Besterman JM.

Department of Cell Biology, Glaxo Inc. Research Institute, Research Triangle Park, North Carolina 27709.

Topoisomerase I has been identified as an intracellular target of camptothecin, a plant alkaloid with anticancer activity. Various lines of evidence suggest that the sensitivity of cells to this drug is directly related to the topoisomerase I content. In humans, the levels of topoisomerase I have been shown to be elevated in colorectal tumors, compared to normal colon mucosa. The aim of our study was to determine whether (a) topoisomerase I levels are elevated in other solid tumors, (b) the elevated enzyme is catalytically active in these tumors, and (c) the increase in topoisomerase I levels in colorectal tumors is a result of increased transcription or translation. Topoisomerase I levels were quantitated in crude extracts from colorectal, prostate, and kidney tumors and their matched normal counterparts by Western blotting and by direct determination of catalytic activity, and mRNA levels were determined by Northern blotting. By Western blotting, colorectal tumors showed 5-35-fold increases in topoisomerase I levels, compared to their normal colon mucosa. In the case of prostate tumors, the increase was 2-10-fold, compared with benign hyperplastic prostate tissue from the same patients. However, no difference was observed in topoisomerase I levels in kidney tumors, compared to their normal counterparts. The catalytic activity of topoisomerase I was determined by a quantitative ³²P-transfer assay in crude homogenates, without isolating nuclei. Colorectal and prostate tumors exhibited 11-40- and 4-26-fold increases, respectively, in catalytic activity. However, kidney tumors did not show any alteration in catalytic activity, compared to their normal matched samples. Thus, for all three tumor types there was a good correlation between enzyme levels and catalytic activity. Finally, colorectal tumors were analyzed for steady state mRNA levels. A 2-33-fold increase in mRNA levels was found in colorectal tumors, compared to normal colon mucosa. These results suggest that alterations in topoisomerase I expression in humans are tumor type specific and that the increase in topoisomerase I levels results from either increased transcription of the topoisomerase I gene or increased mRNA stability.

PMID: 8275492 [PubMed - indexed for MEDLINE]

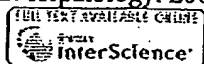
Developmental regulation of acidic fibroblast growth factor (aFGF) expression in bovine retina.

Jacquemin E, Jonet L, Oliver L, Bugra K, Laurent M, Courtois Y, Jeanny JC.

Unite de Recherches Gerontologiques, U. 118 INSERM, Paris, France.

Acidic fibroblast growth factor (aFGF) is a signalling molecule implicated in a wide variety of biological processes such as cell growth, differentiation and survival. It has been purified from bovine retina. The present study was carried out to detect which cells in the bovine retina expressed aFGF at the different stages of embryonic and post-natal development. The specific aFGF mRNA and protein were detected by in situ hybridization employing riboprobes and immunocytochemistry using affinity purified polyclonal human recombinant aFGF antibodies respectively. No signal was detected by either technique until 4-5 months and then there was progressive expression of aFGF with terminal morphogenesis of the retina. By 8-9 months of embryonic development, nuclei of the 3 neuronal layers (ganglion cell layer, inner and outer nuclear layers) were all uniformly and intensely labeled. A slight labeling of the pigmented epithelium of the retina was also visible throughout development and maturation. These results showed a good correlation between message and protein expression in these cell types. In contrast, glial cells in the nerve fiber layer and vascular endothelial cells displayed a nuclear immunostaining for the protein in the absence of message. These data suggest that aFGF plays a role in the late steps of retinal differentiation by autocrine and paracrine mechanisms.

PMID: 7507349 [PubMed - indexed for MEDLINE]



The p21(Cip1) protein, a cyclin inhibitor, regulates the levels and the intracellular localization of CDC25A in mice regenerating livers.

Jaime M, Pujol MJ, Serratos J, Pantoja C, Canela N, Casanovas O, Serrano M, Agell N, Bachs O.

Department of Cell Biology and Pathology, Faculty of Medicine, Institut d'Investigacions Biomediques August Pi Sunyer (IDIBAPS), University of Barcelona, Barcelona, Spain.

Liver cells from p21(Cip1^{-/-}) mice subjected to partial hepatectomy (PH) progress into DNA synthesis faster than those from wild-type mice. These cells also show a premature induction of cyclin E/cyclin-dependent kinase (CDK) 2 activity. We studied the mechanisms whereby cells lacking p21(Cip1) showed a premature induction of this activity. Whereas the levels of CDK2, cyclin E, and p27(Kip1) were similar in both wild-type and p21(Cip1^{-/-}) mice, those of the activator CDC25A were much higher in p21(Cip1^{-/-}) quiescent and regenerating livers than in wild-type animals. Moreover, p21(Cip1^{-/-}) cells also showed a premature translocation of CDC25A from cytoplasm into the nucleus. The ectopic expression of p21(Cip1) into mice embryo fibroblasts from p21(Cip1^{-/-}) mice decreased the levels of CDC25A and delayed its nuclear translocation. The levels of CDC25A messenger RNA in p21(Cip1^{-/-}) cells were higher than in wild-type cells, suggesting that this increase might be responsible, at least in part, for the high levels of CDC25A protein in these cells. Thus, the results reported here indicate that p21(Cip1) regulates the levels and the intracellular localization of CDC25A. We also found a good correlation between CDC25A nuclear translocation and cyclin E/CDK2 activation. In conclusion, premature translocation of CDC25A to the nucleus might be involved in the advanced induction of cyclin E/CDK2 activity and DNA replication in cells from animals lacking p21(Cip1).

PMID: 11981756 [PubMed - indexed for MEDLINE]



Alteration of frizzled expression in renal cell carcinoma.

Janssens N, Andries L, Janicot M, Perera T, Bakker A.

Department of Biochemistry, University of Antwerp, Wilrijk, Belgium.
njansse9@prdbe.jnj.com

To evaluate the involvement of frizzled receptors (Fzds) in oncogenesis, we investigated mRNA expression levels of several human Fzds in more than 30 different human tumor samples and their corresponding (matched) normal tissue samples, using real-time quantitative PCR. We observed that the mRNA level of Fzd5 was markedly increased in 8 of 11 renal carcinoma samples whilst Fzd8 mRNA was increased in 7 of 11 renal carcinoma samples. Western blot analysis of crude membrane fractions revealed that Fzd5 protein expression in the matched tumor/normal kidney samples correlated with the observed mRNA level. Wnt/beta-catenin signaling pathway activation was confirmed by the increased expression of a set of target genes. Using a kidney tumor tissue array, Fzd5 protein expression was investigated in a broader panel of kidney tumor samples. Fzd5 membrane staining was detected in 30% of clear cell carcinomas, and there was a strong correlation with nuclear cyclin D1 staining in the samples. Our data suggested that altered expression of certain members of the Fzd family, and their downstream targets, could provide alternative mechanisms leading to activation of the Wnt signaling pathway in renal carcinogenesis. Fzd family members may have a role as a biomarker.

PMID: 15557753 [PubMed - indexed for MEDLINE]

1. A3
054
v. 25
no. 4
2004
Jul-Aug

1010-4283

Received on: 01-23
Tumour biology: the journal
of the International Society
for Oncodevelopmental
Biology and Medicine.

2004 | 4 | 04

July-August 2004
(Released November 2004)
ISSN 1010-4283
25(4) 157-220 (2004)

The Journal of the International Society for
Oncodevelopmental Biology and Medicine

Tumor Biology

Tumor Markers, Tumor Targeting
and Translational Cancer Research

Research Articles

- 157 Tissue Microarray Analysis of Cyclin D1 Gene Amplification and Gain in Colorectal Carcinomas
Toncheva, D.; Peirova, D.; Tzenova, V.; Dimova, I.; Yankova, R.; Yordanov, V.; Damjanov, D.; Todorov, T.; Zaharieva, B. (Sofia)
- 161 Alteration of Frizzled Expression in Renal Cell Carcinoma
Janssens, N. (Wilrijk/Beerse); Andries, L. (Edegem); Janicot, M.; Perera, T.; Bakker, A. (Beerse)
- 172 Antisense and Dominant-Negative AKT2 cDNA Inhibits Glioma Cell Invasion
Pu, P.; Kang, C.; Li, J. (Tianjin); Jiang, H. (Detroit, Mich.)
- 179 Production and Characterization of a New Antibody Specific for the Mutant EGF Receptor, EGFRvIII, in *Camelus bactrianus*
Omjofar, K.; Rasate, M.J. (Tehran); Modjtahedi, H. (Guilford); Forouzandeh, M.; Taghikhani, M.; Bakhtiari, A.; Paknejad, M.; Kashanian, S. (Tehran)
- 188 Matrix Metalloproteinases 2 and 9 and Their Tissue Inhibitors in Low Malignant Potential Ovarian Tumors
Määttä, M.; Santala, M.; Soini, Y.; Talvensaari-Mattila, A.; Turpeenniemi-Hujanen, T. (Oulu)

- 193 Human Kallikrein 6 Degrades Extracellular Matrix Proteins and May Enhance the Metastatic Potential of Tumour Cells
Ghosh, M.C.; Grass, L.; Soosaipillai, A. (Toronto); Sotiropoulou, G. (Patras); Diamandis, E.P. (Toronto)

Mini Reviews

- 200 The TP53 Tumor Suppressor Gene and Melanoma Tumorigenesis: Is There a Relationship?
Hussein, M.R. (Assuit)
- 208 Strategies to Endow Cytotoxic T Lymphocytes or Natural Killer Cells with Antibody Activity against Carcinoembryonic Antigen
Kuroki, M.; Kuroki, M.; Shibaguchi, H.; Badran, A.; Hachimine, K.; Zhang, J.; Kinugasa, T. (Fukuoka)

Research Commentary

- 217 Up Close and Personal: Molecular Diagnostics in Oncology
Rye, P.D. (Oslo); Nilsson, O. (Göteborg); Rittenhouse, H. (San Diego, Calif.); Stigbrand, T. (Umeå)

S. Karger
Medical and Scientific
Publishers
Basel · Freiburg
Paris · London
New York · Bangalore
Bangkok · Singapore
Tokyo · Sydney

KARGER

Online

Access to full text and tables of contents,
including tentative ones for forthcoming issues:
www.karger.com/tbi_issues

Alteration of Frizzled Expression in Renal Cell Carcinoma

Nico Janssens^{a,c} Luc Andries^b Michel Janicot^c Tim Perera^c
Annette Bakker^c

^aDepartment of Biochemistry, University of Antwerp, Wilrijk, ^bHistoGeneX, Edegem, and ^cOncology Discovery Research, Johnson & Johnson Pharmaceutical Research and Development, Beerse, Belgium

Key Words

β -Catenin · Cyclin D1 · Frizzled receptor · Renal cell carcinoma · Wnt

Abstract

To evaluate the involvement of frizzled receptors (Fzds) in oncogenesis, we investigated mRNA expression levels of several human Fzds in more than 30 different human tumor samples and their corresponding (matched) normal tissue samples, using real-time quantitative PCR. We observed that the mRNA level of Fzd5 was markedly increased in 8 of 11 renal carcinoma samples whilst Fzd8 mRNA was increased in 7 of 11 renal carcinoma samples. Western blot analysis of crude membrane fractions revealed that Fzd5 protein expression in the matched tumor/normal kidney samples correlated with the observed mRNA level. Wnt/ β -catenin signaling pathway activation was confirmed by the increased expression of a set of target genes. Using a kidney tumor tissue array, Fzd5 protein expression was investigated in a broader panel of kidney tumor samples. Fzd5 membrane staining was detected in 30% of clear cell carcinomas, and there was a strong correlation with nuclear cyclin D1 staining in the samples. Our data suggested that altered expression of certain members of the

Fzd family, and their downstream targets, could provide alternative mechanisms leading to activation of the Wnt signaling pathway in renal carcinogenesis. Fzd family members may have a role as a biomarker.

Copyright © 2004 S. Karger AG, Basel

Introduction

The Wnt signaling pathway is evolutionary conserved and controls many events during embryonic development. Members of the Wnt gene family of secreted glycoproteins are involved in embryonic induction, generation of cell polarity, cell proliferation and the determination of cell fate [1, 2]. Recently, it has become evident that the Wnt pathway is also deregulated in a range of tumors [3].

The Wnt signaling pathway is activated when Wnt proteins bind to a cell surface receptor complex consisting of a member of the frizzled receptor (Fzd) family and either low-density-lipoprotein receptor-related protein (LRP5 or LRP6 [4, 5]. A detailed characterization of the Fzds and the immediate downstream events after Wnt binding has been hampered by the lack of pure biologically active Wnts.

Downstream of the receptor complex, three pathways may be initiated, depending on the composition of the

KARGER

Fax +41 61 306 12 34
E-Mail karger@karger.ch
www.karger.com

© 2004 S. Karger AG, Basel
1010-228X/04/0254-0161\$21.00/0

Accessible online at:
www.karger.com/tbi

Nico Janssens
Oncology Discovery Research, JNJPRD
Turnhoutseweg 30
BE-2340 Beerse (Belgium)
Tel. +32 14 603831, Fax +32 14 605403, E-Mail njansse9@prdbe.jnj.com

ligand and receptor complex. The 'Wnt/ β -catenin pathway', the 'Wnt/ Ca^{2+} pathway' or the 'Wnt polarity pathway' [6]. The Wnt/ β -catenin pathway has been linked to carcinogenesis. Genetic alterations in components of this pathway (adenomatous polyposis coli, APC, axin and β -catenin) can result in the accumulation of non-phosphorylated β -catenin [3, 7] and this can promote carcinogenesis. Conversely, neither the Wnt/ Ca^{2+} pathway nor the Wnt polarity pathway involves the activation of β -catenin [for review, see ref. 1, 6].

Mutations in one of the three regulatory genes (APC, β -catenin and axin), overexpression of Wnts and Fzds or the expression of a constitutively active Fzd have been linked to Wnt/ β -catenin pathway activation in various tumors [8, 9].

To evaluate the involvement of Fzds in oncogenesis, we investigated mRNA expression levels of several human Fzds (Fzd2, 3, 5, 6, 7, 8 and 9) in more than 30 different human tumor samples using real-time quantitative PCR. Each sample was compared with its corresponding (matched) normal tissue sample. The most striking observation was the dramatically increased Fzd5 and Fzd8 mRNA expression seen in the renal carcinoma samples. This was confirmed at the protein level using Western blotting. Kidney tumor tissue arrays confirmed Fzd5 membrane staining in 30% of clear cell carcinomas, with nuclear cyclin D1 showing a strong correlation with the Fzd5 membrane labeling. Fzd8 protein expression analysis was not performed due to the lack of suitable reagents. These data suggest that Fzd5 may have a role in renal cell carcinogenesis due to its frequent overexpression observed in these tumor samples. Potential future applications could include uses in tumor targeting or as a potential biomarker.

Materials and Methods

Tissue Samples

Frozen tumor tissue samples with corresponding normal tissue from the same patient were derived either from human biopsy or autopsy material (Department of Pathology, University of Antwerp, kindly provided by Prof. E. Van Marck). Tissue specimens were snap-frozen in liquid nitrogen and kept at -80°C until use. Frozen sections of kidney tumor and normal tissue samples were stained with hematoxylin-eosin to support the pathologist's observations and to confirm the type of kidney tumor. Paraffin-embedded tissue slides of renal carcinoma, lung carcinoma, breast and colon carcinoma were obtained, after encryption, from the Department of Pathology (Middelheim Hospital, Antwerp, Belgium). The CLI human kidney cancer (SuperBioChips Laboratories) tissue array used in this study contained 59 tissue samples consisting of 9 normal kidney tissues,

30 clear cell renal carcinoma samples and another 20 renal cell tumor types (chromophil, chromophobe, papillary type, collecting duct carcinoma and samples with mixed types).

RNA Isolation and Reverse Transcription

Total RNA was extracted from tissue specimens using Ultraspec Reagent (Biotecx, USA) according to the manufacturer's instructions. All total RNA was routinely treated with DNase (DNA-free kit, Ambion, USA). 1 μg of total RNA was used to synthesize cDNA using oligo-dT primers (Superscript; Invitrogen, Merelbeke, Belgium). Reverse transcription was performed at 42°C for 60 min, followed by 70°C for 10 min.

Real-Time PCR

Real-time PCR was performed on either an ABI Prism 7700 or 7900 Sequence detection system (Perkin-Elmer Applied Biosystems, Foster City, Calif., USA) using the 5' nuclease assay (TaqmanTM). Primer and probe sequences were designed using Primer Express (PE Applied Biosystems) and are shown in table I. Quantitative values were obtained from the threshold cycle number (Ct) at which the increase in the signal associated with exponential growth of PCR products is detected using PE Biosystems analysis software, according to the manufacturer's instructions.

We have used the $2^{-\Delta\Delta\text{Ct}}$ method to analyze the relative changes in gene expression of the different genes between tumor and corresponding normal tissue samples. We used the mitochondrial ATP synthase 6 (ATP6) as the endogenous RNA control [10; Janssens et al., in prep.], and each sample was normalized to its ATP6 content. The relative expression of the target gene was also normalized to the corresponding normal tissue sample (calibrator). Results, expressed as the amount of target sample relative to the ATP6 gene and the calibrator, were determined as follows, $N = 2^{-(\Delta\text{Ct}_{\text{sample}} - \Delta\text{Ct}_{\text{calibrator}})}$, where the ΔCt values of the sample and calibrator were determined by subtracting the average Ct value of the sample and the calibrator from the average Ct value of the ATP6 gene. Amplification was done essentially as described previously [10]. Briefly, 50 μl of reaction mixture containing 1 μl of cDNA template were amplified as follows: incubation at 50°C for 2 min, denaturation at 95°C for 10 min, and 50 cycles at 95°C for 15 s and 60°C for 1 min.

Membrane Preparation, Gel Electrophoresis and Immunoblotting

Tissue samples were weighed, suspended at a 40 times dilution [$= 40$ volumes/original wet weight of tissue (v/w)] in 50 mM Tris-HCl buffer, pH 7.4, and homogenized with an Ultra-Turrax homogenizer. After centrifugation for 10 min, 24,000 g at 4°C , the pellet was washed three times by resuspension in the Tris-HCl buffer followed by centrifugation. The final membrane pellets were stored at -80°C in the Tris-HCl buffer at a concentration of 0.5–1 mg/mL. The Bradford protein assay (Pierce, Aalst, Belgium) was used for protein determination. Proteins (50 μg) were separated by 8% SDS-PAGE and transferred to nitrocellulose membranes. After primary and secondary antibody incubation, the antigen-antibody-peroxidase complex was detected by chemiluminescence (Pierce, Aalst, Belgium) according to the manufacturer's instructions.

Immunohistochemistry

Immunohistochemistry was performed on 10- μm -thick cryosections of unfixed tumor tissue and on 6- μm -thick paraffin sections from renal tumor tissue fixed by formalin or by an alcohol-based fixative. Adjacent tissue blocks from renal tumors were processed with

Table 1. Real-time PCR primer and probe sequences

Target cDNA	Primer/probe sequences ^a	Fragment position ^b	Accession No. ^c
FZD2	(a) 5'-atcccggtcccgge-3' (b) 5'-gtattgatcatgtagcgtgaagtc-3' (c) 5'-FAM-tacacgcgcgcgtgctgc-TAMRA-3'	1,548-1,613	AB017364
FZD3	(a) 5'-tcacgccagtgcatggg-3' (b) 5'-ttgtcacccttcaatttattcctcg-3' (c) 5'-FAM-catcccggaacttaacatcatccctt-TAMRA-3'	1,473-1,547	AB039723
FZD5	(a) 5'-tgccaaggcacttccgtt-3' (b) 5'-tctccaagtcgcgcg-3' (c) 5'-FAM-cttcatgggtgctgtgcccc-TAMRA-3'	2,143-2,204	HSU43318
FZD6	(a) 5'-ctagcaccctcaggtaagagaa-3' (b) 5'-ccagagagctctggagatggat-3' (c) 5'-FAM-tgtgggaacgtgctcgcag-TAMRA-3'	2,094-2,170	AF072873
FZD7	(a) 5'-cctgtggaaaggcataactgtg-3' (b) 5'-aaccaacgggaaccctcaga-3' (c) 5'-FAM-aagcaactttataggcaagcagtgcaa-TAMRA-3'	2,687-2,762	AB017365
FZD8	(a) 5'-tggtgctgggtgctctgctt-3' (b) 5'-cgctccatgctgataaggaag-3' (c) 5'-FAM-ccaccttgcgcacgtctcca-TAMRA-3'	853-919	AB043703
FZD9	(a) 5'-ccccgggagctacggac-3' (b) 5'-tagctatgcaagaccacgg-3' (c) 5'-FAM-tggcagcactgccaataaggct-TAMRA-3'	1,696-1,763	HSU82169
ATP5b	(a) 5'-gggtagggtgctccttggtt-3' (b) 5'-gggcgcagtgattataggctt-3' (c) 5'-FAM-aagtggttagggcattttatcttagagcg-TAMRA-3'	580-503	AF368271
c-myc	(a) 5'-accaccgacgacgactcga-3' (b) 5'-tccagcagaaggtagccagact-3' (c) 5'-FAM-accctttgcccaggacgtgctct-TAMRA-3'	1,297-1,413	HSMYCI
Cyclin D1	(a) 5'-gaacctgcccgaatgac-3' (b) 5'-cgctctggcaatttggga-3' (c) 5'-FAM-cgcacgaattcattgaacatt-TAMRA-3'	4,148-4,211	AF511593
PPAR δ	(a) 5'-agcatcttcacggcaaa-3' (b) 5'-gtctgatgctgtggaicaca-3' (c) 5'-FAM-ccagccacacggccct-TAMRA-3'	932-990	NM-006238

^a (a) = Sense primer; (b) = antisense primer; (c) = probe.
^b Fragment positions are given according to the EMBL/GenBank accession No. of cloned sequence.
^c EMBL/GenBank accession No. of cloned sequence.

formalin and with the alcohol-based fixative. Paraffin and cryosections were mounted on poly-L-lysine or 3-aminopropyltriethoxysilane-gelatin-coated slides. The 59 tissue samples on the CL1 human renal cancer tissue array slides were all fixed with formalin and embedded in paraffin, and the sections were mounted on silane-coated slides (SuperBioChips Laboratories). In addition to renal carcinoma tissue, sections from 10 formalin-fixed paraffin-embedded lung carcinomas were stained for Fzd5. Colon and breast tumors

were used as positive controls for β -catenin and cyclin D1 immunostaining.

The following primary antibodies were used: Fzd5 (Upstate Biotechnology), β -catenin (Zymed), cyclin D1 (Zymed), E-cadherin (Novocastra) and cytokeratin 8 (Biogenex). Cryosections were fixed in 4% paraformaldehyde for 5 min; acetone for 5 min at -20°C and 70% ethanol for 5 min. Endogenous peroxidase activity was quenched using 3% H_2O_2 . Paraffin sections of formalin- and alcohol-

Table 2. Fzd mRNA expression in tumor samples

Sample ^a	Tissue	Tumor type	x-fold expression increase ^b						
			FZD2	FZD3	FZD5	FZD6	FZD7	FZD8	FZD9
133702	kidney	adenocarcinoma	0.17	0.5	3.72	2.13	0.06	1.32	-
137770	kidney	renal cell carcinoma	1.23	3.56	8.26	2.61	1.3	8.21	5.44
138844	kidney	renal cell carcinoma	0.31	0.11	6.84	1.18	0.23	3.18	2.8
137146	kidney	renal cell carcinoma	0.47	0.45	3.16	2.23	0.73	4.42	1.37
137564	kidney	renal cell carcinoma	3.43	2.95	9.6	1.57	7.64	3.52	-
133408	kidney	renal cell carcinoma	23.97	0.98	6.39	2.48	5.05	16.72	-
139188	kidney	renal cell carcinoma	3.7	0.56	0.66	1.33	0.37	4.41	1.53
135699	kidney	renal cell carcinoma	2.6	0.36	4.83	0.9	0.34	2.54	2.31
139064	kidney	renal cell carcinoma	5.16	1.82	1.25	2.36	1.8	2.19	2.85
134585	kidney	renal cell carcinoma	1.47	0.72	1.38	0.47	0.09	0.6	-
140279	kidney	renal cell carcinoma	7.33	18.17	3.93	6.05	6.41	4.65	7.91
137252	ovary	carcinosarcoma	0.4	3.39	0.49	0.44	0.92	0.54	0.53
138256	ovary	papillary carcinoma	0.7	5.17	1.22	2.19	0.4	0.11	-
146472	ovary	serous papillary carcinoma	0.39	3.29	2.56	1.34	3.94	0.67	0.59
145845	colon	adenocarcinoma	3.45	3.36	0.58	1.22	1.67	1.24	1.99
146145	colon	adenocarcinoma	5.46	6.74	4.42	6.57	3.36	6.08	0.15
146630	colon	adenocarcinoma	4.01	4.73	0.3	1.16	0.54	0.55	0.12
146633	colon	adenocarcinoma	1.87	1.07	1.62	1.47	0.51	2.07	-
147055	colon	adenocarcinoma	0.66	1.41	1.01	1.33	0.24	0.79	4.87
142253	lung	adenocarcinoma	0.67	5.17	0.43	1.87	0.33	0.59	0.41
143036	lung	adenocarcinoma	0.67	1.24	2.63	1.13	1.11	1.04	9.19
138938	lung	adenocarcinoma	0.93	0.88	1.07	1.3	1.73	0.38	0.76
133563	lung	adenocarcinoma	2.76	1.23	0.31	1.34	0.99	0.78	4.97
144387	lung	adenocarcinoma	12.85	0.43	0.49	0.25	2.73	0.54	-
137304	lung	acinary adenocarcinoma	0.54	9.15	1.65	1.25	0.63	3.41	2.64
144546	lung	epithelial carcinoma	0.1	0.67	0.21	8.11	0.27	0.97	1.32
137621	lung	epithelial carcinoma	1.52	2.19	0.37	2.26	0.52	0.45	1.06
145552	lung	epithelial carcinoma	1.09	-	0.16	0.91	1.47	0.13	0.5
143987	testis	embryonal carcinoma	0.24	0.6	19.43	1.33	23.12	2.43	0.33
137332	stomach	leiomyoma	19.32	3.91	0.45	1.53	18.98	32.82	16.7
139026	stroma	gastrointestinal carcinoma	66.1	3.51	0.03	6.67	8.44	2.28	20.82
136049	rectum	adenocarcinoma	1.71	0.52	0.4	0.54	0.29	0.88	0.28
140794	gall bladder	adenosquamous carcinoma	0.19	-	0.93	3.02	0.2	-	-

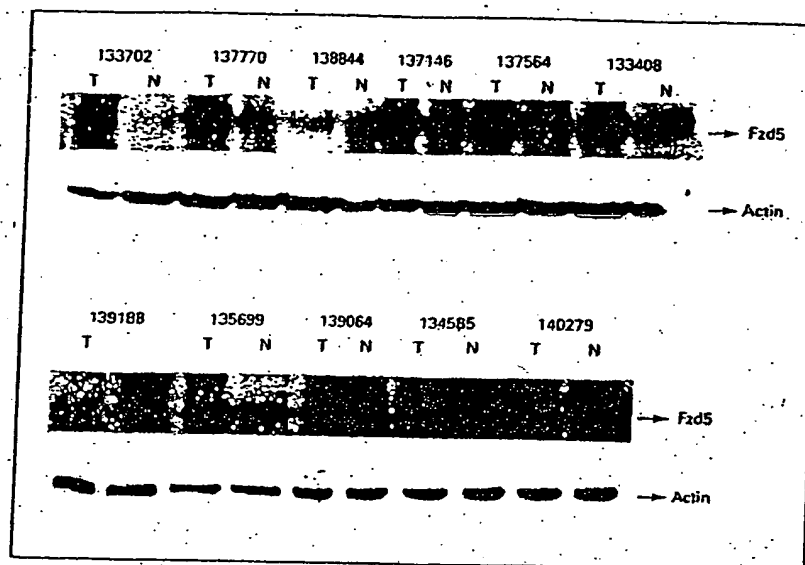
^a Sample identification numbers were given by the pathologist.

^b Results are expressed as x-fold increase of the gene in the tumor tissue sample compared to its matched normal tissue sample after normalizing both samples on the basis of their ATP5b content. A cutoff of 3-fold was used to define differential expression. Significant (> 3-fold) increases in the expression level of the Fzd receptor are shown in italics. - = Expression of the target gene undetectable in one or both samples (tumor and/or normal).

fixed tissue were processed with a trypsin-citrate-microwave pretreatment or with an EDTA-microwave pretreatment to unmask epitopes, respectively. Sections were then sequentially processed with primary antibodies, biotinylated secondary antibodies and streptavidin-biotin-peroxidase (Fzd5, E-cadherin and cytokeratin 8). For β -catenin, polyclonal rabbit antibody with the EnVision detection system (DAKO) was used. The slides were further developed using 3-amino-9-ethylcarbazole, counterstained with hemalaun and mount-

ed with glycerin gelatin. Stained sections were observed with an Axioplan 2 microscope equipped with an Axiocam digital camera. Staining intensity for β -catenin was scored as no staining (value 0), weak and fragmentary staining of cell membranes (value 1), moderate membrane staining of less than 50% of the tumor cells (value 2), moderate membrane staining of more than 50% of tumor cells (value 3) and strong membrane staining of more than 75% of tumor cells (value 4). The cyclin D1 staining was quantified as a percentage of

Fig. 1. Fzd5 protein expression in matched tumor/normal kidney samples. T = Tumor sample; N = matched normal sample. Sample identification numbers are given by the pathologist.



cyclin D1-immunoreactive nuclei in tumor cells in three fields (area: 18,641 μm^2) of each tumor sample. The total number of tumor nuclei ranged from 51 to 164. The correlation between Fzd5 and β -catenin staining, and between Fzd5 and cyclin D1 staining was evaluated by the Mann-Whitney U test.

Results

Fzd mRNA Expression in Matched Human Tumor/Normal Tissue Samples

Fzd expression in tumor tissue was compared with Fzd expression in matched normal tissue samples and normalized to the expression of the housekeeping gene mitochondrial ATP5b (table 2). A 3-fold increase was considered significant.

In the kidney tumor samples, in which 10 of 11 samples were clear cell carcinomas, Fzd5 was upregulated in 8 of the 11 samples. A similar observation was made for Fzd8 and Fzd2, which were upregulated in 7 and 5 renal tumor samples, respectively. None of the other Fzds showed consistent upregulation.

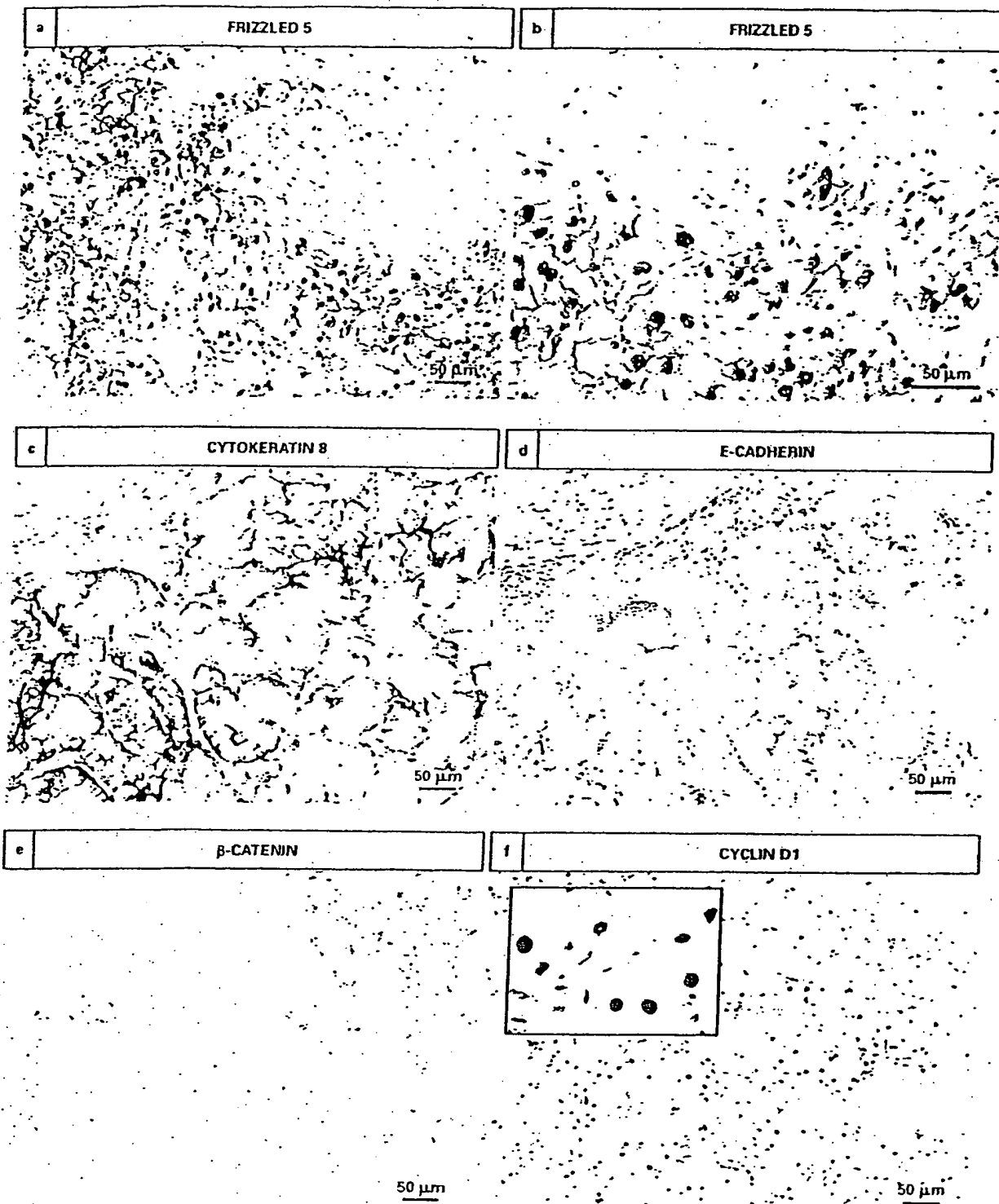
Both Fzd2 and Fzd3 were upregulated in 3 of 5 colon adenocarcinoma samples. No other Fzd expression was significantly different compared to the normal colon tissue sample. Fzd3 showed an increased expression in all 3 ovarian carcinoma samples. Fzd expression was not altered in any of the lung tumor samples. The Fzd expres-

sion level was observed to be relatively low in these lung tissues compared to the other tissues investigated.

Western Blot and Immunohistochemistry Analysis on Renal Carcinomas

Western blotting was used to evaluate Fzd5 protein expression in the renal tissue samples used for mRNA expression analysis. Membrane fractions of the renal carcinoma and corresponding normal tissue samples were prepared. As previously shown (table 2), Fzd5 mRNA upregulation was detected in 8 of the 11 matched tumor/normal samples. Increased expression of Fzd5 protein was seen in membrane fractions from 9 of 11 samples (fig. 1). In most cases, concomitant increases in Fzd5 mRNA and protein levels were observed.

Hematoxylin-eosin staining of the cryosectioned tumors confirmed the presence of clear cell carcinoma. Fzd5 immunostaining in clear cell carcinoma (fig. 2a, b) was observed to be localized to cell membranes and to nuclei. Cytokeratin 8 (fig. 2c) and E-cadherin (fig. 2d) were also detected. E-cadherin labeling of cell membranes in clear cell carcinoma was less intense and patchy compared to epithelial cells of normal renal tissue. β -Catenin staining was confined to the cell membrane. β -Catenin levels in the clear cell carcinoma membranes were highly variable. Nuclear β -catenin staining was not observed in any of the samples. Epithelial cells in normal renal tissue showed intense membrane staining and some cytoplasmic



staining. In addition, weak β -catenin staining of endothelial cells was observed. A high number of cyclin D1-immunoreactive nuclei was observed in clear cell carcinoma (fig. 2f).

On the CL1 human kidney cancer tissue array, 30% ($n = 9$) of the clear cell carcinoma tumor samples ($n = 30$) showed Fzd5 immunoreactivity (fig. 3a). Membrane-associated β -catenin staining was observed in 33% of the Fzd5-positive tumor samples and 57% of Fzd5-negative clear renal cell carcinoma samples (table 3; fig. 3c, d). Again, nuclear β -catenin staining was never observed. Statistical analysis did not reveal a difference in the expression of β -catenin between Fzd5-positive and Fzd5-negative tumor samples (fig. 4a).

Nuclear cyclin D1 was observed in 89% of the Fzd5-positive clear cell carcinoma samples (table 3; fig. 3e). Only 38% of the Fzd5-negative clear cell carcinoma samples contained nuclear cyclin D1. Statistical analysis showed a significantly higher cyclin D1 expression in Fzd5-positive compared to Fzd5-negative tumor samples (fig. 4b).

c-myc, Cyclin D1 and Peroxisome

Proliferator-Activated Receptor δ Expression in Renal Carcinomas

Wnt/ β -catenin pathway activation in the kidney tissue samples was investigated looking at the expression of a number of target genes, which have previously been shown to be upregulated when the pathway is active. Gene expression of *c-myc*, cyclin D1 and peroxisome proliferator-activated receptor δ (PPAR δ) was analyzed. Increased expression of both *c-myc* and cyclin D1 genes have been implicated in cell proliferation, and carcinogenesis, and they represent two of the more important and closely studied target genes of the Wnt signaling pathway.

Expression of PPAR δ was investigated because it represents a direct target of the β -catenin pathway with T cell factor binding sites in its promoter. Expression of *c-myc* was found to be upregulated in 7 of 11, whilst cyclin D1 was upregulated in 10 of 11 kidney tumor samples (table 4). PPAR δ was upregulated in 9 cases. All three selected target genes showed a marked upregulation in the majority of renal tumors, which suggested that the Wnt/ β -catenin pathway was activated in these samples.

Discussion

Fzd family member overexpression has been postulated to play key roles in different tumor types such as esophageal carcinoma [11], gastric cancer [12] and head and neck squamous cell carcinoma [13]. The current study evaluated the potential implication of Fzds as tumor-associated antigens in different tumor types. We screened a number of matched normal/tumor tissue samples for the expression of a variety of Fzds using real-time quantitative PCR.

Results obtained revealed that both Fzd5 and Fzd8 mRNA were overexpressed in the majority of renal carcinoma samples when compared to the matched normal kidney samples. Fzd2 and Fzd3 were upregulated in 3 of 5 colon adenocarcinoma samples. Fzd3 was also upregulated in the ovarian tumor tissue samples compared to the matched normal tissue samples. None of the other Fzds evaluated showed a specific differential expression pattern in any of the samples studied. Fzd5 and Fzd8 show 69.1% similarity and belong to the same subgroup of Fzds [14]. The significantly higher expression of Fzd5 and Fzd8 in the renal tumor samples, as compared to the normal renal samples, suggests a higher probability that this subgroup may be implicated in the progression of renal cancer. Therefore, we decided to further examine the possible role of Fzd5 in renal carcinoma.

We observed, using Western blotting, that protein levels were mostly consistent with mRNA levels in the tumor samples. In order to be able to determine the Fzd5 expression in a broader range of kidney tissues, we utilized a tissue array. Fzd5 membrane staining was detected in 9 of 30 (30%) clear cell carcinomas, and importantly, membrane staining was not detected in the matched 9 normal kidney tissue samples.

Since the Wnt signaling pathway appears to play an important role in embryonic development, in particular embryonic kidney induction [15, 16], activation of this pathway in the adult kidney due to mutation or overex-

Fig. 2. Distribution of Fzd5 (a, b), cytokeratin 8 (c), E-cadherin (d) and β -catenin (e) immunoreactivity in paraffin sections from a renal tumor processed by an alcohol fixative. From the same tumor, a formalin-fixed block was used for cyclin D1 immunostaining (f). Fzd5 immunostaining shows distinct immunoreactivity in cell membranes and in nuclei of clear cell renal carcinoma. Clear cells are immunoreactive for cytokeratin 8. β -Catenin and E-cadherin staining of membranes is rather weak, and not uniform, in clear cell renal carcinoma. Nuclear β -catenin immunoreactivity was not observed. In clear cell renal carcinoma, many nuclei showed cyclin D1 immunoreactivity. The inset in f shows a detailed view of the cyclin D1 labeling of nuclei in clear cell renal carcinoma.

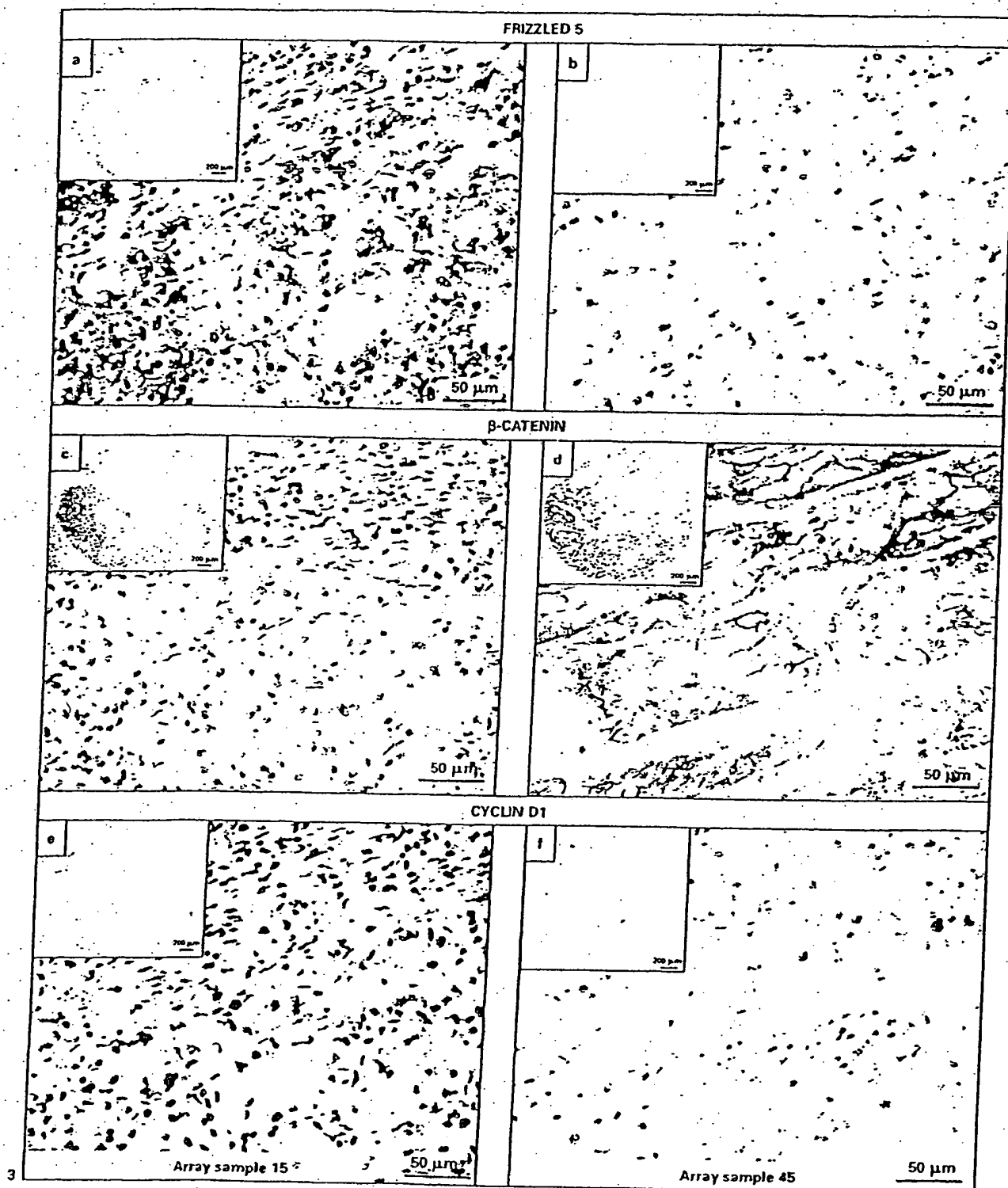


Table 3. Correlation between Fzd5 and β -catenin or cyclin D1 expression

	Fzd5, %	
	+	-
β -Catenin +	33	57
β -Catenin -	67	43
Cyclin D1 +	89	38
Cyclin D1 -	11	62

pression of one of the components of the pathway could be a determining factor in the development of renal cancers. Therefore, several studies have looked into the possible function the Wnt/ β -catenin pathway plays in renal carcinogenesis. APC gene mutations have been demonstrated not to be involved in renal carcinoma [17, 18]. In addition, β -catenin mutations are rare events in renal carcinoma [19, 20]. Nevertheless, cytoplasmic accumulation of β -catenin has been reported in a number of renal cell carcinomas [19], and thus the Wnt signaling pathway.

Table 4. Wnt/ β -catenin target gene mRNA expression in tumor samples

Sample ^a	Tissue	Tumor type	x-fold expression increase ^b		
			c-myc	cyclin D1	PPAR δ
133702	kidney	adenocarcinoma	0.54	4.52	0.52
137770	kidney	renal cell carcinoma	<i>13.9</i>	<i>28.91</i>	<i>5.53</i>
138844	kidney	renal cell carcinoma	2.39	<i>31.49</i>	<i>7.48</i>
137146	kidney	renal cell carcinoma	7.62	<i>15.38</i>	<i>3.15</i>
137564	kidney	renal cell carcinoma	<i>33.82</i>	<i>19.65</i>	<i>8.65</i>
133408	kidney	renal cell carcinoma	7.8	<i>8.92</i>	<i>4.86</i>
139188	kidney	renal cell carcinoma	2.22	<i>9.92</i>	<i>11.67</i>
135699	kidney	renal cell carcinoma	<i>12.18</i>	<i>22.73</i>	<i>5.53</i>
139064	kidney	renal cell carcinoma	<i>22.11</i>	<i>5.04</i>	<i>6.33</i>
134585	kidney	renal cell carcinoma	1.79	1.14	1.67
140279	kidney	renal cell carcinoma	<i>61.68</i>	<i>54.95</i>	<i>14.62</i>

^a Sample identification numbers were given by the pathologist.

^b Results are expressed as x-fold increase of the gene in the tumor tissue sample compared to its matched normal tissue sample after normalizing both samples on the basis of their ATP5b content. A cutoff of 3-fold was used to define differential expression. Significant (>3-fold) increases in the expression level of the Fzd receptors are in italics.

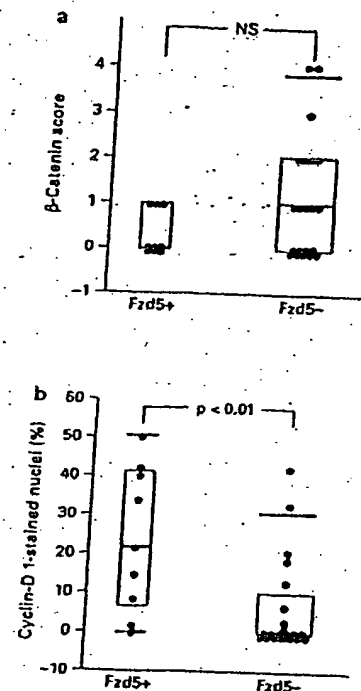


Fig. 3. Fzd5, β -catenin and cyclin D1 immunostaining of the CL1 renal carcinoma tissue arrays. The left column of images represents serial sections from tumor sample 15. Insets show an overview of each tumor section on the serial tissue arrays. The Fzd5-immunoreactive clear cell renal carcinoma (a) of this tumor sample does not express β -catenin (c). Immunostaining for cyclin D1 (e) detects distinct labeling of nuclei in clear cell renal carcinoma. The right column of images is taken from serial sections of tumor sample 45. Clear cell renal carcinoma from this tumor sample does not express Fzd5 (b) and cyclin D1 (f) but does show distinct membrane β -catenin staining (d).

Fig. 4. Box plot charts (thick black line = median) illustrating the relationship between Fzd5 immunostaining and β -catenin (a) and cyclin D1 (b) expression in clear cell renal carcinoma. No significant correlation was observed between the β -catenin scores of Fzd5-positive and -negative clear cell renal carcinoma. Nuclear cyclin D1 staining in clear cell renal carcinoma showed a significant difference between Fzd5-positive and Fzd5-negative tumor samples.

might act as an inducer of tumorigenesis in the kidney. This view is supported by the observation that aberrant activity of the Wnt signaling pathway has been reported in renal-cancer-derived cell lines. Zang et al. [21] observed a higher expression level of Wnt5a and Fzd5 mRNA in the renal cancer cell line GRC-1 than in the normal renal cell line HK-2. Expression of β -catenin was also higher in GRC-1 than in HK-2.

To determine the status of the canonical Wnt signaling pathway in our renal carcinoma samples, we have quantitated the mRNA levels of three important target genes of T cell factor/lymphoid enhancer factor activation by β -catenin. The mRNA levels of these three target genes (c-myc, cyclin D1 and PPAR δ) correlated largely with the expression of Fzd5 in these samples, suggesting that the canonical pathway is activated. On the kidney tissue array, cyclin D1 protein expression showed a highly significant correlation with the Fzd5 expression in the tumor samples (table 3). Cyclin D1 protein is frequently overexpressed in various tumors, but in only a proportion of the cases is it due to amplification of the cyclin D1 gene [22]. Therefore, other mechanisms such as upregulation of gene transcription may play a substantial role in the overexpression of cyclin D1 [23–26]. Our data, showing increased cyclin D1 expression in renal carcinoma samples, are consistent with the results of Stassar et al. [27]. They studied genes that are associated with human renal carcinoma by suppression subtractive hybridization and reported 14 differentially expressed genes, including cyclin D1. Although we would have expected an increased nuclear β -catenin staining, nuclear accumulation of β -cate-

nin was not observed in any of the tumors or on the tissue array. This result is consistent with the data presented for renal cell carcinomas by Kim et al. [19]. They did not detect nuclear β -catenin staining in the 52 renal cell carcinomas examined. The lack of nuclear β -catenin staining has also been reported by others in tumors that might have arisen from Wnt/ β -catenin pathway activation [28–31].

While expression of both Wnt5a and Fzd5 does induce duplication of the *Xenopus* head, exogenous expression of Fzd5 in a *Xenopus* model does not induce duplication of the head [32]. Fzd5 does not activate the β -catenin signaling pathway on its own, as the presence of its endogenous ligand is also required. Our results suggest that Fzd5 may have a role in renal cell carcinogenesis due to its frequent overexpression observed in these tumor samples, and we hypothesize that if Fzd5 is overexpressed, it has a rather limited effect on β -catenin signaling. However, in the presence of its endogenous still unknown ligand, it activates the canonical Wnt signaling pathway. The elucidation of this ligand and its binding characteristics is still under investigation. Ultimately, knowledge of the specific expression patterns of both Wnt and Fzd members could lead to directed tumor targeting or could be used as a tumor marker.

Acknowledgment

We are grateful to Prof E. Van Marck (University of Antwerp) for providing us with the tissue samples.

References

- 1 Pandur P, Maurus D, Kuhl M: Increasingly complex: New players enter the Wnt signaling network. *Bioessays* 2002;24:881–884.
- 2 Dale TC: Signal transduction by the Wnt family of ligands. *Biochem J* 1998;329:209–223.
- 3 Oving JM, Clevers HC: Molecular causes of colon cancer. *Eur J Clin Invest* 2002;32:448–457.
- 4 Pinson KI, Brennan J, Monkley S, Avery BJ, Skarnes WC: An LDL-receptor-related protein mediates Wnt signalling in mice. *Nature* 2000;407:535–538.
- 5 Tamai K, Semenov M, Kato Y, Spokony R, Liu CM, Katsuyama Y, Hess F, Saint-Jeannet JP, He X: LDL-receptor-related proteins in Wnt signal transduction. *Nature* 2000;407:530–535.
- 6 Miller JR: The Wnts. *Genome Biol* 2002, vol 3.
- 7 Satoh S, Daigo Y, Furukawa Y, Kato T, Miwa N, Nishiwaki T, Kawasoe T, Ishiguro H, Fujita M, Tokino T, Sasaki Y, Imaoka S, Murata M, Shimano T, Yamaoka Y, Nakamura Y: AXIN1 mutations in hepatocellular carcinomas, and growth suppression in cancer cells by virus-mediated transfer of AXIN1. *Nat Genet* 2000;24:245–250.
- 8 Vider BZ, Zimmer A, Chastre E, Prevot S, Gespach C, Estlein D, Wolloch Y, Tronick SR, Gazit A, Yaniv A: Evidence for the involvement of the Wnt 2 gene in human colorectal cancer. *Oncogene* 1996;12:153–158.
- 9 Iozzo RV, Eichstetter I, Danielson KG: Aberrant expression of the growth factor Wnt-5A in human malignancy. *Cancer Res* 1995;55:3495–3499.
- 10 Gerard CJ, Andrejka LM, Macina RA: Mitochondrial ATP synthase 6 as an endogenous control in the quantitative RT-PCR analysis of clinical cancer samples. *Mol Diagn* 2000;5:39–46.
- 11 Tanaka S, Akiyoshi T, Mori M, Wands JR, Sugimachi K: A novel frizzled gene identified in human esophageal carcinoma mediates APC/beta-catenin signals. *Proc Natl Acad Sci USA* 1998;95:10164–10169.
- 12 To KF, Chan MW, Leung WK, Yu J, Tong JH, Lee TL, Chan FK, Sung JJ: Alterations of frizzled (FzE3) and secreted frizzled related protein (hsFRP) expression in gastric cancer. *Life Sci* 2001;70:483–489.
- 13 Rhee CS, Sen M, Lu D, Wu C, Leoni L, Rubin J, Corr M, Carson DA: Wnt and frizzled receptors as potential targets for immunotherapy in head and neck squamous cell carcinomas. *Oncogene* 2002;21:6598–6605.

- 14 Saitoh T, Hirai M, Katoh M: Molecular cloning and characterization of human frizzled-8 gene on chromosome 10p11.2. *Int J Oncol* 2001;18: 991-996.
- 15 Dressler GR: Tubulogenesis in the developing mammalian kidney. *Trends Cell Biol* 2003;12: 390-395.
- 16 Vainio SJ, Itaranta PV, Perasaari JP, Uusitalo MS: Wnts as kidney tubule inducing factors. *Int J Dev Biol* 1999;43:419-423.
- 17 Bohm M, Wieland I, Stinboer C, Otto T, Rubben H: Detection of loss of heterozygosity in the APC tumor suppressor gene in nonpapillary renal cell carcinoma by microdissection and polymerase chain reaction. *Urol Res* 1997;25: 161-165.
- 18 Suzuki H, Ueda T, Komiya A, Okano T, Isaka S, Shimazaki J, Ito H: Mutational state of von Hippel-Lindau and adenomatous polyposis coli genes in renal tumors. *Oncology* 1997;54: 252-257.
- 19 Kim YS, Kang YK, Kim JB, Han SA, Kim KJ, Paik SR: Beta-catenin expression and mutational analysis in renal cell carcinomas. *Pathol Int* 2000;50:725-730.
- 20 Ueda M, Gemmill RM, West J, Winn R, Sugita M, Tanaka N, Ueki M, Drabkin HA: Mutations of the β - and γ -catenin genes are uncommon in human lung, breast, kidney, cervical and ovarian carcinomas. *Br J Cancer* 2001;85: 64-68.
- 21 Zang T, Zhuang L, Zhang Z, Xia D, Guo Y: Aberrant activity of WNT/frizzled signaling pathway in renal cancer cell lines. *Chin Sci Bull* 2000;45:1703-1707.
- 22 Ozturk M: Genetic aspects of hepatocellular carcinogenesis. *Semin Liver Dis* 1999;19:235-242.
- 23 Aktas H, Cai H, Cooper GM: Ras links growth factor signaling to the cell cycle machinery via regulation of cyclin D1 and the Cdk inhibitor p27KIP1. *Mol Cell Biol* 1997;17:3850-3857.
- 24 Weber JD, Raben DM, Phillips PJ, Baldassare JJ: Sustained activation of extracellular-signal-regulated kinase 1 (ERK1) is required for the continued expression of cyclin D1 in G1 phase. *Biochem J* 1997;326:61-68.
- 25 Lavoie JN, L'Allemain G, Brunet A, Muller R, Pouyssegur J: Cyclin D1 expression is regulated positively by the p42/p44MAPK and negatively by the p38/HOGMAPK pathway. *J Biol Chem* 1996;271:20608-20616.
- 26 Treinies I, Paterson HF, Hooper S, Wilson R, Marshall CJ: Activated MEK stimulates expression of AP-1 components independently of phosphatidylinositol 3-kinase (PI3-kinase) but requires a PI3-kinase signal to stimulate DNA synthesis. *Mol Cell Biol* 1999;19:321-329.
- 27 Stassar MJ, Devitt G, Brosius M, Rinnab L, Prang J, Schradin T, Simon J, Petersen S, Kopp-Schneider A, Zoller M: Identification of human renal cell carcinoma associated genes by suppression subtractive hybridization. *Br J Cancer* 2001;85:1372-1382.
- 28 Wong SC, Lo SF, Lee KC, Yam JW, Chan JK, Wendy Hsiao WL: Expression of frizzled-related protein and Wnt-signalling molecules in invasive human breast tumours. *J Pathol* 2002; 196:145-153.
- 29 Ueta T, Ikeguchi M, Hirooka Y, Kaibara N, Terada T: Beta-catenin and cyclin D1 expression in human hepatocellular carcinoma. *Oncol Rep* 2002;9:1197-1203.
- 30 Tanaka Y, Kato K, Notohara K, Nakatani Y, Miyake T, Ijiri R, Nishimata S, Ishida Y, Kigasawa H, Ohama Y, Tsukayama C, Kobayashi Y, Horie H: Significance of aberrant (cytoplasmic/nuclear) expression of beta-catenin in pancreaticoblastoma. *J Pathol* 2003;199: 185-190.
- 31 Qiao Q, Ramadani M, Gansauge S, Gansauge F, Leder G, Beger HG: Reduced membranous and ectopic cytoplasmic expression of beta-catenin correlate with cyclin D1 overexpression and poor prognosis in pancreatic cancer. *Int J Cancer* 2001;95:194-197.
- 32 He X, Saint-Jeannet JP, Wang Y, Nathans J, Dawid I, Varmus H: A member of the frizzled protein family mediating axis induction by Wnt-5A. *Science* 1997;275:1652-1654.

Multidrug resistance phosphoglycoprotein (ABCB1) in the mouse placenta: fetal protection.

Kalabis GM, Kostaki A, Andrews MH, Petropoulos S, Gibb W, Matthews SG.

Department of Physiology, University of Toronto, Ontario, Canada.

The multidrug resistance phosphoglycoprotein ATP-binding cassette subfamily B (ABCB1) actively extrudes a range of structurally and functionally diverse xenobiotics as well as glucocorticoids. ABCB1 is present in many cancer cell types as well as in normal tissues. Although it has been localized within the mouse placenta, virtually nothing is known about its regulation. In the mouse, two genes, *Abcb1a* and *Abcb1b*, encode ABCB1. We hypothesized that there are changes in placental *Abcb1a* and *Abcb1b* gene expression and ABCB1 protein levels during pregnancy. Using in situ hybridization, we demonstrated that *Abcb1b* mRNA is the predominant placental isoform and that there are profound gestational changes in the expression of both *Abcb1a* and *Abcb1b* mRNA. Placentas from pregnant mice were analyzed between Embryonic Days (E) 9.5 and 19 (term approximately 19.5d). *Abcb1b* mRNA was detected in invading trophoblast cells by E9.5, peaked within the placental labyrinth at E12.5, and then progressively decreased toward term ($P < 0.0001$). *Abcb1a* mRNA, although lower than that of *Abcb1b* at midgestation, paralleled changes in *Abcb1b* mRNA. Changes in *Abcb1* mRNA were reflected by a significant decrease in ABCB1 protein ($P < 0.05$). A strong correlation existed between placental *Abcb1b* mRNA and maternal progesterone concentrations, indicating a potential role of progesterone in regulation of placental *Abcb1b* mRNA. In conclusion, there are dramatic decreases in *Abcb1a* and *Abcb1b* mRNA and in ABCB1 at the maternal-fetal interface over the second half of gestation, suggesting that the fetus may become increasingly susceptible to the influences of xenobiotics and natural steroids in the maternal circulation.

PMID: 15917342 [PubMed - in process]

Expression of human telomerase reverse transcriptase gene and protein, and of estrogen and progesterone receptors, in breast tumors: Preliminary data from neo-adjuvant chemotherapy.

Kamori M, Izumiyama N, Hashimoto M, Nakamura K, Okano T, Kurabayashi R, Naoki H, Honma N, Ogawa T, Kaminishi M, Takubo K.

Division of Breast and Endocrine Surgery, Department of Surgery, Graduate School of Medicine, The University of Tokyo, Bunkyo-ku, Tokyo 113-8655, Japan. kamori-dis@umin.ac.jp.

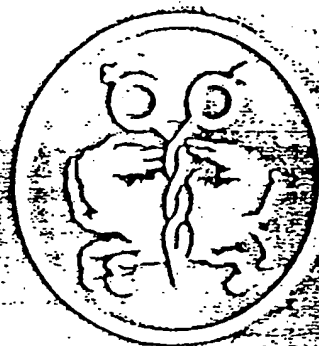
Human telomerase reverse transcriptase (hTERT), the catalytic subunit of telomerase, is very closely associated with telomerase activity. Telomerase has been implicated in cellular immortalization and carcinogenesis. In situ detection of hTERT will aid in determining the localization of telomerase-positive cells. The aim of this study was to detect expression of hTERT mRNA, hTERT protein, estrogen receptor (ER) and progesterone receptor (PR) in paraffin-embedded breast tissue samples and to investigate the relationship between hTERT expression and various clinicopathological parameters in breast tumorigenesis. We used in situ hybridization (ISH) to examine hTERT gene expression, and immunohistochemistry (IHC) to examine expression of hTERT protein, ER and PR, in breast tissues including 64 adenocarcinomas, 2 phyllode tumors and their adjacent normal breast tissues. hTERT gene expression was detected by ISH in 56 (88%) carcinomas, but in neither of the 2 phyllode tumors. hTERT protein expression was detected by IHC in 52 (81%) carcinomas, but in neither of the 2 phyllode tumors. Moreover, ER and PR were expressed in 42 (66%) and 42 (66%) carcinomas, respectively, and in neither of the 2 phyllode tumors. In 4 cases of breast carcinoma that strongly expressed hTERT gene and protein before treatment, neo-adjuvant chemotherapy led to disappearance of gene and protein expression in all cases. There was a strong correlation between detection of hTERT gene expression by ISH and of hTERT protein by ICH in tissue specimens from breast tumors. These results suggest that detection of hTERT protein by ICH can be used to distinguish breast cancers as a potential diagnostic and therapeutic marker.

PMID: 16211220 [PubMed - in process]

161
v. 27
no. 5
2005 Nov

Received on: 05-10-20
International journal of
oncology.

International Journal of Oncology



ISSN 1079-6439

An international journal devoted to Oncology Research and Cancer Treatment

VOLUME 27, NUMBER 5, NOVEMBER 2005



Expression of human telomerase reverse transcriptase gene and protein, and of estrogen and progesterone receptors, in breast tumors: Preliminary data from neo-adjuvant chemotherapy

MAKOTO KAMMORI^{1,2}, NAOTAKA IZUMIYAMA², MASANORI HASHIMOTO¹, KEN-ICHI NAKAMURA²,
TADAO OKANO³, RIE KURABAYASHI¹, HIKI NAOKI¹, NAOKO HONMA², TOSHIHISA OGAWA¹,
MICHIO KAMINISHI¹ and KAIYO TAKUBO²

¹Division of Breast and Endocrine Surgery, Department of Surgery, Graduate School of Medicine,
The University of Tokyo; ²Human Tissue Research Group, Tokyo Metropolitan Institute of Gerontology;

³Tokyo Metropolitan Tama Cancer Detection Center, Tokyo, Japan

Received January 25, 2005; Accepted March 24, 2005

Abstract. Human telomerase reverse transcriptase (hTERT), the catalytic subunit of telomerase, is very closely associated with telomerase activity. Telomerase has been implicated in cellular immortalization and carcinogenesis. *In situ* detection of hTERT will aid in determining the localization of telomerase-positive cells. The aim of this study was to detect expression of hTERT mRNA, hTERT protein, estrogen receptor (ER) and progesterone receptor (PR) in paraffin-embedded breast tissue samples and to investigate the relationship between hTERT expression and various clinicopathological parameters in breast tumorigenesis. We used *in situ* hybridization (ISH) to examine hTERT gene expression, and immunohistochemistry (IHC) to examine expression of hTERT protein, ER and PR, in breast tissues including 64 adenocarcinomas, 2 phyllode tumors and their adjacent normal breast tissues. hTERT gene expression was detected by ISH in 56 (88%) carcinomas, but in neither of the 2 phyllode tumors. hTERT protein expression was detected by IHC in 52 (81%) carcinomas, but in neither of the 2 phyllode tumors. Moreover, ER and PR were expressed in 42 (66%) and 42 (66%) carcinomas, respectively, and in neither of the 2 phyllode tumors. In 4 cases of breast carcinoma that strongly expressed hTERT gene and protein before treatment, neo-adjuvant chemotherapy led to disappearance of gene and protein expression in all cases. There was a strong correlation between detection of hTERT gene expression by ISH and of hTERT protein by ICH in tissue specimens from breast tumors. These results suggest that detection of hTERT

protein by ICH can be used to distinguish breast cancers as a potential diagnostic and therapeutic marker.

Introduction

Breast cancer is the most frequent malignancy in women, affecting up to one in every eight females worldwide. The most important clinicopathological prognostic parameter so far identified is the absence or presence of lymph node metastasis, but the identification of further parameters for both lymph node-positive and -negative patients would facilitate an individually based risk-directed therapy (1). A promising emerging molecular marker is telomerase, a ribonucleoprotein enzyme complex, which when activated or upregulated allows tumor cells to escape from cellular senescence and to proliferate indefinitely (2). The human telomere is a simple repeat sequence of six bases (TTAGGG) that is located at the ends of each chromosome (3). Telomeres are believed to protect against degeneration, reconstruction, fusion, and loss (4) and to promote the homologous pairing of chromosomes (5). The end-to-end chromosome fusions observed in some tumors may result from the loss of telomeres and may be partly responsible for the genetic instability associated with tumorigenesis. Telomerase catalyzes the synthesis of telomere DNA and facilitates cell immortalization through the stabilization of chromosomal structure (6-8). Although the expression of the human RNA component of telomerase (hTERC) is widespread, the restricted expression pattern of the mRNA of hTERT, the human telomerase catalytic subunit gene, is correlated with telomerase activity (8-13). As telomerase activity seems to be the key player in tumor cell immortality, it has importance as a target molecule for anti-cancer therapy. Telomerase activity has been shown to correlate with poor clinical outcome in neuroblastomas and other tumors (14). For breast cancer, however, telomerase activity is a controversial prognostic marker: some studies suggest that telomerase activity, clinicopathological parameters and disease outcome are linked, whereas others do not find this association (14-23).

Correspondence to: Dr Makoto Kammori, Division of Breast and Endocrine Surgery, Department of Surgery, Graduate School of Medicine, The University of Tokyo, 7-3-1 Hongo, Bunkyo-ku, Tokyo 113-8655, Japan
E-mail: kammori-dis@umin.ac.jp

Key words: human telomerase reverse transcriptase, telomerase, estrogen receptor, breast cancer, chemotherapy

We have succeeded in very clearly and sensitively demonstrating hTERT mRNA in thyroid, colorectal, parathyroid and lung tissues by use of an oligonucleotide probe (13,24-26). Strong correlation has been observed between hTERT mRNA and/or protein expression and telomerase in a variety of malignant tumors (13,14,24,25,27,28). In the present study, we used ISH to examine expression of the hTERT gene, and IHC to examine expression of hTERT protein, ER and PR, in 64 carcinomas and 2 phyllodes tumors of breast to determine whether hTERT protein can be used to differentiate breast cancers. We also analyzed hTERT mRNA and protein expression with special reference to clinical features and histological findings to investigate the potential role of hTERT mRNA expression analysis in predicting the biological characteristics of breast cancers. Since hTERT expression in breast tumors has not previously been analysed by ISH or IHC, our investigation also examined various clinicopathological parameters, including age, histopathological type, tumor size, lymph node status, relapses, and the expression of ER and PR.

Materials and methods

Tissue collection. Sixty-six samples were obtained during 66 mastectomies: 64 breast carcinomas, 2 phyllodes tumors and 66 specimens of the adjacent normal breast gland. In 4 cases, samples were obtained during core needle biopsies (CNB) before neo-adjuvant therapy and again during mastectomies after neo-adjuvant therapy; for these cases, all measurements and examinations were performed both before and after the neo-adjuvant therapy. The patients ranged in age from 32 to 90 years. The patients with carcinomas ranged in age from 37 to 90, mean 56, years and were all women. The women with phyllode tumors were aged 32 and 38 years, respectively. The surgical and CNB tissue samples were frozen rapidly with liquid nitrogen and stored at -80°C until fixation. Then, they were fixed in 10% buffer formalin solution and embedded in paraffin. Surgical and CNB samples were collected from the patients after obtaining their informed consent, and the study protocol was approved by the Medical Department of the University of Tokyo Ethics Committee. The pathologic diagnoses were made by the surgical pathological specialists at our institute on the basis of examination of hematoxylin-eosin stained slides. A pathological review was performed for all breast tumors according to the BRE score. pT and pN staging were assigned according to the 1997 WHO classification (7th edition).

MCF-7 human breast cancer cells, kindly provided by the Cell Resource Center for Biomedical Research, Institute of Development, Aging and Cancer, Tohoku University, were used as positive controls. The cells were incubated in RPMI-1640 medium with 25 mM HEPES buffer, L-glutamine, and 10% fetal bovine serum (Gibco; Grand Island, NY) on a chamber-attached slideglass (Lab-Tek® Chamber Slide™; Nalge Nunc International, Naperville, IL) in a humidified 5% CO₂ atmosphere at 37°C. The cells were then fixed with 10% buffered neutral formalin (Sigma Chemical Co., St. Louis, MO). The cultured MCF-7 cell line that was used as a positive control was tested for telomerase with a PCR-based standard TRAP assay (6,13). These cells were also used to prepare cell blocks. Briefly, the cells were fixed in 10% buffered neutral

formalin, resuspended in molten agarose and then embedded in paraffin. Sections from these cell blocks were used as positive procedural controls in ISH and IHC. The negative control in ISH was obtained by replacing the oligonucleotide probe with RNase. The negative control in IHC was obtained by replacing the primary antibody with Tris-buffered saline (TBS).

Oligonucleotide probe for ISH. The specificity of the oligonucleotide sequence was initially determined by a GenEMBL database search using the Genetics Computer Group Sequence Analysis Program (GCG, Madison, WI) based on the fastA algorithm (29); the sequence exhibited 100% homology with the hTERT gene sequence. A d(T)₂₀ oligonucleotide was used to verify the integrity and lack of degradation of the mRNA in each sample. All oligonucleotide probes were synthesized with a hapten-labeled nucleotide, such as digoxigenin-dUTP (Boehringer-Mannheim), at the 3' end via direct coupling by using standard phosphoramidite chemistry (Research Genetics, Huntsville, AL) (30). The probe used for detection of hTERT by ISH was generated from the original sequence for *Homo sapiens* telomerase reverse transcriptase (AF015950), 2766-2800: 5'-GCCTCGTCTTCTACAGGGA AGTTCACCACTGTCTT-3' (13,24-26).

ISH. ISH was performed with the GenPoint nucleic acid hyper-detection system (Dako; Carpinteria, CA) (31). Formalin-fixed, paraffin-embedded tissue sections (5 µm thick) were deparaffinized in xylene and a graded alcohol series. Tissue sections and CNB samples were then pretreated with target retrieval solution (Dako, S1700) at 95°C and proteinase K (Dako, S3004) at room temperature. Next, the tissues and CNB samples were fixed in 0.3% hydrogen peroxide followed by a methyl alcohol series at room temperature. Digoxigenin-labeled anti-sense oligonucleotide in mRNA *in situ* hybridization solution (Dako, S3304) was placed over the tissues and CNB samples. After hybridization at 37°C overnight, the slides were washed in stringent wash solution (Dako, GenPoint System Kit) at 45°C. The tissues and CNB samples were exposed to avidin blocking solution (Dako, X0590) at room temperature followed by biotin blocking solution (Dako, X0590) at room temperature. The tissues and samples were then incubated at room temperature with a sheep monoclonal hapten-labeled anti-digoxigenin antibody (Dako, p5104), and the slides were then fixed with biotinyl tyramine (Dako, GenPoint System Kit) at room temperature. Finally, the slides were incubated with HRP-conjugated streptavidin (Dako, GenPoint System Kit) at room temperature. Since 3,3'-diaminobenzidine tetrahydrochloride (DAB) was used as the substrate, a positive reaction was visible as a brown color under a light microscope. The sections were weakly counterstained with 0.1% hematoxylin.

IHC. IHC was performed by the avidin-biotin complex/horseradish peroxidase method. Tissue sections were stained for hTERT with a commercially available monoclonal antibody (NCL-L-hTERT; Novocastra, Newcastle upon Tyne, UK). Sections were dewaxed in xylene. Antigen retrieval was done by incubating sections immersed in 0.01 M citrate buffer at pH 6.0 in a microwave oven at 99°C. The sections were allowed to cool down at room temperature. The sections

MCF-7 Lysis Case 6 Case 14 Case 23 Case 44 Case 59

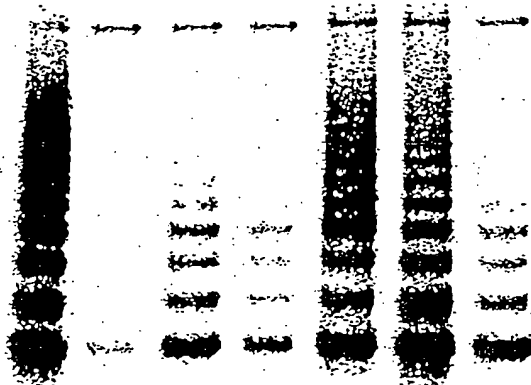


Figure 1. Representative results of the TRAP assay. If functional telomerase is present, the enzyme adds DNA to the substrate in 6-base-pair (bp) increments, resulting in a ladder-like distribution of products. The 6-bp ladder signals are apparent for MCF-7 and breast cancers (case nos. 6, 14, 23, 44 and 59) and are not apparent for lysis buffer as the negative control. An extract of MCF-7 was used as a positive control for the TRAP assay and as an Internal Telomerase Assay Standard (ITAS) positive control for PCR amplification, with lysis buffer as the negative control (Lysis).

were then immersed in 1% hydrogen peroxide (H_2O_2) in methanol to block endogenous peroxidase activity. Following that, the sections were washed in TBS (pH 7.6) before being incubated in normal rabbit serum for 20 min to block non-specific binding. After draining off the excess serum, the sections were incubated with the primary antibody at room temperature. The sections were washed in TBS before being incubated with the secondary antibody (biotinylated rabbit anti-mouse, Dako). The sections were washed again with TBS and incubated with avidin-biotin complex/horseradish peroxidase. After washing the sections with TBS, peroxidase activity was visualized under light microscopy by applying DAB chromogen (Dako). The sections were counterstained with hematoxylin, dehydrated in increasing grades of alcohol and finally mounted in dibutyl phthalate (DPX) mountant.

Homogeneous staining or a speckled/dotted pattern in the nucleus was considered positive staining, and absence of distinct nuclear staining was taken as negative staining. Grading of the percentage of stained cells (hTERT labeling index) was performed by previously published criteria (1) as follows: Grade 1, negative staining; Grade 2, 1-10% positive staining nuclei; Grade 3, 11-50% positive nuclei; and Grade 4, >50% positive nuclei. Immunostained slides for ER and PR were scored as previously described (32,33). In brief, each entire slide was evaluated by light microscopy. First, a proportion score was assigned, which represents the estimated proportion of positive-staining tumor cells (0, none; 1, <1/100; 2, 1/100 to 1/10; 3, 1/10 to 1/3; 4, 1/3 to 2/3; and 5, >2/3). Next, an intensity score was assigned, which represents the average intensity of positive tumor cells (0, none; 1, weak; 2, intermediate; and 3, strong). The proportion and intensity scores were then added to obtain a total score, which ranged from 0 to 8. Slides were scored by pathologists who did not have knowledge of ligand-binding results or patient outcome.

Table I. Relationships between mRNA status (negative/positive) by ISH and standard clinical, pathological, and biological factors in the 66 tumors.

	Total population (%)	No. of patients (%)		P-value ^a
		hTERT negative	hTERT positive	
Total	66	10 (15.2)	56 (84.8)	
Age				NS
≤50	26	6 (23.1)	20 (76.9)	
>50	40	6 (15.0)	34 (85.0)	
Histopathological type				NS
Scirrhous	32	2 (6.4)	30 (93.6)	
Papillotubular	20	2 (10.0)	18 (90.0)	
Solid tubular	6	1 (16.7)	5 (83.3)	
Mucinous	2	1 (50.0)	1 (50.0)	
Non-invasive	4	2 (50.0)	2 (50.0)	
Phyllodes	2	2 (100)	0 (0)	
Tumor size (cm) ^b				NS
T1 (<2.0)	20	0 (0)	20 (100)	
T2 (2.0-5.0)	34	6 (17.6)	28 (82.4)	
T3 (>5.0)	10	2 (20.0)	8 (80.0)	
Lymph node status ^b				NS
pN0	34	6 (17.6)	28 (82.4)	
pN1	26	2 (7.7)	24 (92.3)	
pN2+pNM	4	0 (0)	4 (100)	
Relapse				NS
+	10	0 (0)	10 (100)	
-	56	10 (17.6)	46 (82.4)	
ER expression				NS
+ (≥2)	42	6 (14.3)	36 (85.7)	
- (<2)	24	4 (16.7)	20 (83.3)	
PR expression				NS
+ (≥2)	42	4 (9.5)	38 (90.5)	
- (<2)	24	6 (25.0)	18 (75.0)	

^a χ^2 test. NS, not significant; ^bInformation available for 64 patients.

Statistical analysis. Differences in p-values were analyzed with the χ^2 test for independence, and Fisher's test was used for correlations. In all comparisons, $p < 0.05$ was considered significant.

Results

Representative results of the TRAP assay are shown in Fig. 1. The cultured cells, which were tested for telomerase activity

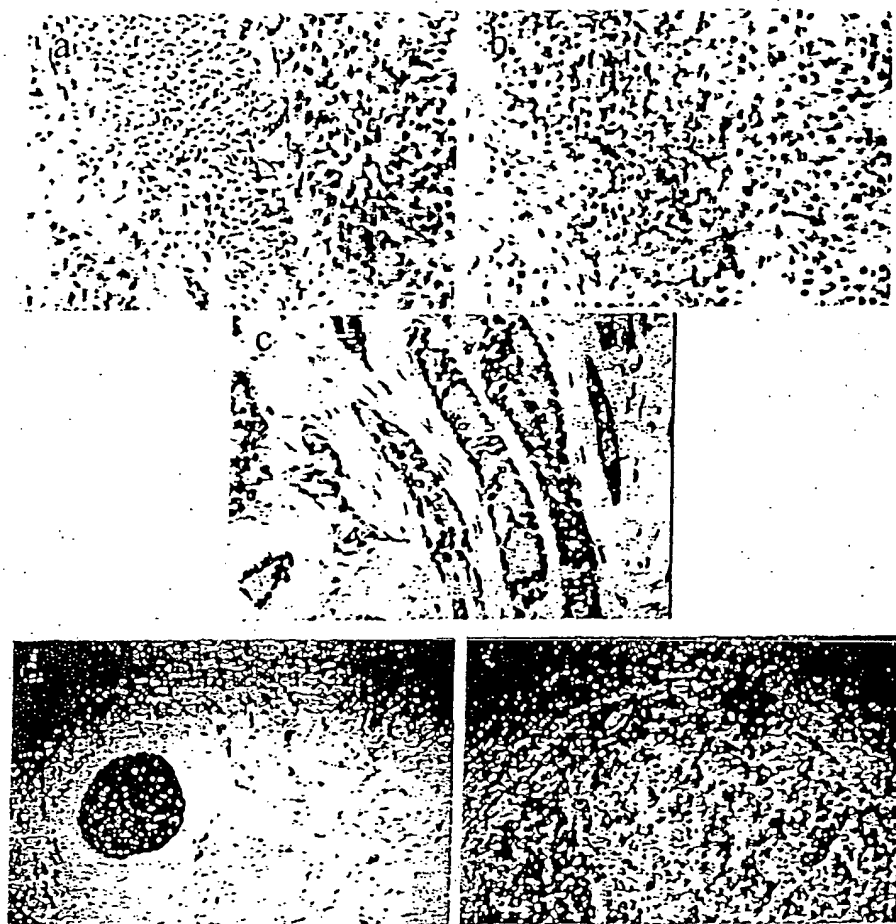


Figure 2. Correlation between histologic diagnosis, human telomerase reverse transcriptase (hTERT) mRNA by ISH, hTERT protein by IHC, estrogen receptor (ER) by IHC and progesterone receptor (PR) by IHC in breast cancers. (a, H&E); (b, hTERT mRNA); (c, hTERT protein); (d, ER) and (e, PR).

with the TRAP assay, gave positive results with all procedural controls (MCF-7 and 5 breast cancer samples) (Fig. 1).

ISH revealed that hTERT mRNA was strongly expressed in the nuclei and cytoplasm of almost all of the MCF-7 human cancer cells (data not shown). Expression of hTERT mRNA was detected in 56 (88%) of the 64 breast cancers and in none of the phyllodes tumors of the breast (Table I) with the anti-sense probe, whereas no expression was detected with the anti-sense probe treated with RNase (data not shown). The levels of expression were heterogeneous within the carcinomatous regions. Strong expression of hTERT mRNA was not confined to the carcinomatous regions but was also detected in infiltrating lymphocytes (Fig. 2a and b). Higher expression levels of both signals of hTERT mRNA were detected in some sections containing both carcinomas and lymphocytes, compared with the adjacent non-cancerous mammary gland, but no clear differences in signal intensity were observed between carcinomas and lymphocytes. The signals in both the normal and cancer tissues were mainly present in the lymphocytes, and the signal intensity was similar in both, although a precise quantitative comparison of the *in situ* signals was impossible.

IHC revealed that hTERT protein was strongly expressed in the nuclei, nuclear membrane and cytoplasm of almost all of the MCF-7 human cancer cells (data not shown). Expression of hTERT protein was detected in 52 (81%) of the 64 breast cancers and in none of the phyllode tumors of the breast (Table II). The levels of expression were heterogeneous within the carcinomatous regions. As shown in Fig. 2c, strong expression of hTERT protein was observed in nuclei, nuclear membrane and cytoplasm, similar to the pattern in MCF-7 human cancer cells. Normal mammary gland and stromal cells generally showed negative immunoreactivity against hTERT protein antibody.

A nuclear signal for the ER (Fig. 2d), as assessed by IHC, was observed in 36 (56%) of the 64 breast cancers and in none of the phyllode tumors of the breast, with positive scores ranging from 2 to 8 (Tables I and II). A nuclear signal for the PR (Fig. 2e), as assessed by IHC, was observed in 38 (59%) of the 64 breast cancers and in none of the phyllode tumors of the breast, with positive scores ranging from 2 to 8 (Tables I and II).

We used ISH and IHC to examine hTERT expression in 4 cases of breast cancer before and after neo-adjuvant

Table II. Relationships between mRNA status (negative/positive) by IHC and standard clinical, pathological, and biological factors in the 66 tumors.

	Total	No. of patients (%)		P-value ^a
		hTERT negative	hTERT positive	
Total	66	14 (21.2)	52 (78.8)	
Age				NS
≤50	26	10 (38.5)	16 (61.5)	
>50	40	4 (10.0)	36 (90.0)	
Histopathological type				NS
Scirrhous	32	2 (6.4)	30 (93.6)	
Papillotubular	20	4 (20.0)	16 (80.0)	
Solid tubular	6	4 (66.7)	2 (33.3)	
Mucinous	2	0 (0)	2 (100)	
Non-invasive	4	2 (50.0)	2 (50.0)	
Phyllodes	2	2 (100)	0 (0)	
Tumor size (cm) ^b				NS
T1 (<2.0)	20	4 (20.0)	16 (80.0)	
T2 (2.0-5.0)	34	6 (17.6)	28 (82.4)	
T3 (>5.0)	10	2 (20.0)	8 (80.0)	
Lymph node status ^b				NS
pN0	34	6 (17.6)	28 (82.4)	
pN1	26	6 (23.1)	20 (76.9)	
pN2+pNM	4	0 (0)	4 (100)	
Relapse				NS
+	10	1 (10.0)	9 (90.0)	
-	56	13 (23.2)	43 (79.6)	
ER expression				NS
+ (≥2)	42	6 (14.3)	36 (85.7)	
- (<2)	24	8 (33.3)	16 (66.7)	
PR expression				NS
+ (≥2)	42	6 (14.3)	36 (85.7)	
- (<2)	24	8 (33.3)	16 (66.7)	

^aχ² test. NS, not significant. ^bInformation available for 64 patients.

chemotherapy. Before chemotherapy, all 4 of the breast carcinomas strongly expressed hTERT by both ISH and IHC. After chemotherapy, hTERT expression completely disappeared in all 4 cases (Table III). hTERT expression by lymphocytes was detectable by ISH and IHC both before and after chemotherapy in all 4 cases, and the level of expression did not appear to be altered by treatment.

No correlation was observed between hTERT mRNA expression and any of the clinicopathological parameters age, histopathological type, tumor size, lymph node status,

Table III. Relationship of hTERT mRNA and protein expression before and after neoadjuvant chemotherapy.

Case	Age	Neoadjuvant	hTERT mRNA		hTERT protein	
			Before	After	Before	After
1	80	Anastrozole	+	-	+	-
2	78	Anastrozole	+	-	+	-
3	35	FEC ^a	+	-	+	-
4	37	AC ^b	+	-	+	-

^aFEC, 5FU (500 mg/m²), Epirubicin (70 mg/m²), Cyclophosphamide (500 mg/m²). ^bAC, Doxorubicin (60 mg/m²), Cyclophosphamide (500 mg/m²). Before, before neoadjuvant chemotherapy. After, after neoadjuvant chemotherapy. +, positive; -, negative.

relapses, and the expression of ER and PR. Similarly, there was no correlation between hTERT protein expression and any of these clinicopathological parameters. There was a correlation between hTERT mRNA expression and hTERT protein expression in breast cancers ($p < 0.005$).

Discussion

This study reports a comparison of hTERT mRNA expression by ISH and hTERT protein expression by IHC in tissue sections from breast tumors. hTERT mRNA was detected by ISH in 56 of the 64 breast cancers and in MCF-7 human breast cancer cells. Breast cancer cell nuclei stained strongly positive with the specific anti-sense probe but not with the anti-sense probe treated with RNase (data not shown). Tissue lymphocytes also stained positively with the anti-sense probe, but the stromal cells did not. Expression of hTERT protein was observed by IHC in 52 of the 64 breast cancers. hTERT mRNA and protein expressions were highly correlated in breast cancers ($p < 0.005$). Detection of the hTERT protein by IHC has permitted further analysis of carcinogenesis and cancer diagnosis (34).

In recent years, there has been disagreement over the suitability of telomerase activity as a prognostic biologic marker in breast cancer that may help to differentiate patients for individually based risk-related therapy. Hiyama *et al* (15), in a study of 140 breast cancer specimens with the TRAP assay, found a strong association between telomerase activity and stage classification and observed telomerase activity in 68% of stage I tumors and 95% of stage IV tumors. Poremba *et al* (1), using tissue microarrays, found a statistically significant correlation between tumor-specific survival (overall survival) and hTERT expression in breast cancer. However, some problems in interpretation may affect this apparent consensus. First, some samples of breast cancer tissue may be extensively contaminated by infiltrating lymphocytes during operative manipulations, especially in advanced disease, causing overestimation of telomerase activity and/or hTERT expression. In our previous reports, higher expression levels

of signals for both hTERT mRNA and protein were detected in some sections containing both carcinoma and lymphocytes in thyroid and colorectal cancers (13,24). Secondly, Poremba *et al* (1) used polyclonal antibodies against hTERT protein as a signal for expression. In our hands, polyclonal antibodies against hTERT protein give rise to strong background signals and are not clearly specific for measuring expression in cancer tissues. We have carefully compared the reactivity against hTERT protein of the monoclonal antibody used in the present study with that of some polyclonal antibodies. Use of the monoclonal antibody in IHC allowed clear demonstration of hTERT protein expression, with results similar to those of ISH for hTERT mRNA expression. Furthermore, IHC is technically much easier to perform than ISH, since contamination of samples by RNase is not an issue in IHC.

To the best of our knowledge, this report is the first on the study of hTERT expression in breast cancer as a function of neo-adjuvant treatment. We examined hTERT expression in 4 cases of breast cancer before and after chemotherapy. Before chemotherapy, hTERT was strongly expressed in all 4 carcinomas, but after chemotherapy hTERT expression had completely disappeared in all 4 cases. hTERT expression by lymphocytes was detectable by ISH and IHC both before and after chemotherapy in all 4 cases, and the level of expression did not appear to be altered by treatment.

In conclusion, determination of hTERT mRNA expression by ISH and hTERT protein expression by IHC can be used to obtain information contributing to a histopathological diagnosis during screening of breast cancers. By use of a monoclonal antibody, we could very clearly and sensitively demonstrate hTERT protein expression in breast cancer tissues but not in non-cancerous tissues. We also demonstrated that 4 carcinomas with originally positive immunoreactivity against hTERT protein became negative after neo-adjuvant chemotherapy. These results suggest that determination of hTERT protein by IHC can be used as a potential diagnostic and therapeutic marker to distinguish breast cancers.

Acknowledgments

We thank Ms. Sachiko Nishimura for her expert technical assistance.

References

- Poremba C, Heine B, Diallo R, Heinecke A, Wai D, Schaefer KL, Braun Y, Schuck A, Lanvers C, Bankfalvi A, Kneif S, Thorhorst J, Zuber M, Kochli OR, Mross F, Dieterich H, Sauter G, Stein H, Fogt F and Boecker W: Telomerase as a prognostic marker in breast cancer: high-throughput tissue microarray analysis of hTERT and hTR. *J Pathol* 198: 181-189, 2002.
- Healy KC: Telomeric dynamics and telomerase activation in tumor progression: prospects for prognosis and therapy. *Oncol Res* 7: 121-130, 1995.
- Shampay J and Blackburn EH: Tetrahymena micronuclear sequences that function as telomeres in yeast. *Nucleic Acids Res* 17: 3247-3260, 1989.
- Levy MZ, Allsopp RC, Futcher AB, Greider CW and Harley CB: Telomere end-replication problem and cell aging. *J Mol Biol* 225: 951-960, 1992.
- Moyzis RK, Buckingham JM, Cram LS, Dani M, Deaven LL, Jones MD, Meyne J, Ratliff RL and Wu JR: A highly conserved repetitive DNA sequence, (TTAGGG)_n, present at the telomeres of human chromosomes. *Proc Natl Acad Sci USA* 85: 6622-6626, 1988.
- Kim NW, Piatyszek MA, Prowse KR, Harley CB, West MD, Ho PL, Coviello GM, Wright WE, Weinrich SL and Shay JW: Specific association of human telomerase activity with immortal cells and cancer. *Science* 266: 2011-2015, 1994.
- Blackburn EH: Telomerase. *Annu Rev Biochem* 61: 113-129, 1992.
- Shay JW and Bacchetti S: A survey of telomerase activity in human cancer. *Eur J Cancer* 33: 787-791, 1997.
- Meyerson M, Counter CM, Eaton EN, Ellisen LW, Steiner P, Caddle SD, Ziaugra L, Beijersbergen RL, Davidoff MJ, Liu Q, Bacchetti S, Haber DA and Weinberg RA: hEST2, the putative human telomerase catalytic subunit gene, is up-regulated in tumor cells and during immortalization. *Cell* 90: 785-795, 1997.
- Nakamura TM, Morin GB, Chapman KB, Weinrich SL, Andrews WH, Lingner J, Harley CB and Cech TR: Telomerase catalytic subunit homologs from fission yeast and human. *Science* 277: 955-999, 1997.
- Kilian A, Bowtell DD, Abud HE, Hime GR, Venter DJ, Keese PK, Duncan EL, Reddel RR and Jefferson RA: Isolation of a candidate human telomerase catalytic subunit gene, which reveals complex splicing patterns in different cell types. *Hum Mol Genet* 6: 2011-2019, 1997.
- Kamori M, Nakamura KI, Kanauchi H, Obara T, Kawahara M, Mijima Y, Kaminishi M and Takubo K: Consistent decrease in telomere length in parathyroid tumors but alteration in telomerase activity limited to malignancies: a preliminary report. *World J Surg* 26: 1083-1087, 2002.
- Kamori M, Nakamura K, Hashimoto M, Ogawa T, Kaminishi M and Takubo K: Clinical application of human telomerase reverse transcriptase gene expression in thyroid follicular tumors by fine-needle aspirations using *in situ* hybridization. *Int J Oncol* 22: 985-991, 2003.
- Poremba C, Scheel C, Hero B, Christiansen H, Schaefer KL, Nakayama J, Berthold F, Juergens H, Boecker W and Dockhorn-Dworniczak B: Telomerase activity and telomerase subunits gene expression patterns in neuroblastoma: a molecular and immunohistochemical study establishing prognostic tools for fresh-frozen and paraffin-embedded tissues. *J Clin Oncol* 18: 2582-2592, 2000.
- Hiyama E, Gollahon L, Kataoka T, Kuroi K, Yokoyama T, Gazdar AF, Hiyama K, Piatyszek MA and Shay JW: Telomerase activity in human breast tumors. *J Natl Cancer Inst* 88: 116-122, 1996.
- Sugino T, Yoshida K, Bolodcoku J, Tahara H, Buley I, Manek S, Wells C, Goodison S, Ide T, Suzuki T, Tahara E and Tarin D: Telomerase activity in human breast cancer and benign breast lesions: diagnostic applications in clinical specimens, including fine needle aspirates. *Int J Cancer* 69: 301-306, 1996.
- Nawaz S, Hashizumi TL, Markham NE, Shroyer AL and Shroyer KR: Telomerase expression in human breast cancer with and without lymph node metastases. *Am J Clin Pathol* 107: 542-547, 1997.
- Clark GM, Osborne CK, Levitt D, Wu F and Kim NW: Telomerase activity and survival of patients with node-positive breast cancer. *J Natl Cancer Inst* 89: 1874-1881, 1997.
- Poremba C, Boecker W, Willenbring H, Schaefer KL, Otterbach F, Burger H, Diallo R and Dockhorn-Dworniczak B: Telomerase activity in human proliferative breast lesions. *Int J Oncol* 12: 641-648, 1998.
- Hoos A, Hepp HH, Kaul S, Ahlert T, Basten G and Wallwiener D: Telomerase activity correlates with tumor aggressiveness and reflects therapy effect in breast cancer. *Int J Cancer* 79: 8-12, 1998.
- Roos G, Nilsson P, Cajander S, Nielsen NH, Arnerlov C and Landberg G: Telomerase activity in relation to p53 status and clinicopathological parameters in breast cancer. *Int J Cancer* 79: 343-348, 1998.
- Mokbel K, Parris CN, Ghilchik M, Williams G and Newbold RF: The association between telomerase, histopathological parameters, and Ki-67 expression in breast cancer. *Am J Surg* 178: 69-72, 1999.
- Umbrecht CB, Sherman ME, Dome J, Carey LA, Marks J, Kim N and Sukumar S: Telomerase activity in ductal carcinoma *in situ* and invasive breast cancer. *Oncogene* 18: 3407-3414, 1999.
- Kamori M, Kanauchi H, Nakamura KI, Kawahara M, Weber TK, Mafune K, Kaminishi M and Takubo K: Demonstration of human telomerase reverse transcriptase (hTERT) in human colorectal carcinomas by *in situ* hybridization. *Int J Oncol* 20: 15-21, 2002.

25. Kamatori M, Nakamura KI, Ogawa T, Mafune KI, Tatutomi Y, Obara T, Onoda N, Fujiwara M, Izumiyama-Shimomura N, Mori M, Kaminishi M and Takubo K: Demonstration of human telomerase reverse transcriptase (hTERT) in human parathyroid tumors by *in situ* hybridization with a new oligonucleotide probe. *Clin Endocrinol* 58: 43-48, 2003.
26. Fukushima M, Shimomura N, Nakamura KI, Kamatori M, Koizumi K, Shimizu K and Takubo K: Demonstration of human telomerase reverse transcriptase by *in situ* hybridization in lung carcinoma. *Oncol Rep* 12: 1227-1232, 2004.
27. Frost M, Bobak JB, Gianani R, Kim N, Weinrich S, Spalding DC, Cass LG, Thompson LC, Enomoto T, Uribe-Lopez D and Shroyer KR: Localization of telomerase hTERT protein and hTR in benign mucosa, dysplasia, and squamous cell carcinoma of the cervix. *Am J Clin Pathol* 114: 726-734, 2000.
28. Kawakami Y, Kitamoto M, Nakanishi T, Yasui W, Tahara E, Nakayama J, Ishikawa F, Tahara H, Ide T and Kajiyama G: Immuno-histochemical detection of human telomerase reverse transcriptase in human liver tissues. *Oncogene* 19: 3888-3893, 2000.
29. Pearson WR and Lipman DJ: Improved tools for biological sequence comparison. *Proc Natl Acad Sci USA* 85: 2444-2448, 1988.
30. Caruthers MH, Beaucage SL, Efcavitch JW, Fisher EF, Goldman RA, De Haseth PL, Mandecki W, Matteucci MD, Rosendahl MS and Stabinsky Y: Chemical synthesis and biological studies on mutated gene-control regions. *Cold Spring Harbor Symp Quant Biol* 47: 411-418, 1982.
31. Tani Y: PCR *In situ* amplification and catalyzed signal amplification: approaches of higher sensitive, non-radioactive *in situ* hybridization. *Acta Histochem Cytochem* 32: 261-270, 1999.
32. Harvey JM, Clark GM, Osborne CK and Allred DC: Estrogen receptor status by immunohistochemistry is superior to the ligand-binding assay for predicting response to adjuvant endocrine therapy in breast cancer. *J Clin Oncol* 17: 1474-1481, 1999.
33. Allred DC, Harvey JM, Berardo M and Clark GM: Prognostic and predictive factors in breast cancer by immunohistochemical analysis. *Mod Pathol* 11: 155-168, 1998.
34. Tahara H, Yasui W, Tahara E, Fujimoto J, Ito K, Tamai K, Nakayama J, Ishikawa F, Tahara E and Ide T: Immunohistochemical detection of human telomerase catalytic component, hTERT, in human colorectal tumor and non-tumor tissue sections. *Oncogene* 18: 1561-1567, 1999.

Expression of the ubiquitin-proteasome pathway and muscle loss in experimental cancer cachexia.

Khal J, Wyke SM, Russell ST, Hine AV, Tisdale MJ.

Pharmaceutical Sciences Research Institute, Aston University, Birmingham, UK.

Muscle protein degradation is thought to play a major role in muscle atrophy in cancer cachexia. To investigate the importance of the ubiquitin-proteasome pathway, which has been suggested to be the main degradative pathway mediating progressive protein loss in cachexia, the expression of mRNA for proteasome subunits C2 and C5 as well as the ubiquitin-conjugating enzyme, E2(14k), has been determined in gastrocnemius and pectoral muscles of mice bearing the MAC16 adenocarcinoma, using competitive quantitative reverse transcriptase polymerase chain reaction. Protein levels of proteasome subunits and E2(14k) were determined by immunoblotting, to ensure changes in mRNA were reflected in changes in protein expression. Muscle weights correlated linearly with weight loss during the course of the study. There was a good correlation between expression of C2 and E2(14k) mRNA and protein levels in gastrocnemius muscle with increases of 6-8-fold for C2 and two-fold for E2(14k) between 12 and 20% weight loss, followed by a decrease in expression at weight losses of 25-27%, although loss of muscle protein continued. In contrast, expression of C5 mRNA only increased two-fold and was elevated similarly at all weight losses between 7.5 and 27%. Both proteasome functional activity, and proteasome-specific tyrosine release as a measure of total protein degradation was also maximal at 18-20% weight loss and decreased at higher weight loss. Proteasome expression in pectoral muscle followed a different pattern with increases in C2 and C5 and E2(14k) mRNA only being seen at weight losses above 17%, although muscle loss increased progressively with increasing weight loss. These results suggest that activation of the ubiquitin-proteasome pathway plays a major role in protein loss in gastrocnemius muscle, up to 20% weight loss, but that other factors such as depression in protein synthesis may play a more important role at higher weight loss.

PMID: 16160695 [PubMed - in process]



Cell type-specific occurrence of caveolin-1alpha and -1beta in the lung caused by expression of distinct mRNAs.

Kogo H, Aiba T, Fujimoto T.

Department of Anatomy and Molecular Cell Biology, Nagoya University Graduate School of Medicine, Showa-ku, Nagoya 466-8550, Japan. hkogo@fujita-hu.ac.jp

Two isoforms of caveolin-1, alpha and beta, had been thought to be generated by alternative translation initiation of an mRNA (FL mRNA), but we showed previously that a variant mRNA (5'V mRNA) encodes the beta isoform specifically. In the present study, we demonstrated strong correlation between the expression of the caveolin-1 protein isoforms and mRNA variants in culture cells and the developing mouse lung. The alpha isoform protein and FL mRNA were expressed constantly during the lung development, whereas expression of the beta isoform protein and 5'V mRNA was negligible in the fetal lung before 17.5 days post coitum, and markedly increased simultaneously at 18.5 days post coitum, when the alveolar type I cells started to differentiate. Immunohistochemical analysis revealed the cell type-specific expression of the two isoforms; the alveolar type I cell expresses the beta isoform predominantly, while the endothelium harbors the alpha isoform chiefly. The mutually exclusive expression of caveolin-1 isoforms was verified by Western blotting of the selective plasma membrane preparation obtained from the endothelial and alveolar epithelial cells. The present result indicates that the two caveolin-1 isoforms are generated from distinct mRNAs in vivo and that their production is regulated independently at the transcriptional level. The result also suggests that the alpha and beta isoforms of caveolin-1 may have unique physiological functions.

PMID: 15067006 [PubMed - indexed for MEDLINE]

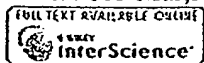
Oncogene and growth factor expression in ovarian cancer.

Kommoss F, Bauknecht T, Birmelin G, Kohler M, Tesch H, Pfeiderer A.

Department of Gynaecology, Albert-Ludwig University, Freiburg, Germany.

The varying tumor-biological behavior of ovarian carcinomas probably influences both their operability and response to chemotherapy, which are the most relevant prognostic factors. The phenotype of different ovarian carcinomas is obviously associated with an activation of the EGF/TGF-alpha signal pathway, including c-myc and c-jun expression. Analysis of EGF-R, TGF-alpha, c-myc and c-jun expression in 33 stage III/IV, and 2 stage I/II ovarian carcinomas with biochemical, molecular-chemical and immunohistochemical methods showed a correlation between the mRNA and protein levels of EGF-R and TGF-alpha for tumors with low or high expressing rates. However, the concentration of measurable free EGF-Rs seems to depend on the amount of TGF-alpha expression by the tumors. The EGF-R binding ligand TGF-alpha is produced by epithelial tumor cells; stromal cells are usually TGF-alpha-negative, as shown by immunohistochemistry. High expression rates of EGF-R, TGF-alpha and c-myc were detected in 6, 7, and 10 out of 35 ovarian carcinomas, respectively. C-jun mRNA was detected in 18/19 cases studied. Non-malignant tissues originating from myometrium or ovary expressed no (or only small amounts of) EGF-R or TGF-alpha mRNA, whereas a high c-myc expression was found in 1/7 normal myometria, and in 2/5 normal ovaries. There was no strong correlation between EGF-R/TGF-alpha and c-myc/c-jun expression. (ABSTRACT TRUNCATED AT 250 WORDS)

PMID: 1502888 [PubMed - indexed for MEDLINE]



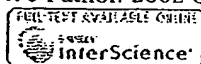
A transcriptomic and proteomic analysis of the effect of CpG-ODN on human THP-1 monocytic leukemia cells.

Kuo CC, Kuo CW, Liang CM, Liang SM.

Institute of BioAgricultural Sciences, Academia Sinica, Taipei, Taiwan.

The CpG motif of bacterial DNA (CpG-DNA) is a potent immunostimulating agent whose mechanism of action is not yet clear. Here, we used both DNA microarray and proteomic approaches to investigate the effects of oligodeoxynucleotides containing the CpG motif (CpG-ODN) on gene transcription and protein expression profiles of CpG-ODN responsive THP-1 cells. Microarray analysis revealed that 2 h stimulation with CpG-ODN up-regulated 50 genes and down-regulated five genes. These genes were identified as being associated with inflammation, antimicrobial defense, transcriptional regulation, signal transduction, tumor progression, cell differentiation, proteolysis and metabolism. Longer stimulation (8 h) with CpG-ODN enhanced transcriptional expression of 58 genes. Among these 58 genes, none except one, namely WNT1 inducible signaling pathway protein 2, was the same as those induced after 2 h stimulation. Proteomic analysis by two-dimensional gel electrophoresis, followed by mass spectrometry identified several proteins up-regulated by CpG-ODN. These proteins included heat shock proteins, modulators of inflammation, metabolic proteins and energy pathway proteins. Comparison of microarray and proteomic expression profiles showed poor correlation. Use of more reliable and sensitive analyses, such as reverse transcriptase polymerase chain reaction, Western blotting and functional assays, on several genes and proteins, nonetheless, confirmed that there is indeed good correlation between mRNA and protein expression after CpG-ODN treatment. This study also revealed that several anti-apoptotic and neuroprotective related proteins, not previously reported, are activated by CpG-DNA. These findings have extended our knowledge on the activation of cells by CpG-DNA and may contribute to further understanding of mechanisms that link innate immunity with acquired immune response(s).

PMID: 15693060 [PubMed - indexed for MEDLINE]



Quantification of CK20 gene and protein expression in colorectal cancer by RT-PCR and immunohistochemistry reveals inter- and intratumour heterogeneity.

Lassmann S, Bauer M, Soong R, Schreglmann J, Tabiti K, Nahrig J, Ruger R, Hoffer H, Werner M.

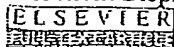
Pathologisches Institut, Universitätsklinikum Freiburg, Albertstrasse 19, 79104 Freiburg, Germany. lassmann@ukl.uni-freiburg.de

Cytokeratin 20 (CK20) is an epithelial protein expressed almost exclusively in the gastrointestinal (GI) tract and is widely used as immunohistochemical marker for routine diagnosis. In contrast, CK20 gene expression is not an established marker for the classification of tumours and the detection of disseminated cancer cells in colorectal cancer. Recently, real-time reverse transcriptase polymerase chain reaction (RT-PCR) has provided the means for reproducible and quantitative investigation of molecular markers. This report directly compares CK20 mRNA and protein expression in serial sections of archival, formalin-fixed, paraffin-embedded (FFPE) colorectal adenocarcinomas. CK20 expression was detected by immunohistochemistry (IHC) in 60/63 (95.2%) cases, by conventional RT-PCR in 58/60 (96.7%) and by quantitative RT-PCR using the LightCycler (LightCycler is a trademark of a Member of the Roche Group) System in 29/32 (90.6%) microdissected cases, one case yielding variable results. Despite the high detection rate of all three techniques, marked heterogeneity of CK20 expression was seen between different cases and also within individual cases. CK20 expression profiles were not related to particular histopathological features of the tumours. A good correlation ($r = 0.8964$) was found between CK20 mRNA and protein expression by comparing quantitative RT-PCR with IHC in 32 cases. This was also true for selected heterogeneous tumour cells within individual cases. Both RT-PCR and IHC are therefore valuable tools for CK20 detection in colorectal adenocarcinoma, with real-time RT-PCR providing supplementary quantitative information. This suggests a promising supportive role for quantitative RT-PCR in molecular pathology. Copyright 2002 John Wiley & Sons, Ltd.

Publication Types:

- Evaluation Studies

PMID: 12237879 [PubMed - indexed for MEDLINE]



Enhanced expressions of arachidonic acid-sensitive tandem-pore domain potassium channels in rat experimental acute cerebral ischemia.

Li ZB, Zhang HX, Li LL, Wang XL.

Institute of Materia Medica, Chinese Academy of Medical Sciences and Peking Union Medical College, Beijing 100050, China.

To further explore the pathophysiological significance of arachidonic acid-sensitive potassium channels, RT-PCR and Western blot analysis were used to investigate the expression changes of TREK channels in cortex and hippocampus in rat experimental acute cerebral ischemia in this study. Results showed that TREK-1 and TRAAK mRNA in cortex, TREK-1 and TREK-2 mRNA in hippocampus showed significant increases 2 h after middle cerebral artery occlusion (MCAO). While the mRNA expression levels of the all three channel subtypes increased significantly 24 h after MCAO in cortex and hippocampus. At the same time, the protein expressions of all the three channel proteins showed significant increase 24 h after MCAO in cortex and hippocampus, but only TREK-1 showed increased expression 2 h after MCAO in cortex and hippocampus. Immunohistochemical experiments verified that all the three channel proteins had higher expression levels in cortical and hippocampal neurons 24 h after MCAO. These results suggested a strong correlation between TREK channels and acute cerebral ischemia. TREK channels might provide a neuroprotective mechanism in the pathological process.

PMID: 15652517 [PubMed - indexed for MEDLINE]



Retinal preconditioning and the induction of heat-shock protein 27.

Li Y, Roth S, Laser M, Ma JX, Crosson CE.

Department of Ophthalmology, Medical University of South Carolina, Charleston, South Carolina 29425, USA.

PURPOSE: Brief periods of ischemia have been shown to protect the retina from potentially damaging periods of ischemia. This phenomenon has been termed ischemic preconditioning or ischemic tolerance. In the present study the cellular changes in levels of heat shock protein (Hsp)27, -70, and -90 mRNA and expression of Hsp in the rat retina associated with ischemic preconditioning were evaluated. **METHODS:** Unilateral retinal ischemia was created in Long-Evans and Sprague-Dawley rats for 5 minutes. Rats were then left for 1 hour to 7 days, to allow the retina to reperfuse. Retinas were dissected, the mRNA and protein isolated, and Northern and Western blot analyses conducted to detect changes in expression of Hsp27, -70, and -90. Immunohistochemical studies were used to identify retinal regions where Hsp changes occurred. Selected animals were subjected to a second ischemic event, 60 minutes in duration, to correlate the changes in expression of Hsp with functional protection of the retina from ischemic injury. **RESULTS:** In control and sham-treated animals retinal Hsp27, -70, and -90 mRNAs were detectable. Five hours after retinal preconditioning, levels of Hsp27 mRNA were elevated above control levels, and 24 hours later, mRNA levels increased 200% over basal levels. Hsp27 expression remained elevated for up to 72 hours and then began to return to control levels. Hsp27 protein levels were increased by 200% over basal levels 24 hours after retinal preconditioning, remained at this level for 72 hours, and then returned to control levels. In contrast, no consistent change in Hsp70 or -90 mRNA or protein levels was observed during the course of the study. Immunohistochemical studies demonstrated that the increase in expression of Hsp27 was localized to neuronal and non-neuronal cells in the inner layers of the retina. Electroretinography studies demonstrated a strong correlation between the protection of retinal function from ischemic injury and the expression of Hsp27. **CONCLUSIONS:** These results provide evidence that the induction of Hsp27 is a gene-specific event associated with ischemic preconditioning in the retina. This increase in expression of Hsp27 occurs in both neuronal and non-neuronal retinal cells, and appears to be one component of the neuroprotective events induced by ischemic preconditioning in the retina.

PMID: 12601062 [PubMed - indexed for MEDLINE]

Increasing expression of tissue plasminogen activator and plasminogen activator inhibitor type 2 in dog gingival tissues with progressive inflammation.

Lindberg P, Kinnby B, Lecander I, Lang NP, Matsson L.

Center for Oral Health Sciences, Malmo University, S-214 21 Malmo, Sweden.
pia.lindberg@od.mah.se

Urokinase and tissue-type plasminogen activators (u-PA and t-PA) are serine proteases that convert plasminogen into plasmin, which degrades matrix proteins and activates metalloproteinases. The PAs are balanced by specific inhibitors (PAI-1 and PAI-2). Local production of t-PA and PAI-2 was recently demonstrated in human gingival tissues. The aim now was to investigate the production and localization of t-PA and PAI-2 in gingival tissues from dogs in three well-defined periodontal conditions; clinically healthy gingiva, chronic gingivitis and an initial stage of ligature-induced loss of attachment. At the start of the experiment the gingiva showed clear signs of inflammation. Clinically healthy gingiva were obtained after 21 days period of intense oral hygiene. Attachment loss was induced by placing rubber ligatures around the neck of some teeth. Biopsies were taken from areas representing the different conditions and prepared for in situ hybridization and immunohistochemistry. In clinically healthy gingiva both t-PA mRNA and antigen were expressed in a thin outer layer of the sulcular and junctional epithelia. No t-PA signals or staining were seen in connective tissue. Both mRNA signaling and immunostaining for t-PA were stronger in chronic gingivitis. In areas with loss of attachment, t-PA mRNA as well as antigen were found in the sulcular and junctional epithelia to a similar degree as in gingivitis. Occasionally the connective tissue was involved, especially in connection with vessels. PAI-2 mRNA was seen in a thin outer layer of the sulcular and junctional epithelia in clinically healthy gingiva, but no signals were seen in connective tissue. PAI-2 antigen was found primarily in the outer layer of the sulcular and junctional epithelia. Some cells in the connective tissue were stained. In gingivitis, PAI-2 signals were mainly found in the same locations, but more intense and extending towards the connective tissue. Immunostaining was seen in the outer half of the sulcular and junctional epithelia as well as in the upper part of the connective tissue, close to the sulcular epithelium. In sites with loss of attachment, PAI-2 mRNA was found throughout the sulcular and junctional epithelia, as was the antigen, which stained intensely. No PAI-2 mRNA was seen in connective tissue; the antigen was found scattered, especially near vessels. This study shows that the expression of both t-PA and PAI-2 increases with experimental gingival inflammation in the dog, and furthermore, the two techniques demonstrate a strong correlation between the topographical distribution of the site of protein synthesis and the tissue location of the antigens for both t-PA and PAI-2. The distribution correlates well with previous findings in humans.

Effect of duration of fixation on quantitative reverse transcription polymerase chain reaction analyses.

Macabeo-Ong M, Ginzinger DG, Dekker N, McMillan A, Regezi JA, Wong DT, Jordan RC.

Oral Pathology, Department of Stomatology, University of California San Francisco, California 94143-0424, USA.

Increasingly, there is the need to analyze gene expression in tumor tissues and correlate these findings with clinical outcome. Because there are few tissue banks containing enough frozen material suitable for large-scale genetic analyses, methods to isolate and quantify messenger RNA (mRNA) from formalin-fixed, paraffin-embedded tissue sections are needed. Recovery of RNA from routinely processed biopsies and quantification by the polymerase chain reaction (PCR) has been reported; however, the effects of formalin fixation have not been well studied. We used a proteinase K-salt precipitation RNA isolation protocol followed by TaqMan quantitative PCR to compare the effect of formalin fixation for 24, 48, and 72 hours and for 1 week in normal (2), oral epithelial dysplasia (3), and oral squamous cell carcinoma (4) specimens yielding 9 fresh and 36 formalin-fixed samples. We also compared mRNA and protein expression levels using immunohistochemistry for epidermal growth factor receptor (EGFR), matrix metalloproteinase (MMP)-1, p21, and vascular endothelial growth factor (VEGF) in 15 randomly selected and routinely processed oral carcinomas. We were able to extract RNA suitable for quantitative reverse transcription (RT) from all fresh (9/9) and formalin-fixed (36/36) specimens fixed for differing lengths of time and from all (15/15) randomly selected oral squamous cell carcinoma. We found that prolonged formalin fixation (>48 h) had a detrimental effect on quantitative RT polymerase chain reaction results that was most marked for MMP-1 and VEGF but less evident for p21 and EGFR. Comparisons of quantitative RT polymerase chain reaction and immunohistochemistry showed that for all markers, except p21, there was good correlation between mRNA and protein levels. p21 mRNA was overexpressed in only one case, but protein levels were elevated in all but one tumor, consistent with the established translational regulation of p21. These results show that RNA can be reliably isolated from formalin-fixed, paraffin-embedded tissue sections and can produce reliable quantitative RT-PCR data. However, results for some markers are adversely affected by prolonged formalin fixation times.

PMID: 12218216 [PubMed - indexed for MEDLINE]



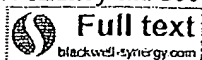
Tightly regulated and inducible expression of a yoked hormone-receptor complex in HEK 293 cells.

Meehan TP, Puett D, Narayan P.

Department of Biochemistry and Molecular Biology, University of Georgia, Athens, Georgia 30602, USA.

We have previously reported the construction of a constitutively active luteinizing hormone receptor by covalently linking a fused heterodimeric hormone to the extracellular domain of the G protein-coupled receptor. This yoked hormone-receptor complex (YHR) was found to produce high levels of cAMP in the absence of exogenous hormone. Stable lines expressing YHR were generated in HEK 293 cells to obtain lines with different expression levels; however, in a relatively short time of continued passage, it was found that YHR expression was greatly reduced. Herein, we describe the development of clonal lines of HEK 293 cells in which the expression of YHR is under the control of a tetracycline-regulated system. Characterization of clonal lines revealed tight control of YHR expression both by dose and time of incubation with doxycycline. These experiments demonstrated a good correlation between expression levels of the receptor and basal cAMP production. Moreover, the reduction in receptor expression following doxycycline removal revealed that YHR mRNA and protein decayed at similar rates, again suggesting a strong linkage between mRNA and protein levels. The controlled expression of YHR in this cell system will allow for a more detailed analysis of the signaling properties associated with constitutive receptor activation and may prove to be advantageous in developmental studies with transgenic animals.

PMID: 14766006 [PubMed - indexed for MEDLINE]



Overexpression of chemokines, fibrogenic cytokines, and myofibroblasts in human membranous nephropathy.

Mezzano SA, Droguett MA, Burgos ME, Ardiles LG, Aros CA, Caorsi I, Egido J.

Division of Nephrology, School of Medicine, Universidad Austral, Valdivia, Chile.
smezzano@uach.cl

Overexpression of chemokines, fibrogenic cytokines, and myofibroblasts in human membranous nephropathy. **BACKGROUND:** Proteinuria plays a central role in the progression of glomerular disease, and there is growing evidence suggesting that it may determine tubular cell activation with release of chemokines and fibrogenic factors, leading to interstitial inflammatory reaction. However, most studies on this subject have been performed in experimental models, and the experience in human kidney biopsies has been scarce. We analyzed the tissue sections of patients with idiopathic membranous nephropathy (IMN), a noninflammatory glomerular disease that may follow a progressive disease with heavy persistent proteinuria, interstitial cell infiltration, and decline of renal function. **METHODS:** Paraffin-embedded biopsy specimens from 25 patients with IMN (13 progressive and 12 nonprogressive) were retrospectively studied by immunohistochemistry [monocyte chemoattractant protein-1 (MCP-1), regulated on activation normal T-cell expressed and secreted chemokine (RANTES), osteopontin (OPN), platelet-derived growth factor-BB (PD-GF-BB)] and in situ hybridization [MCP-1, RANTES, PDGF-BB, transforming growth factor-beta1 (TGF-beta1)]. Moreover, we studied the presence of myofibroblasts, which were identified by the expression of alpha-smooth muscle actin (alpha-SMA), the monocytes/macrophages (CD68-positive cells), and T-cell infiltration (CD4+ and CD8+ cells). All of the patients were nephrotic and without treatment at time of the biopsy. **RESULTS:** A strong up-regulation of MCP-1, RANTES, and OPN expression was observed, mainly in tubular epithelial cells, with a significant major intensity in the progressive IMN patients. A strong correlation between the mRNA expression and the corresponding protein was noted. The presence of these chemokines and OPN was associated with interstitial cell infiltration. TGF-beta and PDGF were also up-regulated, mainly in tubular epithelial cells, with a stronger expression in the progressive IMN, and an association with the presence of myofibroblasts was found. **CONCLUSIONS:** Patients with severe proteinuria and progressive IMN have an overexpression in tubular epithelial cells of the chemokines MCP-1, RANTES, and OPN and the profibrogenic cytokines PDGF-BB and TGF-beta. Because this up-regulation was associated with an interstitial accumulation of mononuclear cells and an increase in myofibroblastic activity, it is suggested that those mediators are potential predictors of progression in IMN. Finally, based on experimental data and the findings of this article, we speculate that severe proteinuria is the main factor responsible for the up-regulation of these factors in tubular epithelial cells.



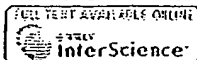
Decreased uncoupling protein expression and intramyocytic triglyceride depletion in formerly obese subjects.

Mingrone G, Rosa G, Greco AV, Manco M, Vega N, Hesselink MK, Castagneto M, Schrauwen P, Vidal H.

Istituto di Clinica Medica and. Clinica Chirurgica and Centro CNR Fisiopatologia Shock, Universita Cattolica S Cuore, Rome, Italy. gmingrone@rm.unicatt.it

OBJECTIVE: To examine the muscular uncoupling protein expression 2 (UCP2) and UCP3 gene expression in morbid obese subjects before and after bariatric surgery [bilio-pancreatic diversion (BPD)]. **RESEARCH METHODS AND PROCEDURES:** Eleven obese subjects (BMI = 49 ± 2 kg/m²) were studied before BPD and 24 months after BPD. Skeletal muscle UCP2 and UCP3 mRNA was measured using reverse transcriptase-competitive polymerase chain reaction and UCP3 protein by Western blotting. Intramyocytic triglycerides were quantified by high-performance liquid chromatography. Twenty-four-hour energy expenditure and respiratory quotient (RQ) were measured in a respiratory chamber. **RESULTS:** After BPD, the average weight loss was approximately 38%. Nonprotein RQ was increased in the postobese subjects (0.73 ± 0.00 vs. 0.83 ± 0.02 , $p < 0.001$). The intramyocytic triglyceride level dropped (3.66 ± 0.16 to 1.60 ± 0.29 mg/100 mg of fresh tissue, $p < 0.0001$) after BPD. Expression of UCP2 and UCP3 mRNA was significantly reduced (from $35.9 \pm 6.1\%$ to $18.6 \pm 4.5\%$ of cyclophilin, $p = 0.02$; from $60.2 \pm 14.0\%$ to $33.4 \pm 8.5\%$, $p = 0.03$; respectively). UCP3 protein content was also significantly reduced (272.19 ± 84.13 vs. 175.78 ± 60.31 , AU, $p = 0.04$). A multiple regression analysis ($R(2) = 0.90$) showed that IMTG levels ($p = 0.007$) represented the most powerful independent variable for predicting UCP3 variation. **DISCUSSION:** The strong correlation of UCP expression and decrease in IMTG levels suggests that triglyceride content plays an even more important role in the regulation of UCP gene expression than the circulating levels of free fatty acids or the achieved degree of weight loss.

PMID: 12740453 [PubMed - indexed for MEDLINE]



Urokinase-mediated posttranscriptional regulation of urokinase-receptor expression in non small cell lung carcinoma.

Montuori N, Mattiello A, Mancini A, Tagliatela P, Caputi M, Rossi G, Ragno P.

Istituto di Endocrinologia ed Oncologia Sperimentale, Consiglio Nazionale delle Ricerche, Naples, Italy.

The urokinase-type plasminogen activator (uPA) and its cellular receptor (uPAR) are involved in the proteolytic cascade required for tumor cell dissemination and metastasis, and are highly expressed in many human tumors. We have recently reported that uPA, independently of its enzymatic activity, is able to increase the expression of its own receptor in uPAR-transfected kidney cells at a posttranscriptional level. In fact, uPA, upon binding uPAR, modulates the activity and/or the level of a mRNA-stabilizing factor that binds the coding region of uPAR-mRNA. We now investigate the relevance of uPA-mediated posttranscriptional regulation of uPAR expression in non small cell lung carcinoma (NSCLC), in which the up-regulation of uPAR expression is a prognostic marker. We show that uPA is able to increase uPAR expression, both at protein and mRNA levels, in primary cell cultures obtained from tumor and adjacent normal lung tissues of patients affected by NSCLC, thus suggesting that the enzyme can exert its effect in lung cells. We investigated the relationship among the levels of uPA, uPAR and uPAR-mRNA binding protein(s) in NSCLC. Lung tissue analysis of 35 NSCLC patients shows an increase of both uPA and uPAR in tumor tissues, as compared to adjacent normal tissues, in 27 patients (77%); 19 of these 27 patients also show a parallel increase of the level and/or binding activity of a cellular protein capable of binding the coding region of uPAR-mRNA. Therefore, in tumor tissues, a strong correlation is observed among these 3 parameters; uPA, uPAR and the level and/or the activity of a uPAR-mRNA binding protein. We then suggest that uPA regulates uPAR expression in NSCLC at a posttranscriptional level by increasing uPAR-stability through a cellular factor that binds the coding region of uPAR-mRNA. Copyright 2003 Wiley-Liss, Inc.

PMID: 12704669 [PubMed - indexed for MEDLINE]



DNA hypermethylation is a mechanism for loss of expression of the HLA class I genes in human esophageal squamous cell carcinomas.

Nie Y, Yang G, Song Y, Zhao X, So C, Liao J, Wang LD, Yang CS.

Laboratory for Cancer Research, College of Pharmacy, Rutgers-The State University of New Jersey, 164 Frelinghuysen Road, Piscataway, NJ 08854-8020, USA.

The three human leukocyte antigen (HLA) class I antigens, HLA-A, HLA-B and HLA-C, play important roles in the elimination of transformed cells by cytotoxic T cells. Frequent loss of expression of these antigens at the cell surface has been observed in many human cancers. Various mechanisms for post-transcriptional regulation have been proposed and tested but the molecular mechanisms for transcriptional regulation are not clear. We show by immunohistochemistry that the HLA class I antigens are absent in 26 of 29 (89%) samples of human esophageal squamous cell carcinomas (ESCC). Eleven of the 26 ESCC samples lost mRNA expression for at least one of the HLA genes, as shown by RT-PCR. DNA from the 29 pairs of ESCC and neighboring normal epithelium were examined for CpG island hypermethylation, homozygous deletion, microsatellite instability (MSI) and loss of heterozygosity (LOH). DNA from normal epithelial tissues had no detectable methylation of the CpG islands of any of these gene loci. Thirteen of 29 ESCC samples (45%) exhibited methylation of one or more of the three HLA loci and six samples (21%) exhibited methylation of all three loci. The HLA-B gene locus was most frequently methylated (38%). HLA-B mRNA expression in an ESCC cell line, where HLA-B was hypermethylated and did not express mRNA, was activated after treatment with 5-aza-2'-deoxycytidine. Homozygous deletion of these three gene loci was not observed. Relatively low rates of LOH and MSI were observed for the microsatellite markers D6S306, D6S258, D6S273 and D6S1666, close to the HLA-A, -B and -C loci, although a high ratio of LOH was observed at a nearby locus (represented by the markers D6S1051 and D6S1560), where the tumor suppressor gene p21(Waf1) resides. A strong correlation between genetic alterations and mRNA inactivation was observed in the ESCC samples. Our results indicate that HLA class I gene expression was frequently down-regulated in ESCC at both the protein and mRNA levels and that hypermethylation of the promoter regions of the HLA-A, -B and -C genes is a major mechanism of transcriptional inactivation.

PMID: 11577000 [PubMed - indexed for MEDLINE]

95: Hum Pathol. 2003 Jul;34(7):639-45.

Related Articles, Links

Comment in:

- Hum Pathol. 2003 Jul;34(7):635-8.

Human Pathology

Molecular and immunohistochemical analysis of HER2/neu oncogene in synovial sarcoma.

Nuciforo PG, Pellegrini C, Fasani R, Maggioni M, Coggi G, Parafloriti A, Bosari S.

Department of Medicine, Surgery and Dental Sciences, University of Milan, A.O.S. Paolo and IRCCS Ospedale Maggiore, Italy.

Amplification and/or overexpression of HER2/neu have been documented in many types of epithelial tumor and recently has been reported in sarcomas, particularly in osteosarcomas. But the role of HER2/neu alterations in soft tissue tumors remains poorly understood. Thus the present study investigates the expression of HER2/neu in 13 patients with synovial sarcoma (SS). In this study, HER2/neu mRNA levels were measured in frozen tissue samples using a real-time reverse transcription-polymerase chain reaction assay; protein expression was assessed by immunohistochemistry using an anti-HER2/neu polyclonal antibody. Six normal skeletal muscle specimens were used to establish basal levels of HER2/neu mRNA. HER2/neu transcripts were detected in all normal tissues and SSs. Four of 13 sarcomas (31%) demonstrated HER2/neu mRNA levels above the mean value, whereas 3 tumors (23%) displayed HER2/neu protein overexpression. Both membranous and cytoplasmic patterns of immunostaining were observed, and a strong correlation was found between protein expression and mRNA level ($P = 0.01$). Increased HER2/neu mRNA levels were significantly associated with a lower risk of developing recurrences ($P = 0.02$). Moreover, none of the patients with HER2/neu overexpression developed metastasis. Our data demonstrate that HER2/neu is expressed in SSs and that both membrane and cytoplasmic HER2/neu expression correlate with mRNA levels. Our results show that the presence of increased levels of HER2/neu in SSs is associated with a more favorable clinical course. Further studies are needed to assess the role of this oncogene in SSs and to evaluate the application of inhibitory humanized monoclonal antibodies in the treatment regimens for this malignancy.

PMID: 12874758 [PubMed - indexed for MEDLINE]

Original Contributions

Molecular and Immunohistochemical Analysis of HER2/neu Oncogene in Synovial Sarcoma

PAOLO GIOVANNI NUCIFORO, MD, CATERINA PELLEGRINI, PhD,
ROBERTA FASANI, MD, MARCO MAGGIONI, MD,
GUIDO COGGI, MD, ANTONINA PARAFIORITI, MD,
AND SILVANO BOSARI, MD

Amplification and/or overexpression of HER2/neu have been documented in many types of epithelial tumor and recently has been reported in sarcomas, particularly in osteosarcomas. But the role of HER2/neu alterations in soft tissue tumors remains poorly understood. Thus the present study investigates the expression of HER2/neu in 13 patients with synovial sarcoma (SS). In this study, HER2/neu mRNA levels were measured in frozen tissue samples using a real-time reverse transcription-polymerase chain reaction assay; protein expression was assessed by immunohistochemistry using an anti-HER2/neu polyclonal antibody. Six normal skeletal muscle specimens were used to establish basal levels of HER2/neu mRNA. HER2/neu transcripts were detected in all normal tissues and SSs. Four of 13 sarcomas (31%) demonstrated HER2/neu mRNA levels above the mean value, whereas 3 tumors (23%) displayed HER2/neu protein overexpression. Both membranous and cytoplasmic patterns of immunostaining were observed, and a strong correlation was

found between protein expression and mRNA level ($P = 0.01$). Increased HER2/neu mRNA levels were significantly associated with a lower risk of developing recurrences ($P = 0.02$). Moreover, none of the patients with HER2/neu overexpression developed metastasis. Our data demonstrate that HER2/neu is expressed in SSs and that both membrane and cytoplasmic HER2/neu expression correlate with mRNA levels. Our results show that the presence of increased levels of HER2/neu in SSs is associated with a more favorable clinical course. Further studies are needed to assess the role of this oncogene in SSs and to evaluate the application of inhibitory humanized monoclonal antibodies in the treatment regimens for this malignancy. HUM PATHOL 34:639-645. © 2003 Elsevier Inc. All rights reserved.

Key Words: HER2/neu, synovial sarcoma, real-time RT-PCR, immunohistochemistry.

Abbreviations: FISH, fluorescence in situ hybridization, RT-PCR, reverse transcription-polymerase chain reaction, SS, synovial sarcoma.

Synovial sarcoma (SS) is an aggressive soft tissue tumor that accounts for up to 10% of sarcomas, with a peak incidence in adolescents and young adults. This tumor occurs in 2 major forms, biphasic and monophasic, and it is cytogenetically characterized by the t(X;18)(p11;q11) translocation, found in >95% of cases. Although traditionally considered to be a high-grade neoplasm, recent investigations have suggested that different factors influence prognosis, including morphological and cytogenetic features, treatment strategies, the ploidy status, and the apoptotic index.¹

The development of new therapeutic advancements, such as the specific targeting of molecular alterations present in human malignancies, has brought to light the

need to identify not only prognostic factors, but also tumor features that are predictive of response to therapy.

One of the most extensively studied molecular targets for therapy is the HER-2/neu proto-oncogene. The HER-2/neu oncogene (also known as c-erbB-2), located on chromosome 17q21, is a member of the tyrosine kinase receptor family and encodes for a 185-kilodalton protein that shows 50% homology with the epidermal growth factor receptor.^{2,3} This gene is amplified and/or overexpressed in 20% to 30% of breast carcinomas^{4,5} and in various other tumors,⁶ and usually is associated with tumor aggressiveness and poor prognosis.^{7,8} Several studies have supported the value of HER-2/neu to predict the response to chemotherapy in breast cancer, and the use of recombinant humanized antibodies to HER-2/neu protein (Trastuzumab) in the care of patients with advanced, metastatic breast tumors has been approved.⁹

The role of HER-2/neu activation in soft tissue tumors remains poorly understood, and scarce molecular data backing immunohistochemical studies have been reported. HER-2/neu protein expression was immunohistochemically studied in 204 sarcomas, including 6 SSs, and overexpression was absent in all these malignant mesenchymal neoplasms.¹⁰

Recently, HER-2/neu alterations have been described in osteosarcoma, with a high incidence of pro-

From the Department of Medicine, Surgery and Dental Sciences, University of Milan, A.O.S. Paolo and IRCCS Ospedale Maggiore, Milan, Italy; Department of Pathology, Orthopedic Institute Gaetano Pini, Milan, Italy; and Interuniversity Center of Cancer Research, Milan, Italy. Accepted for publication March 5, 2003.

Supported by grants from Ministero dell'Istruzione, dell'Università e della Ricerca (MIUR-cofin 1999) and Associazione Italiana per la Ricerca sul Cancro (AIRC).

Address correspondence and reprint requests to Paolo Giovanni Nuciforo, MD, Division of Anatomic Pathology, A.O.S. Paolo, Via A. Di Rudini 8, 20142, Milano, Italy.

© 2003 Elsevier Inc. All rights reserved.

0046-8177/03/3407-0002\$30.00/0

doi:10.1016/S0046-8177(03)00238-7

RT-PCR were purchased from Applied Biosystems (Foster City, CA).

Primers and Probes

Primers and probes for β -actin and HER2/neu mRNA were chosen using the computer program Primer Express (Applied Biosystems). Sequences of the forward primer for HER2/neu mRNA (GenBank accession number X03363) were 5'-TCC TGT GTG CAC CTG GAT GAC-3' and the reverse primer 5'-CCA AAG ACC ACC CCC AAG A-3'; the sequence of the TaqMan probe was 5'(FAM)-ACC ACA ATG CCA ACC ACC GCA GA-(TAMRA)-3'. Sequences of the forward primer for β -actin mRNA (GenBank accession number X00351) were 5'-TCC TTC CTG CCC ATG GAG-3' and the reverse primer 5'-AGG AGG ACC AAT GAT CTT GAT CTT-3'; the sequence of the TaqMan probe was 5'(FAM)-CCT GTG GCA TCC ACG AAA CTA CCT TC-(TAMRA)-3'. Probes were purchased from Applied Biosystems.

Real-Time RT-PCR

To measure HER2/neu expression in these tumors we used a real-time quantitative RT-PCR based on TaqMan methodology, as previously described,¹⁷ with minor modifications. Briefly, this technique allows, by means of fluorescence emission, to find the cycling point when PCR product is detectable (Ct value or threshold cycle). As previously reported, the Ct value correlates to the starting quantity of the target mRNA.¹⁸ To normalize the amount of total RNA present in each reaction, we amplified the housekeeping gene β -actin, which is assumed to be constant in both normal samples and tumor tissues.

Our results are expressed as relative levels of HER2/neu mRNA, referred to a sample, called a "calibrator," chosen to represent 1X expression of this gene. The calibrator was a breast cancer cellular line (MCF-7)¹⁹ that was analyzed on every assay plate with the unknown samples. All of the analyzed tumors expressed n-fold HER2/neu mRNA relative to the calibrator.

The amount of target, normalized to an endogenous reference (β -actin) and relative to the calibrator, was defined by the $\Delta\Delta C_t$ method as described by Livak K (Sequence Detector User Bulletin 2; Applied Biosystems). Specifically, the formula is applied as follows:

$$\text{target amount} = 2^{-\Delta\Delta C_t}$$

where $\Delta\Delta C_t = [C_t(\text{HER2/neu sample}) - C_t(\beta\text{-actin sample})] - [C_t(\text{HER2/neu calibrator}) - C_t(\beta\text{-actin calibrator})]$.

Immunohistochemistry

Formalin-fixed, paraffin-embedded tissue sections were deparaffinized, rehydrated, and exposed to the primary antibody using the EnVision+ system (Dako, Carpinteria, CA). Primary anti-HER2/neu antibody (rabbit polyclonal antibody, catalog number A0485; Dako) was applied in a dilution of 1:2000 for 60 minutes at room temperature. Before exposure to the primary antibody, sections were microwave-treated in EDTA, pH 8.0, to retrieve antigenicity, and incubated with endogenous peroxidase-blocking solution for 10 minutes at room temperature. Positive control, constituted by a breast carcinoma showing more than 80% positive staining for HER2/neu, as well as negative control, in which the primary antibody was omitted, were stained in parallel.

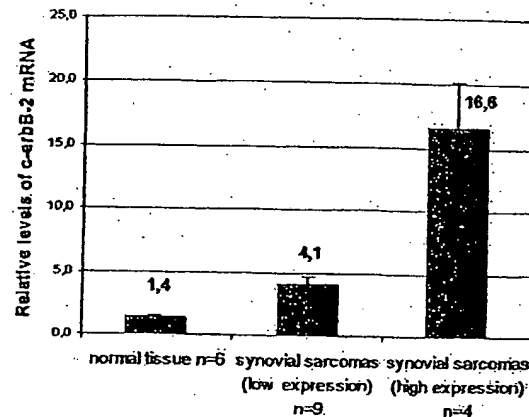


FIGURE 1. Distribution of HER2/neu mRNA levels in normal muscle tissues, and in low- and high-expression sarcomas. Data are expressed as mean and standard error of the mean for each group.

All cases were examined for both cytoplasmic and membrane immunoreactivity. Cytoplasmic staining was evaluated on a semiquantitative scale, according to Kilpatrick et al with minor modifications,²⁰ and reported as 0 (no staining or staining in <10% of cells), 1+ (weak staining in >10% of cells), 2+ (moderate staining in >10% of cells), or 3+ (strong staining in >10% of cells). The presence of a membranous pattern of staining was recorded separately and scored as absent (no staining or weak staining in <10% of cells) or present (complete and/or incomplete staining in >10% of cells). Tumors with a cytoplasmic score of 3+ were considered to have high HER2/neu protein expression.

Statistical Analysis

Statistical differences were calculated by Fisher's exact test. The *t*-test method was used to evaluate the differences between groups. Differences were considered statistically significant when *P* was <0.05.

RESULTS

HER2/neu mRNA Evaluation

All of the tissues analyzed contained detectable levels of HER2-neu mRNA. Six normal tissue samples (skeletal muscle) were used to establish basal level of HER2/neu mRNA. All the normal samples expressed very low levels of HER2/neu mRNA, ranging from 0.9 to 1.9 n (mean, 1.4 n). Among the 13 tumor samples, HER2/neu levels varied greatly, ranging from 2.1 to 24 n. Setting a cutoff level at 7.9 n (a value that represents the mean value of expression distribution of the SSs), 9 cases (69%) had low HER2/neu expression and 4 cases (31%) had high HER2/neu expression (Fig 1; Table 1). The difference between the 2 groups (low and high HER2/neu tumors) was statistically significant (*P* = 0.0004).

TABLE 2. Correlation Between Clinicopathologic Features and HER2/neu Expression as Detected by IHC and RT-PCR

Variable	HER2/neu					
	IHC			PCR		
	L	H	P value	L	H	P value
Age (years)						
<40	3	3		3	3	
>40	7	0	NS	6	1	NS
Sex						
Female	8	0		7	1	
Male	2	3	0.03	2	3	NS
Tumor size (cm)						
<5	3	2		3	2	
>5	7	1	NS	6	2	NS
Histological grade						
II	3	0		3	0	
III	7	3	NS	6	4	NS
Histological type						
MF	5	1		5	1	
BF	2	1		2	1	
PD	3	1	NS	2	2	NS
Chemo/Radiotherapy*						
Yes	4	2		3	3	
No	5	1	NS	5	1	NS
Recurrence†						
Yes	5	0		5	0	
No	2	3	NS	1	4	0.02
Metastasis†						
Yes	3	0		3	0	
No	4	3	NS	3	4	NS

Abbreviations: L, low expression; H, high expression; NS, not significant; MF, monophasic fibrous; BF, biphasic; PD, poorly differentiated (including MF and BF with poorly differentiated areas).

*Information not available for case 7.

†Cases 7, 12, and 13 were excluded from the analysis.

clinicopathologic features, including local recurrence and metastatic disease. Two cases (cases 12 and 13) with follow-up less than 12 months and 1 case (case 7) for which clinical information was not available were excluded from the analysis of recurrences and metastatic behavior.

No correlation was observed between HER2/neu mRNA expression and age, sex, tumor size, tumor grade, histotype, and metastasis. A correlation between sex of the patients and HER2/neu protein expression was found. In fact, none of the female patients showed high HER2/neu protein expression ($P = 0.03$). Patients with high Her2/neu mRNA levels had a lower risk of recurrence than those with low Her2/neu mRNA levels ($P = 0.02$). None of the cases with high HER2/neu mRNA levels developed metastatic foci, although the small number of observations precluded reaching statistical significance ($P = 0.1$). Results are detailed in Table 2.

DISCUSSION

The present work provides the first combined molecular by real-time RT-PCR and immunohistochemical evidence that HER2/neu overexpression occurs in SSs.

Our results indicate that this parameter may provide prognostic information and suggest that a specific therapy with humanized monoclonal antibodies against HER2/neu may be considered in a significant number of SSs.

The HER2/neu oncogene has been extensively investigated as a prognostic factor and more recently as a predictor of response to therapy. It has been demonstrated in breast cancer, where HER2/neu overexpression is usually associated with gene amplification,²¹ and in other epithelial tumors, including ovarian, gastric, lung, and urinary bladder carcinomas.

HER2/neu amplification/overexpression appears to be an early event in oncogenic transformation by interacting with other members of the HER family.³ In breast cancer, it is involved in cell cycle and apoptotic pathways through the antiapoptotic effects mediated by p53 and p21 deregulation.^{22,23}

Whether HER2/neu overexpression plays an important role in mesenchymal neoplasms remains controversial. An immunohistochemical study of sarcomas, using a monoclonal antibody, reported no evidence of immunoreactivity for HER2/neu in 6 SSs as well as in other 197 mesenchymal tumors, with cytoplasmic reactivity observed only in 1 case of peripheral neuroepithelioma.¹⁰ A recent investigation reported gene expression profiles of 41 soft tissue tumors with cDNA microarray analysis. Among these sarcomas, 6 monophasic SSs were characterized by a unique expression pattern of a cluster of 104 genes, including the epidermal growth factor receptor, which shows 50% homology with the HER2/neu gene.²⁴ These data also suggest that the erb-B receptor family plays a significant role in SS. It has been demonstrated that a variable number of osteosarcomas overexpress HER2/neu.¹¹⁻¹⁵ However, more recent studies^{20,25,26} were unable to detect any HER2/neu gene amplification and/or overexpression using fluorescence in situ hybridization (FISH), RT-PCR, and immunohistochemistry.

Differences in the techniques used may play an important role and explain (at least in part) these discrepancies. HER2/neu alterations can be evaluated using different techniques including immunohistochemistry, FISH, Southern hybridization, Northern blot, and competitive, differential, or real-time PCR.²⁷ Immunohistochemistry is the most common method for detection of HER2/neu overexpression, but it is significantly affected by the sensitivity and specificity of the antibodies used, the type of tissue (frozen versus formalin-fixed), and the various interpretative criteria and scoring systems used to evaluate cases. Indeed, most studies of HER2/neu expression in osteosarcoma used immunohistochemical techniques, with different monoclonal or polyclonal antibodies. The discrepancy in results may stem from the use of different antibodies, as well as a lack of standardized evaluation.

For these reasons, to evaluate HER2/neu immunoreactivity in our study, we used a polyclonal antibody (Dako, Carpinteria, CA), arguably the most diffuse and thoroughly tested antibody for HER2/neu assessment. Furthermore, we investigated HER2/neu mRNA ex-

- breast cancer that overexpress *Her2/neu*. *N Engl J Med* 344:783-792, 2001
10. George E, Niehans GA, Swanson PE, et al: Overexpression of the *c-erbB-2* oncogene in sarcomas and small round cell tumors of childhood. An immunohistochemical investigation. *Arch Pathol Lab Med* 116:1033-1035, 1992
11. Onda M, Matsuda S, Higaki S, et al: *ErbB-2* expression is correlated with poor prognosis for patients with osteosarcoma. *Cancer* 77:71-78, 1996
12. Gorlick R, Huvois AG, Heller G, et al: Expression of *HER2/erbB-2* correlates with survival in osteosarcoma. *J Clin Oncol* 17:2781-2788, 1999
13. Akatsuka T, Wada T, Kokai Y, et al: Loss of *ErbB2* expression in pulmonary metastatic lesions in osteosarcoma. *Oncology* 60:361-366, 2001
14. Morris CD, Gorlick R, Huvois G, et al: Human epidermal growth factor receptor 2 as a prognostic indicator in osteogenic sarcoma. *Clin Orthop* 382:59-65, 2001
15. Akatsuka T, Wada T, Kokai Y, et al: *ErbB2* expression is correlated with increased survival of patients with osteosarcoma. *Cancer* 94:1397-1404, 2002
16. Coindre JM, Trojani M, Contesso G, et al: Reproducibility of a histopathologic grading system for adult soft tissue sarcoma. *Cancer* 58:306-309, 1986
17. Marchetti A, Pellegrini C, Buttitta F, et al: Prediction of survival in stage I lung carcinoma patients by telomerase function evaluation. *Lab Invest* 82:729-736, 2002
18. Heid CA, Stevens J, Livak KJ, et al: Real time quantitative PCR. *Genome Res* 6:986-994, 1996
19. Kraus MH, Popescu NC, Amsbaugh SC, et al: Overexpression of the EGF receptor-related proto-oncogene *erbB-2* in human mammary tumor cell lines by different molecular mechanisms. *EMBO J* 6:605-610, 1987
20. Kilpatrick SE, Geisinger KR, King TS, et al: Clinicopathologic analysis of *HER-2/neu* immunoreexpression among various histologic subtypes and grades of osteosarcoma. *Mod Pathol* 14:1277-1283, 2001
21. Slamon DJ, Godolphin W, Jones LA, et al: Studies of the *HER-2/neu* proto-oncogene in human breast and ovarian cancer. *Science* 244:707-712, 1989
22. Harari D, Yarden Y: Molecular mechanisms underlying *ErbB2/HER2* action in breast cancer. *Oncogene* 19:6102-6114, 2000
23. Zhou BP, Liao Y, Xia W, et al: *HER-2/neu* induces p53 ubiquitination via Akt-mediated MDM2 phosphorylation. *Nat Cell Biol* 3:973-982, 2001
24. Nielsen OT, West RB, Linn SC, et al: Molecular characterization of soft tissue tumours: A gene expression study. *Lancet* 359:1301-1307, 2002
25. Thomas DG, Giordano TJ, Sanders D, et al: Absence of *HER2/neu* gene expression in osteosarcoma and skeletal Ewing's sarcoma. *Clin Cancer Res* 8:788-793, 2002
26. Maitra A, Wanzer D, Weinberg AG, et al: Amplification of the *Her-2/neu* oncogene is uncommon in pediatric osteosarcomas. *Cancer* 92:677-683, 2001
27. Hanna W, Kahn HJ, Trudeau M: Evaluation of *HER-2/neu* (*erbB-2*) status in breast cancer: From bench to bedside. *Mod Pathol* 12:827-834, 1999
28. Naber SP, Tsutsumi Y, Yin S, et al: Strategies for the analysis of oncogene overexpression. Studies of the *neu* oncogene in breast carcinoma. *Am J Clin Pathol* 94:125-136, 1990
29. Tetu B, Brisson J: Prognostic significance of *HER-2/neu* oncoprotein expression in node-positive breast cancer. The influence of the pattern of immunostaining and adjuvant therapy. *Cancer* 73:2359-2365, 1994
30. Coombs LM, Pigott DA, Sweeney E, et al: Amplification and over-expression of *c-erbB-2* in transitional cell carcinoma of the urinary bladder. *Br J Cancer* 63:601-608, 1991
31. Kay EW, Mulcahy H, Walsh CB, et al: Cytoplasmic *c-erbB-2* protein expression correlates with survival in Duke's B colorectal carcinoma. *Histopathology* 25:455-461, 1994
32. Roychowdhury DF, Tseng A Jr, Fu KK, et al: New prognostic factors in nasopharyngeal carcinoma: Tumor angiogenesis and *c-erbB-2* expression. *Cancer* 77:1419-1426, 1996
33. Hall PA, Hughes CM, Staddon SL, et al: The *c-erb B-2* proto-oncogene in human pancreatic cancer. *J Pathol* 161:195-200, 1990
34. Sugg SL, Ezzat S, Zheng L, et al: Cytoplasmic staining of *erbB-2* but not mRNA levels correlates with differentiation in human thyroid neoplasia. *Clin Endocrinol (Oxf)* 49:629-637, 1998
35. Keshgegian AA, Cnaan A: *erbB-2* oncoprotein expression in breast carcinoma. Poor prognosis associated with high degree of cytoplasmic positivity using CB-11 antibody. *Am J Clin Pathol* 108:456-463, 1997
36. Kawauchi S, Fukuda T, Oda Y, et al: Prognostic significance of apoptosis in synovial sarcoma: Correlation with clinicopathologic parameters, cell proliferative activity, and expression of apoptosis-related proteins. *Mod Pathol* 13:755-765, 2000
37. Rosen G, Forscher C, Lowenbraun S, et al: Synovial sarcoma: Uniform response of metastasis to high dose ifosfamide. *Cancer* 73:2506-2511, 1994
38. Muss HB, Thor AD, Berry DA, et al: *c-erbB-2* expression and response to adjuvant therapy in women with node-positive early breast cancer. *N Engl J Med* 330:1260-1266, 1994



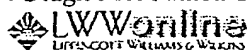
Expression of bcr-abl mRNA in individual chronic myelogenous leukaemia cells as determined by in situ amplification.

Pachmann K, Zhao S, Schenk T, Kantarjian H, El-Naggar AK, Siciliano MJ, Guo JQ, Arlinghaus RB, Andreeff M.

The University of Texas M.D. Anderson Cancer Center, Department of Molecular Haematology and Therapy, 1515 Holcombe Boulevard, Houston, TX 77030, USA.

We present the results of a novel method developed for evaluation of in situ amplification, a molecular genetic method at the cellular level. Reverse transcription polymerase chain reaction (RT-PCR) was used to study bcr-abl transcript levels in individual cells from patients with chronic myelogenous leukaemia (CML). After hybridizing a fluorochrome-labelled probe to the cell-bound RT-PCR product, bcr-abl mRNA-positive cells were determined using image analysis. A dilution series of bcr-abl-positive BV173 into normal cells showed a good correlation between expected and actual values. In 25 CML samples, the percentage of in situ PCR-positive cells showed an excellent correlation with cytogenetic results ($r = 0.94$, $P < 0.0001$), interphase fluorescence in situ hybridization (FISH) ($r = 0.95$, $P = 0.001$) and hypermetaphase FISH ($r = 0.81$, $P < 0.001$). The fluorescence intensity was higher in residual CML cells after interferon (IFN) treatment than in newly diagnosed patients ($P = 0.004$), and was highest in late-stage CML resistant to IFN therapy and lowest in CML blast crisis ($P = 0.001$). Mean fluorescence values correlated with bcr-abl protein levels, as determined by Western blot analysis ($r = 0.62$). Laser scanning cytometry allowing automated analysis of large numbers of cells confirmed the results. Thus, fluorescence in situ PCR provides a novel and quantitative approach for monitoring tumour load and bcr-abl transcript levels in CML.

PMID: 11260080 [PubMed - indexed for MEDLINE]



Correlative immunohistochemical and reverse transcriptase polymerase chain reaction analysis of somatostatin receptor type 2 in neuroendocrine tumors of the lung.

Papotti M, Croce S, Macri L, Funaro A, Pecchioni C, Schindler M, Bussolati G.

Department of Biomedical Sciences and Oncology, University of Turin, Italy.

Somatostatin receptors type 2 (sst2) have been frequently detected in neuroendocrine tumors and bind somatostatin analogues, such as octreotide, with high affinity. Receptor autoradiography, specific mRNA detection and, more recently, antisst2 polyclonal antibodies are currently employed to reveal sst2. The aim of the present study was to investigate by three different techniques the presence of sst2 in a series of 26 neuroendocrine tumors of the lung in which fresh frozen tissue and paraffin sections were available. It was possible, therefore, to compare, in individual cases, RNA analysis studied by reverse transcriptase polymerase chain reaction (RT-PCR), in situ hybridization (ISH), and immunohistochemistry. A series of 20 nonneuroendocrine lung carcinoma samples served as controls. RT-PCR was positive for sst2 in 22 of 26 samples, including 15 of 15 typical carcinoids, 5 of 6 atypical carcinoids, and 2 of 5 small-cell carcinomas. The sst2 mRNA signal obtained by RT-PCR was strong in the majority (87%) of typical carcinoids and of variable intensity in atypical carcinoids and small-cell carcinomas. A weakly positive signal was observed in 5 of 20 control samples. In immunohistochemistry, two different antibodies (anti-sst2) were employed, including a monoclonal antibody, generated in the Department of Pathology, University of Turin. In the majority of samples a good correlation between sst2 mRNA (as detected by RT-PCR) and sst2 protein expression (as detected by immunohistochemistry) was observed. However, one atypical carcinoid and one small-cell carcinoma had focal immunostaining but no RT-PCR signal. ISH performed in selected samples paralleled the results obtained with the other techniques. A low sst2 expression was associated with high grade neuroendocrine tumors and with aggressive behavior. It is concluded that 1) neuroendocrine tumors of the lung express sst2, and there is a correlation between the mRNA amount and the degree of differentiation; 2) immunohistochemistry and ISH are reliable tools to demonstrate sst2 in these tumors; and 3) sst2 identification in tissue sections may provide information on the diagnostic or therapeutic usefulness of somatostatin analogues in individual patients with neuroendocrine tumors.

PMID: 10718213 [PubMed - indexed for MEDLINE]

Volume 9, Number 1, March 2000

Diagnostic Molecular Pathology

WESTON LIBRARY

MAR 07 2000

35125 CLINICAL SCIENCE CENTER
800 HIGHLAND AVE MADISON WI 53792

Co-Editors

Robert A. DeLeellis, M.D.

Robert A. McKee, M.D.



LIPPINCOTT WILLIAMS & WILKINS

Diagnostic Molecular Pathology

Volume 9 □ Number 1 □ March 2000

ORIGINAL ARTICLES

- 1 Strong Association of SYT-SSX Fusion Type and Morphologic Epithelial Differentiation in Synovial Sarcoma
Cristina R. Antonescu, Akira Kawai, Denis H. Leung, Fulvio Lonardo, James M. Woodruff, John H. Healey, and Marc Ladanyi
- 9 Clinical Relevance of Molecular Diagnosis in Childhood Rhabdomyosarcoma
Ana Tobar, Smadar Avigad, Meira Zoldan, Celia Mor, Yakov Goshen, and Rina Zaizov
- 14 Accumulation of Chromosomal Imbalances From Intraductal Proliferative Lesions to Adjacent In Situ and Invasive Ductal Breast Cancer
Michaela M. Aubele, Margaret C. Cummings, Anita E. Mattis, Horst F. Zitzelsberger, Axel K. Walch, Markus Kremer, Heinz Höfler, and Martin Werner
- 20 Routine Analysis of p53 Mutation in Clinical Breast Tumor Specimens Using Fluorescence-Based Polymerase Chain Reaction and Single Strand Conformation Polymorphism
Barry Iacopetta, Hany Elsahh, Fabienne Grieu, David Joseph, Greg Sterrett, and Peter Robbins
- 26 Tumor-Associated Overexpression of the Soluble T1-S Receptor in Lymph Node-Negative Breast Cancer
Anne Katrin Werenskiöld, Dieter Prechtel, Nadia Harbeck, and Heinz Höfler

(continued on next page)

Listed in *Index Medicus*, *Current Awareness in Biological Sciences*, *EMBASE/Excerpta Medica*, *Current Contents/Life Sciences*, and *Science Citation Index*.

Diagnostic Molecular Pathology (ISSN 1052-9551) is published four times per year in March, June, September, and December by Lippincott Williams & Wilkins, Inc., 12107 Insurance Way, Hagerstown, MD 21740. Business offices are located at 530 Walnut Street, Philadelphia, PA 19106-3621. Printed in the U.S.A. Periodicals postage paid at Hagerstown, MD, and at additional mailing offices.

Copyright © 2000 by Lippincott Williams & Wilkins, Inc. All rights reserved.

Address for subscription information, orders, or changes of address: (except Japan) 12107 Insurance Way, Hagerstown, MD 21740, or call 1-800-638-3030; in Maryland, call collect 301-714-2300. In Japan, contact Igaku-Shoin, Ltd., 1-28-36 Hongo, Bunkyo-ku, Tokyo 113, Japan; phone: 81-3-3817-5675; fax: 81-3-3815-6776.

Annual subscription rates: U.S.: \$143.00 individual, \$309.00 institution; Canada and Mexico: \$165.00 individual, \$232.00 institution. (The Canadian GST Tax of 7% will be added to the subscription price of all orders shipped to Canada. The Lippincott Williams & Wilkins, Inc. GST Identification No. is 895524239.) Canada Post International Publications Mail Product Sales Agreement No. 0616168; all other countries (except Japan): \$171.00 individual, \$258.00 institution. (Prices outside North America include \$6.00 for air freight shipping; air freight delivery occurs within 7-21 days worldwide.) International subscriptions must be prepaid. Single copies, when available, may be ordered from the publisher. Single copies \$58.00. Prices are subject to change without notice. Copies will be replaced without charge if the publisher receives a request within 90 days of the mailing date, both in the U.S. and worldwide.

Postmaster: Send changes of address to *Diagnostic Molecular Pathology*, P.O. Box 1550, Hagerstown, MD 21740.

WESTON LIBRARY
MAR 07 2000
J8120 CLINICAL SCIENCE CENTER
800 HIGHLAND AVE MADISON WI 53792

This material may be protected by Copyright law (Title 17 U.S. Code)

Correlative Immunohistochemical and Reverse Transcriptase Polymerase Chain Reaction Analysis of Somatostatin Receptor Type 2 in Neuroendocrine Tumors of the Lung

Mauro Papotti, M.D., Sabrina Croce, M.D., Luigia Maci, M.D.,
Aola Funaro, Ph.D., Carla Pecchioni, Marcus Schindler, M.D., and
Gianni Bussolati, M.D., F.R.C.Path.

Somatostatin receptors type 2 (sst2) have been frequently detected in neuroendocrine tumors and bind somatostatin analogues, such as octreotide, with high affinity. Receptor autoradiography, specific mRNA detection and, more recently, anti-sst2 polyclonal antibodies are currently employed to reveal sst2. The aim of the present study was to investigate by three different techniques the presence of sst2 in a series of 26 neuroendocrine tumors of the lung in which fresh frozen tissue and paraffin sections were available. It was possible, therefore, to compare, in individual cases, RNA analysis studied by reverse transcriptase polymerase chain reaction (RT-PCR), in situ hybridization (ISH), and immunohistochemistry. A series of 20 nonneuroendocrine lung carcinoma samples served as controls. RT-PCR was positive for sst2 in 22 of 26 samples, including 15 of 15 typical carcinoids, 5 of 6 atypical carcinoids, and 2 of 5 small-cell carcinomas. The sst2 mRNA signal obtained by RT-PCR was strong in the majority (87%) of typical carcinoids and of variable intensity in atypical carcinoids and small-cell carcinomas. A weakly positive signal was observed in 5 of 20 control samples. In immunohistochemistry, two different antibodies (anti-sst2) were employed, including a monoclonal antibody, generated in the Department of Pathology, University of Turin. In the majority of samples a good correlation between sst2 mRNA (as detected by RT-PCR) and sst2 protein expression (as detected by immunohistochemistry) was observed. However, one atypical carcinoid and one small-cell carcinoma had focal immunostaining but no RT-PCR signal. ISH performed in selected samples paralleled the results obtained with the other techniques. A low sst2 expression was associated with

high grade neuroendocrine tumors and with aggressive behavior. It is concluded that 1) neuroendocrine tumors of the lung express sst2, and there is a correlation between the mRNA amount and the degree of differentiation; 2) immunohistochemistry and ISH are reliable tools to demonstrate sst2 in these tumors; and 3) sst2 identification in tissue sections may provide information on the diagnostic or therapeutic usefulness of somatostatin analogues in individual patients with neuroendocrine tumors.

Key Words: Neuroendocrine—Lung—Tumors—Somatostatin receptors—Immunohistochemistry—Small cell carcinoma—Reverse transcriptase polymerase chain reaction.

Diagn Mol Pathol 9(1): 47-57, 2000.

The somatostatin receptor family (sst) includes at least five isoforms that have been recently identified and characterized (18,32,41). The ssts are widely distributed in normal human tissues and in human tumors. Sst type 2 is more commonly detected in neuroendocrine tumors (32,37) and binds the somatostatin analogue octreotide with high affinity.

Sst localization had originally been demonstrated by means of binding assays of radiolabeled somatostatin analogues (20,25,31). Subsequently, specific sst messenger RNA (mRNA) detection was obtained by means of in situ hybridization (ISH) and reverse transcriptase polymerase chain reaction (RT-PCR) (14,32,37). Recently, polyclonal antibodies specific for different isoforms of sst were produced and used in immunohistochemistry (10,12,15,18,30,35,36). Given the well-known heterogeneity of neoplastic populations, in situ methods (immunohistochemistry and ISH) allow a more definite mapping of the distribution of the receptor in such tissues.

From the Department of Biomedical Sciences and Oncology (M.P., S.C., L.M., A.F., C.P., G.B.), University of Turin, Italy; and Glaxo Institute of Applied Pharmacology (M.S.), University of Cambridge, United Kingdom.

Supported by grants from the Regione Piemonte (grant no. 165 of Research Project DGR 34-23230) and Ministry of University (Rome), Italy.

A.F. is the recipient of a Research Contract by the University of Turin.

Address correspondence and reprint requests to Prof. M. Papotti, Department of Pathology, University of Turin, Via Santena 7, I-10126 Torino.

This is potentially useful for predicting the responsiveness of a given neoplastic cell population to medical treatment with somatostatin analogues, which are used in the clinical setting for both diagnostic and therapeutic purposes with special reference to neuroendocrine tumors.

The spectrum of neuroendocrine tumors of the lung includes well-differentiated neoplasms (so-called typical carcinoids) and poorly differentiated small-cell carcinomas (SCCs). Intermediate forms sharing features of both the aforementioned types also belong to this spectrum (so-called atypical carcinoids or well-differentiated neuroendocrine carcinomas). Finally, large-cell neuroendocrine carcinoma has been identified and included in this tumor group (4,40). The tissue distribution of *sst2* in neuroendocrine tumors of the lung has not been thoroughly characterized, although individual samples of bronchial carcinoids were found to express *sst* (30). SCCs (but not non-small-cell types) were also shown to be *sst2* positive by receptor binding assay (33). Moreover, *sst2* has been detected in *in vitro* cell cultures of human SSC of the lung (39,42). No study on a series of neuroendocrine tumors of the lung including all neuroendocrine lung tumor types has been reported to date.

The aim of this study was therefore to investigate the presence of *sst2* mRNA and protein in a series of 26 neuroendocrine tumors of the lung, employing different technical approaches, such as RT-PCR, ISH, and immunohistochemistry. To this purpose a monoclonal antibody to *sst2* (N-terminal) was generated in the Department of Pathology, University of Turin. The results were then compared and related to the tumor grade and to other clinicopathologic parameters.

MATERIALS AND METHODS

Case Series and RNA Extraction

Twenty-six samples of neuroendocrine tumors of the lung, in which fresh frozen tissue was available, were retrieved from the surgical pathology file of the University of Turin, Italy. All samples were reviewed applying currently accepted criteria of classification (4,40), and the neuroendocrine nature was confirmed by positive immunostaining for chromogranin A (CgA) (with or without antigen retrieval) or synaptophysin, and by positive RT-PCR for CgA mRNA. According to the classifications described here, these included 15 well-differentiated neuroendocrine tumors (typical carcinoids), 6 well-differentiated neuroendocrine carcinomas (atypical carcinoids), and 5 SCCs.

A series of 20 non-small-cell lung carcinomas (10 squamous, 9 adenocarcinomas, and 1 large-cell anaplastic) lacking neuroendocrine differentiation, as demonstrated by negative immunohistochemistry and RT-PCR for CgA (1), served as a control group. Clinicopathologic data and follow-up information were obtained for all patients.

For hybridization analysis, total RNA was extracted using the guanidine thiocyanate-cesium chloride method (5). The concentration of RNA was estimated by spectrophotometry, and RNA degradation was assessed by agarose gel electrophoresis, as previously reported (37).

Reverse Transcriptase Polymerase Chain Reaction for *sst2* and Chromogranin A

Total RNA (2 μ g) was first digested, with 10 units of RNase-free DNase (Boehringer, Mannheim, Germany) in a 10- μ L solution containing 20 mmol/L $MgCl_2$, to avoid DNA contamination. The solution was kept at room temperature for 10 minutes, then heated for 5 minutes at 70°C to inactivate the DNase molecules; 40 pmol/L of oligodeoxythymidine primers (oligo-dT16) were added and the solution was heated again at 70°C for 10 minutes, then chilled on ice to allow the primer hybridization. The resulting solution was reverse transcribed using 100 units of reverse transcriptase (Gibco BRL, Gaithersburg, MD). Complementary DNA (cDNA) was generated in a 50- μ L final reaction volume containing 50 mmol/L Tris-HCl pH 8.3, 75 mmol/L KCl, 3 mmol/L $MgCl_2$, 10 mmol/L dithiothreitol, 1 mmol/L deoxynucleotide triphosphates (dNTPs), and 20 units of RNasin (Promega, Madison, WI). The solution was heated at 37°C for 90 minutes. Finally, the enzymes were inactivated by heating to 70°C for 10 minutes.

The efficiency of the reverse transcription was determined by performing a PCR reaction having the β_2 -microglobulin "housekeeping gene" as a target. PCR was carried out in a 10- μ L final reaction volume containing 1 μ L of cDNA template, 10 pmol of sense and antisense oligonucleotide primers, 67 mmol/L Tris-HCl pH 8.8, 16 mmol/L $(NH_4)_2SO_4$, 0.01% polysorbate 20, 2 mmol/L dNTPs, 1 mmol/L $MgCl_2$, and 0.5 units of Taq polymerase. β_2 -Microglobulin, *sst2*, and CgA PCR reactions were performed using the same protocol at the following PCR conditions: 35 cycles, each cycle consisting of denaturation at 94°C for 2 minutes, annealing at 55°C for 1 minute for β_2 -microglobulin, at 61°C for *sst2*, and at 68°C for CgA; extension was performed at 72°C for 1 minute. The primers used for RT-PCR (9,11,23,37) are reported in Table 1.

The amplified fragments were run in a 1% agarose gel, containing ethidium bromide. Strict precautions against contamination were undertaken (19) and negative controls (a no-template control and a no-reverse transcriptase control and distilled water to replace the RNA) were included. The RNA extracted from an H716 neuroendocrine colon carcinoma cell line and from a neuroblastoma (37) served as positive controls for CgA and *sst2*, respectively.

Antibodies

Two different antibodies specific for *sst2* were employed. The first one was a monoclonal antibody raised

TABLE 1. Sequences of primers used for reverse transcriptase polymerase chain reaction

	Size of PCR product (bp)	Position	Study
1) β_2 -microglobulin sense: 5' ACC CCC ACT GAA AAA GAT GA 3'	120	286-305	Gussow et al. (8)
2) β_2 -microglobulin antisense: 5' ATC TTC AAA CCT CCA TGA TG 3'		389-408	
3) SSTR2 sense: 5' CAG TCA TGA GCA TCG ACC GA 3'	284	402-421	Sestini et al. (37)
4) SSTR2 antisense: 5' GCA AAG ACA GAT GAT GGT GA 3'		665-684	
5) CgA sense: 5' GCT CCA AGA CCT CGC TCT CC 3'	583	316-335	Helman et al. (11)
6) CgA antisense: 5' GAC CGA CTC TCG CCT TTC CG 3'		878-897	

PCR, polymerase chain reaction.

in the Department of Pathology (University of Turin) specific for an N-terminal sequence of the sst2 (shared by both A and B receptor isoforms). The octapeptide EPYYDLTS, corresponding to amino acids 35 to 42 of the human receptor (and differing by one amino acid from the mouse sequence), was synthesized, having a tyrosine added to the N-terminal. This sequence was similar to that used by other groups to produce polyclonal antibodies (17,18,27). This sequence was rather short but made it possible to avoid extensive homology with sst1. In addition, according to a genbank search using FASTA (28), this protein sequence is unique to human sst2 and has a partial homology only with rat and human nuclear receptor retinoid orphan nuclear receptor-beta (a protein having nuclear localization). Three Balb/c mice were immunized with the peptide conjugated to keyhole limpets hemocyanin (KLH) (Sigma, St. Louis, MO) following the standard procedure. After the first intrasplenic injection (100 μ g of protein) at time 0, the mice were intraperitoneally injected six times with the peptide-KLH conjugate (150 μ g) in the presence of Freund adjuvant. The reactivity of the sera from each animal was evaluated using an enzyme-linked immunosorbent assay, using the peptide coated onto the plastic. The hybridomas were produced by somatic fusion of immunized splenocytes with the mouse myeloma cell line Ag8.X63.653, following the standard technique (21). The monoclonal antibodies of interest were selected on the basis of the reactivity with the target peptide and with appropriate tissue sections. The latter included formalin-fixed and paraffin-embedded sections of pituitary gland and pancreatic islets and were analyzed by means of immunoperoxidase staining. Parallel control experiments were also performed by staining serial sections of these tissues, omitting the primary antibody or with the preimmune serum or with the antibody preadsorbed with high concentrations (1 mg/mL) of the antigenic peptide. In addition, the selected monoclonal antibodies (coded 10C6 and 10G4), both of IgM isotype, were further characterized by Western blotting. Membranes were prepared from stable transfected Chinese hamster ovary (CHO)-K1 cells, individually expressing recombinant human somatostatin receptors (sst1 to sst5). Western blotting was performed as previously described (36). The monoclonal

antibody was used as culture supernatant at 1:3 dilution for 2 hours at room temperature in Tris-buffered saline (TBS), supplemented with 0.1% polysorbate 20. Blots were washed in TTBS and incubated with peroxidase-conjugated goat antimouse IgM, diluted 1:1,500 for 90 minutes at room temperature. Then, blots were washed in TTBS and immunocomplexes were visualized using ECL following manufacturer's instructions (Amersham, Bucks, UK).

A second polyclonal antibody was produced that had been characterized previously (35,36). This antibody (coded K230) was raised in sheep and was specific for a sequence of the C-terminal portion of the sst2A (KSRL-NETTETQRTLLNEDLQ, amino acids 347 to 366).

Immunohistochemistry

Sections 4 or 5 μ thick, adjacent to those used for conventional histopathologic examination and immunostaining for neuroendocrine markers, were collected onto poly-L-lysine-coated slides. The proliferative activity of the tumors was assessed by means of Ki67 immunostaining (clone MIB1, Immunotech, Marseille, France), diluted 1:10 after microwave-based antigen retrieval in citrate buffer). The ascitic fluid of monoclonal antibody 10G4 was used in this study and was applied to tissue sections with prior antigen retrieval (three 3-minute passages in a microwave oven at 800 W in citrate buffer pH 6.0), at the dilution of 1:10,000 or 1:12,000 for 30 minutes at room temperature. The antiserum coded K230 was applied overnight at a dilution of 1:300 with no prior antigen retrieval. The immune reactions were then revealed with the immunoperoxidase technique (13) using the streptavidin-peroxidase kit and diaminobenzidine as chromogen. A weak nuclear counterstain or no counterstain was used in parallel sections. Control stainings for both antibodies included immunoperoxidase of serial sections using preimmune serum or antibody preadsorbed with the antigen or buffer instead of the primary antibody.

In Situ Hybridization

Selected tumors (12 samples) were also analyzed for sst2 mRNA expression by means of a nonradioactive, tyramide deposition-based ISH technique. The proce-

ture of amplification was modified from procedures reported by Kerstens et al. (16), Speel et al. (38), and the GenPoint (biotinyl-tyramide) manufacturer (Dako, Glostrup, Denmark). Briefly, 5- μ m-thick paraffin sections were collected onto silane-coated slides and deparaffinized through xylene and graded alcohols to phosphate buffer saline (PBS). The slides were then incubated for 5 minutes in a microwave oven at 800 W in citrate buffer pH 6.0. After washing in PBS, they were digested with proteinase K (1 μ g/mL) for 10 minutes at 23°C. Endogenous peroxidase activity was blocked with 3% hydrogen peroxide and endogenous biotin was blocked using avidin-blocking reagent for 15 minutes followed by washing in PBS and biotin-blocking reagent for 15 minutes (3). Sections were then prehybridized for 1 hour at room temperature in a mixture composed of 4 \times SSC, 50% formamide, Denhardt's 1 \times , dextran sulfate 5 \times , 500 μ g/mL salmon sperm DNA, and 250 μ g/mL tRNA. Hybridization took place overnight at 42°C in a solution containing the specific probe at a concentration of 1 pmol/mL. The probe was a digoxigenin-labeled 48-base oligonucleotide (32), complementary to positions 91 to 139 of the human *sst2* gene (41). After hybridization, excess hybridization buffer and coverslips were removed by a rapid wash in 4 \times SSC followed by stringent washing in 0.1 \times SSC for 10 minutes at 42°C. The hybrids were revealed by the following incubation steps: peroxidase-labeled antidigoxigenin (diluted 1:100 in PBS) for 30 minutes at room temperature, biotinylated tyramide (diluted 1:5 in PBS) for 15 minutes at room temperature, and peroxidase-labeled streptavidin for 15 minutes at room temperature. Diaminobenzidine was used as chromogen. Controls for ISH included staining of serial sections with sense probe, an unrelated probe (EBER-1 of the Epstein-Barr virus), and omission of the probe in the hybridization mixture, with all other experimental conditions identical to the procedure described here.

RESULTS

Reverse Transcriptase Polymerase Chain Reaction

All neuroendocrine tumors, but no nonneuroendocrine lung carcinomas, were positive for CgA mRNA (Fig. 1). *Sst2* mRNA was amplified in 22 of 26 samples of neuroendocrine tumor. The signals had variable intensities (Fig. 2) and were weak in moderately or poorly differentiated tumors (mostly in SCCs). No amplification was obtained in no-template or no-reverse transcriptase experiments. Control samples (nonneuroendocrine lung carcinomas proven by negative CgA RT-PCR) were weakly positive for *sst2* in 5 of 20 samples only (including 3 adenocarcinomas, 1 squamous, and the large-cell anaplastic carcinoma) (Fig. 3). These differences were statistically significant ($P < 0.01$) by χ^2 test.

Characterization of Monoclonal Antibodies to *sst2*

Several clones were identified having a positive binding by enzyme-linked immunosorbent assay and a parallel immunoreactivity on formalin-fixed paraffin-embedded human endocrine tissues (pituitary and pancreatic islets). In Western blotting experiments, two clones (coded 10C6 and 10G4) specifically developed a band at approximately 70 kD. When the antibodies were used against CHO-transfected cells expressing recombinant somatostatin receptors 1 through 5, a specific band corresponding to *sst2* (at approximately 70 kD) was revealed by the monoclonal antibody 10G4. Monoclonal antibody 10C6 developed a strong band with *sst2* but displayed a weaker reactivity also with *sst1*, 3, and 5, at least in the present experimental conditions (Fig. 4 A,B). The same antibodies were also tested by means of immunoperoxidase staining on formalin-fixed, paraffin-embedded samples of normal human pituitary gland and pancreas. Monoclonal antibody 10G4 gave good results in immunohistochemistry and was used at increasing di-

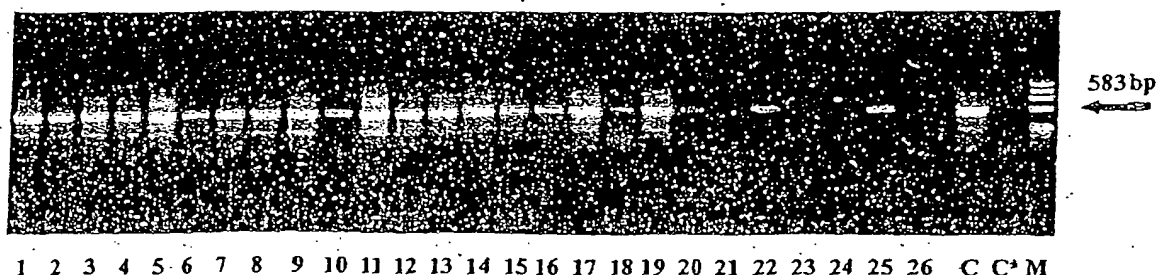


FIG. 1. Reverse transcriptase polymerase chain reaction for chromogranin A (CgA) mRNA in 26 samples of neuroendocrine tumor of the lung. Numbers in each lane correspond to sample numbers in Table 2. CgA mRNA is amplified at 429 bp. C and C* stand for positive (neuroendocrine colon carcinoma cell line, H716) and negative (distilled water) controls, respectively. The last column to the right represents the molecular weight marker. All samples are positive with a variable intensity of the amplification band.

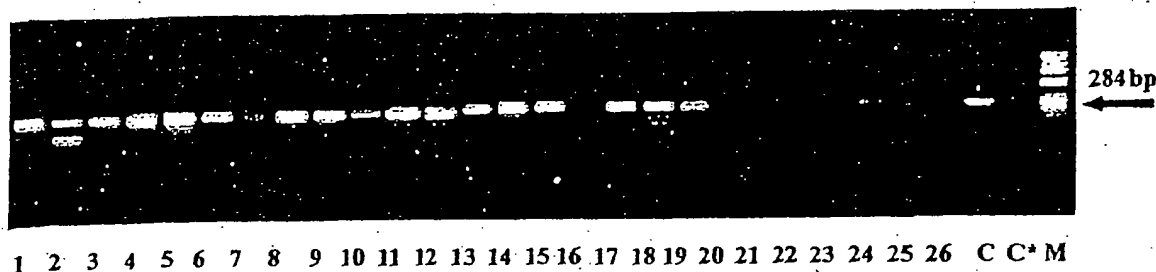


FIG. 2. Reverse transcriptase polymerase chain reaction for *sst2* mRNA in 26 samples of neuroendocrine tumor of the lung. Numbers in each lane correspond to sample numbers in Table 2. *sst2* mRNA is amplified at 284 bp. C and C* stand for positive (a neuroblastoma) and negative (distilled water) controls, respectively. The last column to the right represents the molecular weight marker. Twenty-two of 26 samples are positive with a variable intensity of the amplification band.

lutions (up to 1:15,000) with specific staining. Using thin sections (approximately 4 μ m), a strong membrane-bound and peripheral cytoplasmic immunoreactivity was found in an adenohypophyseal cell population (corresponding to growth hormone-secreting cells, as confirmed by double immunohistochemical analyses) and in pancreatic islets (Fig. 4 C,D). In the latter, the staining was apparently not restricted to a specific hormone-producing cell type and had a peripheral cytoplasmic or membrane distribution. Exocrine pancreatic cells (both acinar and ductal) were only occasionally immunostained. Immunohistochemistry performed on serial control sections, either omitting the primary antibody or using the preimmune serum or antibodies preabsorbed with the synthetic peptide, was negative in both tissues. Monoclonal antibody 10C6 had a relatively higher background staining at similar dilutions.

Immunohistochemistry

The antibodies to *sst2* (monoclonal antibody 10G4 and polyclonal K230) gave slightly different immunoreactions in 25 samples, and staining was not done in 1 sample because of lack of residual paraffin blocks. The monoclonal antibody 10G4 stained 21 of 25 samples, the

negative samples being 1 atypical carcinoid and 3 SCCs (Fig. 5). The tumors had 5% to 25% of the neoplastic cells immunoreactive. The staining was at the periphery of the cytoplasm, and omitting the counterstain its membrane-bound distribution was better outlined in most samples (Fig. 6). One sample of atypical carcinoid (no. 21) was focally immunoreactive for *sst2*, despite negative RT-PCR findings. Conversely, sample no. 26 was immunohistochemistry negative and RT-PCR positive. The antiserum anti-*sst2A* (code K230) gave positive signal in 19 of 25 samples, in 5% to 60% of the neoplastic cell population (Fig. 7). The location of the staining was at the membrane level associated with a weak cytoplasmic reactivity. The same pattern was seen in positive controls, e.g., pancreatic islets (Fig. 7, inset). Two samples (nos. 19 and 26) were negative in spite of a positive RT-PCR signal. Two other tumors (nos. 21 and 22), apparently devoid of *sst2* mRNA, showed a small percentage of immunoreactive cells. Incidentally, one of these latter samples (no. 21) was also immunoreactive with monoclonal antibody 10G4 (Table 2).

The five control samples positive by RT-PCR were also reactive with the antibodies. The type of immunocytochemical location of *sst2* receptors was similar to that described here, being a peripheral cytoplasmic stain-

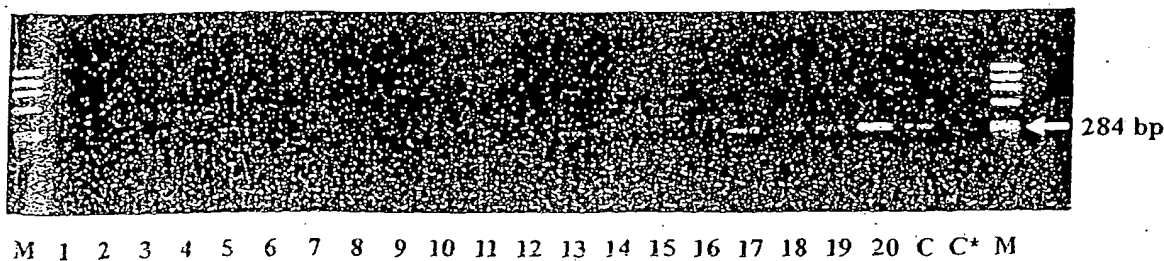


FIG. 3. Reverse transcriptase polymerase chain reaction for *sst2* mRNA in 20 control samples of nonneuroendocrine lung carcinoma. Five of 20 samples show a weak band at 284 bp corresponding to *sst2* mRNA. Control columns (C and C*) are identical to those in Fig. 2.

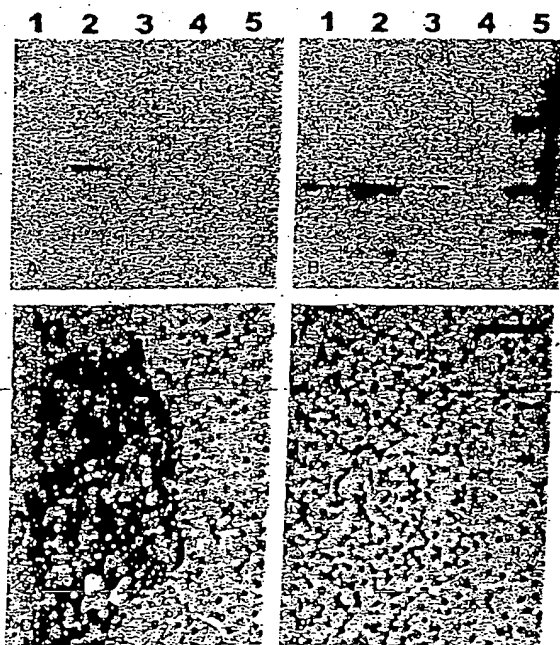


FIG. 4. Western blot analysis of monoclonal antibody clones 10G4 and 10C6 against sst2 in Chinese hamster ovary cells transfected with recombinant sst 1 through 5 (numbers of each column correspond to receptor type). Monoclonal antibody 10G4 shows a specific band at approximately 70 kD for sst2 only (A) as opposed to monoclonal antibody 10C6, which strongly reacts with sst2 but also has some degrees of cross-reactivity with sst 1, 3, and 5 (B). The lower figures show control formalin-fixed paraffin-embedded pancreatic islets immunostained with monoclonal antibody 10G4 without (C) and with (D) preadsorption with the peptide antigen, respectively. The majority of endocrine cells show a membrane-bound immunoreactivity (C) (immunoperoxidase). Bar: 90 µm.

ing present in 40% to 70% of neoplastic cells. A weak and focal staining was also observed in five of the remaining RT-PCR-negative samples, when the antibody K230 was used (but not when the monoclonal was employed).

Several cells in peritumoral tissues were occasionally stained. Ciliated cells of bronchial mucosa had a peripheral staining at the cilia border. Mucous glands were negative. Rare chondrocytes had a membrane staining. The wall of peritumoral as well as of occasional distant vessels was stained at the endothelium level and in occasional smooth muscle cells.

The reactivity of both antibodies was abolished in serial sections when the reagents were preabsorbed with the respective synthetic peptides, but not when an unrelated peptide was used. The peritumoral bronchial mucosa had a focal staining of ciliated cells with both antibodies. This reactivity disappeared when the preabsorbed antibody was applied.

In Situ Hybridization

Eight of 12 samples stained by ISH were positive for sst2 mRNA. The mRNA was present in a percentage of cells (ranging from 10% to 40%) and gave a weak signal (Fig. 8), despite the amplification provided by the tyramide-based procedure. The background level was minimal using diluted biotinylated tyramide. Control sections stained with sense probe or an unrelated probe, or omitting the probe, were consistently negative.

Clinical Data

Clinicopathologic data are summarized in Table 2. At follow-up, the majority of patients with typical carcinoids are free from disease 1 to 11 years after surgery. Two patients are alive with stable metastatic disease. Patients affected by atypical carcinoids had disease progression in one third of samples. Finally, patients with SCC had fatal outcomes within 1 year from diagnosis (except the recent sample). Eight patients had preoperative octreotide scintigraphy performed at the time of diagnosis. All patients had positive octreoscan findings, and, in these patients, also the tumor was positive by RT-PCR and immu-



FIG. 5. sample no. 25 (small cell carcinoma). Absence of immunoreactivity for sst2 with the monoclonal 10G4. This sample was also negative by reverse transcriptase polymerase chain reaction and in situ hybridization. (Immunoperoxidase in a formalin-fixed paraffin-embedded sample. Nuclei slightly counterstained with hemalum.) Bar: 45 µm.

nohistochemistry or ISH. In addition, three of these patients received octreotide therapy administered at the time of tumor recurrence or metastatic spread. Stable disease is recorded at follow-up more than 5 years after diagnosis.

Correlations

Overall, complete overlapping (i.e., RT-PCR, ISH, and immunohistochemistry with two antibodies) between *sst2* gene and protein expression was obtained in 21 of 25 samples (84%) and between RT-PCR results and immunohistochemical findings with at least one of the antibodies in 24 of 25 samples (96%). The monoclonal antibody 10G4 looked highly sensitive, being able to stain all but one sample (no. 26) (95%) positive for *sst2* mRNA by RT-PCR. *Sst2* expression, at mRNA as well as at protein levels, was reduced in high grade tumors, with SCCs being weakly positive in only two of five samples. Decreasing expression of *sst2* appears to cor-

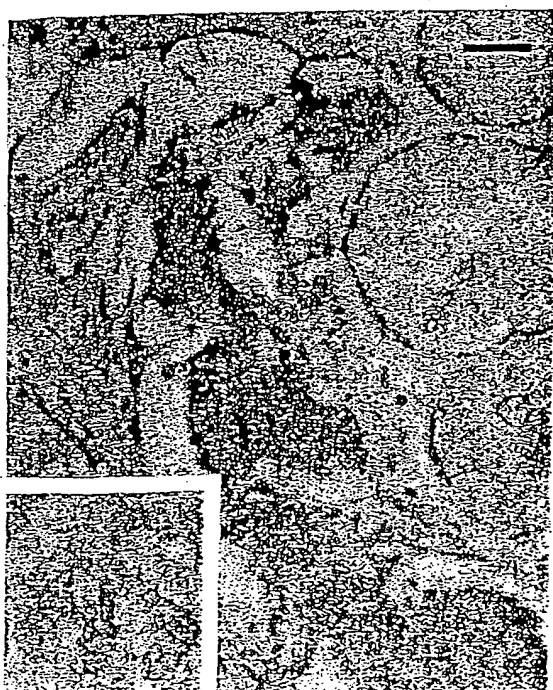


FIG. 6. sample no. 16 (typical carcinoid). Immunohistochemical detection of *sst2* by means of monoclonal antibody 10G4. The neoplastic cells have a peripheral cytoplasmic staining and membrane positivity in some cells, whereas the peribronchial gland adjacent to the tumor is unreactive. (Immunoperoxidase in a formalin-fixed paraffin-embedded sample. Nuclei slightly counterstained with hemalum.) Bar: 45 μ m. The membrane-bound distribution of the immunostaining is better outlined in a parallel section stained for monoclonal antibody 10G4 omitting nuclear counterstain (inset).



FIG. 7. Same sample as in Fig. 6. Immunohistochemical detection of *sst2* by means of the polyclonal antibody K230. The immunostaining is more intense at the cell border (arrows), as observed with the monoclonal antibody. In the inset, a pancreatic islet, used as positive control, shows a predominant membrane-bound immunostaining of many neuroendocrine cells. (Immunoperoxidase in a formalin-fixed paraffin-embedded sample. Nuclei slightly counterstained with hemalum.) Bar: 45 μ m.

relate with high tumor grade and elevated proliferative activity, but not with other parameters such sex, age, or tumor size.

DISCUSSION

In this study, the presence of *sst2* mRNA has been demonstrated in a series of resected neuroendocrine tumors of the lung by means of RT-PCR and confirmed by a sensitive nonradioactive tyramide-based ISH procedure and by immunohistochemistry with anti-*sst2* antibodies. Samples of both carcinoid tumors and SCCs were *sst2* positive, although a reduced or absent signal was observed in poorly differentiated (small-cell) carcinomas. This is the first study of *sst2* expression in a relatively large series of neuroendocrine tumors of the lung. Single samples of human carcinoids and SCCs (including cell lines of the latter) had previously been analyzed and found to express *sst2* (7,15,30,32,33,39,42). Several methods have been used to detect these receptors and partially overlapping results were obtained.

In the present study, the expression of high amounts of

TABLE 2. Clinicopathologic data and somatostatin receptor type 2 (sst2) expression in 26 cases of neuroendocrine lung tumors

Patient no.	Diagnosis	Sex/age	Size (cm)	Follow-up (mo)	CgA IHC	CgA RT-PCR	SYP IHC	Ki67 IHC*	sst2 RT-PCR	sst2 IHC Mab(10G4)	sst2 IHC (K230 Ab)
1	WD NET	F/35	3.5	NED 90	+	+++	+ F	1.5	+++	+	+
2	WD NET	F/29	4	NED 45	+	++	+ F	3	++	+	+
3	WD NET	F/41	2.5	NED 70	+	++	+	0.1	+++	+	+ F
4	WD NET†	F/25	4	NED 21	+	++	+	2.6	+++	+ F	+ F
5	WD NET†	M/58	3.8	NED 23	+	+++	+	13	+++	+ F	+
6	WD NET	M/52	2.5	NED 42	+	++	+	4.5	+++	+ F	+ F
7	WD NET	F/69	3.5	NED 47	+	++	+	1	+	+	+
8	WD NET	M/29	3	NED 70	+	+++	+	1.5	+++	+	+
9	WD NET	M/27	4	NED 108	+	+++	+	NT	+++	+	+
10	WD NE Ca†	M/66	8	AWD 55	+	++	+ F	1.1	++	+ F	+
11	WD NET†	F/29	2	AWD 56	+	+++	+	2.5	+++	+	+
12	WD NET*	F/32	3	NED 26	+	++	+	4	+++	+	+
13	WD NE Ca	M/60	3	NED 133	+	+++	+	1	+++	NT	NT
14	WD NET	M/28	4	NED 130	+	+++	+	1	+++	+	+
15	WD NET†	M/41	1.3	AWD 53	+	+++	+	1.5	+++	+	+
16	WD NET†	F/31	1	NED 13	+	++	++	2.6	+	+	+
17	WD NET	F/53	4	NED 24	+	+++	+ F	4	+++	+ F	+
18	WD NE Ca	M/62	3	NED 6	-	++	-	13	+++	+	+ F
19	WD NE Ca	F/73	5	DOD 20	+	+++	+	3	++	+	-
20	SCC	M/57	6	DOD 12	+	++	+	45	+	+ F	+ F
21	SCC	M/51	4.5	DOD 5	+	+	+	35	-	+ F	+ F
22	WD NE Ca	M/60	6	NED 51	+	++	+	1.5	-	-	+
23	SCC	F/56	6	DOD 11	+	+	+	50	-	-	-
24	WD NE Ca	M/77	2.5	NED 21	+	+	+	24	+	+ F	+ F
25	SCC	M/57	5	DOD 10	+	++	++	80	-	-	-
26	SCC†	M/68	.11	recent case	+	+	++	71	+	-	-

AWD, alive with disease; CgA, chromogranin A; DOD, died of disease; + F, focal; positive in <5% of cells; IHC, immunohistochemistry; Mab, monoclonal antibody; NECa, Neuroendocrine carcinoma; NED, no evidence of disease; NET, neuroendocrine tumor; NT, not tested; RT-PCR, reverse transcriptase polymerase chain reaction; SCC, Small-cell lung carcinoma; SYP, synaptophysin; WD, well differentiated.

* Ki67 IHC: values correspond to percentage of positive nuclei of neoplastic cells.

† Patients who had preoperative octreoscan performed.

‡ Patients who had octreoscan performed and octreotide treatment.

sst2 mRNA was confirmed in well to moderately differentiated neuroendocrine tumors, in agreement with the results obtained by Reubi et al. (32) by means of radioactive ISH. The presence of sst2 mRNA in SCC had never been reported in human specimens, except for two samples included in Reubi et al.'s series (32). Although the data on cell lines support the observation that SCCs contain sst2 (42), slightly discrepant results were found in some of samples described here. Unfortunately, SCCs are rarely operated on, and therefore it is difficult to collect a large number of surgical specimens. The five samples studied in the current series by means of RT-PCR had a low amount (two samples) or absent (three samples) sst2 mRNA. This could be the result of the extensive necrosis commonly present in such tumor types. However, because care was taken to freeze fragments that were macroscopically devoid of necrotic areas, a more likely hypothesis is that sst2 expression is reduced in poorly differentiated tumors. Recently, Reisinger et al. (29) showed that the uptake of somatostatin analogues in patients with SCC undergoing chemotherapy is significantly lower, and therapeutic external factors may affect the receptor status of individual tumors. In addition, the uptake of somatostatin analogues

in metastatic deposits of SCC has been shown to be low or absent (29,2). The present findings suggest that the sst2 mRNA content is related to the degree of tumor differentiation. These data must be confirmed in larger series of nonneuroendocrine tumors to ascertain whether the observed loss or decrease of sst2 expression in neuroendocrine tumors is a common event linked to neoplastic dedifferentiation. In addition, further studies are needed to assess the functionality of such receptors, by comparing the profile of sst2 expression in tumor tissues with binding assays employing labeled somatostatin and with the clinical response to diagnostic and therapeutic administration of somatostatin analogues.

To this purpose, several investigators have demonstrated a correlation between clinical imaging or response to somatostatin analogue treatment and sst2 mRNA content in single samples of carcinoid tumors (15,22). Northern blotting and ISH were the techniques used for sst2 mRNA identification. This kind of correlation is useful for selecting patients for somatostatin analogue treatment, although the demonstration of receptor mRNA in a cell does not imply per se that the receptor is fully functional.

The present study relied on a highly sensitive tech-

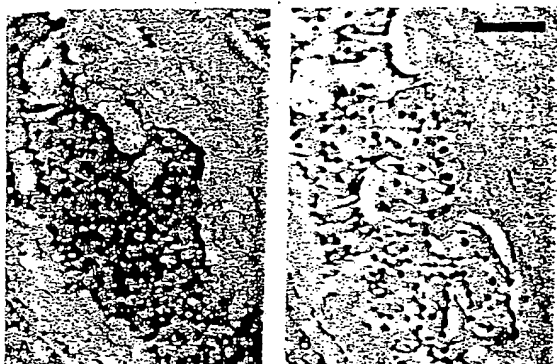


FIG. 8. sample no. 11 (typical carcinoid). In-situ-hybridization (ISH) for sst2 mRNA shows a weak cytoplasmic staining (A) in most tumor cells. An ISH performed with an unrelated probe was negative in a serial section of the same tumor (B). This sample was strongly positive by reverse transcriptase polymerase chain reaction for sst2 mRNA and by immunohistochemistry. (Nonradioactive ISH revealed by peroxidase and diaminobenzidine, as substrate. Nuclei counterstained with hemalum.) Bar: 75 μ m.

nique, RT-PCR, to identify all samples bearing even small amounts of sst2 mRNA. Indeed, in a previous study, single samples exhibiting octreotide-binding sites had no demonstrable sst2 mRNA by means of ISH, possibly due to the low sensitivity of the ISH procedure (34). The RT-PCR has shown sst2 mRNA transcripts in the majority of samples here studied. Only four samples were negative, all belonging to poorly differentiated high grade tumors, which usually follow an aggressive course. A decrease of sst2 mRNA expression in association with neuroendocrine tumor dedifferentiation had also been reported in neuroblastomas (37). In the above report, as well as in the current study, samples having an unfavorable prognosis were found to contain a relatively low amount of sst2 mRNA, as compared with well-differentiated tumors.

In the current sample series, eight samples were investigated before surgery with radiolabeled octreotide. Despite the low figures, all the samples positive at the diagnostic procedure had a strong RT-PCR signal for sst2 mRNA. Three of eight patients were also responsive to octreotide treatment administered at the time of relapse or metastatic spread. More extensive correlative clinicopathologic studies on the sst status are needed to better define the tissue distribution of somatostatin binding sites and their potential clinical role in the treatment of patients.

Sst2 evaluation by means of ISH (14,32) or RT-PCR (26,37) is a highly sensitive and reliable procedure. Unfortunately, these techniques have limitations because frozen tissue is needed for some of them, and radioactive material or costly and time-consuming methods are nec-

essary for others. Immunohistochemical analysis of sst2 by means of specific antibodies represents an ideal, cheap, and rapid alternative, easily applicable to archival material. For these reasons, several investigators have raised polyclonal antibodies specific for sst (8,10,15,17, 18). In the current study, tested tumor fragments adjacent to those snap frozen for RT-PCR analysis were tested with a polyclonal antibody against a C-terminal portion of the sst2A splice variant (35,36). In addition, a monoclonal antibody was produced in the Department of Pathology (University of Turin) against an N-terminal sequence of the human sst2. This antibody was the first monoclonal developed against sst2 and was shown to be highly specific for sst2 in Western blot and immunohistochemical analysis. Both the monoclonal and the polyclonal antibodies specifically reacted with all samples also positive by RT-PCR (with minor discrepancies in two samples, likely due to tumor heterogeneity). The observed correlation between RT-PCR and immunohistochemistry indicates that the latter may be a reliable diagnostic tool and may allow immunohistochemical investigation for sst2 even in small biopsy samples. This in turn may enable a rapid screening of sst2-positive tumors for medical treatment with somatostatin analogues.

Having confirmed in a relatively large series that the vast majority of neuroendocrine tumors of the lung contain variable amounts of sst2 mRNA, a final comment is deserved for sst2 expression in nonneuroendocrine lung carcinomas. No data have been reported thus far in the literature concerning normal human lung, although in the present study some bronchial cells of peritumoral parenchyma were positive for sst2 when immunohistochemical analysis was performed with either antibody. The staining was specific because it was abolished using preabsorbed antibodies. Therefore, it is likely that normal human lung tissue contains sst2. This might be confirmed by alternative techniques (e.g., Western blot, RT-PCR). However, in situ morphologic procedures, such as those employed here, have definite advantages. In fact, the lung is rich in vessels, and in several tissues (either in tumoral or in inflammatory-reactive conditions) the vessels were recently shown to contain sst (6).

A low expression of sst2 was found in 25% of lung carcinomas of nonneuroendocrine type investigated in the present study by means of RT-PCR. Therefore, sst type 2, at least, does not appear to be extensively expressed in nonneuroendocrine carcinomas of the lung. However, because two tumors in the control group (a squamous carcinoma and an adenocarcinoma, respectively) had positive octreotide scintigraphy, but no sst2 mRNA, it is plausible that a heterogeneous distribution of sst occurs in nonneuroendocrine lung tumors. Other receptor types may be expressed in these tumors and may be responsible for the positive results in diagnostic testing. Because sst5 is also known to bind somatostatin

analogues, such as octreotide, with high affinity (24), the expression of this receptor type will be investigated in future studies. □

Acknowledgments: The authors are grateful to Dr. P.L. Filosso (Turin) for clinical data, to Mrs. M. Cerrato and Miss S. Solero for skilful technical help, and to Mr. A. Grua for the photographs.

REFERENCES

1. Abbona GC, Papotti M, Viberù L, Macri L, Stella A, Bussolati G. Chromogranin A gene expression in non-small cell lung carcinomas. *J Pathol* 1998;186:1-6.
2. Berenger N, Moretti JL, Boaziz C, Vigneron N, Moret JF, Breaux JL. Somatostatin receptor imaging in small cell lung cancer. *Eur J Cancer* 1996;32:1429-31.
3. Bussolati G, Gugliotta P, Volante M, Pace M, Papotti M. Retrieved endogenous biotin: a novel marker and potential pitfall in diagnostic immunohistochemistry. *Histopathology* 1997;31:400-7.
4. Capella C, Heitz PU, Hoffer H, Solcia E, Kloppel G. Revised classification of neuroendocrine tumors of the lung, pancreas and gut. *Virchows Arch* 1995;425:547-60.
5. Chirgwin JM, Przybyla AE, MacDonald RJ, Rutter W. Isolation of biologically active RNA from sources enriched in ribonuclease. *Biochemistry* 1979;18:5294-7.
6. Denzler B, Reubi JC. Expression of somatostatin receptors in peritumoral veins of human tumors. *Cancer* 1999;85:189-98.
7. Fujita T, Yamaji Y, Sato M, Murao K, Takahara J. Gene expression of somatostatin receptor subtypes, SSTR1 and SSTR2, in human lung cancer cell lines. *Life Sci* 1994;55:1797-806.
8. Gu WZ, Schonbrunn A. Coupling specificity between somatostatin receptor sst2A and G proteins: isolation of the receptor-G protein complex with a receptor antibody. *Mol Endocrinol* 1997;11:527-37.
9. Gussow D, Rein R, Ginjaar I, Hochstenbach F, Seemann G, Kottman A, Ploegh HL. The human beta 2-microglobulin gene: primary structure and definition of the transcriptional unit. *J Immunol* 1987;139:3132-8.
10. Helboe L, Møller M, Nøregård L, Schiødt M, Sørensen CE. Development of selective antibodies against the human somatostatin receptor subtypes sst1-sst5. *Brain Res Mol Brain Res* 1997;49:82-8.
11. Helman JJ, Ahn TG, Levine MA, et al. Molecular cloning and primary structure of human chromogranin A (secretory protein I) cDNA. *J Biol Chem* 1988;263:11559-63.
12. Hofland LJ, Liu Q, Van Koetsveld PM, et al. Immunohistochemical detection of somatostatin receptor subtypes sst1 and sst2A in human somatostatin receptor positive tumors. *J Clin Endocrinol Metab* 1999;84:775-80.
13. Hsu SM, Raine L, Fanger H. Use of avidin-biotin-peroxidase complex (ABC) in immunoperoxidase techniques: comparison between ABC and unlabelled antibody (PAP) procedures. *J Histochem Cytochem* 1981;29:577-80.
14. Janson ET, Gobl A, Kalkne KM, Oberg K. A comparison between the efficacy of somatostatin receptor scintigraphy and that of in situ hybridization for somatostatin receptor subtype 2 messenger RNA to predict therapeutic outcome in carcinoid patients. *Cancer Res* 1996;56:2561-5.
15. Janson ET, Svendsberg M, Gobl A, Westlin JE, Oberg K. Determination of somatostatin receptors subtype 2 in carcinoid tumors by immunohistochemical investigation with somatostatin receptor subtype 2 antibodies. *Cancer Res* 1998;58:2375-8.
16. Kerstens HJM, Poddighe PJ, Hanselaar AGJM. A novel in situ hybridization signal amplification method based on the deposition of biotinylated tyramine. *J Histochem Cytochem* 1995;43:347-52.
17. Krisch B, Feindt J, Mendlin R. Immunoelectronmicroscopic analysis of the ligand-induced internalization of the somatostatin receptor subtype 2 in cultured human glioma cells. *J Histochem Cytochem* 1998;46:1233-42.
18. Kumar U, Laird D, Srikant CB, Escher E, Patel YC. Expression of the five somatostatin receptors (SSTR1-5) subtypes in rat pituitary somatotrophs: quantitative analysis by double-label immunofluorescence confocal microscopy. *Endocrinology* 1997;138:4473-6.
19. Kwok S, Higuchi R. Avoiding false positives with PCR. *Nature* 1989;339:237-8.
20. Lamberts SWJ, Hofland LJ, Koetsveld PM, Reubi JC, Brünig HA, Bakker WH, Krenning EP. Parallel in vivo and in vitro detection of functional somatostatin receptors in human endocrine pancreatic tumors: consequences with regard to diagnosis, localization and therapy. *J Clin Endocrinol Metab* 1990;71:566-74.
21. Malavasi F, Funaro A, Bellone G, et al. Functional and molecular characterization by the CB04 monoclonal antibody of a cell surface structure exerting C3-complement receptor activity. *J Clin Immunol* 1985;5:412-20.
22. Nilsson O, Kolby L, Wängberg B, et al. Comparative studies on the expression of somatostatin receptor subtypes, outcome of octreotide scintigraphy and response to octreotide treatment in patients with carcinoid tumours. *Br J Cancer* 1998;77:632-7.
23. Pagani A, Forni M, Tonini GP, Papotti M, Bussolati G. Expression of members of the chromogranin family in primary neuroblastomas. *Diagn Mol Pathol* 1992;1:16-24.
24. Panetta R, Greenwood MT, Warszynska A, et al. Molecular cloning, functional characterization and chromosomal localization of a human somatostatin receptor (somatostatin receptor type 5) with preferential affinity for somatostatin-28. *Mol Pharmacol* 1994;45:417-27.
25. Papotti M, Macri L, Bussolati G, Reubi JC. Correlative study on neuroendocrine differentiation and presence of somatostatin receptors in breast carcinomas. *Int J Cancer* 1989;43:365-9.
26. Papotti M, Macri L, Pagani A, Aloï F, Bussolati G. Quantitation of somatostatin receptor type 2 in neuroendocrine (Merkel cell) carcinoma of the skin by competitive RT-PCR. *Endocr Pathol* 1999;10:1-10.
27. Patel YC, Panetta R, Escher E, Greenwood M, Srikant CB. Expression of multiple somatostatin receptor genes in AIT-20 cells: evidence for a novel somatostatin-28 selective receptor subtype. *J Biol Chem* 1994;269:1506-9.
28. Pearson WR, Lipman DJ. Improved tools for biological sequence comparison. *Proc Natl Acad Sci U S A* 1988;85:2444-8.
29. Reisinger I, Bohuslavzki KH, Brenner W, et al. Somatostatin receptor scintigraphy in small-cell lung cancer: results of a multicenter study. *J Nucl Med* 1998;39:224-7.
30. Reubi JC, Kappeler A, Waser B, Laissue J, Hipkin RW, Schonbrunn A. Immunohistochemical localization of somatostatin receptors sst2A in human tumors. *Am J Pathol* 1998;153:233-45.
31. Reubi JC, Maurer R, von Werder K, Torhorst J, Klöppel JGM, Lamberts SWJ. Somatostatin receptors in human endocrine tumors. *Cancer Res* 1987;47:551-8.
32. Reubi JC, Schaefer JC, Waser B, Mengod G. Expression and localization of somatostatin receptors SSTR1, SSTR2, SSTR3 messenger RNA in primary human tumors using in situ hybridization. *Cancer Res* 1994;54:3455-9.
33. Reubi JC, Waser B, Sheppard M, Macaulay V. Somatostatin receptors are present in small-cell but not in non-small-cell primary lung carcinomas: relationship to EGF receptors. *Int J Cancer* 1990;45:269-74.
34. Schaefer JC, Waser B, Mengod G, Reubi JC. Somatostatin receptors subtypes sst1, sst2, sst3 and sst5 expression in human pituitary, gastroentero-pancreatic and mammary tumors: comparison of mRNA analysis with receptor autoradiography. *Int J Cancer* 1997;70:530-7.
35. Schindler M, Holloway S, Humphrey PPA, Waldvogel H, Faull RLM, Berger W, Emson PC. Localization of the somatostatin sst2A receptor in human cerebral cortex, hippocampus and cerebellum. *Neuroreport* 1998;9:521-5.
36. Schindler M, Sellers LA, Humphrey PPA, Emson PC. Immunohistochemical localization of the somatostatin sst2(A) receptor in the rat brain and spinal cord. *Neuroscience* 1997;76:225-40.
37. Sestini R, Orlando C, Peri A, et al. Quantification of somatostatin

- receptor type 2 gene expression in neuroblastoma cell lines and primary tumors using competitive reverse transcription-polymerase chain reaction. *Clin Cancer Res* 1996;2:1757-65.
38. Speel EJM, Saremaslani P, Roth J, Hopman AHN, Komminoth P. Improved mRNA in situ hybridization on formaldehyde-fixed and paraffin-embedded tissue using signal amplification with different haptenized tyramides. *Histochem Cell Biol* 1998;420:1-7.
39. Taylor JE, Theveniau MA, Bashirzadeh R, Reisine T, Eden PA. Detection of somatostatin receptor subtype 2 (SSTR2) in established tumors and tumor cell lines: evidence for sst2 heterogeneity. *Peptides* 1994;15:1229-36.
40. Travis WD, Gal AA, Colby TV, Klimstra DS, Falk R, Koss MN. Reproducibility of neuroendocrine lung tumor classification. *Hum Pathol* 1998;29:272-9.
41. Yamada Y, Post SR, Wang K, Tager H, Bell GI, Seino S. Cloning and functional characterization of a family of human and mouse somatostatin receptors expressed in brain, gastrointestinal tract and kidney. *Biochemistry* 1992;89:251-5.
42. Zhang CY, Yokogoshi Y, Yoshimoto K, Fujimaki Y, Matsumoto K, Saito S. Point mutation of the somatostatin receptor 2 gene in the human small cell lung cancer cell line COR-L103. *Biochem Biophys Res Commun* 1995;210:805-15.



P-cadherin overexpression is an indicator of clinical outcome in invasive breast carcinomas and is associated with CDH3 promoter hypomethylation.

Paredes J, Albergaria A, Oliveira JT, Jeronimo C, Milanezi F, Schmitt FC.

Institute of Pathology and Molecular Immunology of Porto University (IPATIMUP), Braga, Portugal. jparedes@ipatimup.pt

PURPOSE: P-cadherin overexpression has been reported in breast carcinomas, where it was associated with proliferative high-grade histological tumors. This study aimed to analyze P-cadherin expression in invasive breast cancer and to correlate it with tumor markers, pathologic features, and patient survival. Another purpose was to evaluate the P-cadherin promoter methylation pattern as the molecular mechanism underlying this gene regulation. **EXPERIMENTAL DESIGN:** Using a series of invasive breast carcinomas, P-cadherin expression was evaluated and correlated with histologic grade, estrogen receptor, MIB-1, and p53 and c-erbB-2 expression. In order to assess whether P-cadherin expression was associated with changes in CDH3 promoter methylation, we studied the methylation status of a gene 5'-flanking region in these same carcinomas. This analysis was also done for normal tissue and for a breast cancer cell line treated with a demethylating agent. **RESULTS:** P-cadherin expression showed a strong correlation with high histologic grade, increased proliferation, c-erbB-2 and p53 expression, lack of estrogen receptor, and poor patient survival. This overexpression can be regulated by gene promoter methylation because the 5-Aza-2'-deoxycytidine treatment of MCF-7/AZ cells increased P-cadherin mRNA and protein levels. Additionally, we found that 71% of P-cadherin-negative cases showed promoter methylation, whereas 65% of positive ones were unmethylated ($P = 0.005$). The normal P-cadherin-negative breast epithelial cells showed consistent CDH3 promoter methylation. **CONCLUSIONS:** P-cadherin expression was strongly associated with tumor aggressiveness, being a good indicator of clinical outcome. Moreover, the aberrant expression of P-cadherin in breast cancer might be regulated by gene promoter hypomethylation.

PMID: 16115928 [PubMed - in process]



Mammary-derived growth inhibitor protein and messenger ribonucleic acid concentrations in different physiological states of the gland.

Politis I, Gorewit RC, Muller T, Grosse R.

Department of Animal Science, Cornell University, Ithaca 14853.

Expression of mammary-derived growth inhibitor in tissue from lactating and involuting bovine mammary glands was investigated. Seventeen lactating, pregnant (220 to 272 d in gestation) cows were divided in two groups of 8 and 9 cows each. Cows of the first group were slaughtered while in lactation. Cows of the second group (9 involuting cows) were slaughtered at 13 to 52 d following sudden cessation of milking. High concentrations of mammary-derived growth inhibitor (.63% of the total protein) were detected in mammary tissue of lactating cows. Mammary-derived growth inhibitor (less than .10% of the total protein) was dramatically reduced during most of the involution period (13 to 45 d following cessation of milking). Mammary-derived growth inhibitor was again detected (.28% of the total protein) during the last stage of the involution (46 to 53 d after cessation of milking), which coincided with colostrum formation. When steady state concentrations of mammary-derived growth inhibitor mRNA were examined, the results obtained mirrored those obtained at the protein concentration. These data suggest that regulation of mammary-derived growth inhibitor occurs via modulation of the steady state concentration of its mRNA. Furthermore, there is a strong correlation between mammary-derived growth inhibitor expression and lactation in dairy cows.

PMID: 1500548 [PubMed - indexed for MEDLINE]

□ 157: Osteoarthritis Cartilage. 2002 Apr;10(4):253-63.

Related Articles, Links

ELSEVIER
SCIENCE DIRECT

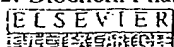
Matrilin-3 in human articular cartilage: increased expression in osteoarthritis.

Pullig O, Weseloh G, Klatt AR, Wagener R, Swoboda B.

Division of Orthopaedic Rheumatology, Department of Orthopaedics, University of Erlangen-Nuremberg, Rathsbberger Str. 57, D-91054 Erlangen, Germany.
oliver.pullig@med.uni-erlangen.de

OBJECTIVE: Matrilin-3 is a member of the recently described matrilin family of extracellular matrix proteins containing von Willebrand factor A-like domains. The matrilin-3 subunit can form homo-tetramers as well as hetero-oligomers together with subunits of matrilin-1 (cartilage matrix protein). It has a restricted tissue distribution and is strongly expressed in growing skeletal tissues. Detailed information on expression and distribution of extracellular matrix proteins is important to understand cartilage function in health and in disease like osteoarthritis (OA). **METHODS:** Normal and osteoarthritic cartilage were systematically analysed for matrilin-3 expression, using immunohistochemistry, Western blot analysis, in situ hybridization, and quantitative PCR. **RESULTS:** Our results indicate that matrilin-3 is a mandatory component of mature articular cartilage with its expression being restricted to chondrocytes from the tangential zone and the upper middle cartilage zone. Osteoarthritic cartilage samples with only moderate morphological osteoarthritic degenerations have elevated levels of matrilin-3 mRNA. In parallel, we found an increased deposition of matrilin-3 protein in the cartilage matrix. Matrilin-3 staining was diffusely distributed in the cartilage matrix, with no cellular staining being detectable. In cartilage samples with minor osteoarthritic lesions, matrilin-3 deposition was restricted to the middle zone and to the upper deep zone. A strong correlation was found between enhanced matrilin-3 gene and protein expression and the extent of tissue damage. Sections with severe osteoarthritic degeneration showed the highest amount of matrilin-3 mRNA, strong signals in in situ hybridization, and prominent protein deposition in the middle and deep cartilage zone. **CONCLUSION:** We conclude that matrilin-3 is an integral component of human articular cartilage matrix and that the enhanced expression of matrilin-3 in OA may be a cellular response to the modified microenvironment in the disease. Copyright 2002 OsteoArthritis Research Society International.

PMID: 11950247 [PubMed - indexed for MEDLINE]



Up-regulation of mitochondrial peripheral benzodiazepine receptor expression by tumor necrosis factor alpha in testicular leydig cells. Possible involvement in cell survival.

Rey C, Mauduit C, Naureils O, Benahmed M, Louisot P, Gasnier F.

INSERM U. 189, Faculte de Medecine Lyon-Sud, BP12, 69921 cedex, Oullins, France.

Porcine Leydig cells in primary cultures are resistant to tumor necrosis factor alpha (TNFalpha) cytotoxicity. Here we report that these cells can be rendered sensitive to TNFalpha killing by treatment with the translational inhibitor cycloheximide, suggesting the existence of proteins that can suppress the death stimulus induced by the cytokine. In search of these cytoprotective proteins, we focused on the constituents of the mitochondrial permeability transition pore (PT pore), whose opening has been shown to play a critical role in the TNFalpha-mediated death pathway. We found that TNFalpha up-regulated mRNA and protein expression of the mitochondrial peripheral benzodiazepine receptor (PBR), an outer membrane-derived constituent of the pore. A strong correlation was established between the resistance of the cells to TNFalpha killing and the density of PBR-binding sites. Concomitantly, TNFalpha down-regulated Bcl-2 mRNA and protein expression. As Bcl-2 has been shown to be an endogenous inhibitor of the PT pore, we hypothesize that the TNFalpha-induced up-regulation of PBR expression may compensate for the decrease in Bcl-2 levels to prevent the opening of the PT pore.

PMID: 11077046 [PubMed - indexed for MEDLINE]

82: Am J Clin Pathol. 2003 Nov;120(5):691-8.

[Related Articles](#), [Links](#)

MetaPress

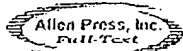
GLUT1 messenger RNA and protein induction relates to the malignant transformation of cervical cancer.

Rudlowski C, Becker AJ, Schroder W, Rath W, Buttner R, Moser M.

Dept of Gynecology and Obstetrics, University Hospital Heidelberg, Vossstr 7-9, D-69115 Heidelberg, Germany.

We studied whether induction of glucose transporters (GLUTs) 1 to 4 correlates with human papillomavirus (HPV)-dependent malignant transformation of cervical epithelium. Tissue samples of cervical intraepithelial neoplasia (CIN; grades 1 to 3), invasive carcinomas, and lymph node metastasis were examined. HPV typing was performed. Tissue sections were immunostained with GLUT1 to GLUT4 antibodies. Messenger RNA (mRNA) in situ hybridization confirmed GLUT1 protein expression. Weak expression of GLUT1 was found in nondysplastic HPV-positive and HPV-negative epithelium; significant expression was observed in preneoplastic lesions, correlating with the degree of dysplasia. In CIN 3 high-risk HPV lesions, cervical cancer, and metastasis, GLUT1 was expressed at highest levels with a strong correlation of GLUT1 mRNA and protein expression. Immunostains for GLUT2 to GLUT4 were negative. Cervical tumor cells respond to enhanced glucose utilization by up-regulation of GLUT1. The strong induction of GLUT1 mRNA and protein in HPV-positive CIN 3 lesions suggests GLUT1 overexpression as an early event in cervical neoplasia. GLUT1 is potentially relevant as a diagnostic tool and glucose metabolism as a therapeutic target in cervical cancer.

PMID: 14608894 [PubMed - indexed for MEDLINE]



UVA irradiation-induced activation of activator protein-1 is correlated with induced expression of AP-1 family members in the human keratinocyte cell line HaCaT.

Silvers AL, Bowden GT.

Department of Radiation Oncology, Arizona Cancer Center, The University of Arizona, Tucson 85724, USA.

To determine whether the transcription factor activator protein-1 (AP-1) could be modulated by ultraviolet A (UVA) exposure, we examined AP-1 DNA-binding activity and transactivation after exposure to UVA in the human immortalized keratinocyte cell line HaCaT. Maximal AP-1 transactivation was observed with 250 kJ/m² UVA between 3 and 4 h after irradiation. DNA binding of AP-1 to the target 12-O-tetradecanoylphorbol-13-acetate response element sequence was maximally induced 1-3 h after irradiation. Both de novo transcription and translation contributed to the UVA-induced AP-1 DNA binding. c-Fos was implicated as a primary component of the AP-1 DNA-binding complex. Other components of the complex included Fra-2, c-Jun, JunB and JunD. UVA irradiation induced protein expression of c-Fos, c-Jun, Fra-1 and Fra-2. Phosphorylated forms of these induced proteins were determined at specific time points. A strong correlation existed between UVA-induced AP-1 activity and accumulation of c-Fos, c-Jun and Fra-1 proteins. UVA irradiation also induced c-fos and c-jun mRNA expression and transcriptional activation of the c-fos gene promoter. These results demonstrate that UVA irradiation activates AP-1 and that c-fos induction may play a critical role in the response of these human keratinocytes to UVA irradiation.

PMID: 11950097 [PubMed - indexed for MEDLINE]

Tumor necrosis factor-alpha upregulates the prostaglandin E2 EP1 receptor subtype and the cyclooxygenase-2 isoform in cultured amnion WISH cells.

Spaziani EP, Benoit RR, Tsibris JC, Gould SF, O'Brien WF.

University of South Florida Health Science Center, Department of Obstetrics & Gynecology, Tampa 33612, USA. espazian@com1.med.usf.edu

Recent studies have demonstrated a strong correlation between infection and preterm labor. Preterm delivery is also associated with high levels of cytokines and prostaglandins in amniotic fluid. The purpose of this study was to investigate the effect of tumor necrosis factor-alpha (TNF-alpha) on the levels of cyclooxygenase, prostaglandin E2 production (PGE2), and expression of the PGE2 receptor subtype EP1 in amnion WISH cell culture. Amnion WISH cell cultures were incubated in increasing concentrations of TNF-alpha (0-50 ng/ml). Changes in cyclooxygenase and EP1 receptor proteins were evaluated by Western blot analysis. Changes in EP1 mRNA were evaluated by Northern blot, and culture fluid concentrations of PGE2 were estimated by enzyme immunoassay (EIA). EP1 protein ($p < 0.01$), EP1 mRNA ($p < 0.05$), cyclooxygenase-2 (COX-2) protein ($p < 0.001$), and PGE2 concentrations ($p < 0.01$) all increased with increasing concentrations of TNF-alpha. Changes in COX-1 protein were not observed following TNF-alpha-incubation. The results suggest that TNF-alpha may play a role in infection-induced preterm labor by its pleiotropic ability to simultaneously stimulate COX-2 activity, PGE2 concentrations, and PGE2 EP1 receptor levels in human amnion.

PMID: 9877447 [PubMed - indexed for MEDLINE]



Specific inhibition of AQP1 water channels in isolated rat intrahepatic bile duct units by small interfering RNAs.

Splinter PL, Masyuk AI, LaRusso NF.

Center for Basic Research in Digestive Diseases, Division of Gastroenterology and Hepatology, Mayo Medical School, Clinic, and Foundation, Rochester, Minnesota 55905, USA.

Cholangiocytes express water channels (i.e. aquaporins (AQPs)), proteins that are increasingly recognized as important in water transport by biliary epithelia. However, direct functional studies demonstrating AQP-mediated water transport in cholangiocytes are limited, in part because of the lack of specific AQP inhibitors. To address this issue, we designed, synthesized, and utilized small interfering RNAs (siRNAs) selective for AQP1 and investigated their effectiveness in altering AQP1-mediated water transport in intrahepatic bile duct units (IBDUs) isolated from rat liver. Twenty-four hours after transfection of IBDUs with siRNAs targeting two different regions of the AQP1 transcript, both AQP1 mRNA and protein expression were inhibited by 76.6-92.0 and 57.9-79.4%, respectively. siRNAs containing the same percent of base pairs as the AQP1-siRNAs but in random sequence (i.e. scrambled siRNAs) had no effect. Suppression of AQP1 expression in cholangiocytes resulted in a decrease in water transport by IBDUs in response to both an inward osmotic gradient (200 mosm) or a secretory agonist (forskolin), the osmotic water permeability coefficient ($P(f)$) decreasing up to 58.8% and net water secretion ($J(v)$) decreasing up to 87%. A strong correlation between AQP1 protein expression and water transport in IBDUs transfected with AQP1-siRNAs was consistent with the decrease in water transport by IBDUs resulting from AQP1 gene silencing by AQP1-siRNAs. This study is the first to demonstrate the feasibility of utilizing siRNAs to specifically reduce the expression of AQPs in epithelial cells and provides direct evidence of the contribution of AQP1 to water transport by biliary epithelia.

PMID: 12468529 [PubMed - indexed for MEDLINE]

Type IV collagenase (M(r) 72,000) expression in human prostate: benign and malignant tissue.

Stearns ME, Wang M.

Department of Pathology, Medical College of Pennsylvania, Philadelphia 19129.

The expression of type IV collagenase (M(r) 72,000) has been examined in tissues from patients with benign prostatic hyperplasia (6 patients) and varying Gleason grades of malignant prostate cancer (18 patients). Immunoperoxidase labeling indicated that expression of the type IV collagenase was weak or nonexistent in benign tissue but consistently strong in the glandular and ductal epithelial cells of prostate tumors diagnosed at Gleason grades 1-8. In moderate to advanced cancer (i.e., Gleason grades 2 to 8), invasive tumor foci in the stromal tissue produced relatively modest amounts of type IV collagenase. The normal stromal tissue (i.e., fibroblasts) uniformly failed to produce detectable levels of type IV collagenase in the 24 patients examined. Northern and quantitative slot blot hybridization assays demonstrated that collagenase type IV mRNA levels were low in benign tissue and high in malignant tumors. In contrast, the stromal cells did not express significant amounts of type IV collagenase mRNA. Enzyme-linked immunosorbent assays demonstrated that the amounts of type IV collagenase protein correlated directly with the mRNA levels in the tumor tissue. The studies suggest that type IV collagenase may be selectively overexpressed by malignant, preinvasive prostatic epithelial cells.

PMID: 7679051 [PubMed - indexed for MEDLINE]

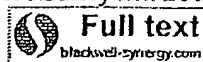
TNF-alpha and IL-8 are upregulated in the epidermis of normal human skin after UVB exposure: correlation with neutrophil accumulation and E-selectin expression.

Strickland I, Rhodes LE, Flanagan BF, Friedmann PS.

Department of Dermatology, University of Liverpool, United Kingdom.

The in vivo response to ultraviolet B (UVB) radiation in skin is characterized by the accumulation of both mononuclear and polymorphonuclear cells within the dermis and an induction of vascular endothelial adhesion molecules. Epidermal production of cytokines (IL-8 and TNF-alpha) has been strongly implicated in the development of UVB-induced inflammation. In the current study, we examined the time course of IL-8 and TNF-alpha mRNA and protein expression in the epidermis over a 24-h period after in vivo UVB irradiation. Also, the induction of adhesion molecule expression and the accumulation of neutrophils within the dermis were followed. We found constitutive expression of both cytokines (mRNA and protein) in the epidermis of unirradiated skin. IL-8 was rapidly upregulated after irradiation and mRNA and protein increased at 4 h, reaching a maximum between 8 and 24 h. TNF-alpha mRNA and protein was minimally increased by 8 h after UVB irradiation and reached a maximum by 24 h. No significant alteration in ICAM-1 or VCAM-1 expression was observed. E-selectin expression, which was absent from control samples, was increased from 4 h onward and also reached a maximum at 24 h, coinciding with peak neutrophil accumulation. A strong correlation ($r = 0.96$) was found between number of E-selectin-positive vessels and numbers of infiltrating neutrophils at this time. Moreover, because E-selectin expression was increased before any apparent increase in TNF-alpha protein (4 h), TNF-alpha does not appear to be involved in the early induction of the adhesion molecule, but cytokines such as TNF-alpha and IL-8 may act subsequently to augment the inflammatory response.

PMID: 9129230 [PubMed - indexed for MEDLINE]



Basic fibroblast growth factor expression is increased in human renal fibrogenesis and may mediate autocrine fibroblast proliferation.

Strutz F, Zeisberg M, Hemmerlein B, Sattler B, Hummel K, Becker V, Muller GA.

Department of Nephrology and Rheumatology, Georg-August-University Gottingen, Germany. fstrutz@gwdg.de

BACKGROUND: Interstitial fibroblasts play a critical role in renal fibrogenesis, and autocrine proliferation of these cells may account for continuous matrix synthesis. Basic fibroblast growth factor (FGF-2) is mitogenic for most cells and exerts intracrine, autocrine, and paracrine effects on epithelial and mesenchymal cells. The aims of the present studies were to localize and quantitate the expression of FGF-2 in normal and pathologic human kidneys and to study the in vitro effects of FGF-2 on proliferation, differentiation, and matrix production of isolated cortical kidney fibroblasts. **METHODS:** FGF-2 protein expression was localized by immunofluorescence double labelings in normal and fibrotic human kidneys. Subsequently, interstitial FGF-2 labeling was determined semiquantitatively in 8 normal kidneys and 39 kidneys with variable degrees of interstitial fibrosis and was correlated with the morphometrically determined interstitial cortical volume. In addition, FGF-2 expression was quantitated by immunoblot analysis in three normal and six fibrotic kidneys. FGF-2 mRNA was localized by in situ hybridizations. Seven primary cortical fibroblast lines were established, and expression of FGF-2 and FGF receptor-1 (FGFR-1) were examined. The effects of FGF-2 on cell proliferation were determined by bromodeoxyuridine incorporation and cell counts, those on differentiation into myofibroblasts by staining for alpha-smooth muscle actin, and those on matrix synthesis by enzyme-linked immunosorbent assay for collagen type I and fibronectin. Finally, proliferative activity in vivo was evaluated by expression of MIB-1 (Ki-67 antigen). **RESULTS:** In normal kidneys, FGF-2 expression was confined to glomerular, vascular, and a few tubular as well as interstitial fibroblast-like cells. The expression of FGF-2 protein was increased in human kidneys, with tubulointerstitial scarring correlating with the degree of interstitial fibrosis ($r = 0.84$, $P < 0.01$). Immunoblot analyses confirmed a significant increase in FGF-2 protein expression in kidneys with interstitial scarring. In situ hybridization studies demonstrated low-level detection of FGF-2 mRNA in normal kidneys. However, FGF-2 mRNA expression was robustly up-regulated in interstitial and tubular cells in end-stage kidneys, indicating that these cells are the source of excess FGF-2 protein. Primary cortical fibroblasts express FGF-2 and FGFR-1 in vitro. FGF-2 induced a robust growth response in these cells that could be blocked specifically by a neutralizing FGF-2 antibody. Interestingly, the addition of the neutralizing antibody alone did reduce basal proliferation up to 31.5%. In addition, FGF-2 induced expression of alpha-smooth muscle actin up to 1.6-fold, but no significant effect was observed on the synthesis of collagen type I and fibronectin. Finally, staining for MIB-1 revealed a good correlation of interstitial FGF-2 positivity

with interstitial and tubular proliferative activity ($r = 0.71$, $P < 0.01$ for interstitial proliferation, $N = 30$). CONCLUSIONS: Interstitial FGF-2 protein and mRNA expression correlate with interstitial scarring. FGF-2 is a strong mitogen for cortical kidney fibroblasts and may promote autocrine fibroblast growth. Expression of FGF-2 correlates with interstitial and tubular proliferation in vivo.

PMID: 10760088 [PubMed - indexed for MEDLINE]



Adiposity elevates plasma MCP-1 levels leading to the increased CD11b-positive monocytes in mice.

Takahashi K, Mizuarai S, Araki H, Mashiko S, Ishihara A, Kanatani A, Itadani H, Kotani H.

Banyu Tsukuba Research Institute in collaboration with Merck Research Laboratories, Tsukuba, Ibaraki 300-2611, Japan.

Obesity is currently considered as an epidemic in the western world, and it represents a major risk factor for life-threatening diseases such as heart attack, stroke, diabetes, and cancer. Taking advantage of DNA microarray technology, we tried to identify the molecules explaining the relationship between obesity and vascular disorders, comparing mRNA expression of about 12,000 genes in white adipose tissue between normal, high fat diet-induced obesity (DIO) and d-Trp34 neuropeptide Y-induced obesity in mice. Expression of monocyte chemoattractant protein-1 (MCP-1) mRNA displayed a 7.2-fold increase in obese mice as compared with normal mice, leading to substantially elevated MCP-1 protein levels in adipocytes. MCP-1 levels in plasma were also increased in DIO mice, and a strong correlation between plasma MCP-1 levels and body weight was identified. We also showed that elevated MCP-1 protein levels in plasma increased the CD11b-positive monocyte/macrophage population in DIO mice. Furthermore, infusion of MCP-1 into lean mice increased the CD11b-positive monocyte population without inducing changes in body weight. Given the importance of MCP-1 in activation of monocytes and subsequent atherosclerotic development, these results suggest a novel role of adiposity in the development of vascular disorders.

PMID: 13129912 [PubMed - indexed for MEDLINE]

FREE full text article at
circ.ahajournals.org

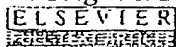
Augmented expression of neuronal nitric oxide synthase in the atria parasympathetically decreases heart rate during acute myocardial infarction in rats.

Takimoto Y, Aoyama T, Tanaka K, Keyamura R, Yui Y, Sasayama S.

Department of Cardiovascular Medicine, Graduate School of Medicine, Kyoto University, Kyoto, Japan.

BACKGROUND: Nitric oxide (NO) synthesized within sinoatrial cells recently has been shown to participate in the autonomic control of heart rate. We hypothesized that NO in the neuronal cells in the heart was increased and parasympathetically regulated heart rate after myocardial infarction (MI). **METHODS AND RESULTS:** We examined heart rate dynamics and neuronal NO synthase (nNOS) expression and activities in the atria of rats with MI 1, 3, 7, and 14 days after MI (n=7 to 22 for each group). Both the mRNA levels of nNOS in the atria determined by competitive reverse transcriptase-polymerase chain reaction and the protein levels determined by Western blotting were significantly increased compared with controls 1, 3, and 7 days after MI. nNOS activity in the atria 1 day after infarction was also increased in MI rats. nNOS immunoreactivity was observed in nerve fibers in the atria. After infusion of a specific inhibitor of nNOS and iNOS, 1-(2-trifluoromethylphenyl) imidazole (TRIM) (50 mg/kg IV), heart rate was significantly ($P<0.01$) increased in MI rats compared with controls 1, 3, and 7 days after MI. The iNOS-specific inhibitor, 1400W (10 mg/kg SC), did not significantly affect the heart rate in rats with MI. The effect of TRIM was abolished by pretreatment with L-arginine (25 mg/kg IV) or by parasympathetic blockade with atropine but not by propranolol. There was a strong correlation ($r=0.837$, $P<0.0001$) between the nNOS protein expression and heart rate change after TRIM infusion. **CONCLUSIONS:** These results indicate that increased nNOS parasympathetically decreased heart rate via the production of NO in rats with acute MI.

PMID: 11815433 [PubMed - indexed for MEDLINE]



Differential upregulation of cellular adhesion molecules at the sites of oxidative stress in experimental acute pancreatitis.

Telek G, Ducroc R, Scoazec JY, Pasquier C, Feldmann G, Roze C.

INSERM U 410, Universite Paris 7 Denis Diderot, 75870 Paris, France.

BACKGROUND: Severe acute pancreatitis (AP)(2) is associated with exaggerated leukocyte adherence and activation. Endothelial cellular adhesion molecules (CAMs) can be induced by cytokines, but also directly by oxygen free radicals (OFRs), mediated by nuclear factor kappa-B (NF-kappa B). We investigated the behavior of inducible CAMs in relation to pancreatic oxidative stress. Our novel modification of cerium capture histochemistry (reaction of OFRs with cerium produces laser reflective Ce perhydroxide precipitates) combined with reflectance confocal laser scanning microscopy (CLSM) allows the histological codemonstration of in vivo OFR production and immunolabeled CAMs, or NF-kappa B. **METHODS:** Taurocholate AP was induced in rats; sham operated and normal animals served as controls. To achieve in situ, in vivo reaction of cerium with OFRs, animals were perfused with CeCl(3) solution at different time points (1, 2, 8, 24 h) and then sacrificed. E-selectin, P-selectin, ICAM-1, VCAM, and NF-kappa B p65 were labeled by immunofluorescence (IF) on frozen sections of cerium perfused pancreata. IF and Ce perhydroxide reflectance were simultaneously detected by CLSM. Pancreatic gene expression of the same CAMs was quantified by competitive RT-PCR (MIMIC internal control). **RESULTS:** Control pancreata showed negligible reflectance and minimal CAM expression. Early (1, 2 h) AP samples were characterized by intense, heterogeneous acinar OFR production, strong P-selectin, and increasing ICAM expression, with nuclear translocation of p65, histologically all colocalizing with the areas of acinar oxidative stress. Adherent polymorphonuclear leukocytes (PMNs) displayed weak OFR formation. Later (8, 24 h), a slowly declining P-selectin, but persisting ICAM-1 expression, was paralleled by widespread adherence of PMNs producing surprisingly large amounts of OFRs. VCAM and E-selectin showed a mild increase at 24 h. CAM gene activation was in good correlation with the protein expression. **CONCLUSIONS:** The early acinar oxidative stress is colocalized with NF-kappa B activation; preferential P-selectin, and ICAM upregulation in this AP model. Subsequently, adherent, activated PMNs become the major source of OFRs, thereby contributing to tissue damage. Copyright 2001 Academic Press.

PMID: 11180997 [PubMed - indexed for MEDLINE]

Myotonic dystrophy: an unstable CTG repeat in a protein kinase gene.

Timchenko L, Monckton DG, Caskey CT.

Department of Molecular and Human Genetics, Baylor College of Medicine, Texas Medical Center, Houston 77030, USA.

Myotonic dystrophy (DM) is caused by the amplification of CTG repeats in the 3' untranslated region of a gene encoding a protein homologous to serine/threonine protein kinases. In DM patients the CTG repeats are extremely unstable, varying in length from patient to patient and generally increasing in length in successive generations. There is a strong correlation between the size of the repeats and the age of onset and severity of the disease. The molecular basis of the effect of the CTG expansion on the development of the DM phenotype continues to be investigated. The first working hypothesis of the molecular mechanism of DM was a reduction in steady-state myotonin-protein kinase (Mt-PK) mRNA and protein levels. However, although the consensus finding is that the Mt PK mRNA and protein levels are decreased in DM patients, it is still not clear if this reduction leads directly to the DM phenotype. In this short review we discuss the molecular aspects of CTG instability and the expression of the myotonin-protein kinase gene in normal and DM populations.

Publication Types:

- [Review](#)
- [Review, Tutorial](#)

PMID: 7620117 [PubMed - indexed for MEDLINE]

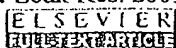
Induction of class 3 aldehyde dehydrogenase in the mouse hepatoma cell line Hepa-1 by various chemicals.

Torronen R, Korkalainen M, Karenlampi SO.

Department of Physiology, University of Kuopio, Finland.

The mouse hepatoma cell line Hepa-1 was shown to express an aldehyde dehydrogenase (ALDH) isozyme which was inducible by TCDD and carcinogenic polycyclic aromatic hydrocarbons. The induced activity could be detected with benzaldehyde as substrate and NADP as cofactor (B/NADP ALDH). As compared with rat liver and hepatoma cell lines, the response was moderate (maximally 5-fold). There was an apparent correlation between this specific form of ALDH and aryl hydrocarbon hydroxylase (AHH) in the Hepa-1 wild-type cell line--in terms of inducibility by several chemicals. However, the magnitude of the response was clearly smaller for ALDH than for AHH. Southern blot analysis showed that a homologous gene (class 3 ALDH) was present in the rat and mouse genome. The gene was also expressed in Hepa-1 and there was a good correlation between the increase of class 3 ALDH-specific mRNA and B/NADP ALDH enzyme activity after exposure of the Hepa-1 cells to TCDD. It is concluded that class 3 ALDH is inducible by certain chemicals in the mouse hepatoma cell line, although the respective enzyme is not inducible in mouse liver in vivo.

PMID: 1505055 [PubMed - indexed for MEDLINE]



Relationship between cyclin D1 and p21(Waf1/Cip1) during differentiation of human myeloid leukemia cell lines.

Ullmannova V, Stockbauer P, Hradcova M, Soucek J, Haskovec C.

Department of Molecular Genetics, Institute of Hematology and Blood Transfusion, U Nemocnice 1, 128 20 Prague 2, Czech Republic. ullman@uhkt.cz

Expression of cell cycle-regulating genes was studied in human myeloid leukemia cell lines ML-1, ML-2 and ML-3 during induction of differentiation in vitro. Myelomonocytic differentiation was induced by phorbol ester (12-o-Tetradecanoyl-phorbol-13-acetate, TPA), tumor necrosis factor alpha (TNFalpha) or interferon gamma (INFgamma), or their combination. Differentiation (with the exception of TNFalpha alone) was accompanied by inhibition of DNA synthesis and cell cycle arrest. Inhibition of proliferation was associated with a decrease in the expression of cdc25A and cdc25B, cdk6 and Ki-67 genes, and with increased p21(Waf1/Cip1) gene expression, as measured by comparative RT-PCR. Expression of the following genes was not changed after induction of differentiation: cyclin A1, cyclin D3, cyclin E1 and p27(Kip1). Surprisingly, cyclin D1 expression was upregulated after induction by TPA, TNFalpha with IFNgamma or BA. Cyclin D2 was upregulated only after induction by BA. The results of the expression of the tested genes obtained by comparative RT-PCR were confirmed by quantitative real-time (RQ) RT-PCR and Western blotting. Quantitative RT-PCR showed as much as a 288-fold increase of cyclin D1 specific mRNA after a 24h induction by TPA. The upregulation of cyclin D1 in differentiating cells seems to be compensated by the upregulation of p21(Waf1/Cip1). These results, besides others, point to a strong correlation between the expression of cyclin D1 and p21(Waf1/Cip1) on the one hand and differentiation on the other hand in human myeloid leukemic cells and reflect a rather complicated network regulating proliferation and differentiation of leukemic cells.

PMID: 12921950 [PubMed - indexed for MEDLINE]



Intestinal carbamoyl phosphate synthase I in human and rat. Expression during development shows species differences and mosaic expression in duodenum of both species.

Van Beers EH, Rings EH, Posthuma G, Dingemanse MA, Taminiau JA, Heymans HS, Einerhand AW, Buller HA, Dekker J.

Pediatric Gastroenterology and Nutrition, Department Pediatrics, Emma Children's Hospital, Academic Medical Center, Amsterdam, The Netherlands.

The clinical importance of carbamoyl phosphate synthase I (CPSI) relates to its capacity to metabolize ammonia, because CPSI deficiencies cause lethal serum ammonia levels. Although some metabolic parameters concerning liver and intestinal CPSI have been reported, the extent to which enterocytes contribute to ammonia conversion remains unclear without a detailed description of its developmental and spatial expression patterns. Therefore, we determined the patterns of enterocytic CPSI mRNA and protein expression in human and rat intestine during embryonic and postnatal development, using in situ hybridization and immunohistochemistry. CPSI protein appeared during human embryogenesis in liver at 31-35 e. d. (embryonic days) before intestine (59 e.d.), whereas in rat CPSI detection in intestine (at 16 e.d.) preceded liver (20 e.d.). During all stages of development there was a good correlation between the expression of CPSI protein and mRNA in the intestinal epithelium. Strikingly, duodenal enterocytes in both species exhibited mosaic CPSI protein expression despite uniform CPSI mRNA expression in the epithelium and the presence of functional mitochondria in all epithelial cells. Unlike rat, CPSI in human embryos was expressed in liver before intestine. Although CPSI was primarily regulated at the transcriptional level, CPSI protein appeared mosaic in the duodenum of both species, possibly due to post-transcriptional regulation.

PMID: 9446830 [PubMed - indexed for MEDLINE]

Malignant transformation of the human endometrium is associated with overexpression of lactoferrin messenger RNA and protein.

Walmer DK, Padin CJ, Wrona MA, Healy BE, Bentley RC, Tsao MS, Kohler MF, McLachlan JA, Gray KD.

Department of Obstetrics and Gynecology, Duke University Medical Center, Durham, North Carolina 27710.

In the mouse uterus, lactoferrin is a major estrogen-inducible uterine secretory protein, and its expression correlates directly with the period of peak epithelial cell proliferation. In this study, we examine the expression of lactoferrin mRNA and protein in human endometrium, endometrial hyperplasias, and adenocarcinomas using immunohistochemistry, Western immunoblotting, and Northern and in situ RNA hybridization techniques. Our results reveal that lactoferrin is expressed in normal cycling endometrium by a restricted number of glandular epithelial cells located deep in the zona basalis. Two thirds (8 of 12) of the endometrial adenocarcinomas examined overexpress lactoferrin. This tumor-associated increase in lactoferrin expression includes an elevation in the mRNA and protein of individual cells and an increase in the number of cells expressing the protein. In comparison, only 1 of the 10 endometrial hyperplasia specimens examined demonstrates an increase in lactoferrin. We also observe distinct cytoplasmic and nuclear immunostaining patterns under different fixation conditions in both normal and malignant epithelial cells, similar to those previously reported in the mouse reproductive tract. Serial sections of malignant specimens show a good correlation between the localization of lactoferrin mRNA and protein in individual epithelial cells by in situ RNA hybridization and immunohistochemistry. Although the degree of lactoferrin expression in the adenocarcinomas did not correlate with the tumor stage, grade, or depth of invasion in these 12 patients, there was a striking inverse correlation between the presence of progesterone receptors and lactoferrin in all 8 lactoferrin-positive adenocarcinomas. In summary, lactoferrin is expressed in a region of normal endometrium known as the zona basalis which is not shed with menstruation and is frequently overexpressed by progesterone receptor-negative cells in endometrial adenocarcinomas.

PMID: 7867003 [PubMed - indexed for MEDLINE]

TPL



Cancer Research

AN OFFICIAL JOURNAL OF THE AMERICAN ASSOCIATION FOR CANCER RESEARCH



March 1, 1995
Volume 55 • Number 5
PP. 975-1197
ISSN 0008-5472 • CNREA 8

LIBRARY OF THE AMERICAN ASSOCIATION FOR CANCER RESEARCH

MAR 06 1995

1001 N. 17TH ST. PHILADELPHIA, PA 19104

UNIVERSITY OF WISCONSIN
HEALTH SCIENCES LIBRARY



1305 Linden Drive
Madison, WI 53706

MAR 0 6 1993

UNIVERSITY OF WISCONSIN
HEALTH SCIENCES LIBRARY

Cancer Research

AN OFFICIAL JOURNAL OF THE AMERICAN ASSOCIATION FOR CANCER RESEARCH

**American Association for
Cancer Research, Inc.**
Publications Staff
Managing Editor
Margaret Foti
Assistant Managing Editor
Mary Anne Mennine
Manager, Editorial Services
Heide M. Puszy
Staff Editors
Lisa A. Chippendale
Pamela M. Griebow
Michael J. Beveridge
Kathleen C. Assenmacher
**Supervisor, Manuscript
Processing**
Margaret A. Pickels
**Assistant Supervisor,
Manuscript Processing**
Theresa A. Griffith
Staff Assistant
Mary Ellen Puring
Editorial Assistants
Valerie L. Taylor
Andrea Conrad
Katherine V. Pawlowaki
Bethann Massarella
Charles W. Wells, Jr.
Administrative Staff
Executive Director
Margaret Foti
Director of Administration
Adam D. Blistine
Controller
Joan D. Brokenshire
**Coordinator, Financial
Operations**
George L. Moore
Meetings Coordinator
Jeffrey M. Ruben
Meeting Planner
Carol L. Kanoff
Public Information Coordinator
Janay Anne Horst-Mertz
**Executive Assistant for
Programs**
Ruth E. Fortson
Administrative Assistant
Robin E. Felder
Systems Specialist
Lydia I. Rodriguez
Staff Assistant
Lori L. Holmes
Secretary
Malika L. Wright
Editorial Secretary
Diana F. Certo
Financial Clerk
Paul Perrault
Office Clerk
James J. Waters
Data Entry Clerk
Robert A. Simms II

Editor-in-Chief
Carlo M. Croce

Associate Editors

Stuart A. Aaronson
Jerry M. Adams
David S. Alberts
Carmen J. Allegra
Frederick R. Appelbaum
James O. Armitage
William M. Baird
Alan Balmain
J. Carl Barrett
Renato Baserga
William T. Beck
Joseph R. Bertino
Mina J. Bissell
Clara D. Bloomfield
Gianni Bonadonna
Ernest C. Borden
G. Tim Bowden
Edward Bresnick
Samuel Broder
Ronald N. Buick
Paul A. Bunn, Jr.
C. Patrick Burns
Fernando Cabanillas
Bruno Calabretta
Eli Canziani
Robert L. Capizzi
Webster K. Cavenee
Bruce D. Cheson
David Colcher
Robert L. Comis
Allan H. Conney
Neal G. Copeland
Joseph G. Cory
William M. Crist
Benoit de Crombrughe

Riccardo Dalla-Favera
Richard L. Davidson
Eugene R. DeSombre
T. Michael Dexter
Ralph E. Dorand
Alan Eastman
Gertrude B. Elion
Leonard C. Erickson
Nelson Fausto
Eric R. Fearon
Isaiah J. Fidler
Robert A. Floyd
Judith Folkman
Kenneth A. Foon
Joseph F. Fraumeni, Jr.
Stephen H. Friend
Minoru Fukuda
Philip Furmanski
Eugene W. Gerner
Elfi Glasstein
David W. Golde
Michael M. Gottesman
J. W. Grisham
F. Peter Guttingerich
Sen-itiroh Hakomori
Phillip C. Hanawalt
Curtis C. Harris
John C. Harshbarger
Stephen S. Hecht
Carl-Henrik Heldin
Brian E. Henderson
Richard B. Hochberg
Wang Ki Hong
Tasuku Honjo
Kay Huebner

John T. Isaacs
Mark A. Israel
Elaine S. Jaffe
Rakesh K. Jain
Peizi A. Jones
V. Craig Jordan
John H. Kersey
Young S. Kim
Kenneth W. Kinzler
Tadamitsu Kishimoto
Alfred G. Knudson, Jr.
Kurt W. Kohle
Lawrence N. Kolonel
Donald W. Kufe
John S. Lazo
Jay A. Levy
Frederick P. Li
Victor Ling
Lance A. Lione
Martin Lipkin
Marc E. Lippman
Gerald Litwack
Leroy F. Liu
Lawrence A. Loeb
Dan L. Longo
Reuben Lotan
David B. Ludlum
Tak W. Mak
Michael J. Mastrangelo
Lynn M. Matrisian
W. Gillies McKenna
Anna T. Meadows
John Mendelsohn
Christopher J. Michrjda
John D. Minna

Beatrice Mintz
Malcolm S. Mitchell
Ruth J. Muschel
Yusuke Nakamura
Garth L. Nicolson
Kenneth Nilsson
Susumu Nishimura
Jeffrey A. Norton
Kenneth Olden
Gilbert S. Omenn
Richard J. O'Reilly
Robert F. Ozols
Michael A. Palladino, Jr.
Peter L. Pedersen
Anthony E. Pegg
Angel Pellicer
Bice Perussia
Gordon L. Phillips
Cecil B. Picken
Jacalyn H. Pierce
Vito Quaranta
Frank J. Rauscher III
Donald J. Reed
Ralph A. Reisfeld
Richard A. Rifkind
Leslie L. Robison
Igor B. Roninson
Howard J. Scher
Robert T. Schirake
J. Schlessinger
Manfred Schwab
Joseph V. Simone
Francis M. Sirotnak
Anna Marie Skalka

Michael B. Sporn
Martha R. Stampfer
Eric J. Stanbridge
Gary S. Stein
Bernard S. Strauss
Takashi Sugimura
Saraswati Sukumar
James A. Swenberg
Paul Talalay
Tadatsugu Taniguchi
Steven R. Tannenbaum
Masaki Terada
Kenneth D. Tew
Donald J. Tindall
George J. Todaro
Jeffrey M. Trent
Giorgio Trinchieri
Takashi Tsuruo
Axel Ullrich
Peter Vaupel
Giancarlo Vecchio
Daniel D. Von Hoff
Michael D. Waterfield
Lee W. Wattenberg
Ralph R. Weichselbaum
I. Bernard Weinstein
Bengt Westermark
Raymond L. White
Gordon F. Whitmore
Max S. Wicha
Walter Willen
H. Rodney Withers
Sheldon Wolff
Stuart H. Yuspa
Harald zur Hausen

Cover Editorial Board
Sidney Weinhouse,
Cover Editor

Hugh J. Creech
Clark W. Heath, Jr.

Edwin A. Mirand
Raymond W. Rudden

Takashi Sugimura
John H. Weisburger

Cancer Research is sponsored by the American Association for Cancer Research, Inc. and receives major support from the American Cancer Society, Inc. Publication costs are also met by a grant from the Elsa U. Pardee Foundation. Accelerated mailing of journals to AACR members in Japan is supported by a generous grant from the Banyu Pharmaceutical Company.

Subscription Information

Cancer Research is published twice a month, one volume per year, by the American Association for Cancer Research, Inc. (AACR). Subscriptions include the *Proceedings of the American Association for Cancer Research*, issued in March of each year. Except for members of the AACR, all subscriptions are payable in advance to *Cancer Research*, P.O. Box 5000, Denville, NJ 07834 (Telephone: (800) 875-2997; FAX: (201) 677-5872), to which all business communications, remittances (in United States currency or its equivalent), and subscription orders should be sent. In Japan, send orders and inquiries to (sole agent): USACO Corporation, Tsutsumi Bldg., 15-12, Shimbashi 1-chome, Minato-ku, Tokyo 105, Japan; Tel. (03) 502-6471. Individuals who are not AACR members may subscribe to Volume 55 (1995) of *Cancer Research* at the rate of \$460 U.S./\$520 foreign. *Cancer Research* is only available to institutions as a combined subscription with *Clinical Cancer Research*. The combined 1995 institutional subscription price of \$495 U.S./\$575 foreign includes a subscription to *Clinical Cancer Research*. Canadian subscribers should add 7% GST. Changes of address notification should be sent 60 days in advance and include both old and new addresses. Member subscribers should send address changes to: AACR Member Services, Public Ledger Bldg., Suite F16, 150 South Independence Mall West, Philadelphia, PA 19106-3483. Nonmember subscribers should send changes of address to: *Cancer Research*, P.O. Box 3000, Denville, NJ 07834. Copies of the journal which are undeliverable because of address changes will be destroyed.

Malignant Transformation of the Human Endometrium Is Associated with Overexpression of Lactoferrin Messenger RNA and Protein

David K. Walmer,¹ Cheryl J. Padin, Mark A. Wrona, Bridget E. Healy, Rex C. Bentley, Ming-Sound Tsao, Matthew F. Kohler, John A. McLachlan, and Karen D. Gray

Department of Obstetrics and Gynecology, Duke University Medical Center, Durham, North Carolina 27710 [D. K. W., B. E. H., M. F. K.]; Department of Obstetrics and Gynecology, University of Michigan, Ann Arbor, Michigan 48109 [C. J. P.]; School of Medicine, University of Maryland, Baltimore, Maryland 21201 [M. A. W.]; Department of Pathology, Duke University Medical Center, Durham, North Carolina 27710 [R. C. B.]; Department of Pathology, Montreal General Hospital, Montreal, Quebec, Canada H3G1A4 [M.-S. T.]; Laboratory of Reproductive and Developmental Toxicology, National Institute of Environmental Health Sciences, Research Triangle Park, North Carolina 27709 [J. A. M.]; and Department of Obstetrics and Gynecology, Uniformed Services University of the Health Sciences, Bethesda, Maryland 20814-7799 [K. D. G.]

ABSTRACT

In the mouse uterus, lactoferrin is a major estrogen-inducible uterine secretory protein, and its expression correlates directly with the period of peak epithelial cell proliferation. In this study, we examine the expression of lactoferrin mRNA and protein in human endometrium, endometrial hyperplasias, and adenocarcinomas using immunohistochemistry, Western immunoblotting, and Northern and *in situ* RNA hybridization techniques. Our results reveal that lactoferrin is expressed in normal cycling endometrium by a restricted number of glandular epithelial cells located deep in the zona basalis. Two thirds (8 of 12) of the endometrial adenocarcinomas examined overexpress lactoferrin. This tumor-associated increase in lactoferrin expression includes an elevation in the mRNA and protein of individual cells and an increase in the number of cells expressing the protein. In comparison, only 1 of the 10 endometrial hyperplasia specimens examined demonstrates an increase in lactoferrin. We also observe distinct cytoplasmic and nuclear immunostaining patterns under different fixation conditions in both normal and malignant epithelial cells, similar to those previously reported in the mouse reproductive tract. Serial sections of malignant specimens show a good correlation between the localization of lactoferrin mRNA and protein in individual epithelial cells by *in situ* RNA hybridization and immunohistochemistry. Although the degree of lactoferrin expression in the adenocarcinomas did not correlate with the tumor stage, grade, or depth of invasion in these 12 patients, there was a striking inverse correlation between the presence of progesterone receptors and lactoferrin in all 8 lactoferrin-positive adenocarcinomas. In summary, lactoferrin is expressed in a region of normal endometrium known as the zona basalis which is not shed with menstruation and is frequently overexpressed by progesterone receptor-negative cells in endometrial adenocarcinomas.

INTRODUCTION

The uterus is a sex steroid-responsive organ that plays a major role in women's health. Hysterectomies were the most frequently performed major surgical procedures in a 20-year study interval (1965-1984; Ref. 1). Fifty-eight to 80% of these 12.5 million procedures were performed for estrogen-related disorders of proliferation. Chronic unopposed estrogen exposure, most commonly associated with type II ovulatory disorders, eventually leads to the development of complex endometrial hyperplasia and adenocarcinoma. Since the sex steroids, estrogen and progesterone, act on their target tissues by regulating the expression of a wide variety of signaling molecules, identifying these regulatory factors will provide critical information towards understanding normal reproduction and reproductive tract pathology. Our current knowledge of estrogen and progesterone action on the reproductive tract is based to a great extent on information collected from rodents (2). Although differences exist

between the reproductive physiology of rodents and humans, the mouse has been a useful model for studying steroid hormone action in the human female reproductive tract (3, 4). One potential regulatory molecule shown to be regulated by estrogen in the mouse reproductive tract is lactoferrin. Lactoferrin is a basic glycoprotein with an extraordinarily high affinity for iron that was originally discovered in milk. This protein is expressed in a wide variety of tissues, most notably in polymorphonuclear leukocytes and most mammalian exocrine glandular secretions. In the mammary gland (5) and the female reproductive tract of the mouse (6-8), lactoferrin is regulated by endocrine hormones. Prolactin stimulates lactoferrin synthesis in the breast; whereas in the uterus and vagina, the ovarian sex steroid, 17 β -estradiol, is the inducer. (6, 7, 9). To date, lactoferrin is one of the few genes that have been identified in the rodent that are directly regulated by estradiol. The lactoferrin gene contains an ERE² that is important for regulating its expression *in vivo* in the mouse reproductive tract. Being linked to estradiol, the expression of lactoferrin by the uterine epithelium parallels the onset of DNA synthesis. Although sequencing information suggests that the human lactoferrin gene also contains a functional imperfect ERE in the 5'-flanking promoter region (10, 11), there is very little data regarding lactoferrin expression in the human female reproductive tract.

The purpose of our study was to examine the expression of lactoferrin in the human endometrium under normal and pathological conditions by immunohistochemistry, immunoblotting, and Northern and *in situ* RNA hybridization techniques. In addition, we looked for correlations between lactoferrin expression and several parameters, such as the stage of the menstrual cycle, the distribution of estrogen and progesterone receptors, HER-2/*neu* expression, markers of cell proliferation, and the histopathological grade and extent of myometrial invasion in the adenocarcinomas. Our data demonstrates that lactoferrin is expressed in a very restricted number of glands in the basal region of normal human endometrium and is markedly overexpressed in a significant number of the uterine adenocarcinomas by PR-negative cells.

MATERIALS AND METHODS

Tissue Preparation and Histological Evaluation. Surgical pathology specimens were obtained from Duke University Medical Center (Durham, NC) and the Department of Pathology at Montreal General Hospital (Quebec, Montreal, Canada). Cycling endometrium was obtained from 22 women (ages 31-49), and atrophic endometrium was obtained from 7 postmenopausal women (ages 64-77). Hysterectomies from cycling women were performed for subserosal leiomyomas ($n = 6$), pelvic relaxation ($n = 8$), pelvic pain ($n = 4$), peritoneal endometriosis ($n = 2$), and cancer of either the exocervix ($n = 1$) or the ovary ($n = 1$). In addition, 12 adenocarcinomas, 3 atypical complex hyperplasias, 5 complex hyperplasias without atypia, and 4 simple hyperplasias were analyzed. Each human uterus was bivalved shortly after

Received 8/15/94; accepted 12/30/94.

The costs of publication of this article were defrayed in part by the payment of page charges. This article must therefore be hereby marked advertisement in accordance with 18 U.S.C. Section 1734 solely to indicate this fact.

¹ To whom requests for reprints should be addressed, at Department of Obstetrics and Gynecology, Box 3145, Duke University Medical Center, Durham, NC 27710.

² The abbreviations used are: ERE, estrogen response element; PCNA, proliferating cell nuclear antigen; ER, estrogen receptor; PR, progesterone receptor.

hysterectomy, and endometrium was removed from the fundal region. A full thickness biopsy was placed into either 10% neutral-buffered formalin or Bouin's solution overnight at room temperature before dehydration, paraffin embedding, and sectioning at 4 μ m on silanized slides. Histological evaluations of hematoxylin and eosin-stained slides were performed blindly by one board-certified pathologist. Normal endometrial samples were dated by the criteria of Noyes *et al.* (12). Endometrial hyperplasias and carcinomas were classified according to the current recommendations of the International Society of Gynecological Pathologists under the auspices of WHO (13). Histological grading of tumors was performed according to Federation Internationale des Gynecologues et Obstetristes criteria (14). Each specimen was read a minimum of three times, and only specimens that were read consistently the same way were included in the study. Unstained sections of the same tissues were used for the cytochemical analysis of protein and mRNA expression using specific reagents. A few endometrial samples were frozen for subsequent protein and RNA extraction, which were evaluated by Western and Northern blotting, respectively. All human tissues were handled with the precautions and the guidelines required by Duke University and National Institute of Environmental Health Sciences.

Immunolocalization. Slides chosen for study were deparaffinized and rinsed in 20% glacial acetic acid at 4°C for 15 s to inhibit endogenous alkaline phosphatase. All subsequent incubations and washes were at room temperature. Sections were next equilibrated in PBS for 20 min and incubated for 20 min with 1.5% normal goat serum diluted in PBS to block nonspecific binding. Detection of lactoferrin was performed primarily with a rabbit anti-human lactoferrin polyclonal antiserum generated in our laboratory and affinity purified. Similar results were also seen with a nonaffinity-purified commercial antiserum (Biogenex, San Ramon, Ca). Following incubation at room temperature with primary antisera for 60 min, the sections were washed in PBS twice for 10 min each, and lactoferrin was localized using an alkaline phosphatase-biotin-streptavidin detection system (Vectastain ABC-AP kit; Vector Laboratories, Burlingame, CA; or the Super Sensitive Detection System; Biogenex, San Ramon, CA). To identify nonspecific staining, preimmune rabbit serum was used in place of the primary antibody. The immunoreaction was quantitated by determining the percentage of glands and the percentage of cells staining for lactoferrin in the zona basalis and the zona functionalis, with a minimum of 300 cells counted in each region. PR antibody was provided by Geoffrey Greene (KD68), and a commercial source was also used (Biogenex, San Ramon, CA). Identical staining patterns were confirmed with both preparations. Other commercially obtained antisera include PCNA (Biogenex, San Ramon, CA), ER (ER1D5; AMAC, Westbrook, Ma), MIB-1 (AMAC), and HER-2/*neu* (Biogenex, San Ramon, CA). The primary antisera incubations were 2 h for the PR, 1 h for PCNA, MIB-1, and ER, and 30 min for HER-2/*neu*. Antisera dilutions were 1:100 for MIB-1 and 1:20 for HER-2/*neu*. Antigen retrieval (Biogenex, San Ramon, CA) was performed before adding the progesterone primary antisera.

Western Blot Analysis. Proteins were extracted from endometrial biopsies by homogenization on ice in 1% Triton-X and 20 mM Tris-HCl (pH 7.4) with protease inhibitors (10 μ g/ml leupeptin, 200 KU/ml aprotinin, and 20 μ g/ml phenylmethylsulfonyl fluoride) and clarified by centrifugation at 45,000 rpm for 30 min in a Beckman 70.1 Ti rotor; then the supernatant was analyzed for protein concentration by the BCA protein assay (Pierce, Rockford, IL). Aliquots of 200 μ g were separated by electrophoresis on an 8.5% SDS polyacrylamide gel, blotted onto nitrocellulose membranes, incubated with polyclonal rabbit antihuman lactoferrin antiserum, and localized with an 125 I-labeled donkey anti-rabbit immunoglobulin, as described previously (7).

In Situ Hybridization. All slides were pretreated with 0.2 N HCl for 30 min at room temperature, digested with 1 μ g/ml proteinase-K (Sigma Chemical Co., St. Louis, MO) in 0.1 M Tris-HCl (pH 7.4)-0.05 M EDTA for 15 min at 37°C, and then treated with 0.1 M methanolamine-0.25% acetic anhydride for 5 min at room temperature and 0.1 M Tris-glycine (pH 7.4) for 30 min at room temperature. The sections were subsequently dehydrated with graded ethanol, air dried, and prehybridized at 50°C for 1 h in 2 \times SSC, 10 mM DTT, 5 \times Denhardt's solution, 100 μ g/ml of both salmon sperm DNA and yeast tRNA, and 50% formamide (15). The slides were then hybridized overnight at 50°C in the same medium with 10% dextran sulfate and 2 \times 10⁶ cpm/ μ l of the specific RNA probe. The lactoferrin oligonucleotide probe was amplified by PCR using primers that spanned nucleotides 718-1654 (10) and cloned into pGEM-4Z. 32 S-labeled sense and antisense RNA probes were made with the

Promega Riboprobe kit (Promega, Madison, WI), washed twice in 1 \times SSC for 10 min at room temperature, digested with RNase [2.8 μ g/ml RNase-A, 0.3 μ g/ml RNase-T1, 10 mM Tris-HCl (pH 7.4), and 15 mM NaCl], and washed again with 1 \times SSC twice for 20 min each time at 50°C, twice for 20 min in 0.1 \times SSC at 55°C, and once for 20 min at 60°C. The sections were then dehydrated and dipped in Kodak autoradiographic emulsion (NTB-2) for detection of specific mRNA expression. The slides were allowed to develop for 2 weeks. After this period, the slides were developed using Kodak D19 developer and Kodak Rapid Fixer.

Northern RNA Analysis. Total cellular RNA was purified from frozen tissue by the guanidine isothiocyanate-cesium chloride method, and poly(A⁺)-RNA was isolated by oligo(dT)-cellulose chromatography using methods described previously (15). For Northern blot analysis, poly(A⁺)-RNA was resolved by electrophoresis on 1.5% formaldehyde agarose gels, stained with ethidium bromide, and transferred to a nylon membrane. The membrane was probed with a 32 P-labeled lactoferrin cDNA derived from human uterus (nucleotides 718-1654; accession no. S52659) using PCR techniques, followed by cloning into pGEM-4Z (Promega, Madison, WI). In order to insure that the quality and quantity of RNA analyzed by Northern blotting was equivalent between control and treated groups, the blot was probed simultaneously for glyceraldehyde-3-phosphate dehydrogenase.

Statistical Analysis. Values are presented as means \pm SD. Differences between the zona basalis and functionalis were tested by the two-tailed Student's *t* test.

RESULTS

Immunohistochemical Analysis of Lactoferrin Protein

Normal Cycling Endometrium. Immunohistochemical studies of normal cycling human endometrium localize lactoferrin protein predominantly to the glandular epithelium deep in the zona basalis and not to the functionalis (Fig. 1A). The association of lactoferrin protein expression with the zona basalis is statistically significant ($P < 0.001$; Fig. 2). Two to 56% of the glands express lactoferrin at any given time during the menstrual cycle. Within positive glands, lactoferrin protein immunolocalization is heterogeneous in that positively staining epithelial cells are interspersed with cells negative for lactoferrin expression. No apparent differences in morphology, PCNA, ER, or PR expression are seen to account for the heterogeneous pattern of intra- and intergland lactoferrin expression in normal endometrium. Similar to our previous findings in mouse uterine epithelial cells, the positive-staining glandular cells of the human endometrium demonstrate two distinct immunostaining patterns for lactoferrin, cytoplasmic and nuclear (Fig. 1B), seen with both formalin and Bouin's fixation. In evaluating the temporal expression of lactoferrin, there is a trend towards more glands expressing lactoferrin during the secretory phase. Because of the large variance, the trend is not statistically significant. As expected, the polymorphonuclear leukocytes in the endometrium also stain intensely for lactoferrin protein, which is stored in their secondary granules (Fig. 3). These results demonstrate, for the first time, that lactoferrin protein is expressed in the human endometrium predominantly by polymorphonuclear leukocytes and epithelial cells of glands located deep in the zona basalis.

Proliferative Endometrial Disorders: Hyperplasias and Adenocarcinomas. Immunohistochemistry reveals that the expression of lactoferrin protein is increased in 66.6% (8 of 12) of the endometrial adenocarcinomas examined. In one-half of these cases (4 of 12), lactoferrin is intensely expressed by malignant epithelial cells throughout the entire tumors (Fig. 4). The other four adenocarcinomas demonstrate increased staining for lactoferrin in concentrated regions of the tumors. In all eight cases where lactoferrin expression is elevated, the cells expressing lactoferrin have one similarity with normal positive glands in that they demonstrate heterogeneous staining of interspersed positive and negative cells. However, the expression of lactoferrin by the malignant cells clearly differs from normal

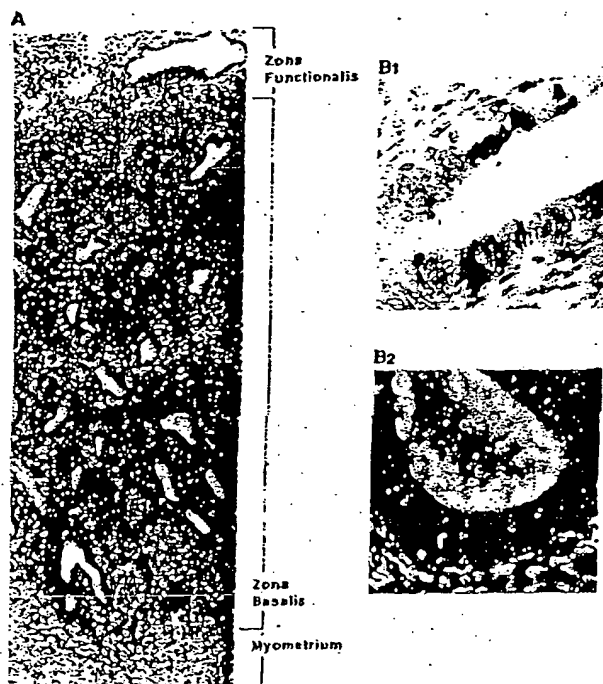


Fig. 1. Localization of lactoferrin protein in normal cycling endometrium by immunohistochemistry using a specific polyclonal antibody. Our analysis reveals that lactoferrin protein is present in a limited number of glands located in the zona basalis of the endometrium (A); $\times 10$. Also, note that lactoferrin is heterogeneous within positive glands, i.e., cells staining for lactoferrin are interspersed with negative-staining epithelial cells throughout the gland. Two immunohistochemical staining patterns are noted for lactoferrin in normal uterine epithelium. In one pattern, lactoferrin protein is immunolocalized primarily over the cytoplasm (B1), and in the other, the staining is seen over the nucleus (B2); $\times 40$.

positive glands in that the lactoferrin is not limited to the basal regions of the tumors, many more cells are positive, and the relative intensity of the staining over individual cells is increased. Although increased lactoferrin expression is associated with malignant transformation, we do not find a correlation between lactoferrin protein presence and the stage, nuclear grade, Federation Internationale des Gynecologues et Obstetristes grade, or the depth of myometrial invasion in the 12 tumors studied (Table 1). In sharp contrast to the common dysregulation of lactoferrin expression found in the malignant endometrium, only 1 of 10 endometrial hyperplasia specimens evaluated contained an increased number of cells staining for lactoferrin. The hyperplastic specimen overexpressing lactoferrin was read as complex without atypia.

In Situ and Northern Analyses of Lactoferrin mRNA Expression in Normal and Malignant Endometrium

To further our understanding of the location of lactoferrin protein synthesis in the human endometrium, we examined lactoferrin mRNA expression by *in situ* and Northern hybridization using specific 35 S-labeled probes for human lactoferrin. No detectable RNA hybridization is observed in the normal endometrium by *in situ* hybridization, even in the presence of immunodetectable protein, using equivalent hybridization conditions and development times as used for the adenocarcinomas. Consistent with the results obtained by *in situ* hybridization, long exposure times were required to demonstrate lactoferrin mRNA in normal endometrium by Northern blot using poly(A)⁺-mRNA. This indicates that lactoferrin mRNA is present in normal

tissue but in very low levels, consistent with the very limited pattern of protein expression in normal endometrium. Equivalent RNA loading and quality for each specimen was demonstrated by ethidium bromide staining of the RNA gels (data not shown) and by probing for the housekeeping gene glyceraldehyde-3-phosphate dehydrogenase that does not fluctuate significantly with the metabolic state of the tissue. A representative Northern blot is shown in Fig. 5. *In situ* hybridization with several adenocarcinomas reveals that there is a direct correlation between the localization of lactoferrin mRNA and the immunostaining of expressed lactoferrin protein (Fig. 4). Lactoferrin mRNA is not associated with polymorphonuclear leukocytes by *in situ* hybridization in either normal or malignant tissue.

Western Blot Analysis

To confirm the specificity of the antisera that we used for immunohistochemistry, we performed Western blot analysis on proteins extracted from both normal and malignant endometrium which were separated by 8.5% SDS-polyacrylamide gel electrophoresis (Fig. 6). Immunoblotting identified a single broad protein band with a molecular weight between 70,000–80,000 in both normal and neoplastic endometrial tissue homogenates, consistent with the reported molecular weight of human lactoferrin. Supporting the immunocytochemical analysis, a representative immunoblot clearly demonstrates that the proportion of protein that is lactoferrin is markedly increased in the adenocarcinomas in comparison to the normal endometrium. The molecular weight of lactoferrin in the adenocarcinomas appears to have a slightly higher molecular weight than the predominant form in normal tissue.

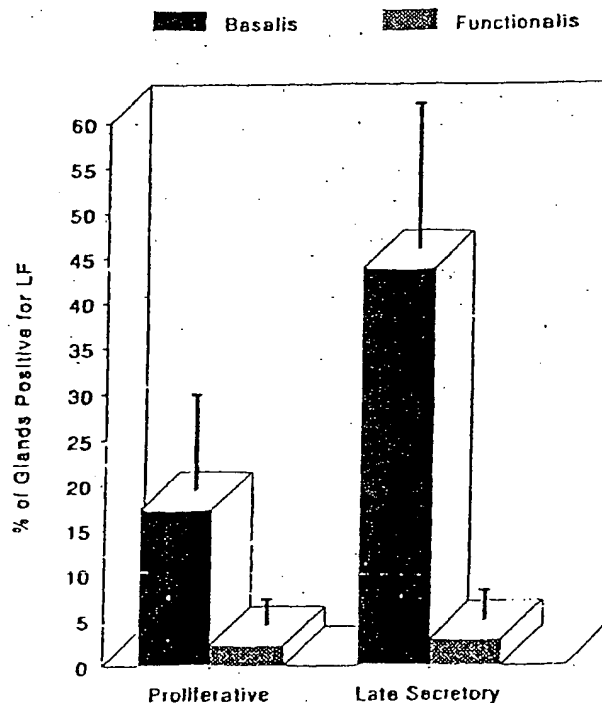


Fig. 2. Percentage of endometrial glands expressing lactoferrin protein by immunohistochemistry. Significantly more glands are positive in the region of the zona basalis than in the zona functionalis of the endometrium ($P < 0.001$). Zona basalis, ■; zona functionalis, □. Although there is a trend towards more of the basalis glands expressing lactoferrin in the secretory phase (right ■ compared with the left ■), this was not statistically significant.

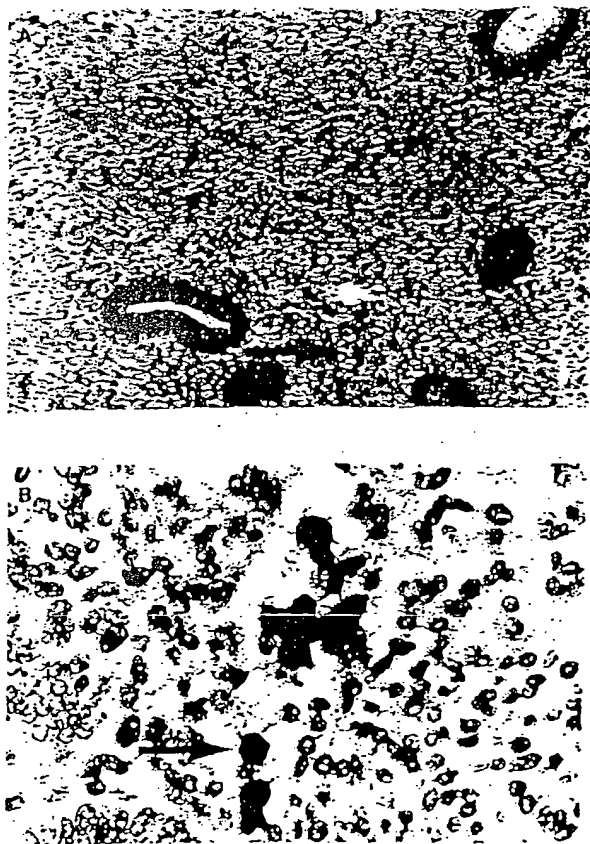


Fig. 3. Polymorphonuclear leukocytes (arrows) are scattered throughout the endometrium and stain intensely for lactoferrin. Lactoferrin is a known component of the secondary granules in polymorphonuclear leukocytes. The presence of a segmented nucleus and lactoferrin protein is an excellent method for identifying this group of inflammatory cells. A, $\times 20$; B, $\times 60$.

Correlation of Lactoferrin Expression with the Expression of PCNA, Ki-67, HER-2/*neu*, ER, and PR

In an attempt to characterize the phenotype of endometrial cells which express lactoferrin, we performed immunohistochemistry on serial sections for the Ki-67 antigen, PCNA, HER-2/*neu*, lactoferrin, ER, and PR. In normal tissue, Ki-67 and PCNA expression are cell cycle-specific markers of cell proliferation (16, 17). Upon analysis of normal cycling endometrium, no relationship between lactoferrin protein expression and ER, PR, or Ki-67 expression was observed. Similarly, in most of the adenocarcinomas evaluated, no relationship was noted between lactoferrin and PCNA protein expression. However, in one adenocarcinoma (Fig. 7), there was a clear inverse relationship seen between lactoferrin and PCNA localization, which was present throughout the entire tumor. Most dramatic, however, was a striking inverse correlation seen between lactoferrin and PR expression in 8 of 8 PR-positive uterine adenocarcinomas (Fig. 7). Two tumors negative for PR also did not express lactoferrin. Although an inverse correlation was also suggested with HER-2/*neu* and PR, the inverse correlation was more precise with lactoferrin in these tumors.

DISCUSSION

In the mouse uterus, lactoferrin is an estrogen-induced uterine secretory protein that is present throughout the epithelium (7), and it

is expressed concomitantly with epithelial cell proliferation. In contrast to lactoferrin's ubiquitous expression in the estrogenized mouse uterine epithelium, lactoferrin protein is limited to glandular epithelial cells in the basal regions of normal human endometrium and usually to glands that were directly adjacent to the myometrium (i.e., the deepest glands of the zona basalis). This regional localization of lactoferrin expression is not surprising in that other biochemical parameters have been reported to show site specificity in primate endometrium. These parameters include the proliferative index and the expression of the secretory component of IgA (18). Similar to our observations in the endometrium, lactoferrin is also expressed regionally in the mammary gland. In bovine breast tissue, lactoferrin is localized primarily to the basal alveolar cells (19); whereas in human breast tissue, the ductal epithelium appears to be the primary source of secreted lactoferrin during lactation (20).

Examining the endometrium on different days of the menstrual cycle demonstrates a trend towards increased lactoferrin expression during the luteal phase. Although this data is not statistically significant, the cyclic variation may be biologically relevant. Kim *et al.* (21) recently reported that the basal endometrial epithelial cells are unique because they proliferate during the postovulatory luteal phase. Interestingly, in the mouse uterus, there is a direct correlation between lactoferrin expression and epithelial cell proliferation (6). Therefore, lactoferrin may have a similar role in the human and mouse endometrium. If lactoferrin expression is cyclic, the ERE in the 5'-flanking promoter region of the human lactoferrin gene may be activated during the luteal phase (10, 11).

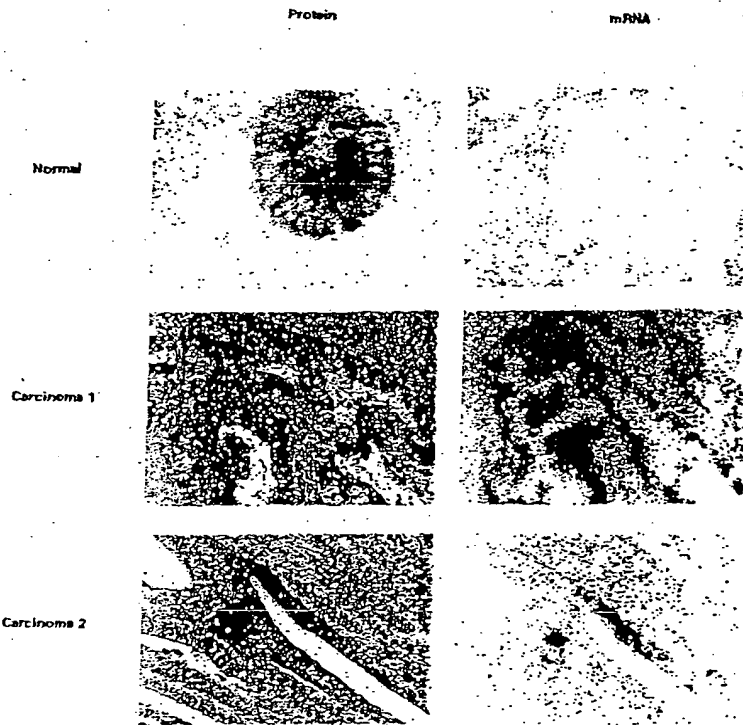
Another similarity between human and mouse uterine lactoferrin expression is the observation of two immunohistochemical staining patterns. In one pattern, the antisera binds primarily over the cytoplasm, and in the other, the nucleus is the primary site of localization. Although this could represent a fixation artifact, we have now observed this pattern in two species and under different fixation conditions. It has been demonstrated that signaling peptides, i.e., platelet-derived growth factor (22), Int-2 (23), and probasin (24), can be selectively directed into the nucleus, cytoplasm, or secreted. It is believed that this differential processing may allow proteins to have intracrine, autocrine, and paracrine roles, depending on the physiological state of the cell. The two localization patterns observed suggest that lactoferrin might have signaling sequences that direct the final destination of the mature peptide.

In normal endometrium, lactoferrin mRNA is present but in very low levels. Prolonged exposure times are needed to visualize the mRNA band with Northern analysis. Although with *in situ* hybridization the lactoferrin mRNA signal is easily seen in adenocarcinomas, we failed to localize the lactoferrin mRNA in normal endometrium using an equivalent exposure time. These low levels of mRNA in normal endometrium suggest that the synthesis and degradation of lactoferrin mRNA is more tightly regulated in normal tissue than in the adenocarcinomas. Because of the low levels of message in normal tissue, we are unable at this time to definitively conclude that lactoferrin mRNA is synthesized by the same epithelial cells which express the protein.

In endometrial adenocarcinomas, malignant transformation of the endometrium is associated with the up-regulation of lactoferrin mRNA and protein biosynthesis. The up-regulation at the RNA level is demonstrated by an increase in steady-state RNA levels using both *in situ* hybridization and Northern analysis techniques. In these cancers, we also observe an increase in the number of lactoferrin-positive cells, which express both the protein and mRNA. In this study, 8 of the 12 adenocarcinomas evaluated overexpress lactoferrin, compared with only 1 of 10 hyperplastic specimens. The form of lactoferrin protein extracted from endometrial adenocarcinomas appears to have

LACTOFERRIN DYSREGULATION IN ENDOMETRIAL CANCER

Fig. 4. Colocalization of lactoferrin protein (left panels) and mRNA (right panels) in a normal proliferative endometrium and endometrial adenocarcinomas by performing immunohistochemistry and *in situ* RNA hybridization on serial sections. Dual analysis of protein and mRNA expression reveals that glands in normal endometrium do not have detectable mRNA, as measured by *in situ* hybridization (top panels; $\times 40$), whereas analysis of the adenocarcinomas clearly demonstrates a direct correlation between protein and RNA expression for lactoferrin (middle and bottom panels; $\times 10$). Note that lactoferrin protein and mRNA is distributed in a heterogeneous pattern in the epithelial cells of the adenocarcinomas. As is shown in Fig. 1, a heterogeneous staining pattern for lactoferrin protein is also seen frequently in normal endometrium.



a slightly higher molecular weight than the protein present in normal tissue. This could be due to alterations in the processing of the lactoferrin mRNA, protein, or glycosylation by the malignant cells. Alternatively, there could be minor differences between lactoferrin protein which is present in neutrophils and the form synthesized by uterine epithelial cells. We suggest two hypotheses to explain lactoferrin overexpression in endometrial adenocarcinomas. In the first hypothesis, lactoferrin biosynthesis is deregulated by the same processes that lead to the malignant transformation of endometrium. If this hypothesis is true then lactoferrin may be a useful marker for endometrial adenocarcinoma investigation, and further research is needed to determine whether lactoferrin plays a contributing role in the malignant transformation. A second hypothesis is that lactoferrin-positive human endometrial adenocarcinomas evolve from the clonal expansion of cells residing in the regenerative zone (zona basalis) of normal endometrium. It is interesting to speculate that lactoferrin expression in endometrial cancer may be linked to estrogen action in

some way, since proliferative disorders of human endometrium are linked to chronic estrogen exposure over several years and sequencing data suggests that the promoter for the human lactoferrin gene does contain an ERE.

Although the function of lactoferrin is unknown, a variety of biological roles have been proposed for lactoferrin which could link this protein to a role in cancer, including the regulation of DNA synthesis (25-29), modulation of the immune response (25, 30, 31), and iron transport (32). Some forms of lactoferrin are reported to have RNase activity (33, 34). Secreted RNases are involved in development, reproductive function, neoplasia, angiogenesis, and immune suppression. (35, 36) If angiogenesis and immunosuppression are components of lactoferrin RNase activity, these properties could promote tumor growth.

In the endometrial adenocarcinomas, we observed a heterogeneous expression pattern for lactoferrin, PCNA, Her-2/*neu*, ER, and PR. With regard to prognosis, patient survival is reportedly worse when

Table 3 Correlation of lactoferrin and PR expression in human endometrial adenocarcinomas

An inverse correlation indicates that lactoferrin and progesterone were not expressed in the same regions of the tumor by immunohistochemical analysis. PR was detected with the antisera KD68, and lactoferrin was detected by a specific polyclonal antisera.

Type of cancer	Age	Stage	Therapy	FIGO ^a grade	Lymph nodes	Myometrial invasion %	Lactoferrin expressed	Inverse correlation with PR
Endometrioid	37	1	None	1	0/12	0	No	No
Endometrioid	61	1	Estrogen	1-3	ND	60	Yes	Yes
Endometrioid	67	1	Estrogen	2-5	ND	60	Yes	Yes
Endometrioid, squamous differentiation	39	1a	None	2	ND	0	Yes	Yes
Endometrioid	69	1b	None	1	ND	29	No	No
Endometrioid	57	1b	None	1	ND	36	Yes	Yes
Endometrioid	72	1b	None	2-2	0/15	5	Yes	Yes
Endometrioid	67	1c	Estrogen	1	ND	50	Yes	Yes
Endometrioid, squamous differentiation	62	2a	None	2	ND	80	No	No
Endometrioid	78	2a	None	2	0/17	5	Yes	Yes
Endometrioid, squamous differentiation	63	3c	None	3	1/27	50	No	No
Endometrioid	64	4b	None	2-3	ND	75	Yes	Yes

^a FIGO, Federation Internationale des Gynecologues et Obstetrisques; ND, not done.

1 2 3 4

Fig. 5. Northern analysis of lactoferrin mRNA expression confirms that endometrial adenocarcinomas (Lanes 3 and 4) significantly overexpress the 2.5-kilobase transcript of human lactoferrin in comparison to normal endometrium (Lanes 1 and 2). The Northern hybridization data supports the *in situ* RNA results and confirms that lactoferrin RNA expression is dysregulated in uterine adenocarcinomas. Normal uterine tissues appear to contain low steady-state RNA levels of lactoferrin, reflecting a controlled pattern of protein expression. Equivalent RNA loading and quality for each specimen was demonstrated by ethidium bromide staining of the RNA gels (data not shown) and by probing for a housekeeping gene (glyceraldehyde-3-phosphate dehydrogenase) that does not fluctuate significantly with the metabolic state of the tissue.

endometrial adenocarcinomas lose sex steroid receptors (37, 38), have a higher proliferative index (39), and demonstrate DNA aneuploidy. During the tumor progression of endometrial adenocarcinomas, it appears that the loss of steroid hormone receptors occurs earlier than either the increase in proliferation rate or the development of DNA aneuploidy (40). In our study, we note a striking inverse correlation between the expression of lactoferrin and PR in the endometrial adenocarcinomas. An inverse relationship also has been described for HER-2/*neu* and PR in endometrial adenocarcinomas that correlates with patient prognosis. Furthermore, in cancers of the human endometrium, ovary and breast Her-2/*neu* expression has been associated with advanced disease and poor survival (41-43). HER-2/*neu* is an oncogene that shares sequence homology with the epidermal growth factor receptor and is speculated to contribute to aberrant growth. Of note is that lactoferrin biosynthesis in the mouse uterus is associated with the expression of the epidermal growth factor. Like HER-2/*neu*, the epidermal growth factor receptor is also frequently overexpressed in PR-negative cells of endometrial adenocarcinomas (44). The amplification of growth factor receptor expression in PR-negative endometrial adenocarcinomas may be associated with the acquisition of growth autonomy and hormone independence, which may contribute to the poorer prognosis of PR-negative endometrial carcinomas (45). Some endometrial adenocarcinomas, including recurrent tumors, can be treated successfully with progesterone therapy (46, 47). Although the significance of the inverse relationship between lactoferrin and PR expression is not known, we speculate that the PR-negative cells do not undergo the normal growth inhibition and secretory differentiation normally associated with progesterone action.

A survey of human tissues reveals that lactoferrin is expressed by most normal mammalian exocrine glands and may be a prognostic marker in tumors (20). Lactoferrin is found in normal ductule breast epithelium and in primary breast carcinomas. In breast tumors, there is an inverse correlation between lactoferrin and ERs (20). Notably, lactoferrin expression in breast cancer may fall into the same category

Fig. 6. Western blot analysis using an antiserum specific for human lactoferrin was performed on proteins extracted from normal and malignant endometrium and separated by SDS-polyacrylamide gel electrophoresis. A broad protein band with a molecular weight between 70,000 and 80,000 is detected in both normal and neoplastic endometrial tissue homogenates, consistent with the reported molecular weight of human lactoferrin (A). The most significant observation from the immunoblotting studies is that lactoferrin protein is markedly elevated in the adenocarcinomas, in comparison to normal endometrium, which supports the immunocytochemical analysis that demonstrates a greater number of cells positive for lactoferrin protein in the uterine tumors. B, the relative amount of protein loaded in each lane by Coomassie blue staining.

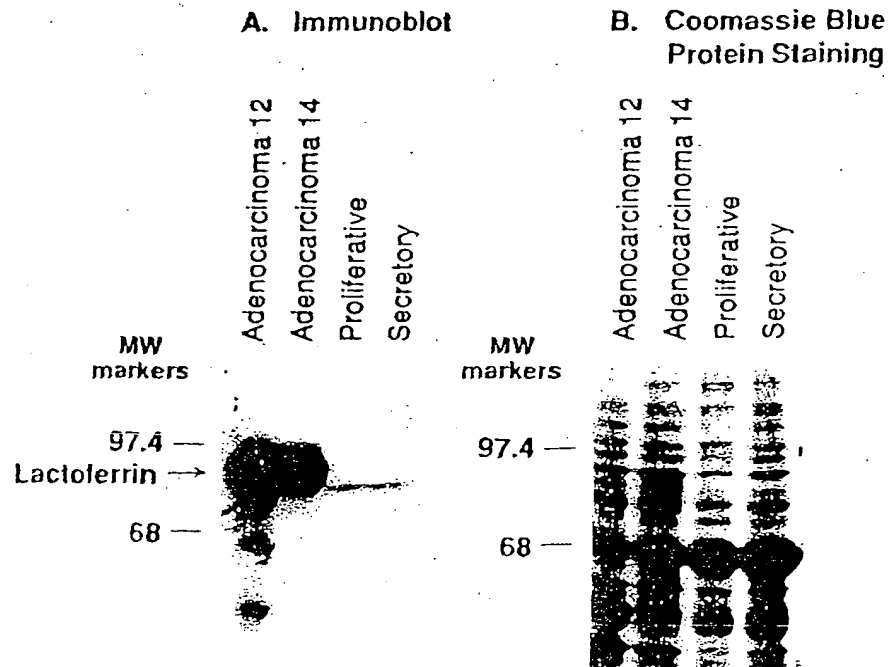
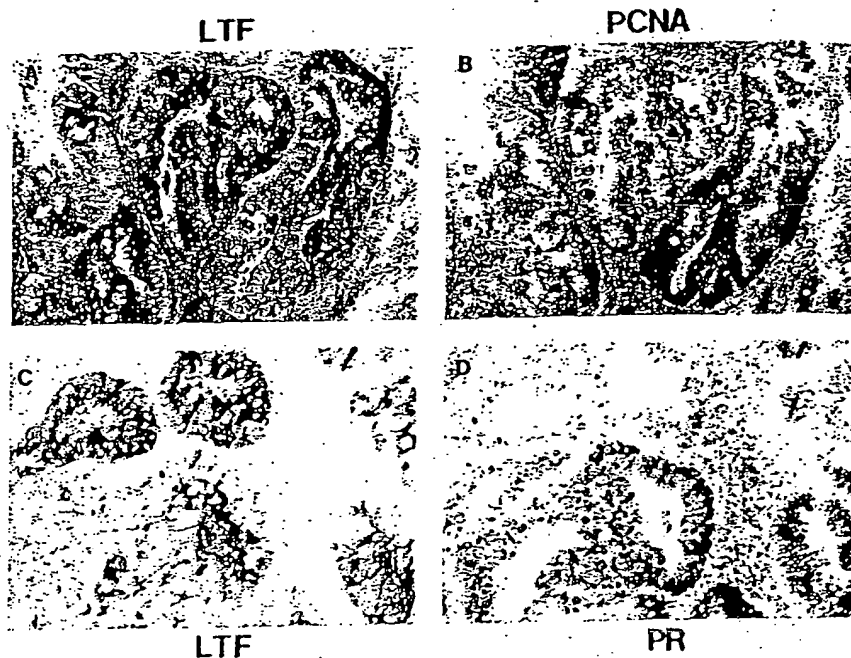


Fig. 7. Correlation of lactoferrin protein expression with the PCNA, a marker of proliferation, and PR as measured by immunohistochemistry performed on serial sections; X 20. In most cases, no relationship between lactoferrin and PCNA expression is found in either normal or malignant endometrium (data not shown). However, in 1 of 12 adenocarcinomas, an inverse correlation is seen between lactoferrin (A) and PCNA (B) localization. This striking pattern was consistent throughout the entire tumor, suggesting the possibility of cell cycle regulation of lactoferrin expression in this adenocarcinoma. The bottom panels exhibit an inverse correlation between lactoferrin (C) and PR expression (D), which was seen in all eight endometrial adenocarcinomas which expressed PR.



as the other markers for ER-negative tumors, such as amplification of EGF receptor, HER-2/neu, and transforming growth factor α expression, which are associated with poor prognosis. In gastric carcinomas, lactoferrin expression is associated with transformation of specific cell types including intestinal-type carcinomas, adenomas, and incomplete intestinal metaplasias (28). Although this is complete speculation at this time, perhaps lactoferrin overexpression in the various malignancies may complement the actions of the growth factor pathway molecules and contribute to the autonomous growth of these tumors.

In conclusion, our studies reveal that lactoferrin is associated with a unique population of epithelial cells in the zona basalis and that lactoferrin overexpression may be associated with malignant transformation of the human endometrium. Further studies are needed to elucidate the role of lactoferrin in normal and pathological endometrial physiology.

ACKNOWLEDGMENTS

We gratefully acknowledge Dr. Geoffrey Greene from the Ben May Institute at the University of Chicago for providing the antisera to the PR (KD68) and the collaborative and collegial relationship between the intramural program at the National Institute of Environmental Health Sciences and the Department of Obstetrics and Gynecology at Duke University Medical Center that made this research possible.

REFERENCES

- Pokras, R., and Hulsagel, V. Hysterectomies in the United States. In: National Health Survey, DHHS Publication PHS 88-1753, Series 13, #92, pp. 1-26, 1987.
- Pollard, J. Regulation of polypeptide growth factor synthesis and growth factor-related gene expression in the rat and mouse uterus before and after implantation. *J. Reprod. Fert.*, 68: 721-731, 1990.
- Martin, L. Estrogens, anti-estrogens and the regulation of cell proliferation in the female reproductive tract in vivo. In: J. McLachlan (ed.), *Estrogens in the Environment*, pp. 105-121. New York: Elsevier North Holland, Inc., 1979.
- Martin, L., and Finn, C. A. Hormonal regulation of cell division in epithelial and connective tissues of the mouse uterus. *J. Endocrinol.*, 41: 365-371, 1968.
- Green, M. R., and Pastewka, J. V. Lactoferrin is a marker for prolactin response in mouse mammary explants. *Endocrinology*, 103: 1510-1513, 1978.
- Walmer, D. K., Wrona, M. A., Hughes, C. L., and Nelson, K. G. Lactoferrin expression in the mouse reproductive tract during the natural estrous cycle: correlation with circulating estradiol and progesterone. *Endocrinology*, 131: 1458-1466, 1992.
- Teng, C. T., Pentecost, B. T., Chen, Y. H., Newbold, R. R., Eddy, E. M., and McLachlan, J. A. Lactoferrin gene expression in the mouse uterus and mammary gland. *Endocrinology*, 124: 992-999, 1989.
- McMaster, M. T., Teng, C. T., Dey, S. K., and Andrews, G. K. Lactoferrin in the mouse uterus: analyses of the preimplantation period and regulation by ovarian steroids. *Mol. Endocrinol.*, 6: 101-111, 1992.
- Teng, C. T., Walker, M. P., Bhattacharya, S. N., Klapper, D. G., DiAugustine, R. P., and McLachlan, J. A. Purification and properties of an oestrogen-stimulated mouse uterine glycoprotein (approx. 70 kDa). *Biochem. J.*, 240: 413-422, 1986.
- Rey, M. W., Woloshuk, S. L., deBoer, H. A., and Pieper, F. R. Complete nucleotide sequence of human mammary gland lactoferrin. *Nucleic Acids Res.*, 18: 5285, 1990.
- Teng, C. T., Liu, Y., Yang, N., Walmer, D. K., and Panella, T. Differential molecular mechanism of the estrogen action that regulates lactoferrin gene in human and mouse. *Mol. Endocrinol.*, 6: 1969-1981, 1992.
- Noyes, R. W., Hertig, A. T., and Rock, J. Dating the endometrial biopsy. *Fertil. Steril.*, 3: 3-25, 1950.
- Silverberg, S. G., and Kurman, R. J. Tumor classification. In: S. G. Silverberg and R. T. Kurman (eds.), *Tumors of the Uterine Corpus and Gestational Trophoblastic Disease*, pp. 15. Washington, DC: Armed Forces Institute of Pathology, 1992.
- Announcement, FIGO Stages: 1988 Revision. *Gynecol. Oncol.*, 35: 125-126, 1989.
- Sambrook, J., Fritsch, E. F., and Maniatis, T. *Molecular Cloning: A Laboratory Manual*. Cold Spring Harbor, NY: Cold Spring Harbor Laboratory, 1989.
- Galand, P., and Degraef, C. Cyclin/PCNA immunostaining as an alternative to thymidine pulse labelling for marking S phase cells in paraffin sections from animal and human tissues. *Cell Tissue Kinet.*, 22: 383-392, 1989.
- Kokeguchi, S., Hayase, R., and Sekiba, K. Proliferative activity in normal endometrium and endometrial carcinoma measured by immunohistochemistry using Ki-67 and anti-DNA polymerase α antibody, and by flow cytometry. *Acta Medica Okayama*, 46: 115-121, 1992.
- Suzuki, M., Ogawa, M., Tamada, T., Nagura, H., and Watanabe, K. Immunohistochemical localization of secretory component and IgA in the human endometrium in relation to menstrual cycle. *Acta Histochem. Cytochem.*, 17: 223-229, 1984.
- Hurley, W. L., and Rejman, J. J. Bovine lactoferrin in involuting mammary tissue. *Cell Biology Int.*, 17: 283-289, 1993.
- Campbell, T., Skilton, R. A., Coombes, R. C., Shousha, S., Graham, M. D., and Luqmani, Y. A. Isolation of a lactoferrin cDNA clone and its expression in human breast cancer. *Br. J. Cancer*, 65: 19-26, 1992.
- Kim, S., Goodman, A. L., Williams, R. F., Hodgen, G. D., Hsu, J. G., and Chwalisz, K. Progesterone induces cyclic renewal in the "basalis" layer of primate endometrium: a possible site of action in anti-progestin-induced endometrial regression. The American Fertility Society Annual Meeting Program, O-065, S32-S35, 1994. (Abstract)
- Lee, B. A., Maher, D. W., Hannink, M., and Donoghue, D. J. Identification of a signal for nuclear targeting in platelet-derived growth-factor-related molecules. *Mol. Cell Biol.*, 7: 3527-3537, 1987.

25. Acland, P., Dixon, M., Peters, G., and Dickson, C. Subcellular fate of the int-2 oncoprotein is determined by choice of initiation codon. *Nature (Lond.)*, 343: 662-665, 1990.
26. Spence, A., Sheppard, P., Davie, J., Matuo, Y., Nishi, N., McKeerhan, W., Dodd, J., and Natusik, R. Regulation of a bifunctional mRNA results in synthesis of secreted and nuclear probasin. *Proc. Natl. Acad. Sci. USA*, 86: 7843-7847, 1989.
27. Gentile, P., and Broxmeyer, H. E. Interleukin-6 ablates the accessory cell-mediated suppressive effects of lactoferrin on human hematopoietic progenitor cell proliferation *in vitro*. *Ann. NY Acad. Sci.*, 628: 74-83, 1991.
28. Rejman, J. J., Oliver, S. P., Muenchen, R. A., and Turner, J. D. Proliferation of the MAC-T bovine mammary epithelial cell line in the presence of mammary secretion whey proteins. *Cell Biol. Int. Rep.*, 16: 993-1001, 1992.
29. Broxmeyer, H. E. Suppressor cytokines and regulation of myelopoiesis. Biology and possible clinical uses. *Am. J. Pediatr. Hematol.-Oncol.*, 14: 22-30, 1992.
30. Tuccari, G., Barresi, G., Arena, F., and Inferrera, C. Immunocytochemical detection of lactoferrin in human gastric carcinomas and adenomas. *Arch. Pathol. Lab. Med.*, 113: 912-915, 1989.
31. Lognani, Y. A., Campbell, T. A., Bennett, C., Coombes, R. C., and Paterson, I. M. Expression of lactoferrin in human stomach. *Int. J. Cancer*, 49: 684-687, 1991.
32. Djcha, A., and Brock, J. H. Effect of transferrin, lactoferrin, and chelated iron on human T-lymphocytes. *Br. J. Haematol.*, 80: 235-241, 1992.
33. Broxmeyer, H. E., Mantel, C., Gentile, P., Srivastava, C., Miyazawa, K., Zucali, J. R., Rado, T. A., Levi, S., and Arosio, P. Actions of H-subunit ferritin and lactoferrin as suppressor molecules of myelopoiesis *in vitro* and *in vivo*. *Curr. Stud. Hematol. Blood Transfus.*, 178-181, 1991.
34. Sanchez, L., Calvo, M., and Brock, J. H. Biological role of lactoferrin. *Arch. Dis. Child.*, 67: 657-661, 1992.
35. Furmanski, P., and Li, Z. P. Multiple forms of lactoferrin in normal and leukemic human granulocytes. *Exp. Hematol.*, 18: 932-935, 1990.
36. Furmanski, P., Li, Z. P., Fortuna, M. B., Swamy, C. V., and Das, M. R. Multiple molecular forms of human lactoferrin: identification of a class of lactoferrins that possess ribonuclease activity and lack iron-binding capacity. *J. Exp. Med.*, 170: 415-429, 1989.
37. Felt, J. W., Snyder, D. J., Lobb, R. R., Alderman, E. M., Bethune, J. L., Riordan, J. F., and Valler, B. L. Isolation and characterization of angiogenin, an angiogenic protein from human carcinoma cells. *Biochemistry*, 24: 5480-5486, 1985.
38. D'Alessio, G., Di Donato, A., Parente, A., and Piccoli, R. Seminal RNase: a unique member of the ribonuclease superfamily. *Trends Biochem. Sci.*, 16: 104-106, 1991.
39. Mayer, T. K., and Mooney, R. A. Laboratory analyses for steroid hormone receptors, and their applications to clinical medicine. *Clin. Chim. Acta*, 172: 1-33, 1988.
40. Vihko, R., Alanko, A., Isomaa, V., and Kauppila, A. The predictive value of steroid hormone receptor analysis in breast, endometrial and ovarian cancer. *Mtd. Oncol. Tumor Pharmacother.*, 3: 197-210, 1986.
41. Rosenberg, P., Wingren, S., Simonsen, E., Sial, O., Risberg, B., and Nordenskjold, B. Flow cytometric measurements of DNA index and S-phase on paraffin-embedded early stage endometrial cancer: an important prognostic indicator. *Gynecol. Oncol.*, 33: 50-54, 1989.
42. Ponninen, R., Mattila, J., Kuoppala, T., and Koivula, T. DNA ploidy, cell proliferation and steroid hormone receptors in endometrial hyperplasia and early adenocarcinoma. *J. Cancer Res. Clin. Oncol.*, 119: 426-429, 1993.
43. Slamon, D. J., Clark, G. M., Wong, S. G., Levin, W. J., Ullrich, A., and McGuire, W. L. Human breast cancer: correlation of relapse and survival with amplification of the HER-2/*neu* oncogene. *Science (Washington DC)*, 235: 177-182, 1987.
44. Slamon, D. J., Godolphin, W., Jones, L. A., et al. Studies of the HER-2/*neu* proto-oncogene in human breast and ovarian cancer. *Science (Washington DC)*, 244: 707-712, 1989.
45. Berchuck, A., Rodriguez, G., Kinney, R. B., Soper, J. T., Dodge, R. K., Clarke-Pearson, D. L., and Bast, R. C., Jr. Overexpression of HER-2/*neu* in endometrial cancer is associated with advanced stage disease. *Am. J. Obstet. Gynecol.*, 164: 15-21, 1991.
46. Bigsby, R. M., Li, A. X., Bomalaski, J., Siehman, F. B., Look, K. Y., and Sutton, G. P. Immunohistochemical study of HER-2/*neu*, epidermal growth factor receptor, and steroid receptor expression in normal and malignant endometrium. *Obstet. Gynecol.*, 79: 95-100, 1992.
47. Lindahl, B., Ferno, M., Gullberg, B., Norgren, A., and Willen, R. 5-year survival rate in endometrial carcinoma stage I-II related to steroid receptor concentration, degree of differentiation, age and myometrial invasion. *Anticancer Res.*, 12: 409-412, 1992.
48. Kohorn, E. I. Gestagens and endometrial carcinoma. *Gynecol. Oncol.*, 4: 398-411, 1976.
49. Creasman, W. T. Clinical correlates of estrogen and progesterone binding protein in human endometrial carcinoma. *Obstet. Gynecol.*, 55: 363-376, 1980.

Comparison of *TP53* Mutations Identified by Oligonucleotide Microarray and Conventional DNA Sequence Analysis¹

Wen-Hsiang Wen, Leslie Bernstein, Jennifer Lescallett, Yasmin Beazer-Barclay, Jane Sullivan-Halley, Marga White, and Michael F. Press²

Department of Pathology [W.-H.W., M.F.P.], The Norris Comprehensive Cancer Center [L.B., J.S.H., M.F.P.], and Department of Preventive Medicine [L.B., J.S.H.], University of Southern California School of Medicine, Los Angeles, California 90033; Affymetrix, Inc., Santa Clara, California 95051 [J.L.]; and Gene Logic, Inc., Gaithersburg, Maryland 20878 [Y.B.-B.]

ABSTRACT

As the rate of gene discovery accelerates, more efficient methods are needed to analyze genes in human tissues. To assess the efficiency, sensitivity, and specificity of different methods, alterations of *TP53* were independently evaluated in 108 ovarian tumors by conventional DNA sequence analysis and oligonucleotide microarray (p53 GeneChip). All mutations identified by oligonucleotide microarray and all disagreements with conventional gel-based DNA sequence analysis were confirmed by re-analysis with manual and automated dideoxy DNA sequencing. A total of 77 ovarian cancers were identified as having *TP53* mutations by one of the two approaches, 71 by microarray and 63 by gel-based DNA sequence analysis. The same mutation was identified in 57 ovarian cancers, and the same wild type *TP53* sequence was observed in 31 ovarian cancers by both methods, for a concordance rate of 81%. Among the mutation analyses discordant by these methods for *TP53* sequence were 14 cases identified as mutated by microarray but not by conventional DNA sequence analysis and 6 cases identified as mutated by conventional DNA sequence analysis but not by microarray. Overall, the oligonucleotide microarray demonstrated a 94% accuracy rate, a 92% sensitivity, and an 100% specificity. Conventional DNA sequence analysis demonstrated an 87% accuracy rate, 82% sensitivity, and a 100% specificity. Patients with *TP53* mutations had significantly shorter overall survival than those with no mutation ($P = 0.02$). Women with mutations in loop2, loop3, or the loop-sheet-helix domain had shorter survival than women with other mutations or women with no mutations ($P = 0.01$). Although further refinement would be helpful to improve the detection of certain types of *TP53* alterations, oligonucleotide microarrays were shown to be a powerful and effective tool for *TP53* mutation detection.

INTRODUCTION

TP53 mutations are the most common genetic alterations in human malignancies. About 570 different *TP53* mutations have been identified by analysis of more than 8000 human cancers since 1989 (1). Most mutations were identified by conventional methods such as SSCP³ and DNA sequencing. Other methods, such as denaturing gradient gel electrophoresis, heteroduplex analysis, and cleavage methods (2), have also been used. In general, these traditional gel-based sequencing methods are relatively time-consuming, labor-intensive, sequential processes. Relatively few studies have analyzed the entire coding sequence from exons 2 through 11. Therefore, current estimates of *TP53* alterations and its mutational spectrum may be incomplete. A more accurate and rapid method would provide more complete information in future studies of *TP53*. Methods based on hybridization of test DNA or RNA with multiple, defined oligo-

nucleotides or cDNA probes attached to a solid glass or nylon matrix have been developed and are referred to as "oligonucleotide microarrays" or "DNA microarrays" or "gene chips." By analyzing different hybridization patterns or levels between control and test DNA or RNA, oligonucleotide microarrays have been used for the analysis of known genes (such as *TP53*, *BRCAl*, the ataxia-telangiectasia gene, the cystic fibrosis transmembrane conductance regulator gene, HIV reverse transcriptase and protease genes, and the cytochrome P450 gene), *de novo* DNA sequencing, comparative sequence analysis, and gene expression studies (3-5). However, relatively little is known about the sensitivity and specificity of microarray methods compared with gel-based DNA sequence analysis. In this study, we compared *TP53* mutations detected by conventional gel-based DNA sequence analysis with those identified by oligonucleotide microarray (p53 GeneChip) in 108 ovarian cancers. The relationship between *TP53* mutations and patient survival was also evaluated.

MATERIALS AND METHODS

Tumor Specimens. Clinical information and *TP53* alterations identified by SSCP and conventional sequence analysis from most of these cases has been reported separately (6). The 108 ovarian carcinomas studied here for *TP53* alterations included 77 serous carcinomas, 5 mucinous carcinomas, 12 endometrioid carcinomas, 5 clear cell carcinomas, 7 mixed epithelial carcinomas, and 2 undifferentiated ovarian adenocarcinomas.

DNA Extraction. Genomic DNA from 108 frozen ovarian epithelial carcinomas, available through the University of Southern California Tumor and Tissue Bank, was analyzed for *TP53* mutations. Frozen tissue sections stained with H&E were used to confirm that the tumor tissue selected for analysis was composed predominantly of tumor cells. DNA was extracted from 10 to 20 serial frozen tissue sections (10 μ m thick) of the tumor collected in Eppendorf tubes. The extraction solution consisted of 300 μ l of 10 mM Tris-HCl, 25 mM EDTA, 100 mM NaCl, 0.5% SDS, and Proteinase K (0.1 mg/ml) incubated overnight at 50°C. After complete digestion, DNA was purified by centrifugation after deproteinization with phenol:chloroform:isoamyl alcohol (50:49:1) treatment and precipitation with ethanol and sodium acetate (3 M; pH 5.2) overnight at -20°C. The DNA yield was determined by spectrophotometry and analyzed by SSCP, DNA sequence analysis (6), automated DNA sequence analysis (7, 8), and p53 GeneChip assay as described below.

SSCP. The PCR was used to amplify each of the exons contributing to the open reading frame of the *TP53* gene. Each of the oligonucleotide primer pairs was designed to span not only the exon of interest but also sufficient flanking intron sequence so that splice junction mutations would be included for analysis. The sequence for each primer pair is described elsewhere (6). Each exon of *TP53* was amplified by the PCR technique through 35 reaction cycles in a thermal cycler using 100 ng of genomic DNA, 4 mM deoxynucleotide triphosphates, 6 μ Ci of [³²P]dATP, 6 μ Ci [³²P]dCTP, and 25 pmol of the appropriate oligonucleotide primer pair. Conformational differences in the PCR products were resolved on nondenaturing mutation detection enhancement polyacrylamide gels with the addition of 5% glycerol at room temperature. All samples identified by SSCP as having altered mobility were further characterized by DNA sequencing for the exon putatively identified as mutated. In previous studies from our laboratory, SSCP has had an 85% sensitivity and a 98% specificity for *TP53* mutations (6).

Manual DNA Sequencing. DNA segments identified as having altered mobility by SSCP were evaluated by manual DNA sequence analysis. Ovarian

Received 6/23/99; accepted 3/17/00.

The costs of publication of this article were defrayed in part by the payment of page charges. This article must therefore be hereby marked advertisement in accordance with 18 U.S.C. Section 1734 solely to indicate this fact.

¹ Supported in part by Grants CA48780 and CA50589 from the National Cancer Institute, Grant DAMD17-94-4234 from the United States Army Medical Research and Materiel Command and a California SEER Registry Special Study grant.

² To whom requests for reprints should be addressed, at USC/Norris Comprehensive Cancer Center, Norris Topping Tower, Room 5409, 1441 Eastlake Avenue, University of Southern California School of Medicine, Los Angeles, CA 90033.

³ The abbreviations used is: SSCP, single-strand conformational polymorphism.

carcinoma template DNA was reamplified with the appropriate PCR primer pair, and amplified PCR product was purified (PCR Purification kit; Qiagen, Inc.). Both the sense and antisense strands were analyzed by the dideoxynucleotide chain termination technique with PCR sense and antisense primers, which were end-labeled using polynucleotide kinase. The products of these sequencing reactions were then separated by electrophoresis on 6% denaturing polyacrylamide gels (National Diagnostics, Atlanta, GA).

Automated DNA Sequence Analysis of All SSCP-negative Samples. Ovarian carcinoma cases with no mobility shift identified by SSCP screening were subjected to complete DNA sequence analysis of each exon contributing to the *TP53* open reading frame (exons 2–11) by automated DNA sequence analysis, as described elsewhere (7), to identify those mutations that SSCP failed to identify.

p53 GeneChip Assay. Oligonucleotide microarrays are manufactured using light-directed combinatorial chemistry. In the context of the p53 GeneChip, the synthesis cycles were repeated until oligonucleotides of ~18 bases in length were constructed. Approximately 65,000 different oligonucleotide probes were synthesized in a 1.2 × 1.2-cm area (grid) consisting of 256 cells in each dimension. Each probe cell (50 μm × 50 μm) was arranged and constructed to accommodate 10⁷ copies of each oligonucleotide. These probes were designed to interrogate each base of exons 2–11 of the human *TP53* coding sequence (~1262 bases) and +2/–2 splice sites in a standard tiling format as well as a redundant tiling format for both sense and antisense strands (Fig. 1A). The first format, standard tiling, was the compilation of complementary probes designed to interrogate the normal sequence and every possible single-base mismatch, single-base deletion, and +2/–2 splice site junctions along the coding region of the *TP53* gene. More specifically, probes in the standard tiles had a common substitution position located at the twelfth base from the 3' end. Each probe set represents A, C, G, T, a 1-bp deletion, and an empty cell for background subtraction (Fig. 1B). Five probes per sense and antisense directions were arranged for each nucleotide position (Fig. 1C). The second format, redundant tiling, was designed to interrogate over 300 common mutations reported more than once in the *TP53* database (9), with the exception of deletions or insertions >1 bp. Each redundantly tiled mutation had 12 probes (6 sense and 6 antisense) designed to interrogate the mismatch. The substitution position was placed at different locations on the probe for maximum hybridization and discrimination of the mutant target. The hybridization pattern and intensity was then determined by laser scanner and analyzed by software based on the mixture detection algorithm. When a mutation occurred, the software called the mutation according to the codon in which the mutation existed. Probes from sense and antisense strands in both tiling formats were used to generate a confidence score for mutations. Mutations that occurred in codons with redundantly tiled nucleotides, in addition to the standard tiling, had the highest confidence score. These scores were higher because of the increased number of probes available to calculate the average intensity from each probe cell. Confidence scores (GeneChip score) ranged from 1 to 36. A score of 36 was the highest indicator that a mutation was present. Cases with scores <10 were regarded as wild-type *TP53*. Through experience prior to initiating this study, we found that samples that showed alternative tiling and on initial processing scored <10 were associated with only standard tiling when processed a second time. These samples proved to be false-positive samples in our pilot investigations with non-study samples. No false-positives produced an alternative tiling pattern when processed on an array a second time.

Tumor DNA from all 108 specimens was analyzed by p53 GeneChip Assay (Affymetrix). Each sample DNA was PCR amplified, fragmented with DNase, labeled with Fluorescein-N6-ddATP (DuPont NEN, Boston, MA) by way of a terminal transferase reaction and hybridized to a p53 GeneChip Array. Fluorescently labeled fragmented DNA samples were washed over the chip and allowed to bind to complementary oligonucleotide probes. Hybridized probe arrays were then read using the GeneArray Scanner (Hewlett-Packard, HP G2500A). As a quality assurance step, a control oligonucleotide was added to each sample during hybridization to examine the signal intensity and proper alignment of the probe array after the scan. Prior to the collection of image data, the scanner confirmed the correct position and alignment of the chip by focusing on a series of defined positions.

To account for any variations that occurred during the assay, each sample batch was processed with human placental DNA as a wild-type control (Sigma

Chemical Co., St. Louis, MO). Any sequence mismatch present in sample DNA was identified by comparison to the control placental DNA (Fig. 1B).

Repeat DNA Sequencing. Automated and/or manual DNA sequencing was used to confirm each mutation identified by the p53 GeneChip assay. In addition, six samples that were wild type by p53 GeneChip but mutated by conventional gel-based assays were also reconfirmed as mutated with automated sequence analysis. Fourteen samples, initially wild type by the above "conventional" gel-based DNA sequence analyses but mutated by p53 GeneChip analysis, were also re-analyzed to confirm the presence of these mutations in either the manual sequence analysis or automated sequence analysis method or in both. Samples were sequenced on an ABI 377 sequencer using the ABI Prism dRhodamine Dye Terminator Cycle Sequencing kit. Each reaction was performed under the conditions outlined by the manufacturer (Perkin-Elmer-Applied Biosystems, Inc., Foster City, CA). Sequencing primers spanned exons 2–11 of the *TP53* gene. Samples were analyzed using the ABI Sequence Navigator Software (version 1.0.1). It was not considered necessary to use a fourth method to confirm the presence of mutations in these samples because re-analysis with either of the "conventional" methods, manual sequencing or automated sequencing, did eventually demonstrate the mutations.

Statistics. Statistical analyses were conducted using the SAS and Epilog software packages. The differences between *TP53* mutations identified by conventional sequence analysis and *TP53* mutations identified by p53 GeneChip were evaluated using Fisher's exact test. Differences in overall survival according to *TP53* status were assessed by log-rank test. Cox proportional hazards analyses were conducted to assess the joint effects of *TP53* alterations, age, grade, stage, and histological type of carcinoma on risk of ovarian cancer death.

RESULTS

***TP53* Mutations Identified by Conventional SSCP and DNA Sequence Analysis.** Among the 108 DNA samples of ovarian carcinoma analyzed, 54 cases were identified by gel shift with SSCP screening of PCR products, and 53 of these SSCP alterations were confirmed by manual gel-based DNA sequence analysis. All ovarian tumor DNAs that lacked SSCP alterations were subjected to complete automated DNA sequence analysis of exons 2–11 (7), and an additional 10 mutations were identified. The 63 cases with mutations, identified by these "conventional" DNA sequence methods, included 57 cases with single-bp substitution mutations, 3 with deletion mutations, and 3 with combined deletion and insertion mutations (Table 1). Among the 57 substitution mutations were 49 missense mutations, 4 nonsense mutations, and 4 splice junction mutations. In addition, 4 cases contained DNA polymorphisms. DNA from 41 cases showed no sequence alteration. Those cases with DNA polymorphisms and those cases with no sequence alterations were both considered to have wild-type *TP53* sequences (45 cases; 42%).

***TP53* Mutations Identified by Oligonucleotide Microarray.** Among the 108 ovarian carcinoma DNA samples, 71 (66%) had GeneChip scores for at least one position that was between 10 and 36 and were, therefore, identified as mutated. Thirty-seven (34%) cases were identified as having wild-type *TP53* gene with either a GeneChip score of <10 or a DNA polymorphism identified. The identified 71 ovarian tumors with mutations included 69 with single-bp substitution mutations and 2 with single-bp deletion mutations. Among the 69 ovarian tumors with substitution mutations were 56 with missense mutations, 7 with nonsense mutations, and 6 with splice junction mutations. Three ovarian tumors had two *TP53* mutations. All three cases had two single-bp substitution mutations for a total of 72 single-bp substitution mutations identified among cases in this cohort. One case with two mutations had both a missense and a splice junction mutation, and the other two cases each had two missense mutations identified. Because no effort was made to characterize more than one mutation using the "conventional" DNA sequence analysis

Table 1 Classification of TP53 mutations identified by conventional DNA sequence analysis and DNA oligonucleotide microarray^a

Mutation type	Sequencing	Microarray	Total
Single-bp substitutions	57	69	71
Missense	49	56	58
Nonsense	4	7	7
Splice junction	4	6	6
Deletion and/or insertion	6	2	6
Single-bp deletion	2	2	2
Multiple bp deletion	1	0	1
Deletion and insertion	3	0	3
Total	63	71	77

^a Cases containing more than one TP53 mutation had the second mutation excluded from this comparison because no attempt was made to characterize more than one TP53 mutation by conventional DNA sequence analyses.

Table 2 Comparison of TP53 mutations identified by conventional DNA sequence analysis and oligonucleotide microarray analysis

	Mutations detected by sequencing	Wild-type by sequencing	Total no.
Mutations detected by microarray	57	14	71
Wild-type by microarray	6	31	37
Total no.	63	45	108

methods described above, only one of the two mutations identified in these three ovarian tumors by p53 GeneChip was included in the comparative evaluation of the methods (Table 1). In addition, among seven cases with a TP53 polymorphism, five also had a missense mutation. These cases were considered in the analysis as showing a single missense substitution.

Comparison of TP53 Mutations Identified by Oligonucleotide Microarray and Conventional DNA Sequence Analysis. A total of 77 ovarian cancers had TP53 mutations identified by at least one of the two approaches. The 77 tumors with identified mutations included 71 with single-bp substitution mutations, 3 with deletion mutations, and 3 with combined deletion/insertion mutations (Table 1). Among the 71 ovarian tumors with substitution mutations were 58 with missense mutations, 7 with nonsense mutations, and 6 with splice junction mutations.

Both methods identified a mutation in 57 ovarian cancers and no mutation in 31 ovarian cancers for a concordance rate of 81% (Table 2). As described previously, 71 ovarian tumors with mutations (71 of 108; 66%) were identified by DNA microarray and 63 (63 of 108; 58%) by conventional gel-based DNA sequence analysis. There were 6 cases identified by conventional DNA sequence analysis but not by DNA oligonucleotide microarray (Table 3) and 14 cases identified as mutated by DNA oligonucleotide microarray but not by conventional DNA sequence analysis (Table 4). These cases were all resequenced and confirmed as mutated by manual or automated DNA sequence analysis or both.

In this cohort of ovarian tumors, one case had an exon 4 (GTG→TTG) Val73Leu missense mutation, which was identified by conventional DNA sequence analysis but not by p53 GeneChip analysis (Table 3). The cohort contained two identical Lys132Arg missense mutations (AAG→AGG). One of these mutations was identified by both approaches; the other was detected initially only by the

oligonucleotide microarray approach (Table 4). A Cys141Trp (TGC→TGG) missense mutation, missed by conventional DNA sequence analysis, was identified by p53 GeneChip analysis (Table 4). A nonsense Gln167Stop (CAG→TAG) mutation was identified by p53 GeneChip analysis but not by conventional DNA sequence analysis (Table 4).

One of two mutations involving codon 195 was detected by conventional DNA sequence analysis but not by the p53 GeneChip. The other mutation at codon 195 was detected by p53 GeneChip but not by conventional DNA sequence analysis. The codon 195 mutation detected by conventional DNA sequence analysis but not by p53 GeneChip analysis was a deletion/insertion mutation involving codons 193–195 (9-bp deletion of CATCTTATC with a 6-bp insertion of GCCCCT, which encoded a deletion of His, Leu, and Ile and an insertion of Ala, Pro; Table 3). The codon 195 mutation detected by p53 GeneChip but not by conventional DNA sequence analysis was an Ile195Asn (ATC→AAC) missense mutation (Table 4). Neither of two Arg196stop (CGA→TGA) mutations were detected by conventional DNA sequence analysis, but both were detected by p53 GeneChip. Missense substitutions at codons 220 and 237 were identified with oligonucleotide microarray analysis but not with conventional DNA sequence analysis (Table 4). On the other hand, a missense mutation at codon 267 (CGG→CCG; Arg267Pro) was detected by conventional DNA sequence analysis but not by p53 GeneChip analysis (Table 3).

Splice site mutations involving the substitution of an A for a G at the –2 position (intron 6 splice site acceptor) and a T for a G at the +2 position (intron 7 splice site donor) were detected by oligonucleotide microarray analysis but were not detected by conventional DNA sequence analysis (Table 4).

Deletion/insertion mutations at codon 219 and codons 247–251 and a deletion at codons 264–265 were identified by conventional DNA sequence analysis but not by p53 GeneChip analysis (Table 3). The deletion/insertion mutation at codon 219 involved the loss of CCC and insertion of GTGTTC (Pro219Val, Phe). The deletion/insertion mutation of codons 247–251 involved a loss of CATCTTATC and an insertion of GCCCCT, predicting the loss of amino acids His, Leu, and Ile and the insertion of Ala, Pro at this position.

Three of the seven mutations at codon 273 were detected by conventional DNA sequence analysis, whereas all seven were detected by p53 GeneChip. Six of the mutations were Arg273Cys mutations, and one was an Arg273Gly mutation. All four of the missed mutations were Arg273Cys mutations.

Overall, TP53 oligonucleotide microarray analysis identified 71 of the 77 mutations, whereas conventional DNA sequence analyses identified 63 of the 77 mutations. This difference in detection between these approaches was marginally statistically significant ($P = 0.091$, Fisher exact test). Sixty-nine of the 71 single-bp substitution mutations, including missense, nonsense, and splice junction mutations (Table 1), were detected by the TP53 oligonucleotide microarray analysis, whereas 57 were detected by conventional DNA sequence analyses. The TP53 oligonucleotide microarray detected significantly more single-bp substitution mutations than conventional DNA se-

Table 3 TP53 mutations detected by conventional DNA sequence analysis but not identified by DNA microarray analysis

Case no.	Genomic location	Codon	DNA sequence change	Predicted amino acid changes	Mutation type
715	Exon 4	73	GTG→TTG	Val→Leu	Missense
805	Exon 6	219	Deletion of CCC. Insertion of GTGTTC	Loss of Pro. Insertion of Val, Phe	Deletion/Insertion
2719	Exon 6	193–195	Deletion of CATCTTATC. Insertion of GCCCCT	Loss of His, Leu, Ile. Insertion of Ala, Pro	Deletion/Insertion
2001	Exon 7	247–251	Deletion of AACC GGAGGCCATC. Insertion of GGGC	Truncated protein	Frameshift/Nonsense
2332	Exon 8	267	CGG→CCG	Arg→Pro	Missense
696	Exon 8	264–265	Loss of ACT	Loss of Leu	Deletion

Table 4 *TP53* mutations identified by DNA microarray but not by conventional DNA sequence analysis

Case no.	Genomic location	Codon	DNA sequence change	Amino acid change	Mutation type	<i>TP53</i> geneChip score
1748	Exon 5	132	AAG→AGG	Lys→Arg	Missense	26
2348	Exon 5	141	TGC→TGG	Cys→Trp	Missense	16
1566	Exon 5	167	CAG→TAG	Gln→stop	Nonsense	11
2741	Exon 6	195	ATC→AAC	Ile→Asn	Missense	24
2729	Exon 6	196	CGA→TGA	Arg→stop	Nonsense	11
2733	Exon 6	196	CGA→TGA	Arg→stop	Nonsense	12
712	Exon 6	220	TAT→TGT	Tyr→Cys	Missense	31
690	Intron 6	Splice acceptor	-2: a→g	NA ^a	Splice junction	33
2347	Exon 7	237	ATG→ATA	Met→Ile	Missense	11
835	Intron 7	Splice donor	+2: t→g	NA	Splice junction	12
2735	Exon 8	273	CGT→TGT	Arg→Cys	Missense	12
993	Exon 8	273	CGT→TGT	Arg→Cys	Missense	12
2311	Exon 8	273	CGT→TGT	Arg→Cys	Missense	11
2327	Exon 8	273	CGT→TGT	Arg→Cys	Missense	11

^a NA, not applicable.

quence analyses ($P = 0.0024$, Fisher exact test). However, *TP53* oligonucleotide microarray detected only two of the six deletion and/or insertion mutations, whereas conventional DNA sequence analyses detected all six. This difference was marginally statistically significant ($P = 0.06$, Fisher exact test).

Of the 49 missense mutations identified by conventional DNA sequencing, DNA microarray analysis detected 47 (96%). Of the four splice junction mutations identified by conventional DNA sequence analysis, microarray technology detected all of them (100%). Of the seven cancers with a premature stop codon identified by conventional DNA sequencing, oligonucleotide microarray analysis detected six, including four nonsense mutations caused by single-bp substitutions and two frameshift mutations caused by single-bp deletions. Among the four cases that had multiple-bp deletions and/or insertions, microarray analysis missed all of them, whether or not the mutation led to a frameshift. In conclusion, microarray achieved a 94% accuracy (102 of 108), a 92% sensitivity (71 of 77), and a 100% (31 of 31) specificity in mutation detection. Conventional DNA sequence analysis demonstrated an 87% (94 of 108) accuracy rate, an 82% (63 of 77) sensitivity, and a 100% (31 of 31) specificity.

Relationship between *TP53* Alterations and Survival. One hundred and four of the 108 patients with survival data available were analyzed for the relationship between *TP53* mutation and overall

survival. The presence of *TP53* mutations was associated with shorter survival ($P = 0.02$; Fig. 2A). Women with mutations in loop2, loop3, or the loop-sheet-helix domain had a significantly shorter survival than women who had other mutations in their ovarian cancers and women who had no mutations in their ovarian cancers ($P = 0.01$; Fig. 2B). Age (Trend test, $P = 0.03$), grade ($P = 0.02$), and stage ($P = 0.002$) were also associated with shortened overall survival. Mucinous histopathology was associated with a lack of *TP53* mutations ($P = 0.023$) but not with survival. Serous (*versus* all others) tumors were not associated with overall survival ($P = 0.94$). Cox proportional hazards analysis, adjusting for the other factors such as size, stage, and grade, suggested that *TP53* was an independent predictor of shortened overall survival after including these factors in the analysis. However, formal statistical significance was not demonstrated ($P = 0.09$), probably because of the limited sample size.

DISCUSSION

This study was designed to assess the sensitivity, specificity, and accuracy of DNA microarrays (p53 GeneChip) in identifying *TP53* mutations relative to conventional gel-based DNA sequence analysis. Overall, the two methods showed a high level of concordance, with 88 of the 108 tumors (81%) showing the same result. With the inclusion

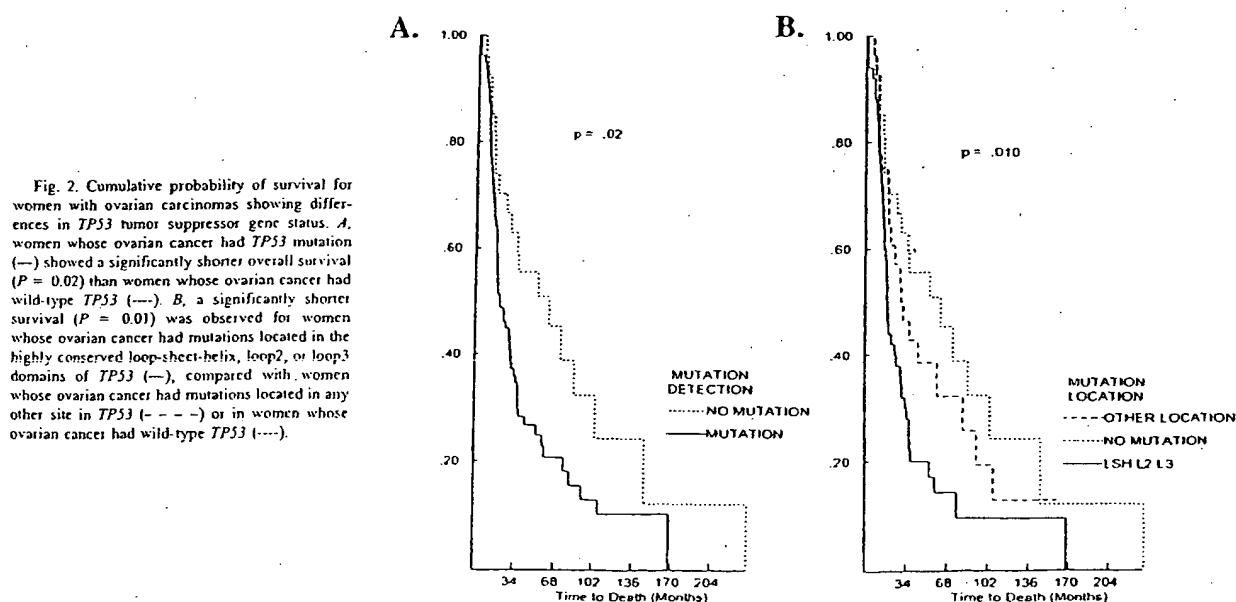


Fig. 2. Cumulative probability of survival for women with ovarian carcinomas showing differences in *TP53* tumor suppressor gene status. A, women whose ovarian cancer had *TP53* mutation (—) showed a significantly shorter overall survival ($P = 0.02$) than women whose ovarian cancer had wild-type *TP53* (---). B, a significantly shorter survival ($P = 0.01$) was observed for women whose ovarian cancer had mutations located in the highly conserved loop-sheet-helix, loop2, or loop3 domains of *TP53* (—), compared with women whose ovarian cancer had mutations located in any other site in *TP53* (---) or in women whose ovarian cancer had wild-type *TP53* (----).

of 14 mutations initially not identified with conventional sequence analysis, the DNA microarray achieved an accuracy of 94% (102 of 108), whereas conventional DNA sequence analysis, including the six mutations not identified with p53 GeneChip analysis, achieved an accuracy of 87% (94 of 108) relative to the final *TP53* status determined from assessment of both approaches together. In addition, three cases were identified with double mutations, two with double missense mutations, and one with a missense mutation and a splice junction mutation. Microarray analysis also detected polymorphisms in seven cases, five of which had coexistent missense mutations. These observations provided an estimate of the frequency of cases with multiple alterations in the *TP53* gene, which has probably been underestimated and underreported in the past (1, 10).

Although there was a high level of concordance between the microarray analysis and conventional DNA sequence analysis, six mutations identified by conventional DNA sequence analysis were not identified by microarray analysis. Four of these mutations (four of six; 67%) involved multiple-bp deletions and/or insertions, including two cases with in-frame deletions and insertions, one case with a frameshift mutation attributable to a 15-bp deletion and 4-bp insertion, and one case with an in-frame 3-bp deletion (Table 3). The two other cases not identified by microarray had missense mutations. The detection rate for nucleotide deletions and insertions was lower with microarray (two of six; 33%) than with conventional DNA sequence analysis (six of six; 100%).

The p53 GeneChip assay showed a higher detection rate for single-bp substitutions of any type including missense mutations, nonsense mutations, and splice junction mutations than did conventional DNA sequence analysis [56 of 58 (97%) versus 49 of 58 (84%); 7 of 7 (100%) versus 4 of 7 (57%); and 6/6 (100%) versus 4 of 6 (67%); Table 1], respectively. Overall, p53 GeneChip assay identified 97% (69 of 71) of single-base substitutions, whereas conventional DNA sequence analysis identified 80% (57 of 71). For single-bp deletion mutations, p53 GeneChip showed the same detection rate as sequence analysis (two of two; 100%). All 14 mutations missed by conventional DNA sequence analysis (Table 4) were of the single-bp substitution type, whereas four of the six (67%) mutations missed by p53 GeneChip assay were deletions >1 bp or complex frameshift mutations. Among the 14 mutations missed by first round of DNA sequencing, no minor bandshift was seen, even after rechecking the SSCP gel or gel-based sequencing data; therefore, misinterpretation of the original sequence was unlikely. Because a majority (9 of 14; 64%) of these cases had a GeneChip score between 11 and 12, it was possible that these DNA samples had less mutant target DNA hybridizing to the probe cell on the array, which was difficult to detect by SSCP and DNA sequencing.

On the other hand, mutations missed by the p53 GeneChip were mostly multiple-base deletion/insertion, which had clear nucleotide changes on DNA sequencing gels. The p53 microarray could be improved by introduction of oligonucleotides designed to identify all previously observed multiple-bp deletion or insertion mutations. Alternatively, p53 microarrays could be used for initial analysis of *TP53* mutations, with all apparently wild-type DNA samples subjected to conventional DNA sequence analysis.

Although a variety of oligonucleotide microarrays have emerged in the market during the past few years, few studies have compared the mutations or sequences identified by both the microarray and conventional sequence approaches (11, 12). In a previous study, exon 11 of *BRCA1* was characterized in 15 patients and 20 control samples. Fourteen of the 15 patient samples with previously known mutations were correctly diagnosed, with no false-positive results identified. The *BRCA1* chip achieved a sensitivity of 93% (14 of 15) and specificity of 100% (20 of 20). Eight single-nucleotide polymorphisms were also

detected. In the second report, the *BRCA1* DNA was used for sequence comparisons of *BRCA1* exon 11 in human, chimpanzee, gorilla, and orangutan DNA samples.

While our manuscript was in review, another paper reported a comparison of *TP53* mutations in 100 lung cancers determined by oligonucleotide microarray and gel-based DNA sequence analysis (13). Dideoxynucleotide sequence analysis of exons 5–9 detected 76% of mutations within this region of the gene. The p53 GeneChip assay detected 80% of the mutations within this same region (exons 5–9) of the gene and 81% of all mutations in exons 2–11 (13). Similar to our experience reported here, the p53 GeneChip detected 46 of 52 missense mutations (88%) but none of five frameshift mutations (13). Accordingly, the p53 GeneChip appears to perform best when analyzing single-base mismatch substitution mutations and single-bp deletion mutations. Conversely, in our hands it failed to identify deletions or insertions >1 bp. The prevalence of deletions and insertions in *TP53* is, however, relatively low, depending on the tumor type. The occurrence of deletions and/or insertions >1 bp is estimated to be 7% in the *TP53* database (9). This value correlated well with our results in these 108 ovarian carcinoma samples. On the other hand, the majority of *BRCA1* mutations are not single-bp substitutions but insertions and deletions. However, oligonucleotide microarray did achieve a high sensitivity and specificity in a relatively small number of cases. The sensitivity of the DNA microarray for mutation detection in *BRCA1* (14 of 15; 93%) was similar to the sensitivity achieved here for *TP53* (71 of 77; 92%).

Overall, *TP53* mutations in these ovarian cancers occurred predominantly in exons 5–8. Nineteen (25%) mutations were in exon 5, 11 (14%) mutations were in exon 6, 15 (20%) mutations were in exon 7, 24 (31%) mutations were in exon 8. Six (8%) mutations were located in introns at splice junctions, and only one mutation was identified in exon 4 (1%) and exon 9 (1%). Most of the studies analyzing the entire open reading frame of *TP53* (14–18) in ovarian cancer had a limited number of cases analyzed. Two of the five studies (17, 18) that analyzed more than 60 cases identified 15 and 18% of mutations outside exon 5–8, with a predominance of deletion/insertion mutations in these regions. However, we did not find a similar distribution in our study. Because we confirmed all SSCP-positive cases by manual sequencing and rescreened SSCP-negative cases by automated DNA sequencing, as well as reanalyzed all DNAs by a p53 GeneChip assay, it is unlikely that a significant number of mutations were missed. Therefore, our estimate of *TP53* mutations in ovarian cancer is considered to be representative. The difference in mutation spectrum among studies might be attributed to environmental mutagenic exposure and/or endogenous factors, such as genetic differences, that contribute to carcinogenesis.

The most frequently mutated codons in our study were codon 273 (seven mutations), codon 179 (four mutations), and codon 234 (four mutations). Two of these (codon 179 and codon 273) are also "hot-spots" of tobacco-associated lung cancers, but most of the mutations (10 of 12; 83%) in these two codons in ovarian cancer were transition mutations rather than transversion mutations as observed in lung cancer (19). On the other hand, mutations frequently related to benzo(a)pyrene exposure in lung cancer, such as mutations in codon 157 (GTC→TTC), codon 248 (CGG→CTG), or related to aflatoxin exposure in liver cancer, such as mutations in codon 249 (AGG→AGT), were not identified. The higher overall percentage of transition (60%) compared with transversion mutations (32%) in our study suggest that most ovarian cancers arise spontaneously rather than because of exogenous carcinogen exposure.

The significance of *TP53* alteration as a prognostic factor in ovarian cancers varies among different studies (reviewed in Ref. 6). The factors that cause variable results include insufficient samples, differ-

ence in screening methods, and incomplete analysis of the open reading frame. In our study, we tried to minimize these factors by using both conventional gel-based DNA sequencing and microarray analysis to analyze mutations in the entire open reading frame of *TP53* in 108 ovarian carcinomas: (a) the high percentage (77 of 108; 71%) of *TP53* mutations indicates that *TP53* function is abrogated mostly by mutation of the gene itself in ovarian cancer, although other nonmutational mechanisms, such as defects in *TP53* pathway that mediate its function or loss of mechanisms that activate *TP53* (20), could be involved in the pathogenesis of those cancers that have wild type *TP53*; (b) the DNA-binding structural motifs (loop-sheet-helix, loop2, and loop3) of *TP53* overlap almost exclusively with the conserved regions of the protein sequence, where the majority of mutations are found and affect its sequence-specific DNA binding activity (21). These "hot-spot" amino acids are highly conserved and are believed to represent regions of structural or functional importance (22). In our analysis, *TP53* mutation was shown to be a predictor of overall survival in ovarian cancer. Patients with mutations in loop2, loop3, or the loop-sheet-helix domain had shorter survival than patients with mutations in other locations or no mutation. This observation supports the current concept that these sequence-specific DNA binding domains are functionally important, and mutations in these areas could have more deleterious effects as opposed to other mutant and/or wild-type *TP53*. Further *in vivo* functional characterization, such as the biological activity of these mutants, would provide more information.

A few possible mechanisms of false-negative and false-positive mutations detected by DNA microarray have been described. These include microarray design, imperfect hybridization conditions, and molecular interactions on microarrays (23, 24). The addition of more probes, such as redundant tiling based on common mutations related to deletion/insertion mutations, as well as other mutations, is expected to improve the sensitivity of the microarray in overall detection. In addition, enzyme approaches, such as polymerase and ligase, have also been adapted for use with microarray (24). It has been suggested that deletion and insertion would lead to the formation of energetically favored duplexes containing bulged nucleotides with wild-type probes over duplexes containing single-bp mismatches (23). All of these possibilities suggest that microarray detection can be improved. Although sequencing the entire coding region is a sensitive technique for overall detection of mutations, it is more time consuming and labor intensive than analysis by DNA microarray technology. For example, screening of the entire coding region of *TP53* requires the amplification of 11 PCR products (exon 4 is split in two amplicons), 22 sequencing lanes, and the manual examination of over 1262 bases. The high costs and increased turnaround times impedes the usage of this technology on a regular basis. On the other hand, the time from purified DNA to data analysis was ~4.5 h for the p53 GeneChip. The average batch size/day was 12 samples, including a reference sample and negative control (blank). In conclusion, although there was a high concordance rate between the two methods, the p53 GeneChip assay detected more mutations, had greater overall accuracy for detection of sequence alterations, and was more effective in terms of time and cost.

ACKNOWLEDGMENTS

We thank Ivonne Villalobos, Norris Cancer Center, University of Southern California School of Medicine, for preparing the manuscript and Dr. Timothy

Triche for the assistance of the Children's Cancer Group Microarray Core Facility at Children's Hospital Los Angeles, USC/Norris Comprehensive Cancer Center.

REFERENCES

- Hainaut, P., Hernandez, T., Robinson, A., Rodriguez-Tome, P., Flores, T., Hollstein, M., Harris, C., and Montesano, R. IARC Database of p53 gene mutations in human tumors and cell lines: updated compilation, revised formats and new visualisation tools. *Nucleic Acids Res.*, 26: 205-213, 1998.
- Cotton, R. Slowly but surely towards better scanning for mutations. *Trends Genet.*, 13: 43-46, 1997.
- Wallace, R. DNA on a chip: serving up the genome for diagnostics and research. *Mol. Med. Today*, 3: 384-389, 1997.
- Southern, E. M. DNA chips. Analysing sequence by hybridization to oligonucleotides on a large scale. *Trends Genet.*, 12: 110-115, 1996.
- Lipshutz, R., Fodor, S., Gingeras, T., and Lockhart, D. High density synthetic oligonucleotide arrays. *Nat. Genet. Suppl.*, 21: 20-24, 1999.
- Wen, W., Reles, A., Sullivan-Halley, J., Bernstein, L., Jones, L., El-Naggar, A., Felix, J., Runnebaum, I., and Press, M. p53 mutations and expression in ovarian cancer: correlation with overall survival. *Int. J. Gynecol. Pathol.*, 18: 29-41, 1999.
- Wang-Gohrke, S., Hees, S., Pochon, A., Wen, W., Reles, A., Press, M., Kreienberg, R., and Runnebaum, I. Genomic semi-automated cycle sequencing as a sensitive screening technique for p53 mutations in frozen tumor samples. *Oncol. Rep.*, 5: 65-68, 1998.
- Runnebaum, I., Kohler, T., Stuckler, E., Kieback, H., and Kreienberg, R. p53 mutation is associated with high S-phase fraction in primary fallopian tube adenocarcinoma. *Br. J. Cancer*, 74: 1157-1160, 1996.
- Beroud, C., Verdier, F., and Soussi, T. p53 gene mutation: software and database. *Nucleic Acids Res.*, 24: 147-150, 1996.
- Beroud, C., and Soussi, T. p53 gene mutation: software and database. *Nucleic Acids Res.*, 26: 200-204, 1998.
- Hacia, J., Brody, L., Chee, M., Fodor, S., and Collins, F. Detection of heterogeneous mutations in BRCA1 using high density oligonucleotide arrays and two-color fluorescence analysis. *Nat. Genet.*, 14: 441-447, 1996.
- Hacia, J., Makalowski, W., Edgermon, K., Erdos, M., Robbins, C., Fodor, S., Brody, L., and Collins, F. Evolutionary sequence comparisons using high-density oligonucleotide arrays. *Nat. Genet.*, 18: 155-158, 1998.
- Ahrendt, S., Halachmi, S., Chow, J., Wu, L., Halachmi, N., Yang, S., Wehage, S., Jen, J., and Sidransky, D. Rapid p53 sequence analysis in primary lung cancer using an oligonucleotide probe array. *Proc. Natl. Acad. Sci. USA*, 96: 7382-7387, 1999.
- Kihana, T., Tsuda, H., Teshima, S., Okada, S., Matsura, S., and Hirohashi, S. High incidence of p53 gene mutation in human ovarian cancer and its association with nuclear accumulation of p53 protein and tumor. *DNA aneuploidy. Jpn. J. Cancer Res.*, 33: 978-984, 1992.
- Kupryjanczyk, J., Thor, A., Beauchamp, R., Merritt, V., Edgermon, S., Bell, D., and Yandell, D. p53 gene mutations and protein accumulation in human ovarian cancer. *Proc. Natl. Acad. Sci. USA*, 90: 4961-4965, 1993.
- Kupryjanczyk, J., Bell, D., Dimco, D., Beauchamp, R., Thor, A., and Yandell, D. p53 gene analysis of ovarian borderline tumors and stage I carcinomas. *Hum. Pathol.*, 26: 387-392, 1995.
- Skilling, J., Sood, A., Nicmann, T., Lager, D., and Buller, R. An abundance of p53 null mutations in ovarian carcinoma. *Oncogene*, 13: 117-123, 1996.
- Casey, G., Lopez, M., Ramos, J., Plummer, S., Arboleda, M., Shaughnessy, M., Karlan, B., and Slamon, D. DNA sequence analysis of exons 2 through 11 and immunohistochemical staining are required to detect all known p53 alterations in human malignancies. *Oncogene*, 13: 1971-1981, 1996.
- Bennett, W., Hussain, S., Vahakangas, K., Khan, M., Shields, P., and Harris, C. Molecular epidemiology of human cancer risk: gene-environment interactions and p53 mutation spectrum in human lung cancer. *J. Pathol.*, 187: 8-18, 1999.
- Kubburat, M., and Voudsen, K. Keeping an old friend under control: regulation of p53 stability. *Mol. Med. Today*, 4: 250-256, 1998.
- Arrowsmith, C., and Morin, P. New insights into p53 function from structural studies. *Oncogene*, 17: 1379-1385, 1998.
- Walker, D., Bond, J., Tarone, R., Harris, C., Makalowski, W., Boguski, M., and Greenblatt, M. Evolutionary conservation and somatic mutation hotspot maps of p53: correlation with p53 protein structural and functional features. *Oncogene*, 18: 211-218, 1999.
- Hacia, J. Resequencing and mutational analysis using oligonucleotide microarrays. *Nat. Genet. Suppl.*, 21: 42-47, 1999.
- Southern, E., Mir, K., and Shepchinov, M. Molecular interactions on microarrays. *Nat. Genet. Suppl.*, 21: 5-9, 1999.

Down-regulation of prostate-specific antigen expression by finasteride through inhibition of complex formation between androgen receptor and steroid receptor-binding consensus in the promoter of the PSA gene in LNCaP cells.

Wang LG, Liu XM, Kreis W, Budman DR.

Department of Medicine, New York University, Manhasset 11030, USA.

As a specific competitive inhibitor of 5 α -reductase, an intracellular enzyme that converts testosterone to dihydrotestosterone, finasteride is being extensively used for the treatment of benign prostatic hyperplasia and in experimental settings for prostate cancer. In this study, we showed that finasteride markedly inhibited prostate-specific antigen (PSA) secretion and expression. The promoter of the PSA gene contains several well-known cis-regulatory elements. Among them, steroid receptor-binding consensus (SRBC) has been identified as a functional androgen-responsive element. Our previous study showed that PSA was not only present in conditioned medium of the PSA-positive LNCaP cells but was also detectable in small amounts in PSA-negative cell lines, PC-3 and DU-145 (L. G. Wang et al., *Oncol. Rep.*, 3: 911-917, 1996). A strong correlation between binding of nuclear factors to SRBC and the level of PSA present in the conditioned medium and cell extracts was found in these three cell lines, whereas no such correlation with binding was obtained using Sp1 oligonucleotide as a probe. Binding of LNCaP cell nuclear proteins to SRBC was diminished when the cells were exposed to 25 microM finasteride, at which concentration 50% of both PSA mRNA and protein were inhibited. As a major component of DNA-protein complexes, the level of androgen receptor was dramatically decreased in the cells treated with finasteride. Our data indicate that inhibition of complex formation between SRBC and nuclear proteins due to the remarkable decrease in the level of androgen receptor plays a key role in the down-regulation of PSA gene expression by finasteride in LNCaP cells.

PMID: 9044850 [PubMed - indexed for MEDLINE]

Expression of calcyclin in human melanocytic lesions.

Weterman MA, van Muijen GN, Bloemers HP, Ruiter DJ.

Department of Biochemistry, University of Nijmegen, The Netherlands.

When comparing two subsequent stages of melanocytic tumor progression we identified calcyclin as a new potential progression marker, the expression of which was correlated with metastatic behavior of various human melanoma cell lines in nude mice. In this study, we describe a good correlation between RNA and protein levels in the xenografts of these cell lines and extended these experiments to a panel of 120 routinely processed human melanocytic cutaneous lesions. Northern blot analysis demonstrated that calcyclin RNA expression was elevated in melanoma metastases as compared to several types of nevocellular nevi. Calcyclin staining using a specific polyclonal antiserum showed a more complex pattern. A stronger staining in a higher percentage of positive cells was observed in thick primary melanoma (≥ 1.5 mm) as compared to thin primary melanoma (< 1.5 mm). Calcyclin expression was also present in a higher percentage of cells showing a stronger staining in melanomas with higher Clark levels ($> II$) corresponding to the vertical growth phase of primary melanomas. Protein expression in nevocellular nevi was confined to the dermal part and was highest in the lower parts of the dermis. Remarkably, dysplastic nevi (atypical moles), potential precursors of melanoma, did not show any expression at all, either in junctional or dermal parts. Confinement of the expression to the dermal part of nondysplastic nevi and primary melanomas may reflect interactions with the microenvironment of the reticular dermis that occurs with vertical growth.

PMID: 8261423 [PubMed - indexed for MEDLINE]

Severely decreased MARCKS expression correlates with ras reversion but not with mitogenic responsiveness.

Wojtaszek PA, Stumpo DJ, Blackshear PJ, Macara IG.

Department of Pathology, University of Vermont College of Medicine, Burlington 05405.

Phorbol ester-inducible phosphorylation of MARCKS, the '80-kDa' substrate of protein kinase C, was undetectable in several phenotypically dominant, non-transformed revertants independently derived from the ras-transformed cell line NIH3T3 DT-ras. Extremely low expression of MARCKS protein accounted for this apparent lack of phosphorylation. MARCKS-encoding mRNA levels were correspondingly decreased relative to normal and ras-transformed cells in all four ras revertant cell lines studied: C-11 and F-2, derived by 5-azacytidine treatment and selection with ouabain; CHP 9CJ, derived by ethylmethane sulfonate mutagenesis and selection with cis-hydroxy-L-proline; and 12-V3, derived by transfection with the human Krev-1 gene. However, re-expression of MARCKS after transfection of a cloned MARCKS cDNA into the C-11 ras revertant cells was not sufficient to induce retransformation. In fact, no significant difference in sensitivity to mitogenic stimulation by phorbol esters was observed among several cell lines expressing widely varying levels of MARCKS. This evidence argues against a direct role for MARCKS in mitogenic signaling. However, the strong correlation between attenuation of MARCKS expression and phenotypically dominant ras reversion suggests that a common negative regulatory mechanism might be responsible for both effects, presenting a potentially useful strategy for identifying factors involved in transducing the ras signal.

PMID: 8437859 [PubMed - indexed for MEDLINE]

[Expression of human telomerase reverse transcriptase in cervix cancer and its significance]

[Article in Chinese]

Xi L, Zhu T, Wu P, Xu Q, Huang L, Li KZ, Lu YP, Ma D.

Department of Obstetrics and Gynecology, Tongji Hospital, Tongji Medical College, Huazhong University of Science and Technology, Wuhan 430030, China.

OBJECTIVE: To investigate the expression of human telomerase reverse transcriptase (hTERT) mRNA and protein in cervix cancer, cervical intraepithelial neoplasia (CIN) and normal cervix. **METHODS:** Expression of hTERT mRNA and the other two subunits of telomerase, human telomerase RNA component (hTR), human telomerase-associated protein (hTP1) was determined by RT-PCR in 3 cervix cancer cell lines, 2 diploid cell lines, 38 cases of cervix cancer, 16 cases of CIN and 20 cases of normal cervix. Telomerase activity was also examined by telomeric repeat amplification protocol enzyme-linked immunosorbent assay (TRAP-ELISA). Expression of hTERT protein was detected in all the cell lines and 101 cases of paraffinized cervix tissue sections. **RESULTS:** hTERT mRNA expression was detected in all of the three cervix cancer cell lines, 81.6% of cervix cancer, 37.5% of CIN, 5.0% of normal cervix, while in neither of the two diploid cell lines. The other two subunits of telomerase were prevalently expressed in all of the cell lines and most cervix tissues. There was a strong correlation between hTERT mRNA expression and telomerase activity. Immunostaining also revealed that hTERT protein was expressed in all three cervix cancer cell lines, 65.5% of cervix cancer, 28.0% of CIN and 4.8% of normal cervix. **CONCLUSION:** Up-regulation of hTERT may play an important role in the development of CIN and cervix cancer, hTERT could be used as an early diagnostic biomarker for cervix cancer.

PMID: 16008894 [PubMed - in process]

A transcriptomic and proteomic analysis of the effect of CpG-ODN on human THP-1 monocytic leukemia cells

Cheng-Chin Kuo¹, Chu-Wei Kuo², Chi-Ming Liang³ and Shu-Mei Liang¹

¹ Institute of BioAgricultural Sciences, Academia Sinica

² Graduate Institutes of Life Sciences, National Defense Medical Center

³ Institute of Biological Chemistry, Academia Sinica, Taipei, Taiwan, Republic of China

The CpG motif of bacterial DNA (CpG-DNA) is a potent immunostimulating agent whose mechanism of action is not yet clear. Here, we used both DNA microarray and proteomic approaches to investigate the effects of oligodeoxynucleotides containing the CpG motif (CpG-ODN) on gene transcription and protein expression profiles of CpG-ODN responsive THP-1 cells. Microarray analysis revealed that 2 h stimulation with CpG-ODN up-regulated 50 genes and down-regulated five genes. These genes were identified as being associated with inflammation, antimicrobial defense, transcriptional regulation, signal transduction, tumor progression, cell differentiation, proteolysis and metabolism. Longer stimulation (8 h) with CpG-ODN enhanced transcriptional expression of 58 genes. Among these 58 genes, none except one, namely WNT1 inducible signaling pathway protein 2, was the same as those induced after 2 h stimulation. Proteomic analysis by two-dimensional gel electrophoresis, followed by mass spectrometry identified several proteins up-regulated by CpG-ODN. These proteins included heat shock proteins, modulators of inflammation, metabolic proteins and energy pathway proteins. Comparison of microarray and proteomic expression profiles showed poor correlation. Use of more reliable and sensitive analyses, such as reverse transcriptase polymerase chain reaction, Western blotting and functional assays, on several genes and proteins, nonetheless, confirmed that there is indeed good correlation between mRNA and protein expression after CpG-ODN treatment. This study also revealed that several anti-apoptotic and neuroprotective related proteins, not previously reported, are activated by CpG-DNA. These findings have extended our knowledge on the activation of cells by CpG-DNA and may contribute to further understanding of mechanisms that link innate immunity with acquired immune response(s).

Received: May 13, 2004
Revised: November 13, 2004
Accepted: November 15, 2004

Keywords:

ADP-ribosylation factor 3 / CpG-ODN / Heat shock protein / Microarray

Correspondence: Dr. Shu-Mei Liang, Institute of BioAgricultural Sciences, Academia Sinica, Taipei 115, Taiwan, Republic of China
E-mail: smyang@gate.sinica.edu.tw
Fax: +886-2-26515120

Abbreviations: ARF3, ADP-ribosylation factor 3; FPLI, formyl peptide receptor-like 1; HEK293, human embryonic kidney 293 cells; HSP, heat shock protein; IL, interleukin; JNK, c-Jun NH₂-terminal kinase; LPS, lipopolysaccharide; LxR, nuclear receptor subfamily 1; MyD88, myeloid differentiation factor 88; PKC, protein kinase C gamma; PGK, phosphoglycerate kinase; TLR9, toll-like receptor 9; WISP-2, WNT1 inducible signaling pathway protein.

1 Introduction

Mammals protect themselves against pathogen infection primarily via innate and adaptive immunity [1]. The innate immune system relies on a set of pattern recognition receptors (e.g., Toll-like receptors) to recognize foreign molecular structures such as lipopolysaccharide (LPS) and bacterial DNA [2, 3]. Innate immune cells recognize these molecular structures and initiate not only innate but also adaptive immunity by producing immunomodulatory cytokines and activating T and B immune cells [1]. Bacterial DNA can directly activate B cells to

proliferate and secrete immunoglobulins in a T cell-independent manner [4–6]. It also induces B cells and monocytes to activate transcription factor NF- κ B and secrete cytokines, including interleukin (IL) 12, tumor necrosis factor α (TNF- α), and interferon α/β [7–10]. The immunostimulatory activity of bacterial DNA has been assigned to unmethylated CpG motifs (GACGTT for murine, GTCGTT for human) [11]. Recent evidence shows that synthetic oligodeoxynucleotides containing a CpG motif (CpG-ODN), like bacterial DNA with the CpG moiety (CpG-DNA), induce potent Th1-like immune responses that are protective against several infectious agents and immune disorders in animal models [12, 13]. Biologically active CpG-ODN, like bacteria DNA, activates macrophages and immature dendritic cells to increase expression of MHC class II and costimulatory molecules, thereby transcribing cytokine mRNAs, and producing pro-inflammatory cytokines including TNF α , IL-1, IL-6 and IL-12 [9, 14–16]. CpG-ODN can therefore serve as an adjuvant and immunomodulator in vaccines against a wide variety of targets, including infectious agents, cancer antigens and allergens [17].

It has been suggested that unmethylated CpG-DNA-mediated immune activation functions through a toll-like receptor 9 (TLR9) signaling pathway [18]. Endocytosis and sequentially endosomal maturation as well as binding of heat shock protein (HSP) 90 to CpG-DNA are essential for induction of TLR9 signal transduction [19, 20]. It has also been shown that recognition of CpG-DNA causes TLR to form a dimer, which recruits the adaptor molecule, myeloid differentiation factor 88 (MyD88), through interaction between their C-terminal Toll/IL-1R domains. This recruitment of MyD88 to the Toll/IL-1R domain of TLR9 initiates a signaling pathway that sequentially involves IL-1R-associated kinase 1 and TNF- α receptor-associated factor 6 [18, 21, 22]. Studies using gene-deficient mice and RAW264.7 cells transiently transfected with dominant-negative forms of these molecules have indicated that the MyD88-mediated signaling pathway is essential for CpG-DNA-induced activation of NF- κ B and c-Jun NH₂-terminal kinase (JNK), as well as subsequent production of cytokines in monocytic cells [18, 21, 22]. The precise mechanism of action of CpG-DNA and CpG-ODN, nonetheless, is still not thoroughly understood. To further elucidate the molecular events after binding of CpG-ODN to TLR9, in this study, we treated CpG-ODN responsive THP-1 cells with CpG-ODN and evaluated changes by using DNA microarray and proteomic approaches. We have discovered up-regulation of more than 50 distinguished genes/proteins and identified induction of several anti-apoptotic and neuroprotecting genes by CpG-ODN treatment.

2 Materials and methods

2.1 Reagents

Phosphorothioate-modified CpG-ODN and GpC-ODN were synthesized by MDBio (Taipei, Taiwan). Human specific ODN sequences are: CpG-ODN, 5'-TCG TCG TTT TGT CGT

TTT GTC GTT-3'; GpC-ODN, 5'-TGC TGC TTT TGT GCT TTT GTG CTT-3'. The mouse specific CpG-ODN sequence is 5'-TCC ATG ACG TTC CTG ATG CT-3'. CHCA was from Sigma (St. Louis, MO, USA).

2.2 Cell culture

Cell lines were obtained from the American Type Culture Collection (Rockville, MD). Mouse RAW264.7 macrophage and human embryonic kidney 293 cells (HEK293) were cultured in DMEM supplemented with 10% heat inactivated fetal bovine serum, 100 U/mL penicillin, 100 μ g/mL streptomycin sulfate, 200 mmol/L L-glutamine, and 50 μ M β -mercaptoethanol in a humidified atmosphere of 5% CO₂ at 37°C. The medium was changed every 2 days for all experiments. Human THP-1 monocytic leukemia cells, which have been shown to express TLR9 and respond to CpG-DNA stimulation [23, 24], were cultured in RPMI1640 with the same supplements as for RAW264.7 cell cultures.

2.3 Human cDNA microarray

Total RNAs extracted from cultured THP-1 cells were isolated with TRIzol (Invitrogen, Leek, The Netherlands) and submitted to Genasia Biotechnology (Taipei, Taiwan) for further processing. In brief, 4 μ g of total RNA from CpG-ODN stimulated, or normal THP-1 cells was labeled with a fluorescence marker (U-vision, (Taipei, Taiwan)). Different colored fluorescence dyes (Cy5 and Cy3) were used to distinguish total RNA from normal and ODN stimulated cells. The labeled RNA was used for hybridization with the Human 1 cDNA microchip from Agilent Technologies (Palo Alto, CA, USA). The chips were scanned and the expression pattern was analyzed using genechip software. Genes showing up-regulation or down-regulation of RNA levels were analyzed and identified on a genomic database as suggested by the manufacturer of the microchip.

2.4 Protein preparation

THP-1 cells were seeded in a 175 cm² tissue culture flask at a density of 10⁶ cells per milliliter in culture medium. The cells were stimulated with or without 1.5 μ M CpG-ODN at defined times and harvested by centrifugation at 4°C, 1000 \times g for 15 min. Cell pellets were washed twice with ice-cold PBS, resuspended and sonicated in extraction buffer containing 25 mM Tris-HCl (pH 7.5), 2 mM β -mercaptoethanol and protease inhibitor cocktail. After centrifugation at 10 000 \times g for 20 min, ammonium sulfate was added to the supernatant until the final concentration reached 50% saturation w/v. The solution was stirred at 4°C for 30 min and centrifuged at 10 000 \times g for 30 min at 4°C. The supernatant fraction was then transferred into a fresh tube, and the precipitated protein pellet solubilized in extraction buffer. To remove salts and other contaminants, the extracts were treated with a pre-cooled (–20°C) solution of 10% TCA in acetone with 0.07% β -mercaptoethanol. Proteins were allowed to precipitate overnight at –20°C.

After centrifugation, the pellet was washed with ice-cold acetone, containing 0.07% β -mercaptoethanol. The supernatant was discarded and the pellet dried in a SpeedVac system (Model AES1010; Savant, Holbrook, NY, USA).

2.5 2-DE

2-DE was performed using an IPGphor IEF and a Hofer DALT vertical unit (Amersham Biosciences, Piscataway, NJ, USA). One milligram of dried protein sample was dissolved in 350 μ L of rehydration buffer solution, containing 7 M urea, 2 M thiourea, 4% w/v CHAPS, 5 mM tributyl phosphine, and 2% IPG and loaded onto an immobilized pH 3–10 linear gradient strip (18 cm), followed by rehydration for 16 h. IEF was then performed in the following manner: 100 V for 30 min, 250 V for 30 min, 500 V for 30 min, 1000 V for 30 min, 4000 V for 30 min, 6000 V for 55 000 Vh. At the end of IEF, the IPG strips were equilibrated for 15 min in buffer containing 6 M urea, 2% w/v SDS, 30% v/v glycerol, and 50 mM Tris, pH 6.8, then reduced with 65 mM dithioerythritol (DTE) and subsequently alkylated with 135 mM iodoacetamide for another 15 min. After equilibration, the IPG strips were immediately placed on top of a 12% SDS-PAGE (1.5 mm, 20 \times 24 cm). The second dimension gels were then overlaid with molten 0.8% agarose solution in SDS electrophoresis buffer. Electrophoresis was performed at 16°C, starting at 10 mA per gel for 1 h, followed by 45 mA per gel until the dye front reached the bottom of the gels.

2.6 Staining and image acquisition

Immediately after electrophoresis, gels were stained with SYPRO Ruby (Molecular Probes, Eugene, OR, USA). In brief, gels were fixed for 30 min in 10% methanol, 7% acetic acid, and then stained overnight in SYPRO Ruby stain. The staining solution was removed and gels were washed in 10% methanol and 7% acetic acid for 3 h. After staining, image acquisition was carried out on a Typhoon 9200 (Amersham Biosciences). To identify a protein, spot detection, quantification and matching of 2-D results were analyzed using ImageMaster software (Amersham Biosciences). The M_r of the proteins were calibrated according to the LMW-SDS Marker Kit (Amersham Biosciences), and their pI values were estimated from the position of the protein spots on the 2-D gel and confirmed with the information supplied by the manufacturer. Since most of the pI values for the truncated proteins had not been reported previously, the pI values of the truncated proteins were estimated from the position of the observed spots. To omit the variation due to the use of separate gels, after background subtraction, the intensity levels of protein spots on each gel were normalized as a proportion of one reference spot, and protein quantities were calculated by integrating the density over the spot area. Protein spots that showed reproducible modulation exceeding ~80% after CpG-ODN treatment in three experiments were further analyzed by MS.

2.7 In-gel digestion with trypsin and extraction of peptides

Protein spots were excised from stained gels and cut into pieces. In brief, gel spots were dehydrated with ACN for 10 min and dried in a vacuum centrifuge. Gel pieces were reswelled with 55 mM DTE in 25 mM ammonium bicarbonate (pH 8.5) at 37°C for 1 h. The solution was then exchanged with alkylation solution, which contained 100 mM iodoacetamide in 25 mM ammonium bicarbonate (pH 8.5), at room temperature for 1 h. After alkylation, the gel pieces were washed twice with 50% ACN in 25 mM ammonium bicarbonate (pH 8.5) for 15 min. The wash solution was discarded and the pieces of gel were dehydrated with ACN for 10 min and dried in a vacuum centrifuge. Tryptic digestion was initiated by reswelling the gel in 25 mM ammonium bicarbonate solution with 25 ng of trypsin (Promega, Madison, WI, USA). After incubation at 37°C for 16 h, tryptic peptides were extracted twice with 50% ACN containing 5% formic acid for 15 min with moderate sonication. The extracted solutions were pooled and evaporated to dryness in a vacuum centrifuge. The dried peptide mixture was dissolved in 0.1% formic acid and used for MS.

2.8 MALDI-Q-TOF MS and protein identification

Tryptic peptides analyses were performed using a Micromass Q-TOF Ultima MALDI (Micromass, Wythenshawe, U.K.) equipped with a 337 nm nitrogen laser and operated in reflection positive ion mode. Peptide mixtures (1 μ L) were premixed with 1 μ L of the matrix (5 mg CHCA in 50% ACN with 0.1% TFA) then spotted onto the MALDI target plate. Mass spectra were acquired for the mass range of 900–3500 Da and the individual spectra from MALDI MS or MS/MS were processed using the Micromass MassLynx 4.0 software. The generated peak list files were used to query the Swiss-Prot database using the MASCOT program (<http://www.matrixscience.com>) with the following parameters: peptide mass tolerance, 50 ppm; MS/MS ion mass tolerance, 0.25 Da; allowance of missed cleavage, 1; and consideration for variable modifications such as oxidation of methionine and carboxyamidomethylation of cysteines. Only significant hits as defined by MASCOT probability analysis were considered initially. In addition, when the PMF matches were between 5 and 9, at least one peptide sequence was manually checked by MALDI MS/MS analysis.

2.9 RT-PCR analysis

cDNA from THP-1 cells was produced with Superscript II reverse transcriptase (Invitrogen) using a oligo(dT)₁₈ primer for 1 h at 42°C. PCR of cDNA was performed using specific primers for the gene of interest and control β -actin. All PCR products were electrophoresed on a 1.5% agarose gel, and DNA bands were visualized by staining the gel with ethidium bromide.

2.10 Immunoblotting

Human THP-1 or mouse macrophage RAW264.7 cells ($5 \times 3 \times 10^6$ /well) were cultured in a six-well culture plate and treated with or without $1.5 \mu\text{M}$ CpG-ODN for the designated times. After stimulation, cells were harvested by centrifugation at $1000 \times g$ for 15 min in a refrigerated centrifuge and washed twice with cold PBS buffer. The cells were lysed on ice for 15 min with 300 μL lysis buffer (Pierce, Rockford, USA), supplemented with protease inhibitor cocktail (Sigma). The lysates were centrifuged at $12000 \times g$ for 15 min at 4°C , and protein concentrations of supernatant were determined using the Bio-Rad Protein Assay (Hercules, CA, USA). The lysates (50 μg of protein/lane) were subjected to 12% SDS-PAGE and transferred to NC membranes (Amersham Biosciences). The membranes were blocked in PBS-0.1% Tween 20 (PBST) containing 5% non-fat skim milk at room temperature for 1 h, followed by staining with anti-ADP-ribosylation factor 3 (ARF-3) monoclonal antibody (0.1 $\mu\text{g}/\text{mL}$; Sigma). The membranes were then incubated with horseradish peroxidase-conjugated secondary antibody (dilution, 1:3000) for 1 h. After washing three times with PBST, specific bands were detected by chemiluminescence according to the manufacturer's protocol (Amersham Biosciences).

2.11 Cell transfection and luciferase assay

HEK293 cells ($5 \times 3 \times 10^6$ /well) were transfected using FuGENE 6 (Roche Molecular Biochemicals, Indianapolis, IN, USA) plus 0.1 μg p5xNF- κB -luc (Stratagene, La Jolla, CA, USA), 0.05 μg pCDNA3.1- β -galactosidase, and pCDNA3.1-hTLR9 overnight. The cells were incubated with or without $1.5 \mu\text{M}$ CpG-ODN for 8 h and then lysed. NF- κB luciferase activity assays were performed as recommended by the manufacturer (Promega). β -galactosidase activity was used to normalize the data.

2.12 Enzyme activity assay

Pyruvate kinase activity was assayed in a solution (1 mL) containing 100 mM Tris-HCl (pH 8.0), 100 mM KCl, 10 mM MgCl_2 , 0.2 mM NADH, 10 mM PEP, 1.5 mM ADP, 1 unit of lactate dehydrogenase, and an appropriate amount of cell lysate from CpG-ODN untreated or treated THP-1 cells. The reaction was monitored at 30°C for a period of time by measuring the decrease in absorbance at 340 nm. PGK activity was assayed in a coupled reaction with glyceraldehyde 3-phosphate dehydrogenase (GAPDH) as described by Lee [25]. In brief, the assay was performed at 30°C in a total volume of 1 mL containing 100 mM Tris-HCl (pH 7.9), 10 mM MgCl_2 , 0.15 mM NADH, 2 mM ATP, 6 mM 3-phosphoglycerate, 0.1 mg/mL BSA, 50 mg of GAPDH, and an appropriate amount of cell lysate. NADH consumption was monitored at 340 nm.

3 Results

3.1 Effect of CpG-ODN on gene expression profiles of human THP-1 cells

To elucidate the effect of CpG-ODN on gene expression, THP-1, a cell line known to express TLR9 and respond to CpG-DNA [23, 24] was cultured with or without CpG-ODN. Since preliminary experiments showed that $1.5 \mu\text{M}$ CpG-ODN caused more contrasting results between normal and CpG-ODN treated cells, $1.5 \mu\text{M}$ CpG-ODN was used throughout the experiments. To distinguish CpG-ODN treated samples from the control, total cellular RNA of normal and CpG-ODN treated cells was isolated and labeled with the fluorescence dyes, Cy5 and Cy3, respectively. The labeled RNA was then used for hybridization with a Human 1 cDNA microchip from Agilent Technologies. Of the 13000 human genes represented on the gene array, a total of 55 genes changed expression significantly after 2 h CpG-ODN treatment. Among these, 50 genes were up-regulated while five genes were down-regulated by a factor ≥ 2 . These genes were sorted by functions and are listed in Tables 1 and 2. They included notably, IL-18 receptor accessory protein, MSGA beta gene, thioredoxin, pro-pol-dUTPase polyprotein, Sp140, connexin 59 gene, Grb2-like 2, enoyl-coenzyme A hydratase, propionyl-coenzyme A carboxylase, cytochrome P450, and WNT1 inducible signaling pathway protein 2 (WISP-2) etc. The function of these genes are known to be related to inflammatory responses, antimicrobial defense, transcriptional regulation, intracellular signal transduction, tumor progression, cell differentiation, proteolysis etc.

Table 1. Genes up-regulated (≥ 2 fold) in human THP-1 cells after 2 h of CpG-ODN treatment

Gene name and description (changed fold ≥ 2)	Genebank number
Inflammation and receptor	
IL-18 receptor accessory protein	AF077346
T cell receptor V beta gene	X58806
MSGA, beta gene	U03019
Antigen gene (PA)	M21896
TIED	NM_004791
Platelet activating receptor	AF002986
Antimicrobial defence	
Thioredoxin	NM_003329
Pro-Pol-dUTPase polyprotein	AC004748
Nuclear body protein Sp140	U63420
Transcriptional regulation	
Putative transcription factor LUZP	A1986271
General transcription factor II, I, pseudogene 1	A1700706
Connexin 59 gene	L29277
Basic helix-loop-helix protein class B 1 (BHLHB1)	AF221520

Table 1. Continued

Gene name and description (changed fold ≥ 2)	Genebank number
Regulatory protein	
Advillin	AF041449
Channel and transport	
Small GTP binding protein Rab9	U44103
FXD domain-containing ion transport regulator 1	AI125364
Signal transduction	
SH3-domain Grb2-like 2	AF036268
Titin	X90568
Titin associated protein (165 kD protein)	X69089
KIAA1451 protein	AB040884
Vasoactive intestinal peptide receptor	U11087
Enzyme and protease	
Enoyl-Coenzyme A, hydratase	AI800553
Nephrin, B-type metallopeptidase	U65090
Propionyl Coenzyme A carboxylase	AB011145
Acyloxyacyl hydrolase (neutrophil)	M62840
Cytochrome P450	U79716
Intestinal alkaline phosphatase	M31008
Tumor progression and cell differentiation	
Retinoblastoma 1	L11910
Human genomic DNA of 9q32 anti-oncogene of flat Epithelium cancer, segment 6/10	AB036268
WNT1 inducible signaling pathway protein 2 (WISP-2)	AF100780
Structure protein	
Collagen, type IV, alpha 6	D21337
Beta Myosin heavy chain	M58018
Other	
Homo sapiens Cri-du-chat region mRNA, clone NIBB11	U52827
Human mRNA for laminin alpha 5 chain, partial cds.	AB010099
NIK like and Thyroxin-binding globulin precursor	Z83850
Hypothetical protein DKFZp434M0331	AL137720
Hypothetical protein FLJ11021 similar to splicing factor	AK023985
Hypothetical protein	AL049851
Chromosome 18 open reading frame 1	NM_004338
Arlapin 1	AW408785
Zinc finger protein 8 (ZFP8)	M29581
Zinc finger protein 137 (clone pHZ-30)	U09414
Olfactomedin related ER localized protein	AI738468
Cyclin-dependent kinase 8	BE467537
Integrin, alpha 1	D87462
KIAA0421 protein	AB007881
KIAA1233 protein	AB033059
Unnamed protein product	AK026362
NBL4	X75535
BC331191_1	AAD39268

Table 2. Genes down-regulated (≥ 2 fold) in human THP-1 cells after 2 h of CpG-ODN treatment

Gene name and description (changed fold ≥ 2)	Genebank number
Zinc-finger homeodomain protein 4	BAB03600
Human protein kinase MEKK2b mRNA, complete cds.	AF239798
Glypican 5	U66033
Human genomic DNA, chromosome 22q11.2, clone N75A12.	AP000362
Collagen, type I, alpha 1	Z74615

Longer stimulation of THP-1 cells with CpG-ODN (8 h) resulted in the up-regulation of 58 genes. These genes included notably IL-10 receptor beta, formyl peptide receptor-like 1 (FPR1), vitamin D receptor, nuclear receptor subfamily 1 (LxR), early B-cell factor, protein kinase C gamma (PKC), Nck, Ash, phospholipase C binding protein (NAP4), phosphoriboxyl pyrophosphate amidotransferase, disheveled 3, WISP-2 *etc.* Analysis of the functions of the 58 up-regulated genes showed that they are associated with anti-inflammation, transcriptional regulation, intracellular signal transduction, tumor progression, cell differentiation, proteolysis, neurodegeneration, neuroprotection *etc.* (Table 3). We also found that the stimulation of THP-1 cells with CpG-ODN for different periods of times resulted in different profiles. Several defense related genes such as IL-18 receptor accessory protein, Pro-Pol-dUTPase polypeptide, Sp140 and connexin 59 were transiently up-regulated at 2 h short stim-

Table 3. Genes up-regulated (≥ 2 fold) in human THP-1 cells after 8 h of CpG-ODN treatment

Gene name and description (changed fold ≥ 2)	Genebank number
Inflammation and receptor	
IL-10 receptor (beta)	U08988
Formyl peptide receptor-like 1 (FPR1)	AF081535
Vitamin D receptor	J03258
NMDAR1	Z32774
CD44 antigen	AW028346
Nuclear receptor subfamily 1 (LxR)	NM_005693
Neuromedin B receptor	M73482
Transcriptional regulation	
Early B-cell factor (ebf)	AF208502
Neurogenic differentiation 1 (Neuro D)	AB018693
MAX dimerization protein (NESH protein)	AB037886
Ribosomal protein S6 kinase	AF090421
ASH2L	AB022785
Regulatory protein	
Hypothetical protein DKFZp434H0820	AL137555
Peroxisomal farnesylated protein	X75535
LTBP4	AF051344
Neuronal pentraxin II	U29195

Table 3. Continued

Gene name and description (changed fold ≥ 2)	Genebank number
Channel and transport	
Gamma-aminobutyric [61] A receptor	NM_004961
ATP synthase subunit F6	M37104
Transient receptor potential channel 1	Z73903
Choroideremia (Rab escort protein 1)	X57637
Signal transduction	
Protein kinase C, gamma	Z15114
Regulator of G-protein signaling 5	AI674877
Nck, Ash and phospholipase C binding protein (NAP4)	AB005216
Highly similar to adenylyl kinase gene	AB016886
Enzyme and protease	
Phenylalanine hydroxylase	AA203389
Carboxypeptidase A1	X67318
Xylulokinase	AK001205
Pancreatic lipase	J05125
Ubiquitin specific protease 12	AF022789
Transmembrane protease, serine2	U75329
Aspartate beta-hydroxylase	U03109
Phosphoribosyl pyrophosphate amidotransferase	D13757
Tumor progression and cell differentiation	
CDC23	AF053977
WISP-2	AF100780
Microseminoprotein, beta	M34376
Dishevelled 3	NM_004423
Structure protein	
Trichohyalin	L09190
Keratin	AF061809
Other	
Human transferrin pseudogene	M22376
TIMP-2	U44383
Collagen-like protein	U67921
Human genomic DNA, chromosome 21q, section 60/105	AP001716
Human genomic DNA, chromosome 21q, section 64/105	AP001720
KIAA0136	D50926
KIAA0379	AB002377
KIAA0489	AB007958
KIAA1114	AL049732
KIAA1451	AB040884
KIAA0756	AB018299
Zinc finger protein 267	AF220492
Hypothetical protein FLJ10633	AK001495
Hypothetical protein EUROMAGE 1955967	AK026108
Myb1 homolog like 1	AK001893
Antizyme inhibitor	D88674
Disintegrin-like and metalloprotease (reprolysin type) with Thrombospondin type 1 motif, 3	AB002364
ADP-ribosylation factor 3 (ARF-3)	M74491
Testis specific protein, Y-linked	M98525
Unnamed protein	AK026042

Table 4. List of antimicrobial and anti-inflammatory genes modulated by CpG-ODN treatment of THP-1 cells

Gene name	Genebank number	Expression fold	
		2 h	8 h
Connexin 59 gene	L29277	2.12 \pm 0.05	1.74 \pm 0.08
IL-18 receptor accessory protein	X58806	2.32 \pm 0.21	1.19 \pm 0.13
Integrin, alpha 1	X68742	2.01 \pm 0.03	1.05 \pm 0.10
Nuclear body protein Sp140	U63420	2.22 \pm 0.11	1.39 \pm 0.04
Pro-Pol-dUTPase polyprotein	AC004748	2.33 \pm 0.18	0.95 \pm 0.03
Thioredoxin	NM_003329	2.20 \pm 0.08	1.07 \pm 0.01
FPRL1	AF081535	0.95 \pm 0.06	2.13 \pm 0.11
IL-10 receptor	U08988	1.22 \pm 0.18	2.21 \pm 0.07
LxR	NM_005693	0.90 \pm 0.03	2.37 \pm 0.31
Vitamin D receptor	J03258	1.37 \pm 0.23	2.39 \pm 0.11

Expression fold is designated as the ratio of CpG-ODN treated over control

ulation but were down-regulated thereafter, while anti-inflammatory associated genes such as FPRL1, IL10 receptor, vitamin D receptor and LxR were up-regulated after 8 h stimulation (Tables 1, 3 and 4).

3.2 Verification of the microarray results with RT-PCR or Western blotting

To verify the results from the microarray analysis, we also performed RT-PCR on the up-regulated genes (Fig. 1). Consistent with results obtained in the microarray gene expression analysis, RT-PCR studies showed that the mRNA levels of some selected genes, including ubiquitin specific protease 12, regulator of G-protein signaling 5, NAP4 and ASH2L, were increased in response to CpG-ODN (Fig. 1, Table 3). In addition, the protein expression level of ARF-3

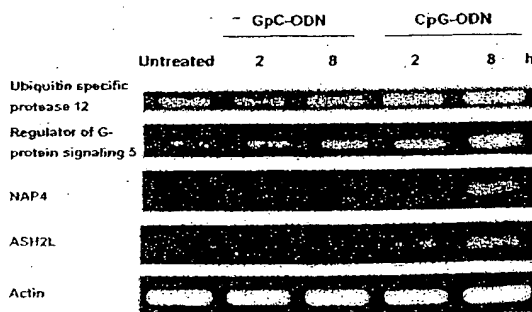


Figure 1. Induction of various genes by CpG-ODN. THP1 cells were stimulated with medium alone, 1.5 μ M GpC-ODN (as the negative control) or CpG-ODN for the indicated times. RT-PCR was then performed to analyze gene expression levels. β -actin was used as an internal control. The experiment was repeated three times with similar results.

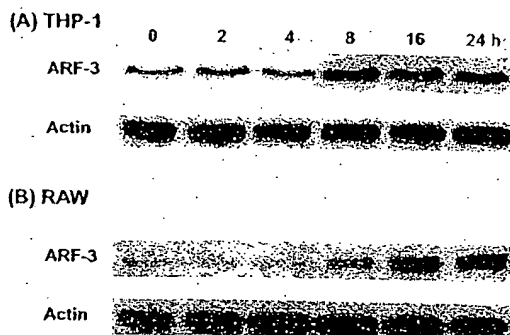


Figure 2. CpG-ODN induced ARF-3 protein expression in human THP-1 or mouse RAW264.7 cells. THP-1 (A) or mouse RAW264.7 (B) cells were incubated with 1.5 μ M CpG-ODN for the indicated time points. The protein expression level of ARF-3 was determined by Western blotting of cell extracts using anti-ARF-3 antibody. The experiment was repeated three times with similar results.

was shown to increase in Western blotting analysis in cell lysates from THP-1 cells treated with CpG-ODN for 8–24 h (Fig. 2A). Similar studies showed that the ARF-3 protein was also induced by mouse specific CpG-ODN in other TLR9 expression cell lines such as the mouse macrophage RAW264.7 cell line (Fig 2B).

3.3 Proteins regulated in CpG-ODN stimulated THP-1 cells

To further assess whether there was any correlation between regulation of gene expression and expression of cellular proteins, a proteomic approach was adopted to identify protein expression profiles. THP-1 cells were treated with CpG-ODN for defined times (from 8 to 40 h), and their cytoplasmic proteins were extracted for 2-DE analysis. Although the use of high concentrations of urea might give us a broader view of all the proteins affected by CpG-ODN, preliminary results from 2-D gels showed that the resolution of the protein mixtures were not satisfactory. To improve and get the best resolution from 2-DE, total proteins were roughly separated into supernatant and precipitated fractions using 50% saturated ammonium sulfate solution. To remove salts and other contaminants, both protein fractions were precipitated with TCA solution and then subjected to 2-DE. By protein spot determination analysis, about 500 and 450 well-resolved spots were observed on each pH 3.0–10.0 gel for precipitated or supernatant fractions, respectively. Comparative analysis of 2-DE between treatments and control showed that the intensities of the protein spots from the ammonium sulfate precipitated fraction did not change, while several protein spots were up-regulated by at least ~80% in the supernatant fraction of 8 h CpG-ODN stimulated THP-1 cells (Fig. 3).

The protein spots were individually excised from gels for further identification. After trypsin digestion, several protein spots were identified without ambiguity by MS MALDI-

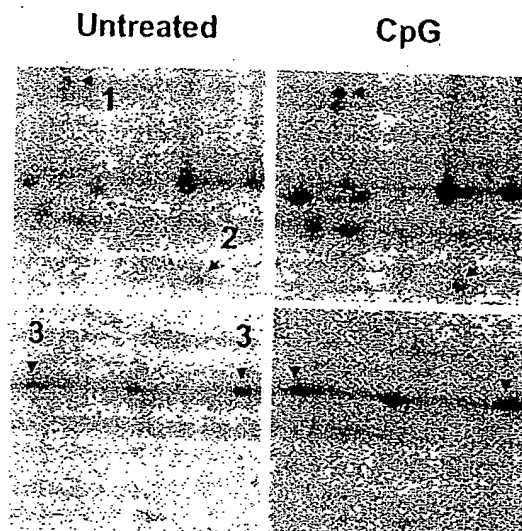


Figure 3. The effect of CpG-ODN on the 2-DE profile of THP-1 cells. THP-1 cells were treated with or without 1.5 μ M CpG-ODN for 8 h. Total proteins were extracted and roughly separated into two fractions by 50% saturation with ammonium sulfate. The supernatant fraction was then separated by 2-DE. Protein spots were visualized by SYPRO Ruby staining. Comparison of CpG-ODN treated THP-1 cells to untreated cells showed that these proteins changed in intensity by over 80%. Protein spots were identified by trypsin digestion and MS. Localization of protein spots 1 (enol-coenzyme A hydratase), 2 (proteasome α) and 3 (cyclophilin A; two isoforms) are shown. The experiment was repeated three times with similar results.

TOF. These proteins included HSP60, HSP90, cyclophilin A, enol-coenzyme A hydratase, eukaryotic translation elongation factor, proteasome α and β chain and ATP synthase beta chain (Table 5). Similar experiments on cells treated for a longer period of time with CpG-ODN stimulation (25 h) revealed that 27 protein spots were changed in intensity by at least ~80%. These protein spots contained members of HSPs (HSP27, hsc70, grp78 and grp94), metabolic enzymes (phosphoglycerate kinase (PGK) and pyruvate kinase (PYK)), macrophage capping protein and cyclophilin A (Table 6). Among these proteins, macrophage capping protein, PGK, PYK, cyclophilin A and HSP27 (Figs. 4 and 5A) were found to be up-regulated. Interestingly, we found that a truncated form of grp78 with an expected mass of 25 kDa and pI of 5.3 was up-regulated while grp78 itself was down-regulated. A similar situation was also found for grp94 and hsc70 and their truncated derivatives (Table 7 and Fig. 5). In addition, we also observed six down-regulated protein spots on 2-D gels in samples after 25 h CpG-ODN treatment. Among these six proteins, we have successfully identified three as 40s ribosomal protein SA, grp78 and hsc70, respectively (Table 6), while the other three, due to their relative low abundance, have not been identified yet.

Table 5. List of proteins modulated by 8 h CpG-ODN treatment

Protein name	Accession no.	M_r (theor.)	pI (theor.)	Matched no.	Coverage%	Score	Expression fold
ATP synthase beta-chain	gi114549	56 525	5.26	16	58	171	2.33 ± 0.06
Cyclophilin A	P05092	17 870	7.82	5	35	62	2.85 ± 0.13
Enoyl-Coenzyme A hydratase	gi4503447 ^{a)}	35 971	6.61	11	44	62	2.52 ± 0.05
Eukaryotic translation elongation factor	gi4503481	50 087	6.25	6	25	68	3.41 ± 0.21
HSP60	P10809 ^{b)}	57 963	5.24	13	27	76	2.78 ± 0.03
HSP90-beta	P08238	83 133	4.97	10	18	65	2.36 ± 0.10
Proteasome α chain	gi4506181	25 882	6.92	11	59	80	2.52 ± 0.11
Proteasome β chain	gi4506193	26 472	8.27	9	46	84	3.85 ± 0.17

Expression fold is designated as the ratio of CpG-ODN treated over control

a). NCBI accession number

b) Swiss-Prot accession number

Table 6. List of proteins modulated by 16 and 25 h CpG-ODN treatment

Protein name	Swiss-Prot no.	M_r (theor.)	pI (theor.)	Matched no.	Coverage%	Score	Expression fold	
							16 h	25 h
Cyclophilin A	P05092	17 870	7.82	5	35	62	2.53 ± 0.02	2.48 ± 0.15
78 kDa glucose regulated protein (grp78)	P11021	72 288	5.07	13	30	148	0.61 ± 0.04	0.29 ± 0.06
HSP27	P04792	22 768	5.98	12	59	124	1.00 ± 0.01	2.61 ± 0.12
Heat shock cognate 70 kDa protein (hsc70)	P11142	70 854	5.37	16	34	114	0.64 ± 0.01	0.31 ± 0.03
Macrophage capping protein	P40121	38 494	5.88	9	30	58	1.31 ± 0.01	2.58 ± 0.03
Phosphoglycerate kinase	P00558	44 284	7.052	11	33	71	2.32 ± 0.11	4.23 ± 0.19
Pyruvate kinase	P14618	57 710	7.95	17	32	114	1.65 ± 0.07	2.70 ± 0.12
40s ribosomal protein SA (RSP40)	P08865	32 833	4.79	5	23	61	0.33 ± 0.02	0.35 ± 0.05

Table 7. List of truncated proteins detected in THP-1 cells after 25 h CpG-ODN treatment

Protein name	Swiss-Prot no.	M_r (obs.)	pI (obs.)	Matched no.	Coverage%	Score	Expression fold
94 kDa glucose-regulated protein (grp94)	P14625	~59 700	~5.00	12	14	104	New ^{a)}
Truncated form of grp78	P11021	~25 000	~5.30	12	22	75	New
Truncated form of hsc70	P11142	~22 000	~5.80	12	20	96	New
Truncated form of hsc70	P11142	~19 000	~6.10	11	18	113	New

a) New designated proteins detected in the CpG-ODN treated gel but not in the corresponding control gel

3.4 Comparison of microarray and proteomic results

Table 8 shows the expression of six genes and their corresponding proteins that were modulated by 8 h treatment of THP-1 cells with CpG-ODN. Besides enoyl-coenzyme A hydratase, there was poor correlation between the expression

of genes and their corresponding proteins (Table 8), suggesting that more in-depth studies were needed. To further evaluate whether changes observed in protein expression correlated with changes in mRNA levels, we randomly chose two proteins (PGK and PYK) that were induced after 16 h CpG-ODN treatment and determined their mRNA levels by

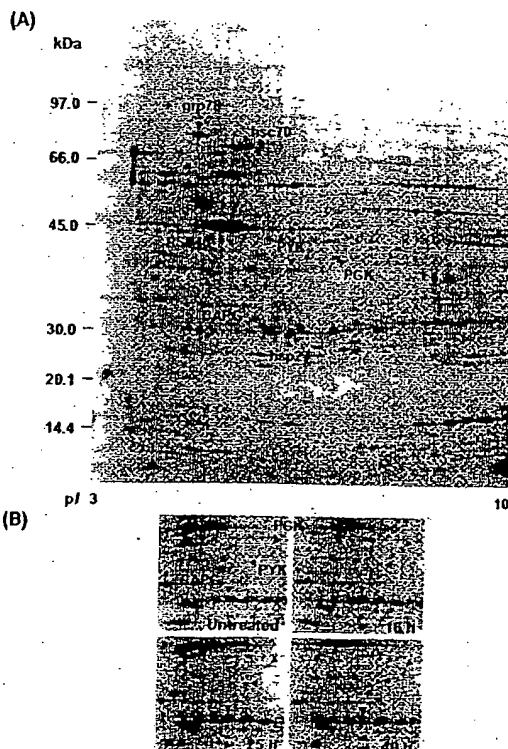


Figure 4. 2-D gel electrophoretic analysis of CpG-ODN-treated THP-1 cells. (A) Total cell protein from unstimulated THP-1 cells was subjected to 2-DE. (B) THP-1 cells were treated with or without 1.5 μ M CpG-ODN for defined times. Cellular proteins were extracted and separated by 2-DE. Several up-regulated proteins are shown in the SYPRO Ruby staining gel. Comparison of CpG-ODN treated THP-1 cells to untreated cells showed that these proteins changed in intensity by over 80%. The experiment was repeated three times with similar results.

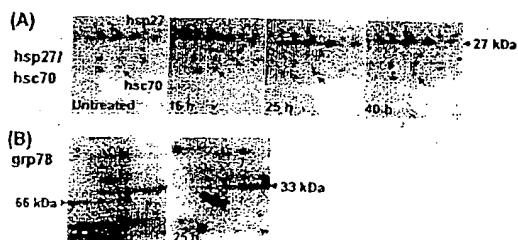


Figure 5. 2-D gel electrophoretic analysis of CpG ODN-treated THP-1 cells. THP-1 cells were treated with or without 1.5 μ M CpG-ODN for defined times. Cellular proteins were extracted and separated by 2-DE. Protein spots were detected by SYPRO Ruby staining. (A) Expression of HSP27 was induced by increasing the period of CpG-ODN stimulation. A truncated form of hsc70 was detected on the gel. (B) The native form of grp78 was detected in untreated cells, while the truncated form of grp78 was observed after 25 h stimulation. The experiment was repeated three times with similar results.

Table 8. Comparison of gene and protein expression levels in THP-1 cells after 8 h CpG-ODN treatment

Protein name	Gene expression fold from microarray	Protein expression fold from 2-D gel
Enoyl-Coenzyme A hydratase	1.72 \pm 0.31	2.52 \pm 0.05
Eukaryotic translation elongation factor	0.95 \pm 0.01	3.41 \pm 0.21
HSP60	0.94 \pm 0.07	2.78 \pm 0.03
HSP90-beta	1.58 \pm 0.11	2.36 \pm 0.10
Proteasome α chain	0.98 \pm 0.03	2.52 \pm 0.11
Proteasome β chain	1.09 \pm 0.11	3.85 \pm 0.17

RT-PCR. Our results showed that mRNA levels of PYK increased after 16 h CpG-ODN treatment, while mRNA levels of PGK were dramatically increased after 24 h stimulation (Fig. 6). In addition, we also performed enzyme activity analysis and found that the activity of PGK and PYK were

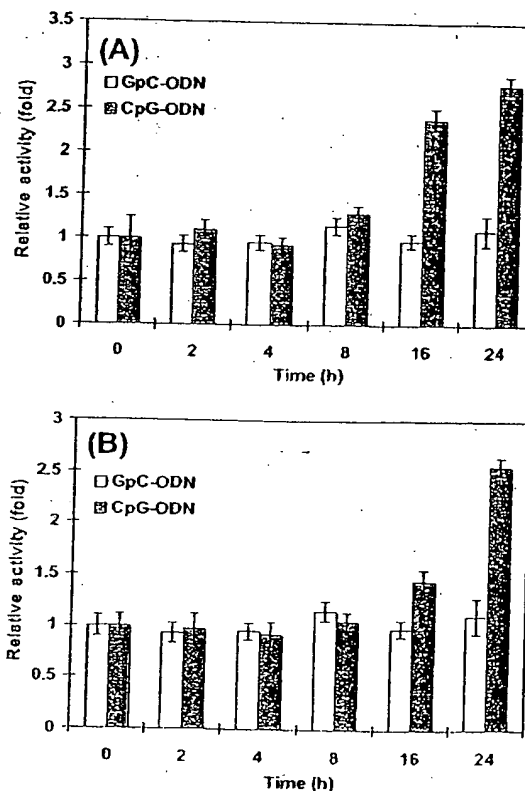


Figure 6. Activities of PYK and PGK induced by CpG-ODN. THP-1 cells were stimulated with medium alone, 1.5 μ M GpC-ODN (as the negative control) or CpG-ODN for the indicated times. Cell lysates were extracted and assayed for (A) PYK and (B) PGK activities. Data represent mean \pm SEM. (n = 3).

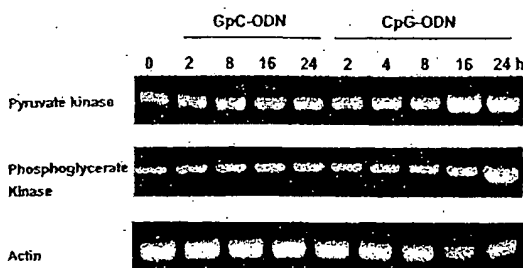


Figure 7. Induction of PYK and PGK transcripts by CpG-ODN. THP1 cells were stimulated with medium alone, 1.5 μ M CpC-ODN or CpG-ODN for the indicated times. RT-PCR was then performed to analyze gene expression. β -actin was used as an internal control. The experiment was repeated three times with similar results.

indeed increased by a factor ~ 2.5 after CpG-ODN stimulation (Fig. 7). To confirm that mRNA induced by CpG-ODN would also be accompanied by an increase in protein expression even though it was not detected in 2-D gel analysis, we used more sensitive and specific Western blotting analysis. As shown in Table 3 and Fig. 2, ARF-3 was identified in the microarray gene profile but not in the proteomic expression profile. Nevertheless, we observed enhanced protein expression of ARF-3 after CpG-ODN stimulation by Western blotting. Moreover, to investigate whether the up-regulation of ARF-3 by CpG-ODN is mediated through the TLR9 pathway, TLR9-deficient HEK293 cells were transiently cotransfected with hTLR9 and luciferase-reporter gene driven by a NF- κ B-dependent promoter. Our data showed that NF- κ B activity of untransfected HEK293 cells were not responsive to CpG-ODN stimulation, while in transfected HEK293 cells expressing hTLR9, NF- κ B luciferase activity was up-regulated 12-fold after 8 h CpG-ODN stimulation. The activation of NF- κ B induced by CpG-ODN was blocked by pretreatment of the transfected cells with an ARF-3 inhibitor, such as brefeldin A (Fig. 8), suggesting CpG-ODN induces ARF-3 and activates NF- κ B after the interaction of CpG-ODN with TLR9.

4 Discussion

In this study both microarray and proteomic approaches were used to evaluate the effect of CpG-ODN on gene/protein expression profiles of THP-1 cells at several time points. Comparison of the gene expression profiles showed that stimulation of the cells with CpG-ODN for different periods of time resulted in different profiles (Tables 1–4). The differences in mRNA expression between the cells with short and long stimulation could be attributable to the low reproducibility. However, to avoid experimental variations, we not only used the same batch of microarrays from the same manufacturer but also applied the samples of short and long term stimulation at the same time. In this way, we found that the

changes in expression fold of mRNA after CpG-ODN treatment were quite reproducible as shown by their mean \pm SEM (Table 4). A more likely explanation for the difference in the expression level of mRNA after different periods of stimulation with CpG-ODN is that the transient increase or decrease in these mRNA by CpG-ODN plays a significant role in modulating biological functions. For example, we found that the IL-18 receptor accessory protein from THP-1 cells was up-regulated after 2 h of CpG-ODN stimulation. The IL-18/IL18R system is known to activate Th1-mediated immune responses that play a critical role in host defense against infection [26]. Together with IL-18/IL18 R, several genes for antimicrobial defense were also increased, including thioredoxin, Pro-Pol-dUTPase polyprotein and Sp140. After 8 h of CpG-ODN stimulation, however, none of these genes was activated any more (Table 4). Since sustained or excessive production of these antimicrobial molecules might lead to inflammation and cellular damage [27], a plausible explanation is that THP-1 cells fight against the invasion of pathogens by up-regulating antimicrobial defense-associated genes at an early stage of stimulation and then shut them down to avoid over-activation. Whether this explanation is true remains to be verified.

It is noteworthy that our data also identified the up-regulation of several anti-inflammatory associated genes after 8 h of CpG-ODN stimulation. These genes included FPRL1, IL-10 receptor, vitamin D receptor, and LxR (Table 3). FPR and FPRL1 have been defined as chemotactic factors involved in host defense against bacterial infection and in the clearance of damaged cells. Additional studies have indicated that FPRL1 interacts with a menagerie of structurally diverse pro- and anti-inflammatory ligands associated with diseases, including amyloidosis, Alzheimer's diseases, prion disease and HIV [28, 29]. Therefore, FPRL1 may play an important role in regulating and/or balancing the production of pro- and anti-inflammatory molecules in CpG stimulated THP-1 cells. Additionally, a recent study has demonstrated that LxRs and their ligands act as negative regulators of macrophage inflammatory gene expression and inhibit the expression of inflammatory mediators such as inducible nitric oxide synthase, cyclooxygenase and IL-6 in response to bacterial infection or LPS stimulation [30]. Of interest, we found that a transcription factor gene connexin 59, a regulator of IL-6 expression, was up-regulated after 2 h of CpG-ODN stimulation. It is thus likely that CpG-ODN stimulation of THP-1 cells for 2 h may induce the expression of the pro-inflammatory cytokine IL-6 through the up-regulation of the connexin 59 gene, while 8 h of CpG-ODN treatment may counter-balance the initial inflammatory response by inducing LxR to inhibit IL-6 production.

Signal transduction molecules play an important role in cellular activation. Intracellular signal transduction systems employing various intermolecular interactions through docking elements, including SH2 and SH3 domains, have been reported [31–33]. Here we found that THP-1 cells treated with CpG-ODN for 2 h up-regulated gene expression

of Grb2-like protein (which contains an SH3 domain), while 8 h of stimulation induced Nck, Ash and phospholipase C binding protein (NAP4 which contains an SH2 domain). It is thus possible that Grb2-like protein and NAP4 may play important roles in CpG-ODN mediated signaling pathways. Furthermore, recent studies have also revealed that binding of CpG-DNA to TLR9 results in activation of JNK [34]. Since JNK is activated by Nck adaptor protein and Nck interacting kinase [35, 36], it is possible that CpG-ODN may activate JNK via up-regulation of NAP4. Although a recent publication described the gene expression profiles of a cultured mouse macrophage cell line after CpG-DNA stimulation [34], their microarray results were only conducted at one time-point (6 h stimulation). Moreover, they did not report the measurement of protein expression profiles in response to CpG-ODN stimulation.

Comparison of the gene and protein expression profiles showed that there was discordance between mRNA and protein levels (Table 8). Similar discordance between the expression pattern of genes and proteins was also reported in other system using different stimuli [37–41]. The discordance between mRNA and protein levels could be due to screening capability, such as detection sensitivity, choice of cut-off point, quantitativity of microarray and 2-D gels, as well as time discrepancy between gene and protein expression [39, 40, 42, 43]. Alternatively, it could also be explained by post-transcriptional events, such as alternative splicing or PTM [39, 40, 42, 43]. Another possible explanation is that most of the spots observed in the 2-D gels are isoforms of some proteins. The intensity of each spots does not necessarily represent total amount of a certain protein and thus does not correlate with its mRNA level. Our finding that microarray results correlated better with Western blotting results (e.g., ARF-3 in Fig. 2), an approach more suitable than 2-D gels for determining the total amount rather than isoforms of a given protein, seems to suggest that formation of isoforms should be carefully taken into consideration when one tries to correlate mRNA and protein expression data.

Using a proteomics approach, we found that CpG-ODN treatment up-regulated the expression of many proteins including HSPs, metabolic enzymes, structural proteins, as well as macrophage capping protein, cyclophilin and proteasome α and β chain *etc.* HSPs are the most abundant and ubiquitous soluble intracellular proteins. They are up-regulated by various stressors including temperature, glucose deprivation, microbial infection and cancer [44]. They function as molecular chaperones to prevent protein aggregation and contribute to the folding of nascent and altered proteins. In addition, they are able to regulate immune responses, including production of inflammatory cytokines and chemokines and activation or maturation of immune cells [45, 46]. Beside HSPs, cyclophilin as well as proteasome α and β chain have also been reported to be involved in the immune response [39, 47]; proteasome β chain is consistently up-regulated in human neutrophils following LPS exposure [39]. Our finding that the protein levels of HSPs, cyclophilin, and

proteasome α and β chain were increased after CpG-ODN treatment suggests that these molecules might play a role in the immunostimulating effect of CpG-ODN. To what extent these proteins contribute to the immune responses of the cells to CpG-ODN is currently under study. Proteomic analysis also showed that truncated forms of grp78, grp94 and hsc70 were induced, a phenomenon similar to calreticulin observed by Richards and his coworkers [48]. The expression of full length hsc70 and grp78 were decreased while the levels of their truncated derivatives was increased after CpG-ODN treatment. These results suggest that the degradation of these proteins has been enhanced. We also found that proteasome α and β chains as well as ubiquitin specific protease 12 were increased by CpG-ODN. Whether these enzymes or other enzymes were responsible for the generation of truncated hsc70 and grp78 remains to be elucidated.

Cells rely on multiple signaling pathways to determine their fates of survival, proliferation or apoptosis [49]. In fact, apoptosis plays an important role in regulating pathogen infection. To be able to grow and replicate in the target cells, pathogens may have to block apoptosis. Results from several laboratories have made it clear that HSP70 and HSP27 protect cells not only from heat, but also from most apoptotic stimuli [48, 50] by binding to Akt and subsequently mediating anti-apoptotic activity through activation of Akt [51–53]. Since our data revealed that CpG-ODN induced the expression of HSP90 and HSP27, it is possible that CpG-ODN might prevent apoptosis by up-regulation of HSPs.

Interestingly, our microarray data also showed that CpG-ODN mediated the induction of a set of genes associated with tumor progression and cell proliferation. Among these, one gene, WISP-2, was up-regulated by CpG-ODN after both 2 and 8 h stimulation. WISP genes were first identified as downstream targets of the Wnt-1 β -catenin signaling pathway. They belong to the CCN family of growth factors that have been receiving increasing attention lately due to some of the family members having been reported to be involved in angiogenesis and tumorigenesis [54]. It would be interesting to evaluate whether CpG-ODN plays a role in angiogenesis and tumorigenesis by regulating WISP-2. In addition, we found that some genes associated with neurodegeneration or neuroprotection, such as FPRL1, NMDAR (NMDA) receptor, PKC and dishevelled 3 were up-regulated. To our knowledge, this is the first report to suggest an association between these genes and CpG-ODN stimulation. As mentioned above, FPRL1 plays a crucial role in proinflammatory aspects of systemic amyloidosis and neurodegenerative disease such as Alzheimer's disease and prion disease [28]. NMDAR, PKC and dishevelled are involved in modulating amyloid precursor protein metabolism, which is central to the pathogenesis of Alzheimer's disease [55–57]. Most notably, recent studies have shown that the TLR4-dependent pathway is involved in neurodegeneration of the central nervous system [58]. Whether CpG-ODN moieties of pathogens play any role in neurodegenerative diseases such as Alzheimer's remains to be elucidated.

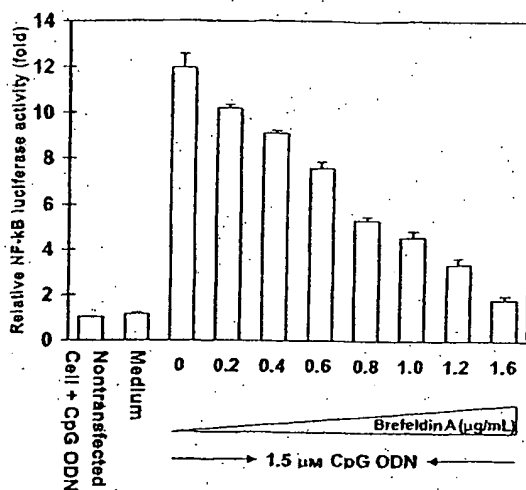


Figure 8. ARF-3 participates in the CpG-ODN-TLR9-NF-κB pathway. HEK293 cells were cotransfected with p5xNF-κB and human TLR9. After overnight transfection, the cells were incubated with or without 1.5 μM CpG-ODN for 8 h in the presence or absence of increasing concentrations of the ARF-3 inhibitor brefeldin A. After incubation, cells were lysed and NF-κB luciferase activity was measured. Data represent mean ± SEM. ($n = 3$).

Exposure of cells to LPS or microbial infection has been known to induce several genes encoding metabolic enzyme [34, 39]. Our microarray data also revealed that a large number of genes encoding proteins involved in energy synthesis and fatty acid oxidation, such as enoyl-coenzyme A hydratase, propionyl coenzyme A carboxylase and cytochrome p450 were activated by CpG-ODN treatment. In addition, we found that other proteins such as ARF-3 were up-regulated (Table 3, Fig. 8). ARFs are 20 kDa GTPases of the ras superfamily that are critical to vesicular trafficking, including exocytic protein transport and endocytosis [59, 60]. This study demonstrates for the first time that ARF-3 is involved in the activation of NF-κB induced by CpG-ODN (as shown in Fig. 8).

CpG-DNA/ODN has been shown to elicit primarily responses via the TLR9/MyD88 dependent pathway [18, 21, 22]. Chromosome location analysis showed that instead of localizing on one or two chromosome, the genes/proteins modulated by CpG-ODN stimulation are scattered on all chromosomes except chromosomes 23 and 24. These results seem to suggest that CpG-ODN either affects multiple chromosomes simultaneously or subsequently via cascades of cellular messengers. More studies are needed to elucidate its mechanism of actions.

5 Concluding remarks

In summary, by using microarray and proteomic approaches to evaluate the effect of CpG-ODN at different time points, we have found that genes/proteins regulated by CpG-ODN

are related to inflammatory responses, antimicrobial defense, transcriptional regulation, intracellular signal transduction, tumor progression, cell differentiation, proteolysis, anti-apoptosis as well as neurodegeneration and neuroprotection. Our results may help delineate the CpG-ODN mediated pathway and contribute to further understanding of mechanisms that link innate immunity with acquired immune response(s).

We thank Mr. Yen-Chieh Huang and Ms. V. R. Kavitha for technical assistance in RT-PCR analysis. We also thank the Core Facilities for Proteomics Research at the Academia Sinica, Taiwan for mass spectrometry analyses. This work was supported by the National Science Council (Grant NSC 91-3112-P001-002-Y) and Academia Sinica (Grant AS 911BC3PP), Republic of China.

6 References

- [1] Akira, S., Hemmi, H., *Immunol. Lett.* 2003, **85**, 85–95.
- [2] Janeway, C. A. Jr., Medzhitov, R., *Semin. Immunol.* 1998, **10**, 349–350.
- [3] Wagner, H., *Curr. Opin. Microbiol.* 2002, **5**, 62–69.
- [4] Halpern, M. D., Kurlander, R. J., Pisetsky, D. S., *Cell. Immunol.* 1996, **167**, 72–78.
- [5] Messina, J. P., Gilkeson, G. S., Pisetsky, D. S., *J. Immunol.* 1991, **147**, 1759–1764.
- [6] Yi, A. K., Krieg, A. M., *J. Immunol.* 1998, **160**, 1240–1245.
- [7] Tokunaga, T., Yamamoto, H., Shimada, S., Abe, H. et al., *J. Natl. Cancer Inst.* 1984, **72**, 955–962.
- [8] Yamamoto, S., Kuramoto, E., Shimada, S., Tokunaga, T., *Jpn. J. Cancer Res.* 1988, **79**, 866–873.
- [9] Stacey, K. J., Sweet, M. J., Hume, D. A., *J. Immunol.* 1996, **157**, 2116–2122.
- [10] Yi, A. K., Tuetken, R., Redford, T., Waldschmidt, M. et al., *J. Immunol.* 1998, **160**, 4755–4761.
- [11] Krieg, A. M., Yi, A. K., Matson, S., Waldschmidt, T. J. et al., *Nature* 1995, **374**, 546–549.
- [12] Kline, J. N., Waldschmidt, T. J., Businga, T. R., Lemish, J. E. et al., *J. Immunol.* 1998, **160**, 2555–2559.
- [13] Shirota, H., Sano, K., Hirasawa, N., Terui, T. et al., *J. Immunol.* 2001, **167**, 66–74.
- [14] Lipford, G. B., Sparwasser, T., Bauer, M., Zimmermann, S. et al., *Eur. J. Immunol.* 1997, **27**, 3420–3426.
- [15] Sparwasser, T., Miethke, T., Lipford, G., Borschert, K. et al., *Nature* 1997, **386**, 336–337.
- [16] Sparwasser, T., Miethke, T., Lipford, G., Erdmann, A. et al., *Eur. J. Immunol.* 1997, **27**, 1671–1679.
- [17] Takeda, K., Akira, S., *Genes Cells* 2001, **6**, 733–742.
- [18] Hemmi, H., Takeuchi, O., Kawai, T., Kaisho, T. et al., *Nature* 2000, **408**, 740–745.
- [19] Hacker, H., Mischak, H., Miethke, T., Liptay, S. et al., *EMBO J.* 1998, **17**, 6230–6240.
- [20] Bandholtz, L., Guo, Y., Palmberg, C., Mattsson, K. et al., *Cell. Mol. Life Sci.* 2003, **60**, 422–429.

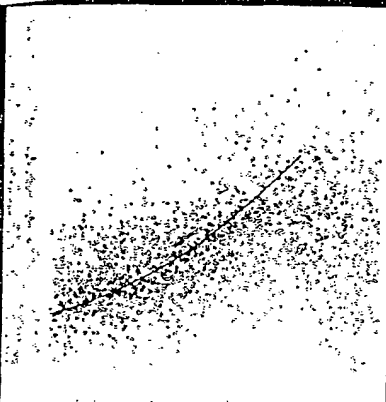
- [21] Bauer, S., Kirschning, C. J., Hacker, H., Redecke, V. *et al.*, *Proc. Natl. Acad. Sci. USA* 2001, 98, 9237–9242.
- [22] Hacker, H., Vabulas, R. M., Takeuchi, O., Hoshino, K. *et al.*, *J. Exp. Med.* 2000, 192, 595–600.
- [23] Takeshita, F., Leifer, C. A., Gursel, I., Ishii, K. J. *et al.*, *J. Immunol.* 2001, 167, 3555–3558.
- [24] Akhtar, M., Watson, J. L., Nazli, A., McKay, D. M., *FASEB J.* 2003, 17, 1319–1321.
- [25] Lee, C. Y., *Methods Enzymol.* 1982, 90 Pt E, 121–126.
- [26] Kawakami, K., *J. Immunother.* 2002, 25 Suppl. 1, S12–19.
- [27] Nakanishi, K., Yoshimoto, T., Tsutsui, H., Okamura, H., *Annu. Rev. Immunol.* 2001, 19, 423–474.
- [28] Le, Y., Oppenheim, J. J., Wang, J. M., *Cytokine Growth Factor Rev.* 2001, 12, 91–105.
- [29] Le, Y., Murphy, P. M., Wang, J. M., *Trends Immunol.* 2002, 23, 541–548.
- [30] Joseph, S. B., Castrillo, A., Laffitte, B. A., Mangelsdorf, D. J., Tontonoz, P., *Nat. Med.* 2003, 9, 213–219.
- [31] Cohen, G. B., Ren, R., Baltimore, D., *Cell* 1995, 80, 237–248.
- [32] Pawson, T., *Nature* 1995, 373, 573–580.
- [33] Birge, R. B., Knudsen, B. S., Besser, D., Hanafusa, H., *Genes Cells* 1996, 1, 595–613.
- [34] Gao, J. J., Diest, V., Wittmann, T., Morrison, D. C. *et al.*, *J. Leukocyte Biol.* 2002, 72, 1234–1245.
- [35] Minden, A., Lin, A., Claret, F. X., Abo, A., Karin, M., *Cell* 1995, 81, 1147–1157.
- [36] Becker, E., Huynh-Do, U., Holland, S., Pawson, T. *et al.*, *Mol. Cell Biol.* 2000, 20, 1537–1545.
- [37] Anderson, L., Seilhamer, J., *Electrophoresis* 1997, 18, 533–537.
- [38] Gygi, S. P., Rochon, Y., Franza, B. R., Aebersold, R., *Mol. Cell Biol.* 1999, 19, 1720–1730.
- [39] Fessler, M. B., Malcolm, K. C., Duncan, M. W., Worthen, G. S., *J. Biol. Chem.* 2002, 277, 31291–31302.
- [40] Kim, C. H., Kim do, K., Choi, S. J., Choi, K. H. *et al.*, *Proteomics* 2003, 3, 2454–2471.
- [41] Scheurer, S. B., Raybak, J. N., Rosli, C., Neri, D., Elia, G., *Proteomics* 2004, 4, 1737–1760.
- [42] Corthals, G. L., Wasinger, V. C., Hochstrasser, D. F., Sanchez, J. C., *Electrophoresis* 2000, 21, 1104–1115.
- [43] Hegde, P. S., White, I. R., Debouck, C., *Curr. Opin. Biotechnol.* 2003, 14, 647–651.
- [44] Robert, J., *Dev. Comp. Immunol.* 2003, 27, 449–464.
- [45] Basu, S., Srivastava, P. K., *Cell Stress Chaperones* 2000, 5, 443–451.
- [46] Berwin, B., Nicchitta, C. V., *Traffic* 2001, 2, 690–697.
- [47] Fluckiger, S., Fijten, H., Whitley, P., Blaser, K., Cramer, R., *Eur. J. Immunol.* 2002, 32, 10–17.
- [48] Richards, J., Le Naour, F., Hanash, S., Beretta, L., *Ann. N. Y. Acad. Sci.* 2002, 975, 91–100.
- [49] Underhill, D. M., Ozinsky, A., *Annu. Rev. Immunol.* 2002, 20, 825–852.
- [50] Somersan, S., Larsson, M., Fonteneau, J. F., Basu, S. *et al.*, *J. Immunol.* 2001, 167, 4844–4852.
- [51] Rane, M. J., Pan, Y., Singh, S., Powell, D. W. *et al.*, *J. Biol. Chem.* 2003, 278, 27828–27835.
- [52] Solit, D. B., Basso, A. D., Olshen, A. B., Scher, H. I., Rosen, N., *Cancer Res.* 2003, 63, 2139–2144.
- [53] Sato, S., Fujita, N., Tsuruo, T., *Proc. Natl. Acad. Sci. USA* 2000, 97, 10832–10837.
- [54] Pennica, D., Swanson, T. A., Welsh, J. W., Roy, M. A. *et al.*, *Proc. Natl. Acad. Sci. USA* 1998, 95, 14717–14722.
- [55] Lipton, S. A., *Cell Death Differ.* 1999, 6, 943–951.
- [56] Du, J., Zhou, S., Coggeshall, R. E., Carlton, S. M., *Neuroscience* 2003, 118, 547–562.
- [57] Mudher, A., Chapman, S., Richardson, J., Asuni, A. *et al.*, *J. Neurosci.* 2001, 21, 4987–4995.
- [58] Lehnardt, S., Massillon, L., Follett, P., Jensen, F. E. *et al.*, *Proc. Natl. Acad. Sci. USA* 2003.
- [59] Lenhard, J. M., Kahn, R. A., Stahl, P. D., *J. Biol. Chem.* 1992, 267, 13047–13052.
- [60] Morinaga, N., Adamik, R., Moss, J., Vaughan, M., *J. Biol. Chem.* 1999, 274, 17417–17423.
- [61] Balog, R. P., de Souza, Y. E., Tang, H. M., DeMasellis, G. M. *et al.*, *Anal. Biochem.* 2002, 309, 301–310.

PROTEOMICS

www.proteomics-journal.de

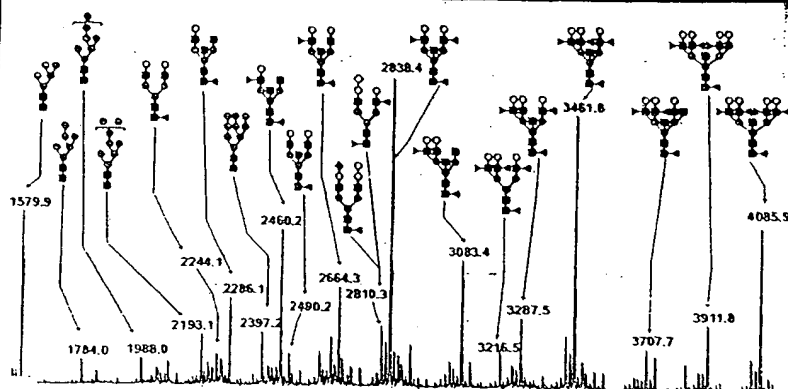
Q
7P93847

4'05



IPC '03

Proceedings of the 3rd International
Proteomics Conference (IPC '03)
held conjointly with the
1st Taiwan Proteomics Conference and the
2nd AOHUPO Congress
Taipei, Taiwan, 14–17 May 2004



EBLING LIBRARY
UNIVERSITY OF WISCONSIN

MAR 28 2005

750 Highland Avenue
Madison, WI 53705

Editor:
Richard J. Simpson



Now
18 Issues
Per Year

WILEY-VCH

ISSN 1615-9853 • PROTC 5 (4) 831–1184 (2005) • Vol. 5 • No. 4 • March 2005

CONTENTS

Volume 5 Issue 4
March 2005
Proteomics 5 (4) 831–1184 (2005)

SPECIAL


IPC '03

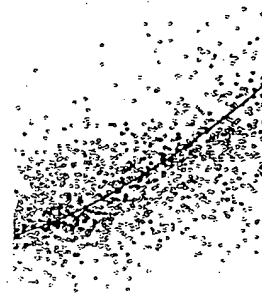
Proceedings of the 3rd International Proteomics
Conference held conjointly with the
1st Taiwan Proteomics Conference and the
2nd AOHUPO Congress
Taipei, Taiwan, 14–17 May 2004

Editor: Richard J. Simpson

- 831 EDITORIAL
IPC '03
Richard J. Simpson

Technology

- 840 SHORT COMMUNICATION
A new application of microwave technology to proteomics
Hsueh-Fen Juan, Shing-Chuan Chang, Hsuan-Cheng Huang
and Shui-Tein Chen
- 843 The development of an algorithm for the mass spectral interpretation
of phosphoproteins
Yupeng Zhao and Yen-Han Lin
 Supporting information see www.proteomics-journal.de
- 846 Tryptic transpeptidation products observed in proteome analysis
by liquid chromatography-tandem mass spectrometry
Heike Schaefer, Daniel C. Chamrad, Katrin Marcus, Kai A. Reidegeld,
Martin Blüggel and Helmut E. Meyer



Cover Illustration

has kindly been provided by
Takao Kawakami,
Clinical Proteome Center,
Tokyo Medical University,
Tokyo, Japan. This issue, p. 861

Localization of Tissue Inhibitor of Metalloproteinases 1 (TIMP-1) in Human Colorectal Adenoma and Adenocarcinoma

Mads N. Holten-Andersen^{1,2*}, Ulla Hansen³, Nils Brünner², Hans Jørgen Nielsen⁴, Martin Illemann¹ and Boye Schnack Nielsen¹

¹The Finsen Laboratory, Rigshospitalet, Denmark

²The Institute for Pharmacology and Pathobiology, The Royal Veterinary and Agricultural University, Denmark

³Department of Pathology, University Hospital Hvidovre, Denmark

⁴Department of Surgical Gastroenterology, University Hospital Hvidovre, Denmark

Tissue inhibitor of matrix metalloproteinases 1 (TIMP-1) inhibits the proteolytic activity of matrix metalloproteinases and hereby prevents cancer invasion. However, TIMP-1 also possesses other functions such as inhibition of apoptosis, induction of malignant transformation and stimulation of cell-growth. We have previously demonstrated that TIMP-1 is elevated in blood from colorectal cancer patients and that high TIMP-1 levels predict poor prognosis. To clarify the role of TIMP-1 in colorectal tumorigenesis, the expression pattern of TIMP-1 in benign and malignant colorectal tumors was studied. In all of 24 cases of colorectal adenocarcinoma TIMP-1 mRNA was detected by *in situ* hybridization. In all cases TIMP-1 expression was found in fibroblast-like cells located at the invasive front but was seen only sporadically in normal mucosa. No TIMP-1 mRNA was seen in any of the cases in benign or malignant epithelial cells, in vascular cells or smooth muscle cells. Comparison of sections processed for TIMP-1 *in situ* hybridization with sections immunohistochemically stained with antibodies against TIMP-1 showed good correlation between TIMP-1 mRNA and immunoreactivity. Combining TIMP-1 *in situ* hybridization with immunohistochemical staining for α -smooth muscle actin or CD68 showed TIMP-1 mRNA in myofibroblasts but not in macrophages. TIMP-1 mRNA was detected in 2 of 7 adenomatous polyps in the adenoma area: in both cases associated with focal stromal inflammation at the epithelial-stromal interface. In conclusion, TIMP-1 expression is a rare event in benign human colon tissue but is highly expressed by myofibroblasts in association with invading colon cancer cells.

Key words: TIMP-1; MMP; *in situ* hybridization; immunohistochemistry; myofibroblast

A prerequisite for cancer cell invasion and metastasis is the breakdown of tissue barriers mediated by proteolytic enzymes such as the matrix metalloproteinases (MMP).^{1,2} Under normal physiologic conditions, the tissue degrading activities of the MMPs are kept at bay by the presence of the naturally occurring inhibitors: tissue inhibitors of metalloproteinases (TIMP). TIMP-1, a 28 kDa glucoprotein demonstrated to be present in most bodily tissues and fluids, binds and inhibits MMPs in a 1:1 stoichiometric manner.^{3,4} Overexpression of TIMP-1 in various cancer models has shown a suppressive role in the malignant progression.⁵ However, as opposed to this anti-invasive role of TIMP-1, several recent studies have demonstrated quite different functions of this MMP-inhibitor including stimulation of cell growth, malignant transformation and inhibition of apoptosis, suggesting a possible tumor-promoting role of TIMP-1 in very early stages of tumorigenesis.^{6–10} Thus, it has been speculated that TIMP-1 may actually play a dual role in cancer progression and metastasis.¹¹

Several studies have demonstrated that tumor tissue levels of MMP mRNA and protein are significantly increased in various malignant diseases and that such MMP elevations are correlated with cancer cell invasion, metastasis and short patient survival.^{12,13} In addition, many reports have described similar overexpression of TIMP-1 mRNA and protein in several cancer types.^{14–20} Moreover, we and others have demonstrated that measurement of increased plasma levels of TIMP-1 by immunoassay serves as a strong marker for short survival and recurrence of disease in patients with colorectal cancer.^{21–23} Similarly, a strong correlation

between high protein levels and poor prognosis is known for the type-1 plasminogen activator inhibitor (PAI-1).^{24,25} Considering the protease inhibiting function of these inhibitors, these findings seemed controversial; however, alternative functions have been reported both for TIMP-1 as mentioned above as well as for PAI-1.²⁶

In order to better understand the role of TIMP-1 in colorectal cancer, histochemical analyses may provide some indications. A number of studies of the localization of TIMP-1 in colorectal cancer have been published; however, the results of these reports are somewhat contradictory. Newell and colleagues²⁷ reported that TIMP-1 mRNA was expressed both in invasive adenocarcinoma, carcinoma *in situ* and adenoma and that the expression was observed in both the stromal as well as the epithelial compartment of the tissues studied. In contrast, Zeng and colleagues^{12,20} reported that TIMP-1 mRNA was expressed only in the stromal compartment of colorectal adenocarcinomas in spindle-shaped cells surrounding the invasive cancer cells. The results of immunohistochemical studies of TIMP-1 in colon are also conflicting: Hewitt and colleagues¹⁹ reported that TIMP-1 was expressed in the connective tissue and basement membrane in both normal mucosa, adenomas and adenocarcinomas with only little staining of the neoplastic epithelium. On the other hand, Tomita and colleagues²⁸ reported that TIMP-1 was expressed in both stromal and epithelial cells in colonic polyps and adenomas, as well as in adenocarcinomas, in which the neoplastic cells were strongly immunoreactive.

In order to resolve these inconsistencies, we undertook our study and by *in situ* hybridization and immunohistochemistry demonstrated that TIMP-1 is expressed in myofibroblasts in the stroma at the invasive front of colorectal adenocarcinomas. Because TIMP-1 was virtually absent from normal colorectal epithelium, we evaluated the possibility of using TIMP-1 as a diagnostic tool to differentiate colorectal adenomas from Dukes' stage A colorectal adenocarcinomas.

Material and methods

Tissue samples

All tissue material included was obtained from University Hospital of Hvidovre (Copenhagen, Denmark) in accordance with a permission given by the local scientific ethical committee (KF 01-078/93). Fourteen archival samples (formalin fixed and paraffin embedded) collected from 1989 to 1993 included Dukes' stage A colorectal adenocarcinomas ($n = 8$) and colorectal adenomatous polyps ($n = 6$, 3 were pedunculated (1 with mild and 2 with

Grant sponsor: The Danish Cancer Society; Grant sponsor: European commission; Grant number: QLGI-CT-2000-0111131; Grant sponsor: Weimann Foundation.

*Correspondence to: Mads N. Holten-Andersen, The Institute for Pharmacology and Pathobiology, The Royal Veterinary and Agricultural University, Denmark.

Received 16 February 2004; Accepted after revision 7 June 2004
DOI 10.1002/ijc.20566

Published online 13 September 2004 in Wiley InterScience (www.interscience.wiley.com).

moderate dysplasia) and 3 were sessile (1 with moderate and 2 with focally severe dysplasia). Samples from 16 colorectal adenocarcinomas (1 Duke's stage A, 6 Duke's stage B, 8 Duke's stage C and 1 Duke's stage D), 1 villous adenoma and 1 malignant colon lymphoma were prospectively collected during 1999–2000. These prospectively collected tissue specimens were dissected so that samples contained both normal mucosa and tumor tissue and were obtained within 30 min following surgical bowel resection. The specimens were immediately fixed in 4% neutral buffered formalin for 20–24 hr and then paraffin embedded. The 14 archival samples had also been formalin fixed and paraffin embedded.

Generation of nonoverlapping TIMP-1 cDNA fragments by PCR

The full length TIMP-1 cDNA (GenBank NM_003254) cloned in pSP64 vector²⁹ was used as template to generate 2 nonoverlapping PCR fragments for *in vitro* transcription, and named f104 (bp 56–378) and f106 (bp 398–680). First, the whole insert (~780 bp) was cut out by digestion with *Hind* III and *Bam* HI and purified after agarose gel electrophoresis using the Qiaex II gel extraction kit (Qiagen, Crawley, United Kingdom). To generate nonoverlapping antisense probes and the corresponding sense probe, 2 PCR fragments were generated using upstream primers flanked by a linker sequence containing an *Eco*RI restriction enzyme site (underlined nucleotides) and a T3 polymerase binding sequence (boldface) 5'-(**gagaattcattacccctactaaaggaga**)-3', and downstream primers flanked by a linker sequence containing a *Bam*HI restriction enzyme site and a T7 polymerase binding sequence 5'-(**ggatcctaatacgtactactataggag**)-3'.⁹ The TIMP-1 specific upstream primers were 5'-accaccatggcccccttg-3' for f104 and 5'-(linker)-gcaggatggactctgcaca-3' for f106, and the downstream primers were 5'-(linker)-actccgcgtcgggttg-3' for f104 and 5'-(linker)-tatctggaccgcaggag-3' for f106. PCR using the 2 f104 primers or the 2 f106 primers was done as previously described.³⁰

The PCR products were purified by column chromatography using S-200HR microspin columns (Amersham Pharmacia Biotech, Inc., Piscataway, NJ), and their size tested by agarose gel electrophoresis. Both migrated as ~300 bp fragments in accordance with the predicted size (322 and 282 bp, respectively). An ABI PRISM 310 genetic analyzer was employed for DNA sequencing analysis and was performed according to the manufacturer's instructions (Perkin Elmer, Applied Biosystems, Foster City, CA) using the primers specified above. The DNA sequences obtained were confirmed by comparison with the specific TIMP-1 cDNA nucleic acid sequence (GenBank NM_003254).

Plasmids containing human MMP-2 cDNA (pCol7201, bp 647–1284) and human MMP-9 cDNA (pCol9202, bp 1751–2326) have been described elsewhere.³¹

In vitro transcription

Antisense and sense riboprobes were labeled with ³⁵S UTP (NEN, Boston, MA) by *in vitro* transcription using T7 and T3 RNA polymerases (Roche, Basel, Switzerland). The DNA template was digested with DNase (Promega, Madison, WI). Nonincorporated ³⁵S UTP and DNA was removed by column chromatography using S-200HR microspin columns (Amersham Pharmacia Biotech, Inc., Piscataway, NJ). The ³⁵S activity was adjusted for every probe by dilution to 500,000 cpm/μl.

In situ hybridization

In situ hybridization was performed essentially as described previously.³² In brief, 3 μm paraffin sections were deparaffinized in xylene, hydrated with graded ethanol and boiled in a microwave oven for 10–12 min in 10 mM citrate buffer, pH 6.0. After additional 20 min at room temperature, the sections were dehydrated with graded ethanol and the ³⁵S labeled probes (2 × 10⁶ cpm in 20 μl hybridization mixture³¹ per slide) incubated overnight at 55°C in a humidified chamber. Sections were washed in Hellen-dahl chambers with SSC buffers containing 0.1% SDS and 10 mM DTT at 150 rpm at 55°C using a Bühler incubation shaker (Johanna Otto GmbH, Hechingen, Germany) for 10 min in 2 × SSC,

10 min in 0.5 × SSC, and 10 min in 0.2 × SSC. Sections were then RNase A treated for 10 min to remove nonspecifically bound riboprobe. Subsequent wash was performed in 0.2 × SSC as specified above. Sections were dehydrated and soaked into an autoradiographic emulsion (Ilford), exposed for 5–7 days if not otherwise stated and finally developed. Sections were counterstained with haematoxylin and eosin.

Immunoperoxidase staining

Immunohistochemistry was performed essentially as described previously.³² Five micrometer paraffin sections were deparaffinized with xylene and hydrated through ethanol/water dilutions. Tissue pretreatment was performed with protease-K (5 μg/ml) digestion for 20 min. Sections were blocked for endogenous peroxidase activity by treatment with 1% hydrogen peroxide for 15 min. The sections were washed in 50 mM Tris 150 mM NaCl, pH 7.6, containing 0.5% Triton X-100 (TBS-T). Incubation with antibodies was done overnight at 4°C. Sheep polyclonal antibodies (pAb) against TIMP-1 and nonimmune goat IgG were used at a final concentration of 4.0 μg/ml. Two monoclonal antibodies (MAb) against TIMP-1,³³ NM4 (clone rTIX6A, NeoMarkers, Fremont, CA) and CalB2 (clone 147-6D11, CalBiochem, Oncogene Res. Products, Cambridge, MA), and a MAb against trinitrophenyl (TNP)³⁴ were all incubated at 1.0 μg/ml (all 3 MABs are IgG1). CalB2 MAB recognizes both free TIMP-1 and TIMP-1 in complex with MMPs.³³ NM4 MAB only recognizes free TIMP-1.³³ According to the manufacturer's descriptions, both MABs are raised using recombinant human TIMP-1. The sheep polyclonal antibodies were raised by immunization with TIMP-1 purified from human dermal fibroblasts. The IgG was obtained by triple precipitation using ammonium sulfate and characterized by immunodiffusion and rocket immunoelectrophoresis.³⁵ In addition, we have shown that the pAb recognize both free and MMP-complexed TIMP-1.³⁶ Furthermore, the specificity of the antibodies was analyzed by Western blotting analysis against recombinant human TIMP-1 expressed in NSO mouse myeloma cells. Here, the antibody preparation recognizes a band of approximately 28 kDa in accordance with the molecular weight of TIMP-1. To certify that the pAb recognize TIMP-1 in colon tumors, the antibodies were immobilized on a sepharose column. Total protein extracted from 3 colon adenocarcinomas was passed through the column 5 times and the bound and subsequently eluted protein analyzed in a Western blot using a TIMP-1 monoclonal antibody (MAC15). A single band of approximately 28 kDa was revealed in accordance with the molecular weight of TIMP-1 (results not shown). In immunohistochemistry, the sheep pAb were detected with biotinylated rabbit-anti-goat IgG, which cross-react with sheep IgG (1:100, code E466, DakoCytomation) followed by horseradish peroxidase in complex with streptavidin (code K377, DakoCytomation). The MABs were detected with the Envision-mouse reagent (EnVision reagent, K4003, DakoCytomation), followed by tyramine amplification, using biotinyl tyramine substrate as specified by the manufacturer (Nen, Boston, MA). Sections were developed with NovaRed substrate as specified by the manufacturer (Vector Laboratories, Burlingame, CA) for 15 min. Finally, sections were counterstained in Mayers haematoxylin, dehydrated in ethanol and mounted.

Combined in situ hybridization and immunohistochemistry

Double labeling by combining *in situ* hybridization and immunohistochemistry on paraffin sections has been described previously.³² In brief, using MAB against α-sm-actin (clone 1A4) diluted 1:1000, against cytokeratin (clone AE1/AE3) diluted 1:1000, or against CD68 (clone PGM1) diluted 1:200, sections were incubated for 2 hours at room temperature and then detected with anti-mouse-IgG/horse radish peroxidase-conjugated polymers (Envision-mouse reagent, DakoCytomation, Glostrup, Denmark). Sections were developed with diaminobenzidine (DAB) for 7–10 min, and immediately dehydrated for *in situ* hybridization, which was performed as described above using the antisense probes of f104. Sections were counterstained with haematoxylin.

Results

Analysis of TIMP-1 probes and antibodies for *in situ* hybridization and immunohistochemistry

Histopathological diagnosis of prospectively collected specimens from 18 colorectal lesions revealed 16 colorectal adenocarcinomas, 1 villous adenoma and 1 malignant lymphoma. ³⁵S-labeled antisense and sense RNA probes were generated by *in vitro* transcription from 2 nonoverlapping DNA sequences of the human TIMP-1 cDNA and tested by *in situ* hybridization on adjacent sections from 5 of the colorectal adenocarcinomas. The 2 antisense probes showed an identical hybridization pattern in all the 5 cases, located in the stromal compartment surrounding the invading cancer cells, while no specific signal was seen with the 2 sense probes (Fig. 1). To test whether the TIMP-1 mRNA was accompanied by TIMP-1 protein expression, immunohistochemistry was performed on 8 of the adenocarcinomas (including the 5 mentioned above) and the malignant lymphoma using sheep anti-human TIMP-1 polyclonal antibodies on sections adjacent to TIMP-1 *in situ* hybridized sections. The TIMP-1 mRNA and immunoreactivity was observed in the same cells in all of the 9 cases tested (Fig. 2A), including the malignant lymphoma. The anti-TIMP-1 polyclonal antibodies did not react with other cell populations in all of 8 adenocarcinomas and the malignant lymphoma apart from some normal and malignant epithelial cells that were weakly stained on the luminal apical surface. Two MABs against TIMP-1 (CalB2 and NM4) required strong signal amplification but showed a staining pattern similar to that of the polyclonal antibody preparation (Fig. 2B), with the only exception that neither of the 2 MABs stained the luminal apical surface of the normal and malignant epithelium. No signal was obtained with nonimmune goat serum or a MAB (of same subclass as CalB2 and NM4) directed against the synthetic hapten trinitrophenyl (TNP).

TIMP-1 mRNA expression patterns in colon cancer

Expression of TIMP-1 mRNA was then analyzed in the remaining 9 colorectal lesions by *in situ* hybridization. TIMP-1 mRNA

expression was in all the cases of colon-adenocarcinoma (including those mentioned above) highly expressed in stromal fibroblast-like cells located at the invasive front (Fig. 3a,d). TIMP-1 mRNA signal was also observed in fibroblast-like cells located in the tumor stroma towards the colonic lumen in 8 of 10 cases where this tissue structure was present (data not shown). No or little TIMP-1 mRNA was detected in the central part of the carcinomas. In 5 of the 16 colorectal adenocarcinomas, we observed TIMP-1 mRNA signal in some fibroblast-like cells located around the muscle layer of some arteries located in the submucosa distant from the cancer area. The normal colonic mucosa, including the lamina propria that was present in all samples tested, was generally negative (Fig. 3b,e). Only a relatively weak TIMP-1 mRNA signal was detected in stromal fibroblast-like cells surrounding one or a very few normal crypts (Fig. 3c,f) in 3 out of 6 cases tested with extended exposure time (10 days vs. usually 5 days). In the villous adenoma, we saw only a few TIMP-1 mRNA positive cells associated with focal inflammation (data not shown). In the malignant lymphoma of the colon, TIMP-1 mRNA expressing fibroblast-like cells were, different from the adenocarcinomas, located in a diffuse pattern throughout the whole tumor. No TIMP-1 mRNA signal was observed in any of the 18 cases in the cancer cells, smooth muscle cells or vascular cells.

Characterization of TIMP-1 mRNA expressing cells

To test whether the TIMP-1 mRNA positive fibroblast-like cells could be (myo)fibroblasts and/or macrophages, sections from 4 colorectal adenocarcinomas and the malignant lymphoma were first immunohistochemically stained with antibodies directed against α -sm-actin [for detection of myofibroblast/smooth muscle cells (SMC)] or CD68 (for detection of macrophages) and subsequently incubated with a TIMP-1 mRNA antisense probe. In normal colon tissue, α -sm-actin is expressed by vascular smooth muscle cells, smooth muscle cells of lamina muscularis mucosae and tunica muscularis as well as pericryptal myofibroblasts.³⁷ In colon tumors, α -sm-actin is expressed by tumor-associated fibroblast-like cells located throughout the tumor stroma, which are defined as myofibroblasts. No TIMP-1 mRNA was detected in any α -sm-actin positive smooth muscle cells, including those of the vessels, the lamina muscularis mucosae and the tunica muscularis. In addition, no TIMP-1 mRNA was detected in the α -sm-actin positive pericryptal myofibroblasts of the lamina propria in any of the 5 lesions. TIMP-1 mRNA signal was in contrast seen in α -sm-actin-positive tumor associated myofibroblasts located at the invasive front of the colon cancers. In 3 of the adenocarcinomas, more than 80% of TIMP-1 mRNA-positive cells located close to the invading cancer cells were α -sm-actin-positive (Fig. 4). TIMP-1 mRNA positive fibroblast-like cells located more distant from the invasive cancer cells, towards the submucosa, expressed little or no α -sm-actin. In 1 adenocarcinoma and in the malignant lymphoma approximately 50% of the TIMP-1 mRNA positive cells expressed α -sm-actin. Thus, the TIMP-1 mRNA expressing cells constitute a subpopulation of tumor-associated myofibroblasts located at the invasive front of the tumor. No TIMP-1 mRNA signal could be identified in any of the CD68-positive cells (Fig. 4).

Expression of TIMP-1 and MMP-2 and 9 in colon cancer

MMP-2 and MMP-9 are 2 type IV collagenases expressed in the invasive cancer tissue of colorectal adenocarcinomas. Thus MMP-2 has been reported to be expressed by fibroblast-like cells in the cancer stroma,^{12,31} and MMP-9 by macrophages at the leading edge of the invasive cancer.³³ To directly compare the expression patterns of MMP-2 and MMP-9 with that of TIMP-1, adjacent sections from 5 colorectal adenocarcinomas were hybridized with probes for TIMP-1, MMP-2 and MMP-9 mRNAs. We found that the expression of TIMP-1 mRNA was localized characteristically at the invasive front of the growing tumor, whereas the expression of MMP-2 mRNA was most intense in the central areas, showing decreased expression towards the invasive front (Fig. 5a). MMP-9 mRNA expressing cells were found at the

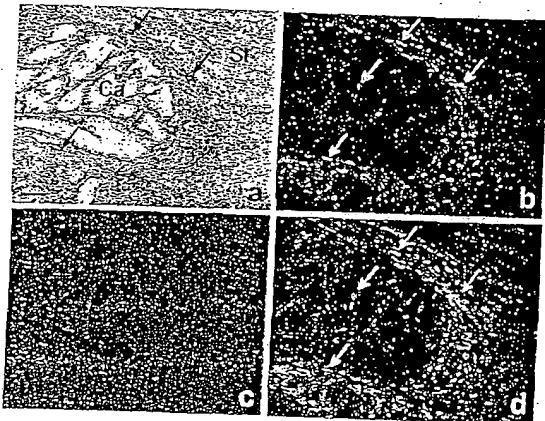


FIGURE 1—*In situ* hybridization with 2 nonoverlapping TIMP-1 specific probes in human colon cancer. Three adjacent sections from a colon adenocarcinoma were incubated with 2 nonoverlapping ³⁵S-labeled antisense probes for TIMP-1 mRNA (f106 (a,b) and f104 (d)) and a corresponding TIMP-1 sense probe, f106 (c). The *in situ* hybridization signal is identified as black silver grains and demonstrated in brightfield (a) and as a white pattern in darkfield illumination (b-d). The 2 antisense probes show the same hybridization pattern and the hybridization signal is seen in the same cells (arrows in a, b and d), whereas no specific signal is seen with the sense probe (c). Note that the TIMP-1 mRNA signal is located in the tumor stroma (indicated by St) surrounding the invasive cancer cells (Ca) that are devoid of TIMP-1 *in situ* hybridization signal. (a)-(d): Bar = 100 μ m.

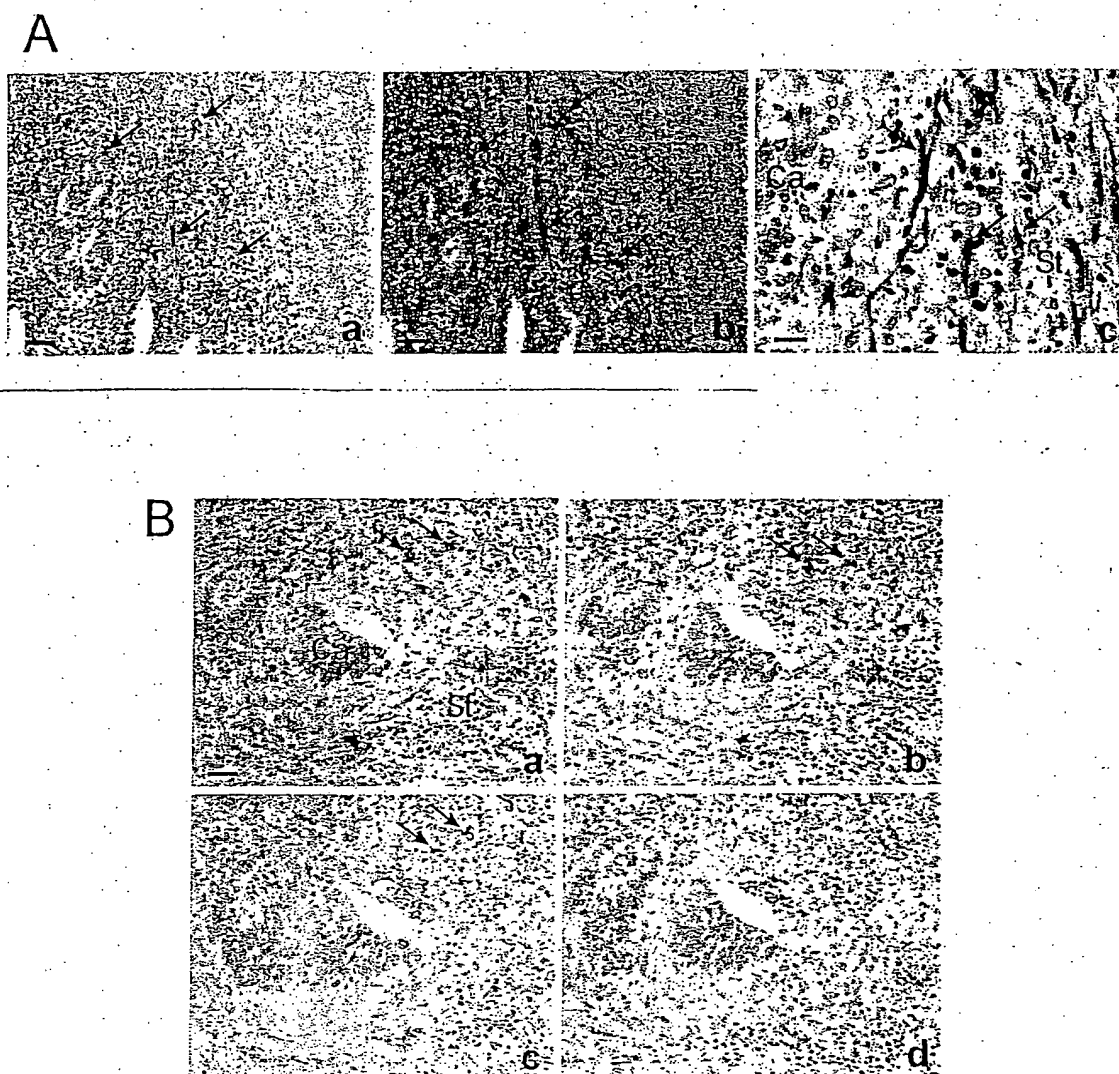


FIGURE 2 - *In situ* hybridization and immunohistochemistry for TIMP-1 in human colon cancer. (A) Two adjacent sections from a human colon adenocarcinoma were incubated with polyclonal antibodies against TIMP-1 (a,c) and a TIMP-1 mRNA antisense probe (b). The TIMP-1 immunoreactivity (red-brown color, arrows in a and c) and the TIMP-1 mRNA (silver grains, arrows in b) are identified in the same cells (arrows in a,b). Immunoperoxidase staining with the TIMP-1 pAb reveals the TIMP-1-positive cells as fibroblast-like cells (arrows in c) located in the stroma (St). No TIMP-1 immunoreactivity is seen in cancer cells (Ca). a,b: bars = 50 μ m; c: bars = 13 μ m. (B) Four consecutive adjacent sections were incubated with CalB2 MAb anti-TIMP-1 (a), NM4 MAb (b), sheep anti TIMP-1 pAb (c) or mouse anti TNP (d). The 3 MABs were detected with Envision reagent followed by TS amplification and the sheep pAb with biotinylated rabbit anti-goat followed by HRP-conjugated streptavidin (see Material and methods). The 3 TIMP-1 antibodies react with the same cells (arrows). No immunoreactivity is seen when the sections are incubated with anti-TNP.

invasive front like those expressing TIMP-1 mRNA but with a distinctly different distribution. Foci with high expression of TIMP-1 mRNA were not accompanied with increased expression of MMP-9 mRNA and vice-versa (Fig. 5b). Thus, TIMP-1 mRNA expression is not coregulated with MMP-2 or MMP-9 mRNA expression.

TIMP-1 in adenomas and Dukes' stage A carcinomas

TIMP-1 antigen can readily be measured in blood and we have previously reported that levels of TIMP-1 in blood are significantly

elevated in colorectal cancer patients compared to healthy donors and that high plasma TIMP-1 levels are associated with short survival of colorectal cancer patients.^{21,56} TIMP-1 has therefore been suggested to be a novel marker for detection of early stage colorectal cancer and for prognostic stratification of colorectal cancer patients.^{21,39} These findings, together with the characteristic expression pattern of TIMP-1 at the invasive front of virtually all the colon cancers and the absence or minute TIMP-1 expression in normal and benign colon mucosa, prompted the evaluation of TIMP-1 expression as a marker for early invasive colon cancer.

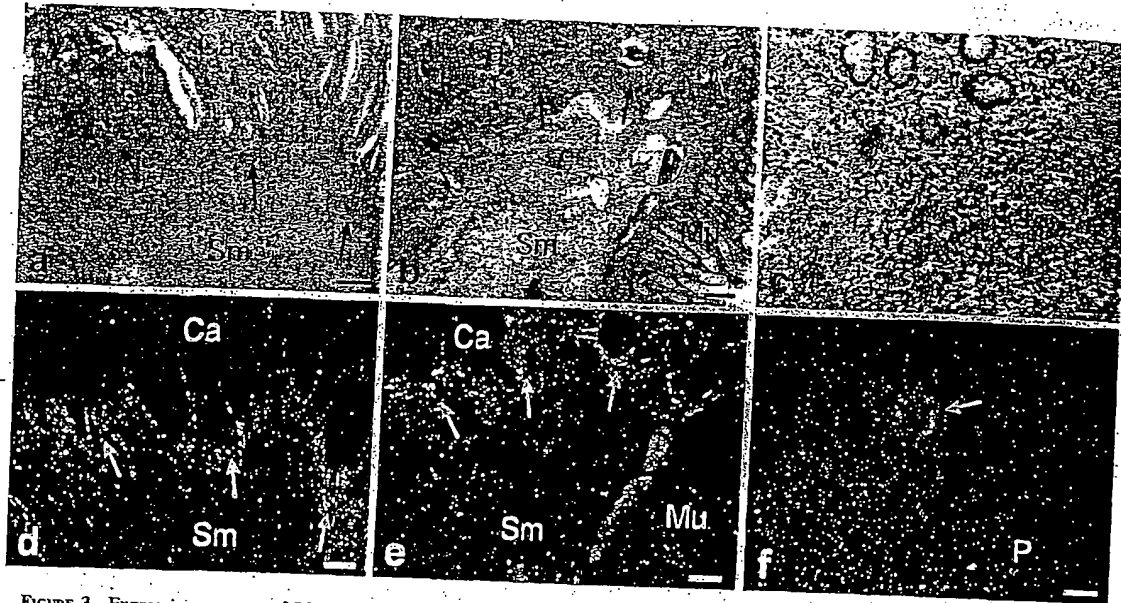


FIGURE 3 - Expression patterns of TIMP-1 mRNA in human colon cancer. Sections were incubated with an antisense probe for TIMP-1 mRNA. The TIMP-1 mRNA signal is demonstrated in brightfield (a-c) and darkfield (d-f). The TIMP-1 mRNA is highly expressed in a subpopulation of stromal fibroblast-like cells at the invasive front of the cancer (a,d), whereas a low hybridization signal is seen within central parts of the cancer area (Ca) and in the submucosa (Sm). The normal mucosa (indicated by Mu in b and e) is negative. A low *in situ* hybridization signal was detected in a few stromal cells surrounding a few normal-looking glands (c,f), see also text. Exposure time: a,b,d,e, 5 days; d,f, 10 days. (a,b,d,f) bars = 200 μ m; (c,f) bars = 25 μ m.

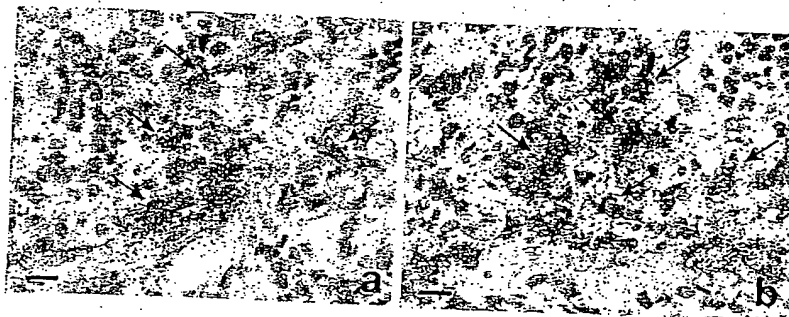


FIGURE 4 - Double labeling for TIMP-1 mRNA and α -sm-actin or CD68 in human colon cancer. Sections were first processed for immunohistochemistry incubating antibodies against α -sm-actin (a) or CD68 (b) and subsequently by *in situ* hybridization using the f104 TIMP-1 specific antisense probe. TIMP-1 mRNA signal is colocalized with α -sm-actin immunoreactivity in fibroblast-like cells that are considered as myofibroblasts (black arrows in a), whereas no CD68 immunoreactivity is seen in the TIMP-1 mRNA positive cells (black arrows in b) in an area with several CD68-positive macrophages (red arrows in b). Note that some of the α -sm-actin-positive myofibroblasts have little or no TIMP-1 mRNA signal (red arrows in a). Bars = 13 μ m.

Therefore, we compared TIMP-1 mRNA expression in an additional 6 colorectal adenomatous polyps with the expression in an additional 8 Dukes' stage A colorectal adenocarcinomas. TIMP-1 mRNA signal was detected in 2 of the 6 adenomas, whereas all 8 Dukes' stage A carcinomas showed TIMP-1 mRNA signal at the invasive front (Fig. 6). In 1 positive adenoma (pedunculated type), TIMP-1 mRNA expression was confined to a single focus in fibroblast-like cells associated with focal stromal inflammation (Fig. 6). However, histological analysis of additional sections from this sample clearly revealed disruption of the dysplastic epithelium in the same area. In the other TIMP-1 mRNA positive adenoma (sessile type), a few TIMP-1 mRNA expressing fibroblasts were located around small arteries not directly associated with the tumor area (data not shown).

Taken together, all of the 9 Dukes' stage A carcinomas analyzed showed TIMP-1 mRNA expression in myofibroblasts located at the invasive front of the tumors, whereas expression was detected in only 3 of 7 adenomas, and in these was seen in fibroblast-like cells associated with focal inflammation at the epithelial-stromal interface in 2 of the cases and with arteries in the submucosa in 1 case.

Discussion

Our study was undertaken to clarify the expression and cellular localization of the MMP inhibitor TIMP-1 in human colon adenocarcinomas. Our studies were founded on the use of 2 specific antisense RNA probes derived from 2 nonoverlapping TIMP-1

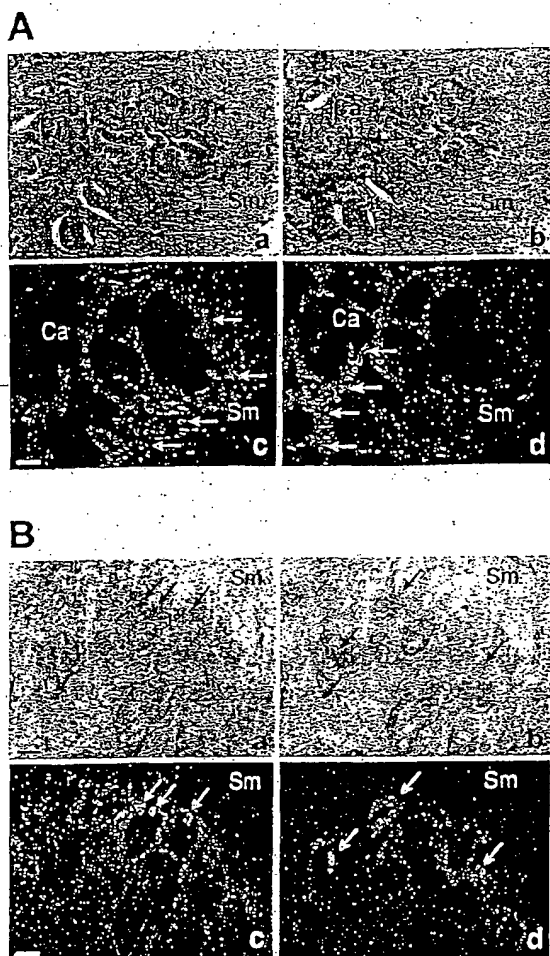


FIGURE 5—*In situ* hybridization for TIMP-1, MMP-2 and MMP-9 in human colon cancer. (A) Adjacent sections were incubated with probes specific for TIMP-1 mRNA (a,c) and MMP-2 mRNA (b,d), respectively, and is shown in brightfield (a,b) and darkfield illumination (c,d). The TIMP-1 mRNA signal increases towards the submucosa (Sm) whereas the MMP-2 mRNA signal decreases and is most intense in the central areas (Ca). (B) Adjacent sections were incubated with probes specific for TIMP-1 mRNA (a,c) and MMP-9 mRNA (b,d), respectively, and is here shown in brightfield (a,b) and darkfield illumination (c,d). Both the TIMP-1 mRNA signal and the MMP-9 mRNA signal are most intense at the invasive front towards the submucosa (Sm), but their expression patterns are quite different, with MMP-9 showing the most restricted expression. Bars = 100 μ m.

cDNA fragments and specific pAb and MABs against human TIMP-1. The TIMP-1 mRNA signal in all colorectal adenocarcinomas investigated was seen in fibroblast-like cells located in the tumor periphery. An identical hybridization pattern was observed with the 2 antisense TIMP-1 probes and application of complementary sense probes on neighboring tissue sections as negative controls did not result in any hybridization signal; therefore, we conclude that the hybridization signal generated with the antisense probes represents the genuine TIMP-1 mRNA. TIMP-1 immunoreactivity was also distinctly located in fibroblast-like stromal cells in the tumor periphery, and these cells were identified to be the same cells as the TIMP-1 mRNA expressing cells. A preparation

of sheep pAb against human TIMP-1³⁵ and 2 well-characterized MABs stained the very same cells in the tumor stroma. Weak staining of the apical surface of some normal and malignant epithelial cells was observed with the pAb in some of the samples. No staining was obtained when the anti-TIMP-1 antibodies were substituted with nonimmune goat serum or anti-TNP MAB incubated at the same concentrations. These immunohistochemical findings strongly suggest that the TIMP-1 antigen detected in the fibroblast-like cells represents the genuine TIMP-1 protein.

In our study, we found TIMP-1 mRNA expression in stromal fibroblast-like cells located in the tumor periphery in all colorectal adenocarcinomas tested, whereas no expression was detected in the cancer cells in any of the cases tested. This finding is in agreement with studies by Zeng and colleagues,^{12,20} but is partly in disagreement with findings by Newell and colleagues.²⁷ In addition to TIMP-1 mRNA signal in fibroblast-like cells in the tumor periphery, Newell and colleagues²⁷ detected a weak TIMP-1 mRNA signal in both benign and malignant epithelial cells.²⁷ This observation was, however, based on the use of probes from a single TIMP-1 cDNA subclone and no additional controls to verify the expression pattern. The difference between our results and those of Newell and colleagues may be explained by methodological differences, since the procedure employed by Newell and colleagues was in several steps different from the one used in the present study, e.g., Newell and colleagues used ³H-labeled probes, whereas we used ³⁵S-labeled probes. It is in this context noteworthy that in order to look for a low expression level of TIMP-1 mRNA, we performed *in situ* hybridization experiments with prolonged exposure time (10 days vs. usually 5 days) with both our TIMP-1 antisense probes and both TIMP-1 sense probes, but with this challenge we did not detect any TIMP-1 mRNA in any epithelial cells. It cannot be excluded though that the TIMP-1 mRNA is expressed in epithelial cells below the detection limit of our *in situ* hybridization procedure.

An interesting observation in our study was the characteristic intense TIMP-1 mRNA and protein expression in the tumor periphery of all colon adenocarcinomas, while little or no expression was seen in the center of the carcinomas. Only in the colorectal lymphoma did we find TIMP-1 mRNA and protein expression in fibroblast-like cells located throughout the tumor tissue. The TIMP-1 expression pattern in the colon adenocarcinomas is in contrast to the expression pattern reported by Hewitt and colleagues,¹⁹ who found that the TIMP-1 staining in most colorectal adenocarcinomas was equally intense in fibroblasts throughout the tumors and that some of the cases even showed decreased TIMP-1 signal intensity towards the tumor periphery. This difference may be explained by possible cross-reactivity of the polyclonal antibodies employed by Hewitt and colleagues or that Hewitt and colleagues employed cryostat sections, while we analyzed paraffin sections.

The TIMP-1 expressing cells had a fibroblast-like morphology and using combined *in situ* hybridization for TIMP-1 mRNA and immunohistochemistry for α -sm-actin, we found that many, generally more than 50%, of the TIMP-1 mRNA positive cells coexpressed α -sm-actin. According to the cellular morphology of the TIMP-1 expressing cells and their localization in the invasive front, we could conclude that the cells were myofibroblasts and not smooth muscle cells.

The myofibroblast is a cell type present in the normal colon mucosa, that originally was described as a pericryptal fibroblast^{37,40} and later was identified with antibodies against α -sm-actin.³⁷ In the lamina propria, the myofibroblasts form a continuous cell layer just below the intestinal epithelium. The pericryptal myofibroblasts are phenotypically different from the neighboring quiescent interstitial fibroblasts that do not express markers of smooth muscle cells.⁴¹ During early steps of colonic tumorigenesis the number of myofibroblasts is significantly increased.⁴¹ The TIMP-1 expressing myofibroblasts may be generated after activation of the pericryptal myofibroblasts and/or the quiescent inter-

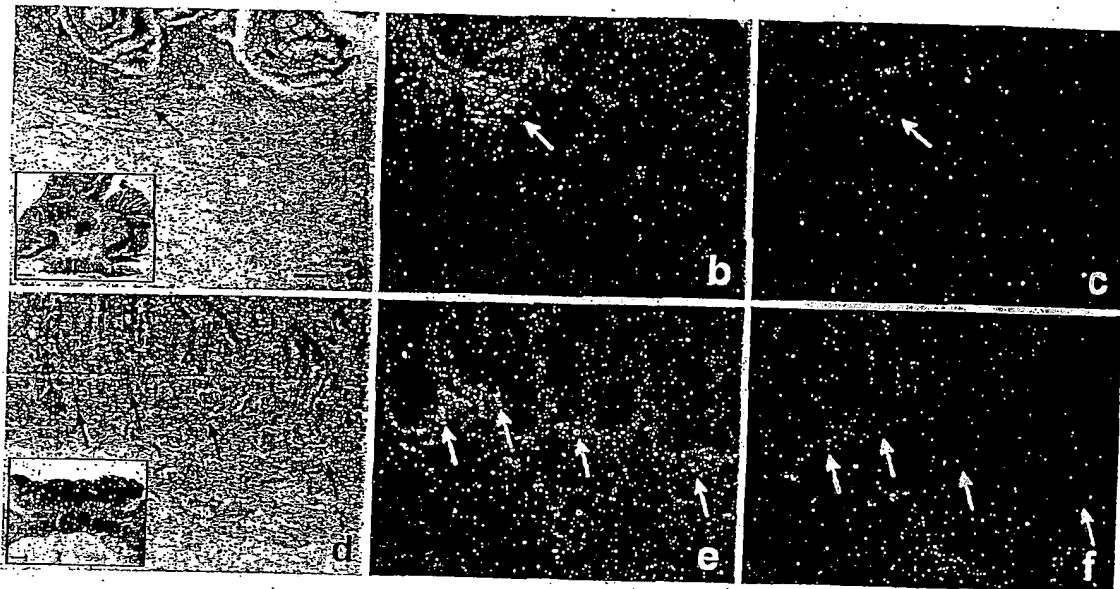


FIGURE 6—*In situ* hybridization for TIMP-1 in colon adenoma and Dukes' stage A adenocarcinoma. Sections from a moderate dysplastic sessile adenoma of the colon (a-c) and a Dukes' A colon carcinoma (d-f) were hybridized with TIMP-1 antisense (a,b and d,e) and sense (c,f) probes, shown in brightfield (a and d) and darkfield illumination (b,c and e,f). Inserts in a and d show virtually the whole tissue section with the arrow indicating the magnified area. TIMP-1 mRNA expression is confined to a single focus in the adenoma (arrows in a,b), whereas the TIMP-1 mRNA is detected along the invasive front in the Dukes' A colon carcinoma (arrows in d,e). (a)-(f): bar = 200 μ m. Bar in inserts = 1,250 μ m.

stitial fibroblasts. Adegboyega and colleagues⁴¹ hypothesized that the tumor-associated myofibroblasts originate from the quiescent interstitial fibroblasts of the lamina propria, rather than from pericryptal myofibroblast or smooth muscle cells, which may help to explain why we found some of the TIMP-1 mRNA expressing fibroblast-like cells α -sm-actin-positive and some α -sm-actin-negative.

Several MMPs including MMP-2, MMP-11 and MMP-14 are expressed by fibroblast-like cells in human colon cancer,^{27,31,42-44} some of which may indeed be myofibroblasts. The role of the (myo-) fibroblasts in colon cancer progression is not known. Since TIMP-1 in human colon cancer appears only to be expressed by fibroblast-like cells most of which are myofibroblasts, and since high TIMP-1 levels measured in blood or tumor extracts from colon cancer patients are strongly associated with a poor prognosis,^{20,21,27,28} it could be argued that the TIMP-1 expressing myofibroblasts play a tumor-promoting role. Immunohistochemical localization studies of proteins involved in the activation and regulation of the efficient serine protease plasminogen, including urokinase plasminogen activator (uPA) and its specific inhibitor PAI-1 show that both are mainly expressed by myofibroblasts in human breast cancer.^{45,46} High levels of uPA and PAI-1 are strongly correlated with poor prognosis in breast cancer,^{47,48} supporting the assumption that the myofibroblast express a promoting role in cancer invasion. We recently reported that the predominant PAI-1 expressing cell in human colorectal cancer also is the myofibroblast,⁴⁹ and earlier studies indicated that elevated levels of PAI-1 in colon cancer patients are associated with poor prognosis.²⁵ Together these findings indicate that myofibroblasts are strongly contributing to the expression of proteins involved in the regulation of extracellular matrix degrading proteases that facilitate cancer invasion and metastasis.

A particularly interesting finding of the present study was the absence of TIMP-1 mRNA in 4 of 7 adenomas, whereas in all of 9 Dukes' stage A carcinomas the TIMP-1 mRNA was expressed in fibroblast-like cells along the invasive front. In the 2 benign lesions, in which the TIMP-1 mRNA was seen in the adenoma area, the

TIMP-1 mRNA positive cells were confined to a single focus with locally increased inflammation related to the dysplastic epithelium. Evident disruption of the dysplastic epithelium was observed in the adenoma with most intense TIMP-1 mRNA signal. Intestinal inflammation may be caused by disruption of the mucous epithelium that leads to focal leakage of mucinous colon material into the lamina propria. Increased intestinal permeability is a common deficiency in Crohn's disease and interestingly TIMP-1 mRNA was found in the intestinal granulation tissue of Crohn's disease⁵⁰ and is expressed by myofibroblasts isolated from Crohn's disease.⁵¹ Induction of TIMP-1 in myofibroblasts in a benign or preinvasive tumor may also be a response to locally increased MMP activity or a response to the presence of a specific MMP in the local microenvironment. MMP-2 and MMP-9 mRNA expression, however, did not appear to be coregulated with TIMP-1 mRNA expression in the colorectal adenocarcinomas. Specific MMPs may indeed be involved in the transition of noninvasive to invasive disease; in studies of preinvasive lesions (ductal carcinoma *in situ*) of the human breast we recently reported that MMP-13 is specifically expressed in myofibroblasts associated with microinvasive events.⁵² Future studies may clarify whether TIMP-1 expression in colorectal adenomas is correlated with expression of specific MMPs, cytokines and/or growth factors, such as TGF- β 1 and TGF- β 251, and whether TIMP-1 can be used as a histopathological marker for malignancy in colorectal tumors.

Acknowledgements

We thank Dr. G. Murphy for the TIMP-1 cDNA, the polyclonal antibodies against TIMP-1, MAC15 and recombinant TIMP-1. We are grateful to P.G. Knudsen and C. Lönborg for their excellent technical assistance, and to L.H. Engelholm for designing the primers. We appreciate the critical comments to the article by Dr. G. Kellermann.

References

- Liotta LA, Steeg PS, Stetler-Stevenson WG. Cancer metastasis and angiogenesis: an imbalance of positive and negative regulation. *Cell* 1991;64:327-36.
- Stetler-Stevenson WG, Yu AE. Proteases in invasion: matrix metalloproteinases. *Semin Cancer Biol* 2001;11:143-52.
- Murphy G, Kokkiliis P, Carne AF. Dissociation of tissue inhibitor of metalloproteinases (TIMP) from enzyme complexes yields fully active inhibitor. *Biochem J* 1989;261:1031-4.
- Welgus HG, Stricklin GP. Human skin fibroblast collagenase inhibitor. Comparative studies in human connective tissues, serum, and amniotic fluid. *J Biol Chem* 1983;258:12259-64.
- Khokha R, Waterhouse P. The role of tissue inhibitor of metalloproteinase-1 in specific aspects of cancer progression and reproduction. *J Neurooncol* 1994;18:123-7.
- Docherty AJ, Lyons A, Smith BJ, Wright EM, Stephens PE, Harris TJ, Murphy G, Reynolds JJ. Sequence of human tissue inhibitor of metalloproteinases and its identity to erythroid-potentiating activity. *Nature* 1985;318:66-9.
- Guedez L, Courtemanche L, Stetler-Stevenson M. Tissue inhibitor of metalloproteinase (TIMP)-1 induces differentiation and an antiapoptotic phenotype in germinal center B cells. *Blood* 1998;92:1342-9.
- Hewitt RE, Brown KE, Corcoran M, Stetler-Stevenson WG. Increased expression of tissue inhibitor of metalloproteinases type 1 (TIMP-1) in a more tumorigenic colon cancer cell line. *J Pathol* 2000;192:455-9.
- Guedez L, Stetler-Stevenson WG, Wolff L, Wang J, Fukushima P, Mansoor A, Stetler-Stevenson M. In vitro suppression of programmed cell death of B cells by tissue inhibitor of metalloproteinases-1. *J Clin Invest* 1998;102:2002-10.
- Li G, Fridman R, Kim HR. Tissue inhibitor of metalloproteinase-1 inhibits apoptosis of human breast epithelial cells. *Cancer Res* 1999;59:6267-75.
- Jiang Y, Goldberg ID, Shi YE. Complex roles of tissue inhibitors of metalloproteinases in cancer. *Oncogene* 2002;21:2245-52.
- Zeng ZS, Guillem JG. Distinct pattern of matrix metalloproteinase 9 and tissue inhibitor of metalloproteinase 1 mRNA expression in human colorectal cancer and liver metastases. *Br J Cancer* 1995;72:575-82.
- Gomez DE, Alonso DF, Yoshiji H, Thorgerirsson UP. Tissue inhibitors of metalloproteinases: structure, regulation and biological functions. *Eur J Cell Biol* 1997;74:111-22.
- Guillem JG, Levy MF, Hsieh LL, Johnson MD, LoGerfo P, Forde KA, Weinstein IB. Increased levels of p16, c-myc, and ornithine decarboxylase RNAs in human colon cancer. *Mol Carcinog* 1990;3:68-74.
- Lu XQ, Levy M, Weinstein IB, Santella RM. Immunological quantitation of levels of tissue inhibitor of metalloproteinase-1 in human colon cancer. *Cancer Res* 1991;51:6231-5.
- Mimori K, Mori M, Shiraiishi T, Fujie T, Baba K, Haraguchi M, Abe R, Ueo H, Akiyoshi T. Clinical significance of tissue inhibitor of metalloproteinase expression in gastric carcinoma. *Br J Cancer* 1997;76:531-6.
- Fong KM. TIMP1 and adverse prognosis in non-small cell lung cancer. *Clinical Cancer Research* 1996;2:1369-72.
- Ree AH, Florenes VA, Berg JP, Mastrandrea GM, Nesland JM, Fodstad O. High levels of messenger RNAs for tissue inhibitors of metalloproteinases (TIMP-1 and TIMP-2) in primary breast carcinomas are associated with development of distant metastases. *Clin Cancer Res* 1997;3:1623-8.
- Hewitt RE, Leach JH, Powe DG, Clark IM, Cawston TE, Turner DR. Distribution of collagenase and tissue inhibitor of metalloproteinases (TIMP) in colorectal tumours. *Int J Cancer* 1991;49:666-72.
- Zeng ZS, Cohen AM, Zhang ZF, Stetler-Stevenson W, Guillem JG. Elevated tissue inhibitor of metalloproteinase 1 RNA in colorectal cancer stroma correlates with lymph node and distant metastases. *Clin Cancer Res* 1995;1:899-906.
- Holten-Andersen MN, Stephens RW, Nielsen HJ, Murphy G, Christensen IJ, Stetler-Stevenson W, Brunner N. High preoperative plasma tissue inhibitor of metalloproteinase-1 levels are associated with short survival of patients with colorectal cancer. *Clin Cancer Res* 2000;6:4292-9.
- Oberg A, Hoyhtya M, Tavelin B, Stenling R, Lindmark G. Limited value of preoperative serum analyses of matrix metalloproteinases (MMP-2, MMP-9) and tissue inhibitors of matrix metalloproteinases (TIMP-1, TIMP-2) in colorectal cancer. *Anticancer Res* 2000;20:1085-91.
- Pellegrini P, Contasta I, Berghella AM, Gargano E, Mammarella C, Adorno D. Simultaneous measurement of soluble carcinoembryonic antigen and the tissue inhibitor of metalloproteinase TIMP1 serum levels for use as markers of pre-invasive to invasive colorectal cancer. *Cancer Immunol Immunother* 2000;49:388-94.
- Grondahl-Hansen J, Christensen U, Rosenquist C, Brunner N, Mouridsen HT, Dano K, Blichert-Toft M. High levels of urokinase-type plasminogen activator and its inhibitor PAI-1 in cytosolic extracts of breast carcinomas are associated with poor prognosis. *Cancer Res* 1993;53:2513-21.
- Nielsen HJ, Pappot H, Christensen U, Brunner N, Thordarsson-Ussing O, Moesgaard F, Dano K, Grondahl-Hansen J. Association between plasma concentrations of plasminogen activator inhibitor-1 and survival in patients with colorectal cancer. *BMJ* 1998;316:829-30.
- Wind T, Hansen M, Jensen JK, Andreasen PA. The molecular basis for anti-proteolytic and non-proteolytic functions of plasminogen activator inhibitor type-1: roles of the reactive centre loop, the shutter region, the flexible joint region and the small serpin fragment. *Biol Chem* 2002;383:21-36.
- Newell KJ, Witty JP, Rodgers WH, Matrisian LM. Expression and localization of matrix-degrading metalloproteinases during colorectal tumorigenesis. *Mol Carcinog* 1994;10:199-206.
- Tomita T, Iwata K. Matrix metalloproteinases and tissue inhibitors of metalloproteinases in colonic adenomas-adenocarcinomas. *Dis Colon Rectum* 1996;39:1255-64.
- O'Shea M, Willenbrock F, Williamson RA, Cockett ML, Freedman RB, Reynolds JJ, Docherty AJ, Murphy G. Site-directed mutations that alter the inhibitory activity of the tissue inhibitor of metalloproteinases-1: importance of the N-terminal region between cysteine 3 and cysteine 13. *Biochemistry* 1992;31:10146-52.
- Engelholm LH, Nielsen BS, Netzel-Arnett S, Solberg H, Chen XD, Lopez Garcia JM, Lopez-Otin C, Young MF, Birkedal-Hansen H, Dano K, Lund LR, Behrendt N, et al. The urokinase-plasminogen activator receptor-associated protein/endostatin is coexpressed with its interaction partners urokinase plasminogen activator receptor and matrix metalloproteinase-13 during osteogenesis. *Lab Invest* 2001;81:1403-14.
- Pyke C, Ralfkiaer E, Huhala P, Hurskainen T, Dano K, Tryggvason K. Localization of messenger RNA for Mr 72,000 and 92,000 type IV collagenases in human skin cancers by *in situ* hybridization. *Cancer Res* 1992;52:1336-41.
- Nielsen BS, Rank F, Lopez JM, Balbin M, Vizoso F, Lund LR, Dano K, Lopez-Otin C. Collagenase-3 expression in breast myofibroblasts as a molecular marker of transition of ductal carcinoma *in situ* lesions to invasive ductal carcinomas. *Cancer Res* 2001;61:7091-100.
- Holten-Andersen MN, Brunner N, Maimonis P, Jensen V, Murphy G, Piironen T. Characterization of monoclonal antibodies to tissue inhibitor of metalloproteinases-1. *Journal of clinical ligand assay* 2002;25:87-90.
- Shulman M, Wilde CD, Kohler G. A better cell line for making hybridomas secreting specific antibodies. *Nature* 1978;276:269-70.
- Hembry RM, Murphy G, Reynolds JJ. Immunolocalization of tissue inhibitor of metalloproteinases (TIMP) in human cells. Characterization and use of a specific antiserum. *J Cell Sci* 1985;73:105-19.
- Holten-Andersen MN, Murphy G, Nielsen HJ, Pedersen AN, Christensen IJ, Hoyer-Hansen G, Brunner N, Stephens RW. Quantitation of TIMP-1 in plasma of healthy blood donors and patients with advanced cancer. *Br J Cancer* 1999;80:495-503.
- Sappino AP, Dietrich PY, Skalli O, Widgren S, Gabbiani G. Colonic pericyclic fibroblasts. Differentiation pattern in embryogenesis and phenotypic modulation in epithelial proliferative lesions. *Virchows Arch A Pathol Anat Histopathol* 1989;415:551-7.
- Nielsen BS, Timshel S, Kjeldsen L, Schested M, Pyke C, Borregaard N, Dano K. 92 kDa type IV collagenase (MMP-9) is expressed in neutrophils and macrophages but not in malignant epithelial cells in human colon cancer. *Int J Cancer* 1996;65:57-62.
- Holten-Andersen MN, Christensen IJ, Nielsen HJ, Stephens RW, Jensen V, Nielsen OH, Sorensen S, Overgaard J, Lilja H, Harris A, Murphy G, Brunner N. Total levels of tissue inhibitor of metalloproteinases 1 in plasma yield high diagnostic sensitivity and specificity in patients with colon cancer. *Clin Cancer Res* 2002;8:156-64.
- Kaye GI, Lane N, Pascal RR. Colonic pericyclic fibroblast sheath: replication, migration, and cytodifferentiation of a mesenchymal cell system in adult tissue. II. Fine structural aspects of normal rabbit and human colon. *Gastroenterology* 1968;54:852-65.
- Adegboyega PA, Mifflin RC, DiMari JF, Saada JJ, Powell DW. Immunohistochemical study of myofibroblasts in normal colonic mucosa, hyperplastic polyps, and adenomatous colorectal polyps. *Arch Pathol Lab Med* 2002;126:829-36.
- Poulsom R, Pignatelli M, Stetler-Stevenson WG, Liotta LA, Wright PA, Jeffery RE, Longcroft JM, Rogers L, Stamp GW. Stromal expression of 72 kDa type IV collagenase (MMP-2) and TIMP-2 mRNAs in colorectal neoplasia. *Am J Pathol* 1992;141:389-96.
- Rouyer N, Wolf C, Chenard MP, Rio MC, Chambon P, Bellocq JP, Basset P. Stromelysin-3 gene expression in human cancer: an overview. *Invasion Metastasis* 1994;14:269-75.

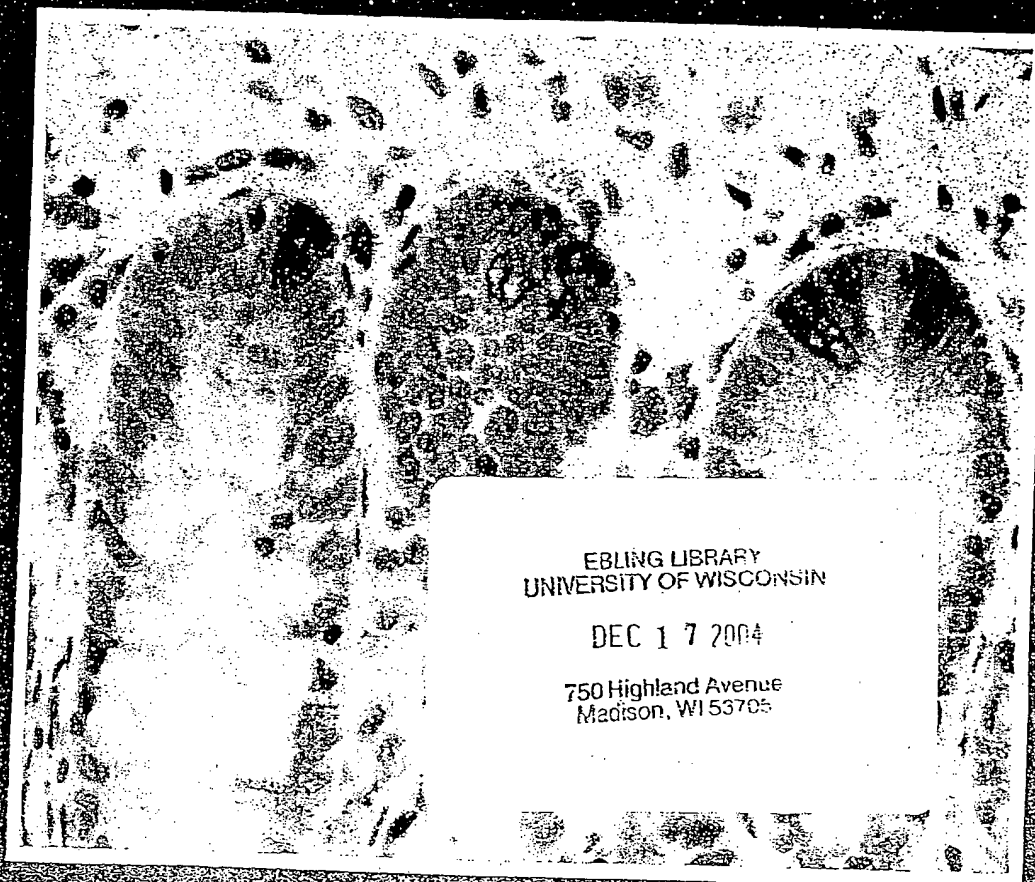
44. Okada A, Bellocq JP, Ronyer N, Chenard MP, Rio MC, Chambon P, Basset P. Membrane-type matrix metalloproteinase (MT-MMP) gene is expressed in stromal cells of human colon, breast, and head and neck carcinomas. *Proc Natl Acad Sci U S A* 1995;92:2730-4.
45. Nielsen BS, Sebested M, Dunn S, Rank F, Timshel S, Rygaard J, Johnsen M, Dano K. Urokinase plasminogen activator is localized in stromal cells in ductal breast cancer. *Lab Invest* 2001;81:1485-501.
46. Offeren BV, Nielsen BS, Hoyer-Hansen G, Rank F, Hamilton-Dutoit S, Overgaard J, Andreassen PA. The myofibroblast is the predominant plasminogen activator inhibitor-1 expressing cell type in human breast carcinomas. *Am J Pathol* 2003;163:1887-99.
47. Duffy MJ, Reilly D, O'Sullivan C, O'Higgins N, Fennelly JJ, Andreassen P. Urokinase-plasminogen activator, a new and independent prognostic marker in breast cancer. *Cancer Res* 1990;50:6827-9.
48. Grondahl HJ, Christensen JJ, Rosenquist C, Brunner N, Mouridsen HT, Dano K, Blichert TM. High levels of urokinase-type plasminogen activator and its inhibitor PAI-1 in cytosolic extracts of breast carcinomas are associated with poor prognosis. *Cancer Res* 1993;53:2513-21.
49. Illemann M, Hansen U, Nielsen HJ, Andreassen PA, Hoyer-Hansen G, Lund LR, Dano K, Nielsen BS. Leading edge myofibroblasts in human colon cancer express PAI-1. *Am J Clin Pathol* 2004;122:256-65.
50. Saarialho-Kere UK, Vaalamo M, Puolakkainen P, Airola K, Parks WC, Karjalainen-Lindberg ML. Enhanced expression of matrilysin, collagenase, and stromelysin-1 in gastrointestinal ulcers. *Am J Pathol* 1996;148:519-526.
51. McKaig BC, McWilliams D, Watson SA, Mahida YR. Expression and regulation of tissue inhibitor of metalloproteinase-1 and matrix metalloproteinases by intestinal myofibroblasts in inflammatory bowel disease. *Am J Pathol* 2003;162:1355-1360.



Q
7IN84115

INTERNATIONAL

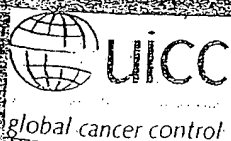
Journal of Cancer



EBLING LIBRARY
UNIVERSITY OF WISCONSIN

DEC 17 2004

750 Highland Avenue
Madison, WI 53705



Publication of the International Union Against Cancer
Published for the UICC by Wiley-Liss, Inc.

Articles published online in Wiley InterScience
25 August 2004 - 8 October 2004

www.internationaljournalofcancer.com

JCN: 0020-7179



International Union Against Cancer

global cancer control

COUNCIL

J. SEFFRIN, President (USA)
L.J. DENIS, Treasurer (Belgium)
J. BAITY, Chair, Finance Committee (USA)

G. BRIEN (Australia)
R.C. BURTON (Australia)
M. DAUBE (Australia)
K.A. DINSHAW (India)
L. ELOVAINIO (Finland)
M.K. GOSPODAROWICZ (Canada)
R.T. HUDSON (Ireland)

T. KITAGAWA (Japan)
A. PUNDLIK KURKURE (India)
R.E. LENHARD (USA)
A. LLOMBART-BOSCH (Italy)

M. LUWIA (Indonesia)
C. MALLINSON (UK)
L.H. MARCHESI (Brazil)
H.F. MICKELSON (USA)
K. NILSSON (Sweden)
S. OMAR (Egypt)
T. PHILIP (France)
E. ROBINSON, Past President (Israel)
Y. SALOOJEE (South Africa)
H. SANCHO-GARNIER (France)

R.J. SCHWEITZER (USA)
O. SOREIDE (Norway)
K. TAJIMA (Japan)
W. WEBER (Switzerland)
S. WILKINSON (UK)
D. ZACKS (USA)
D. ZARIDZE (Russia)
Y. HUI ZHANG (China)
M. ZIV (Israel)
H. ZUR HAUSEN (Germany)

UICC, URL: <http://www.uicc.org>

UICC, E-mail: info@uicc.org

The International Union Against Cancer (UICC) is devoted exclusively to all aspects of the world-wide fight against cancer. Its objectives are to advance scientific and medical knowledge in research, diagnosis, treatment and prevention of cancer, and to promote all other aspects of the campaign against cancer throughout the world. Particular emphasis is placed on professional and public education.

Founded in 1933, the UICC is a non-governmental, independent association of more than 290 member organizations in over 80 countries. Members are voluntary cancer leagues and societies, cancer research and/or treatment centers, and in some countries ministries of health.

The UICC is non-profit, non-political, and non-sectarian. Its headquarters are in Geneva, Switzerland. It creates and carries out programs around the world in collaboration with hundreds of volunteer experts. Supported by membership dues, national subscriptions, grants and donations, its annual budget is about US \$4 million.

The UICC is governed by its members which meet in General Assembly every 4 years. Its elected Council and Executive Committee are responsible for Program structure and implementation.

The UICC organizes an International Cancer Congress every 4 years as well as annual symposia, workshops, and training courses. It publishes the *International Journal of Cancer* (30 issues per year), *UICC News* (quarterly), the *International Calendar of Meetings on Cancer* (bi-annually), and a number of technical reports, textbooks and manuals.

SUBSCRIPTION INFORMATION

© 2005 Wiley-Liss, Inc., a Wiley Company. All rights reserved. No part of this publication may be reproduced in any form or by any means, except as permitted under section 107 or 108 of the 1976 United States Copyright Act, without either the prior written permission of the publisher, or authorization through the Copyright Clearance Center, 222 Rosewood Drive, Danvers, MA 01923, telephone: (978) 750-8400, fax: (978) 750-4470. Requests to the publisher for permission should be addressed to the Permissions Department, c/o John Wiley & Sons, Inc., 111 River St., Hoboken, NJ 07030. Fax: (201) 748-6008; Tel.: (201) 748-6011; <http://www.wiley.com/go/permissions>.

International Journal of Cancer (Print ISSN 0020-7136; Online ISSN 1097-0215) is published 30 times a year, semi-monthly with extra issues in January, March, May, July, September, and November, by Wiley-Liss, Inc., through Wiley Subscription Services, Inc., a Wiley Company. Send subscription inquiries in care of John Wiley & Sons, Inc., Attn: Journals Admin Dept UK, 111 River St., Hoboken, NJ 07030, (201) 748-6645.

Advertising inquiries should be addressed to Advertising Department, c/o John Wiley & Sons, Inc., 111 River St., Hoboken, NJ 07030. Telephone: (201) 748-6921.

Offprint sales and inquiries should be directed to the Customer Service Department, in care of John Wiley & Sons, 111 River St., Hoboken, NJ 07030. Telephone: (201) 748-8776.

Subscription price: Volumes 113-117, 2005 (30 issues). Print only: \$2,905 worldwide. Electronic only: \$2,905 worldwide. A combination price of \$3,195 worldwide includes the subscription in both electronic and print formats. A special personal rate is available to individuals for \$295 worldwide. All subscriptions containing a print element, shipped outside the U.S., will be sent by air. Payment must be made in U.S. dollars drawn on U.S. bank. Periodicals postage paid at Hoboken, NJ and at additional mailing offices. Postmaster: send address changes to INTERNATIONAL JOURNAL OF CANCER, Subscription Distribution, c/o John Wiley & Sons, Inc., 111 River St., Hoboken, NJ 07030. Change of address: Please forward to the subscriptions address listed above 6 weeks prior to move; enclose present mailing label with change of address. Claims for missing issues: Claims for undelivered copies will be accepted only after the following issue has been received. Please enclose a mailing label or cite your subscriber reference number. Missing copies will be supplied when losses have been sustained in transit and where reserve stock permits. Send claims in care of John Wiley & Sons, Inc., Attn: Journals Admin Dept UK, 111 River St., Hoboken, NJ 07030. Indexed by: EMBASE/Excerpta Medica • Current Contents/Life Sciences • Science Citation Index • Scisearch • BIOSIS Data Base • Index Medicus • Cambridge Scientific Abstracts • Chemical Abstracts • Reference Update • Smoking and Health Database.

This journal is printed on acid-free paper.

INTERNATIONAL JOURNAL OF CANCER

2005 Wiley-Liss, Inc.

The *International Journal of Cancer* is published for the International Union Against Cancer by Wiley-Liss, Inc., a division of John Wiley & Sons, Inc. Five volumes are issued annually, each consisting of six numbers.

Abstracting and other journals may reprint the summaries of articles without requesting authorization. Authors alone are responsible for views expressed in signed articles. The mention of specific companies or of certain manufacturers' products does not imply that they are endorsed or recommended by the International Union Against Cancer.

References: When quoting from the *International Journal of Cancer*, please use the official abbreviation:
Int. J. Cancer

Thyroid

VOLUME 7

NUMBER 5

OCTOBER 1997

CLINICAL RESEARCH

Levothyroxine Suppressive Therapy is Partially Effective in Treating Patients with Benign, Solid Thyroid Nodules and Multinodular Goiters.

NICOLAU LIMA, MEYER KNOBEL, HUMBERTO CAVALIERE,
CLAUDIA SZTEJNSZNAJD, EDUARDO TOMIMORI, and
GERALDO MEDEIROS-NETO

691

Is Percutaneous Ethanol Injection a Useful Alternative for the Treatment of the Cold Benign Thyroid Nodule? Five Years' Experience.

NADIA CARACCIO, ORLANDO GOLETTI, PIERO VINCENZO LIPPOLIS,
ARTURO CASOLARO, ENRICO CAVINA, PAOLO MICCOLI, and FABIO MONZANI

699

Value of Combined Technetium-99m Hydroxy Methylene Diphosphonate and Thallium-201 Imaging in Detecting Bone Metastases from Thyroid Carcinoma.

MD. SAYEEDUL ALAM, RYO TAKEUCHI, KANJI KASAGI, TAKASHI MISAKI,
SHINICHI MIYAMOTO, YASUHIRO IIDA, AKINARI HIDAKA, and JUNJI KONISHI

705

Human Thyroid Carcinoma Cell Lines and Normal Thyrocytes: Expression and Regulation of Matrix Metalloproteinase-1 and Tissue Matrix Metalloproteinase Inhibitor-1 Messenger-RNA and Protein.

G. AUST, A. HOFMANN, S. LAUE, A. ROST, T. KÖHLER, and W.A. SCHERBAUM

713

MUC1 Mucin Gene, Transcripts, and Protein in Adenomas and Papillary Carcinomas of the Thyroid.

IVAN BIÈCHE, EMMANUEL RUFFET, ALAIN ZWEIBAUM, FRANÇOISE VILDÉ,
ROSETTE LIDEREAU, and BRIGITTE FRANC

725

Incidence and Clinical Characteristics of Thyroid Carcinoma After Iodine Prophylaxis in an Endemic Goiter Country.

C. BACHER-STIER, G. RICCABONA, M. TÖTSCH, G. KEMMLER, W. OBERAIGNER,
and R. MONCAYO

733

Opposite Changes in Serum Soluble CD8 in Patients at the Active Stages of Graves' and Hashimoto's Diseases.

MIKIO WATANABE, NOBUYUKI AMINO, KAZUNORI HOCHITO,
KIYOSHI WATANABE, KANJI KUMA, and YOSHINORI IWATANI

743

Urinary Iodine Excretion During Normal Pregnancy in Healthy Women Living in the Southwest of France: Correlation with Maternal Thyroid Parameters.

PHILIPPE CARON, MADELEINE HOFF, SAMUEL BAZZI, ALAIN DUFOR,
GÉRARD FAURE, IMAD GHANDOUR, PATRICK LAUZU, YVAN LUCAS,
DOMINIQUE MARAVAL, FRÉDÉRIC MIGNOT, PASCAL RÉSSIGÉAC,
FRANÇOISE VERTONGEN, and VÉRONIQUE GRANGÉ

749

(continued)

Human Thyroid Carcinoma Cell Lines and Normal Thyrocytes: Expression and Regulation of Matrix Metalloproteinase-1 and Tissue Matrix Metalloproteinase Inhibitor-1 Messenger-RNA and Protein

G. AUST,¹ A. HOFMANN,² S. LAUE,² A. ROST,³ T. KÖHLER,³ and W.A. SCHERBAUM⁴

ABSTRACT

Matrix metalloproteinase-1 (MMP-1) and tissue matrix metalloproteinase inhibitor 1 (TIMP-1) play an important role in remodeling the extracellular matrix in normal and pathological processes. The effect of phorbol-myristate acetate (PMA), interleukin-1 (IL-1), and tumor necrosis factor- α (TNF- α) on MMP-1 and TIMP-1 expression was studied on highly purified thyrocytes and undifferentiated 8505 C, C 643, HTb 74, SW 1736 thyroid carcinoma cells compared with thyroid-derived fibroblasts. Messenger RNA (mRNA) levels were monitored by competitive semiquantitative reverse transcriptase polymerase chain reaction (RT-PCR) after 24 hours. Culture supernatants were assayed for free and/or complexed MMP-1 and TIMP-1 after 48 hours using enzyme-linked immunosorbent assay (ELISA) systems (detection limit: <2 ng/mL). MMP-1 and TIMP-1 mRNA were present in all cell types, although thyrocytes showed MMP-1 mRNA levels near the detection limit. 8505 C expressed MMP-1 mRNA levels of up to 10^6 times those of the other cells analyzed. PMA and IL-1 increased MMP-1 mRNA in most cell types. TIMP-1 mRNA increased after treatment with PMA in all cells except 8505 C, whereas only slight effects were shown after IL-1 stimulation. MMP-1 protein was undetectable in normal thyrocyte cultures, but was secreted spontaneously by all cell lines ([ng/mL]: C 643: 15 ± 7 ; HTb 74: 81 ± 1 ; SW 1736: 13 ± 2 ; 8505C: 2097 ± 320). There was a strong correlation between levels of MMP-1 mRNA and protein ($r = 0.99$, $p < .0001$). PMA and IL-1 increased MMP-1 secretion in all cell types after 48 hours. Fibroblasts ([ng/mL] 517 ± 55) and the cell lines (C 643: 142 ± 48 ; HTb 74: 115 ± 13 ; SW 1736: 202 ± 14 ; 8505 C: 120 ± 19) secreted TIMP-1 in unstimulated cultures, whereas only a trace amount was detected in thyrocyte cultures, even after PMA treatment. IL-1 upregulated TIMP-1 secretion after 48 hours in SW 1736, HTb 74, and C 643 cells. Our data suggest that in contrast to normal thyrocytes, dedifferentiated thyroid carcinoma cell lines are potential producers of MMP-1 as well as TIMP-1. High MMP-1 or MMP-1/TIMP-1 expression may play a role in tissue invasion of undifferentiated thyroid cancer cells.

INTRODUCTION

MATRIX METALLOPROTEINASES, (MMPs) constitute a family of structurally related proteolytic enzymes responsible for the proteolytic degradation of extracellular matrix (ECM) components. They are important participants in normal tissue remodeling and contribute to the phenotype of several pathological conditions that are associated with progressive ECM degradation. MMPs are highly regulated at different levels (1). At the transcriptional level, MMP expression can be directly induced or

suppressed on external stimulation, ie, with cytokines, phorbol 12-myristate 13-acetate (PMA), lipopolysaccharide (LPS), or retinoic acid (2,3). After secretion at post-transcriptional level, latent MMP proenzymes are regulated by proteolytic activation and interaction with tissue inhibitors of matrix metalloproteinase (TIMPs), their specific inhibitors. Any imbalance between the proteolytic MMPs activities and the TIMPs that could be influenced and caused by cytokines could potentially lead to pathological conditions (4).

MMP-1, although known as an interstitial collagenase,

¹Institut of Anatomy, ²Department of Internal Medicine III, and ³Institute of Clinical Chemistry and Pathobiochemistry, University of Leipzig, Germany. ⁴Department of Endocrinology, University of Duesseldorf.

is the only enzyme active at neutral pH that can degrade extracellular fibers comprised of collagen types I, II, and III. With this initial step, MMP-1 provides the cleavage products to other collagenase types (5). The major specific inhibitor of MMP-1 is TIMP-1, a 28.5-kd glycoprotein, which forms 1:1 stoichiometric complexes with the protease (6). Cytokines and growth factors have been shown to regulate the expression of both MMP-1 and TIMP-1 (1,7,8).

Although the participation of MMP-1 as the initial collagenase in tissue breakdown during tumor development is well documented (9–11), only one study has described the expression (12) but no study has as yet investigated the regulation of this enzyme in different thyroid tumors. Few studies have been published investigating the role of other MMPs in normal and pathological thyroid tissue by *in situ* hybridization and immunohistochemistry (13–16). Furthermore, tissue remodeling includes both the action of MMPs and their inhibitors; thus, these enzymes could be involved in autoimmune and other nonautoimmune thyroid diseases during morphological changes (17,18). It is still unknown whether or not thyrocytes are able to express MMPs and TIMPs. Although type IV collagenases (MMP-2 and MMP-9) were detected in various human epithelial cells of different tissue origin (19,20), only one study described the secretion of MMP-1 by epithelial cells (21).

Highly purified normal thyrocytes and four thyroid carcinoma cell lines were included in this study to investigate the involvement of these cells in MMP-1 and TIMP-1 production during thyroid tissue remodeling processes and in malignant thyroid neoplasms. MMP-1 and TIMP-1 expression were studied at both the mRNA and protein level by semiquantitative RT-PCR and ELISA measurement, respectively.

In unstimulated carcinoma cell lines both MMP-1 and TIMP-1 mRNA were expressed, partly at a high level, followed by the spontaneous secretion of the proteins. The various conditions for the stimulation of the different cell lines by cytokines and PMA were defined. In contrast to the cell lines, normal thyrocytes did not secrete MMP-1 and only trace amount of TIMP-1, even after stimulation with PMA.

MATERIALS AND METHODS

Preparation of tissues, thyroid-derived cells, and cell lines

Thyrocytes were prepared from surgical thyroid specimens from 3 patients (1 Graves' disease, 2 nontoxic goiter; mean age 54.3 ± 5.0 years). Fibroblasts were separated from thyroid tissue of 5 other patients (3 Graves' disease, 2 nontoxic goiter; mean age 43.6 ± 6.4 years). Graves' disease and nontoxic goiter were diagnosed on the strength of clinical, biochemical, and immunologic features as well as thyroid scintiscans.

Thyroid tissue was trimmed of fat and connective tissue immediately after surgery. Thyroid-derived cells were enriched after gradual enzymatic digestion of tissue and cultured over a period of 16 hours as described. Thyrocytes were obtained from the adherent fraction by incubating

the cell monolayer with phosphate buffered saline (PBS) without $\text{Ca}^{2+}/\text{Mg}^{2+}$ for 45 minutes (22). Residual fibroblasts were removed after subsequent incubation of the cells with the fibroblast-specific mab FibAS01 (22) and goat-anti-mouse IgG-DYNABEADS® M450 (DYNAL, Hamburg, Germany) according to the manufacturer's protocol.

Thyroid-derived fibroblasts were obtained after culturing small pieces of thyroid tissue in Dulbecco's Modified Eagle's Medium (DMEM) with 10% fetal calf serum (FCS) and harvested in the 5th to 7th passage. The purity of the thyrocytes and fibroblasts was determined by using indirect immunofluorescence technique on a FACS-Scan (Becton Dickinson GmbH, Heidelberg, Germany) as described (22).

The following human anaplastic thyroid carcinoma cell lines were cultured in DMEM with 10% FCS: C 643 (23); SW 1736 (23); and HTh 74 (24). The cell line 8505 C (25) was purchased from the German Collection of Microorganisms and Animal Cell Cultures (DSM ACC219). This cell line was established from a primary thyroid tumor characterized histologically as a undifferentiated carcinoma that was partially composed of poorly differentiated papillary cells (25). This is a feature of a subgroup of anaplastic carcinoma (26). The majority of these coexistent better differentiated carcinoma foci in anaplastic carcinoma were papillary (26).

In vitro cultures

Using 24-well plates, 1×10^5 cells were cultured for 24 hours. The medium was aspirated and replaced with 500 μL OPTI-MEM (GIBCO BRL, Grand Island, NY) without FCS to eliminate possible stimulation of MMP-1 and TIMP-1 production by FCS. The medium contained the desired concentration of human IL-1 α (10 U/mL; Pepro Tech EC Ltd., London, UK), TNF- α (100 U/mL; Pepro Tech EC Ltd.), interferon- γ (IFN- γ) (500 U/mL; Pepro Tech EC Ltd.), or 10 ng/mL PMA (SIGMA).

Triplicate cultures of each stimulator were analyzed after 3, 6, and 24 hours at the mRNA and after 24 and 48 hours at the protein level. The supernatants were removed and stored at -80°C for further use. First, a collagenolytic assay based on the digestion of type I collagen was performed. This method showed direct evidence of free pro-MMP-1 enzyme in the cell culture supernatants of unstimulated and IL-1 α stimulated 8505 C, HTh 74, and C634 cells (data not shown). However, the method does not allow quantitation of MMP-1 enzyme activity. Thus, the cell culture supernatants were assayed for MMP-1, TIMP-1, and MMP1/TIMP-1 complex by ELISA (Amersham Life Sciences, Braunschweig, Germany). The MMP-1 assay (sensitivity: 1.7 ng/mL) detected only total human MMP-1, ie, free MMP-1 and MMP-1 complexed with inhibitors such as TIMP-1. It did not detect MMP-1 bound by the nonspecific protease inhibitor α_2 -macroglobulin. The MMP-1/TIMP-1 assay (sensitivity: 1.5 ng/mL) detected MMP-1/TIMP-1 complex, ie, activated MMP-1 that has been subsequently complexed with the specific MMP-1 inhibitor TIMP-1. It did not detect free active MMP-1, free TIMP-1, or pro-MMP-1. There was no cross-reactivity with active MMP-1 bound by the nonspecific protease inhibitor α_2 -macroglobulin. The TIMP-1 assay (sensitivity:

1.25 ng/mL) detected total human TIMP-1, ie, free TIMP-1 and that complexed with MMPs. The assay did not fully cross-react with TIMP-1 in complexes with other MMP. It did not cross-react with TIMP-2.

RNA extraction and cDNA synthesis

For gene expression studies, 5 mL RNazol™ B (Biotex Laboratories Inc., Houston, TX) was added to the cell culture wells. The content of three wells of any cell type was pooled and then stored frozen for further mRNA analysis in liquid nitrogen. Total cellular RNA (cDNA) was isolated from the probes according to the manufacturer's protocol. RNA was fractionated on a denaturing 1.0% agarose gel and stained with ethidium bromide to confirm that spectrophotometric measurements were accurate and that the RNA had not been degraded. Five micrograms total RNA was reverse-transcribed to cDNA using the First-strand cDNA synthesis kit of Pharmacia (Uppsala, Sweden) in a total reaction volume of 15 μ L.

mRNA analysis by competitive RT-PCR

To correct for variations across different cDNA preparations, all samples were first adjusted to contain equal input glyceraldehyde-3-phosphate dehydrogenase (GAPDH) cDNA concentrations. Semi-quantitative GAPDH RT-PCR was used with a heterologous synthetic competitor fragment. The generation of the specific PCR products from the competitor and the cDNA with the GAPDH primers were published earlier (22,27).

We then estimated the MMP-1 and TIMP-1 cDNA in these adjusted samples. The primers were selected using the DNAsis computer program (Hitachi Software Engineering Co, Yokohama, Japan). The primer pairs span one or more introns to allow unambiguous discrimination between cDNA and unwanted contaminating genomic DNA. In quantitating MMP-1 and TIMP-1 cDNA, a rapid one-step method was introduced to synthesize an internal homologous competitor (plan diagram of procedure: Fig. 1, exemplary for MMP-1 [28]). A hybrid primer was synthesized (MMP-1hy) that consisted of two segments (seg₁, seg₂). It

had a length of 40 nucleotides, in which 20 nucleotides (seg₁) at the 3' end corresponded to the opposite strand of the target sequence a predetermined distance from primer MMP-1f, and 20 nucleotides at the 5' end (seg₂ = MMP-1r) that corresponded to the target sequence upstream from the segment seg₁. Amplification with the primers MMP-1f and MMP-1hy from the cDNA resulted in a 478-base pair (bp) (polymerase chain reaction (PCR) product. It was freed from excess primers and deoxynucleoside-triphosphates (dNTPs) using the Qiaquick Gel Extraction Kit (Qiagen GmbH, Hilden, Germany) and quantified. A known number of copies of the competitor was introduced in the GAPDH-adjusted samples and amplified with the primers MMP-1f and MMP-1r. With this approach, two products were generated, one derived from the cDNA (560 bp) and another, 82 bp smaller in size derived from the internal competitor (Fig. 1). PCR products were resolved by gel electrophoresis (1.5% agarose gel). The relative amounts of sample cDNA and competitor were quantified by measuring the intensity of ethidium fluorescence with a CCD image sensor and analyzing the data with the EASY program (Herolab, Wiesloch, Germany). The initial amounts of sample cDNA and competitor were assumed to be equal in those reactions where the ratio of the two products was judged to be equal. This was expressed in arbitrary units (AU) (22,29). One AU was defined as the lowest concentration of competitor yielding a detectable amplification product when added to PCR alone. For example, if equivalence between sample cDNA and competitor was reached using a 100-fold concentrated competitor the relative sample cDNA concentration was 100 AU. Thyrocytes and the cell lines were analyzed for the expression of thyroid-specific and cytokine receptor mRNAs in a simple RT-PCR. The sequences of the TPO and cytokine receptor primer pairs have been published by Watson et al. (30) and Tada et al. (31) and gave the following product sizes: TPO: 506 bp; IL-1R type I (p80): 300 bp; IL-1R type II (p68): 392 bp; TNF- α R (p75): 324 bp; TNF- α R (p55): 587 bp and IFN- γ R: 899 bp. The thyroglobulin (Tg) and thyroid stimulating hormone receptor (TSH-R) primer pairs were selected according to the published sequences using the DNAsis program (Table 1).

Each 25- μ L amplification reaction contained 2.5 μ L 10 \times concentrated PCR buffer (15 mM MgCl₂, Boehringer Mannheim, Germany), 0.3 U Taq DNA polymerase (Boehringer Mannheim, Germany), 100 μ M dNTPs (Perkin Elmer, Weiterstadt, Germany), 0.1 μ M of each primer (IMB, Jena, Germany), and 1 μ L cDNA and competitor in adjusted dilution. Furthermore, restriction mapping (restriction enzymes: Boehringer Mannheim GmbH, Germany) was carried out to confirm the originality of the PCR product (Fig. 1, Table 1).

Statistics

Protein levels of thyrocyte or fibroblast cultures from the different patients and of the thyroid carcinoma cell lines obtained from three separate experiments were presented as mean \pm SEM values. Statistical comparisons between unstimulated and stimulated cell cultures were performed by the alternate (Welch) t-test. The correlation between basal mRNA levels and the unstimulated protein secretion in all cell types was calculated according to the Spearman method.

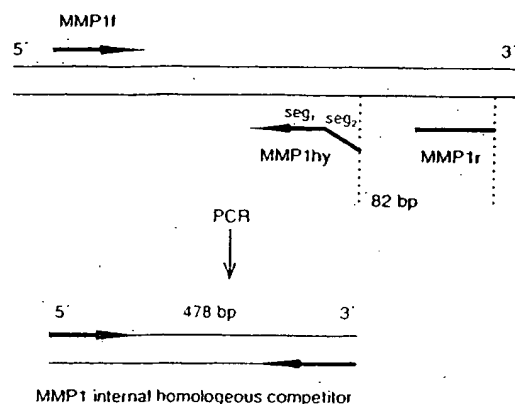


FIG. 1. General scheme for generating homologous competitors used for quantitative PCR.

TABLE 1. PRIMERS, LENGTH OF AMPLIFIED TEMPLATES, RESTRICTION MAPPING AND ASSAY CONDITIONS FOR RT-PCR

		Primer	Length of -3' cDNA (bp)	Length of competitor (bp)	Annealing temperature	Number of cycles
Tg	forward	GCAGATCTTACTGAGTGGCT	416		60	35
	reverse	TGTCAGCACAGTGGCAATAC				
TSH-R	forward	ACTTGCTGCAGCTGGTGCT	354		65	35
exons 1-4	reverse	TGAGGGCATCAGGGTCTATG				
TSH-R	forward	GAAATTCGGAATACCAGGAACCTTA ACT	896		53	35
exons 4-10	reverse	AACTCATCGGACITGGGGGTACA				
MMP-1	forward	TGGGAGCAAACACATCTGAC	560	478	64	33
	reverse	ATCACTTCTCCCGAATCGT				
	hybrid	ATCACTTCTCCCGAATCGT CCATATATGGCTTGGATGCC				
TIMP-1	forward	CTTAGGGGATGCCGTGACA	351	274	64	30
	reverse	GGCAGGCAGGCAAGGTGACG				
	hybrid	GGCAGGCAGGCAAGGTGACG GGATGGATAAACAGGGAAAC				

Tg indicates thyroglobulin; TSH-R, thyroid stimulating hormone receptor; MMP-1, matrix metalloproteinase-1; TIMP-1, tissue inhibitor of metalloproteinase-1; bp, base pair.

RESULTS

Thyroid specific and cytokine receptor mRNA expression

Isolated thyrocytes as well as 8505 C cells expressed Tg and thyroperoxidase (TPO) mRNA, whereas transcripts of the TSH-R (exons 1-4, 354 bp, exons 4-10, 896 bp) were present only in the thyrocytes. The three anaplastic thyroid carcinoma cell lines SW 1736, C 634, and HTh 74 were completely negative for the Tg, TPO, and TSH-R mRNAs (Fig. 2). All cell lines and thyrocytes expressed IL-1R (type I and type II), TNF- α R (p75 and p55) and IFN- γ R mRNA (Fig. 2).

Basal MMP-1 and TIMP-1 mRNA and protein expression

In most stimulation experiments, mRNA levels did not increase until 24 hours of incubation. The 24-hour mRNA levels are shown in Figures 3 and 4. The 3- and 6-hour levels are demonstrated in those experiments where the mRNA levels reached their peak before 24 hours of stimulation. If not otherwise indicated, the MMP-1 levels were measured using the ELISA system, which recognizes free/complexed MMP-1.

MMP-1 and TIMP-1 mRNA were found during unstimulated culture in all investigated cell types, although the mRNA levels varied over a great range. 8505 C showed a basal MMP-1 mRNA level 20 times as high as those of the HTh 74 cells, 6×10^4 times as high as C 643, and 2×10^6 times as high as SW 1736 cells. In thyrocytes, MMP-1 mRNA levels were found near the detection limit (Figs. 3 and 4).

Generally, when analyzing the noted cell types, the measured basal MMP-1 or TIMP-1 mRNA levels correlated well with the basal protein expression (MMP-1: $r = 0.99$, $p < .0001$; TIMP-1: $r = 0.98$, $p < .002$). Corresponding to the high MMP-1 mRNA level, 8505 C cells secreted extremely high levels of MMP-1. No MMP-1 or TIMP-1 was

detected in unstimulated thyrocyte cultures at any time-point examined. All other cell types showed a spontaneous MMP-1 and TIMP-1 secretion (Figs. 5 and 6). Thyroid-derived fibroblasts produced basal TIMP-1 levels of up to 4 times higher in the four carcinoma cell lines, which secreted nearly the same amounts of basal TIMP-1 protein. Nevertheless, TIMP-1 secretion of fibroblasts was found at lower levels than expected after TIMP-1 mRNA measurement in 4 of 5 analyzed patients. The results of the fibroblast cultures from patient five showing a higher TIMP-1 expression than those from the 4 other patients (basal 24 hour: 50 ± 2 ; PMA 24 hour: 90 ± 6 ng/mL TIMP-1) was omitted in Figure 6.

Comparing the basal amount of free/complexed and TIMP-1 complexed MMP-1 after 24 hours of stimulation, a significant level of MMP-1 was not complexed with TIMP-1 in 8505 C cultures, whereas in fibroblast cultures most of the MMP-1 activity was inhibited by TIMP-1. The anaplastic carcinoma cell line HTh 74 did not show such a great discrepancy between free/complexed and TIMP-1 complexed MMP-1 level as 8505 C cells (Fig. 7).

Effects of IL-1 α on MMP-1 and TIMP-1 mRNA and protein expression

Experiments were performed to determine whether human thyroid epithelial cells and thyroid carcinoma cell lines could produce or increase basal MMP-1 and TIMP-1 secretion after exposure to various stimuli. The results from these stimulation experiments are summarized in Figures 3 through 5. Generally, there was a delay in protein secretion level in comparison to the mRNA expression level. At the protein level, the cytokine-mediated stimulating or inhibiting effect is more distinct after 48 hours compared with 24 hours, even when the mRNA level had already decreased after 6 hours.

IL-1 upregulated MMP-1 mRNA in SW 1736-cells up to 100 times and, in thyroid-derived fibroblasts, up to 12 times after 24 hours of incubation (Fig. 3). This increased mRNA level was accompanied by a significantly enhanced

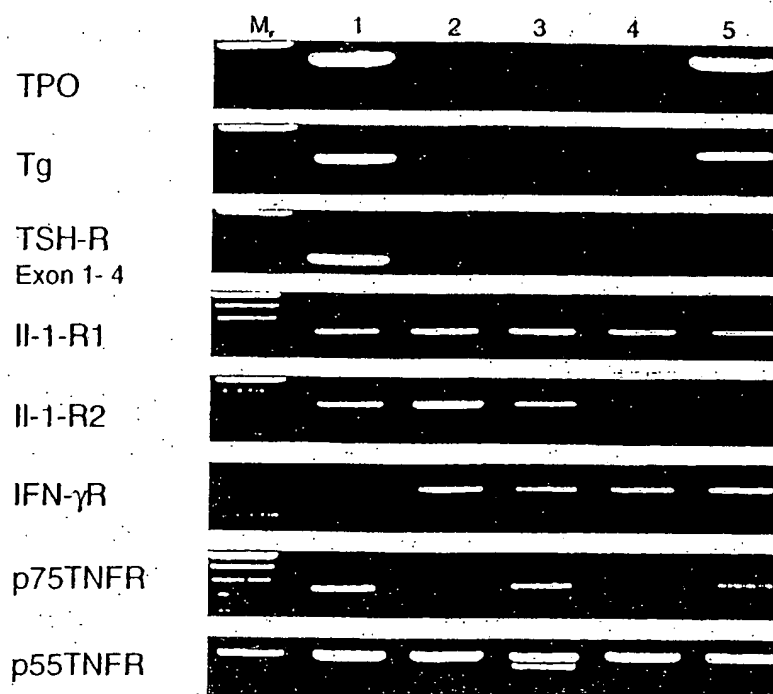


FIG. 2. Amplification of thyroid specific and interleukin-receptor mRNA in thyrocytes (1), SW 1736 (2), C 643 (3), HTh 74 (4) and 8505 C (5) cells using RT-PCR; M, = 100-bp ladder (GIBCO).

MMP-1 secretion after 48 hours. Furthermore, IL-1 α increased MMP-1 mRNA expression in thyrocytes up to seven times after 6 hours, but no MMP-1 protein could be detected in thyrocyte cultures. IL-1 had no stimulatory effect on MMP-1 mRNA expression in C 643, HTh 74, and 8505 C cells after 24 hours, although a significant increase of MMP-1 secretion was found in HTh-74 and SW 1736 cells after 48 hours of incubation (Fig. 5). This discrepancy may be explained by a possible increase in MMP-1 mRNA level after 24 hours of stimulation. The same effect could also be observed in the IL-1 stimulated TIMP-1 at the mRNA as well as the protein level: the only slight effect of IL-1 on TIMP-1 mRNA expression in carcinoma cell lines after 24 hours was accompanied by a significant increase of TIMP-1 secretion in 8505 C and HTh 74 cells after 48 hours (Figs. 4 and 6).

Effects of TNF- α on both MMP-1/TIMP-1 mRNA and protein expression

In contrast to IL-1, TNF- α did not stimulate the MMP-1 and TIMP-1 mRNA and protein levels in all carcinoma cell lines and thyrocytes. Only thyroid-derived fibroblasts responded with a slight upregulation of MMP-1 and TIMP-1 mRNA expression after TNF- α stimulation, which was not accompanied by an increase of MMP-1 and TIMP-1 secretion.

Effects of PMA, and IFN- γ on MMP-1 and TIMP-1 mRNA and protein expression

PMA was included in our study as a positive control because it is known to upregulate or induce both MMP-1 and TIMP-1 secretion in various cell types (1,32). Indeed, PMA was able to induce or enhance MMP-1 mRNA levels in all cell types investigated, although the detected levels varied to a large extent (Fig. 3). This result is in good correlation with the significantly increased MMP-1 protein levels that were already detectable after 24 hours of stimulation (Fig. 5). PMA upregulated TIMP-1 mRNA levels by up to 20 times in C 643, and up to 2 times in SW 1736 and HTh 74 cells, fibroblasts and thyrocytes, but it did not change the TIMP-1 mRNA content in 8505 cells (Fig. 4). At the protein level, we found a significant stimulation of TIMP-1 secretion in C 643 and HTh 74 cells, as well as in thyroid-derived fibroblasts (Fig. 6).

In contrast to PMA, IFN- γ was without effect on stimulation or downregulation of MMP-1 and TIMP-1 mRNA or protein in any of the cell types investigated (Figs 5 and 6).

The main inhibitor of MMP-1 is TIMP-1, which forms 1:1 stoichiometric complexes with MMP-1, although some other inhibitors can also bind MMP-1. On the other hand, TIMP-1 can bind other MMP types.

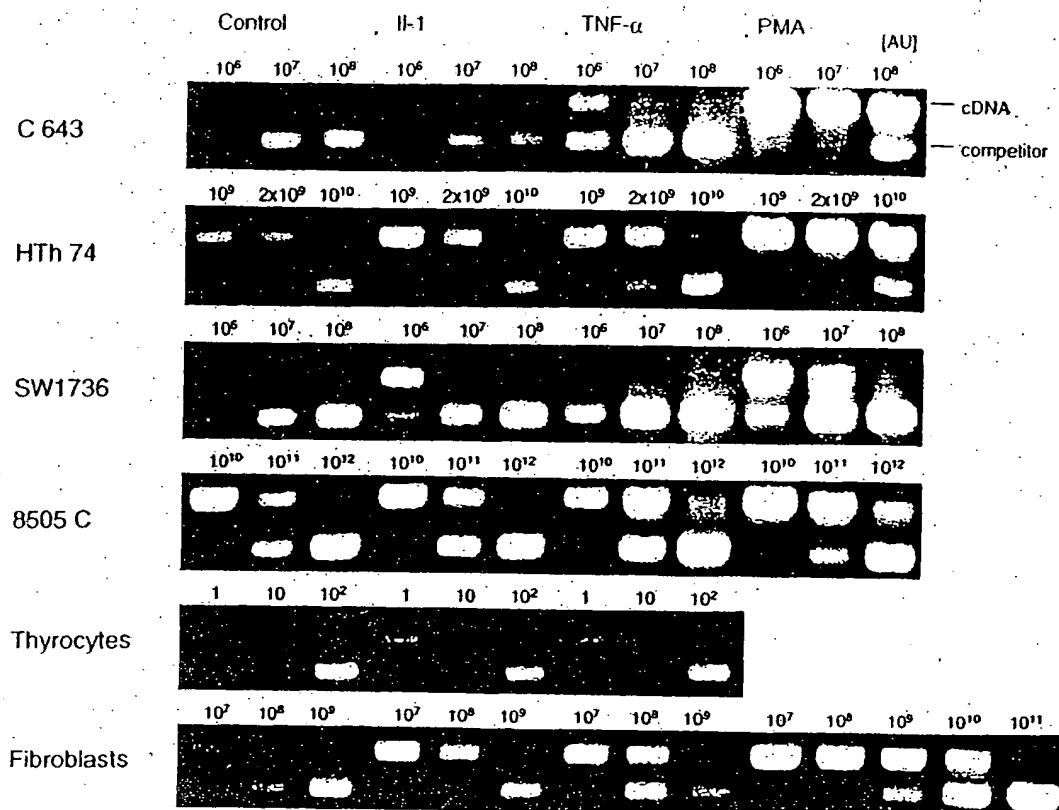


FIG. 3. Representative samples of competitive amplified MMP-1 mRNA of thyrocytes, thyroid-derived fibroblasts and thyroid carcinoma cell lines without stimulation (control) and after stimulation with 10 U/mL IL-1 α and 100 U/mL TNF- α and 10 ng/mL PMA after 24 hours. Serial dilutions of known amounts of the competitor fragment were coamplified with identical aliquots of cDNA. The 560-bp (cDNA) and 478-bp (competitor) PCR products were visualized by agarose gel electrophoresis and ethidiumbromide staining. The relative concentration of the added competitor was given in arbitrary units (AU) in the figure. One AU was defined as the lowest concentration of the competitor yielding a detectable amplification for MMP-1 mRNA. The ratio of competitor to cDNA fragments was determined by measuring the intensity of ethidium fluorescence with a CCD image sensor and analysis of data. Measured cDNA concentration can be expressed in AU.

DISCUSSION

Our findings demonstrate for the first time that thyroid carcinoma cell lines are able to express MMP-1 and TIMP-1 mRNA and protein at significant levels *in vitro*. The observation of spontaneous release of MMP-1 and TIMP-1 corresponds well with earlier studies covering the secretion of these proteins by several carcinoma cell lines (33,34).

However, in contrast to its clear physiological function in extracellular matrix breakdown, the role of MMP-1 in tumor growth and metastases is still controversial (9–11,35). Recently, Murray et al. (10) demonstrated that MMP-1 is associated with poor prognosis in colorectal cancer, and has a prognostic value independent of the Duke's stage. Therefore, MMP-1 could be a target for therapeutic intervention in such tumors. Furthermore, the hypothesis of whether or not cancer cells themselves are able to

produce MMP, or whether cancer cells stimulate the surrounding stromal cells to secrete MMP *in vivo*, is disputed. MMP-1 mRNA and protein were detected by both *in situ* hybridization and immunohistochemistry in stromal as well as tumor cells of head, neck, gastric, colorectal, and mammary carcinomas (9,10,36,37). In contrast, Kameyama (12) demonstrated by *in situ* hybridization that the MMP-1 mRNA was not expressed in the cancer cells but in the surrounding fibrous capsules of strongly differentiated papillary thyroid carcinoma tissue. Highly differentiated follicular carcinomas and follicular adenomas were depleted for MMP-1 transcripts. Undifferentiated follicular, papillary, and aggressive anaplastic carcinomas that showed poor prognosis and strong tumor invasive and metastatic potential and that can be compared in their morphological, genetic and growth features with undifferentiated thyroid carcinoma cell lines were not included this

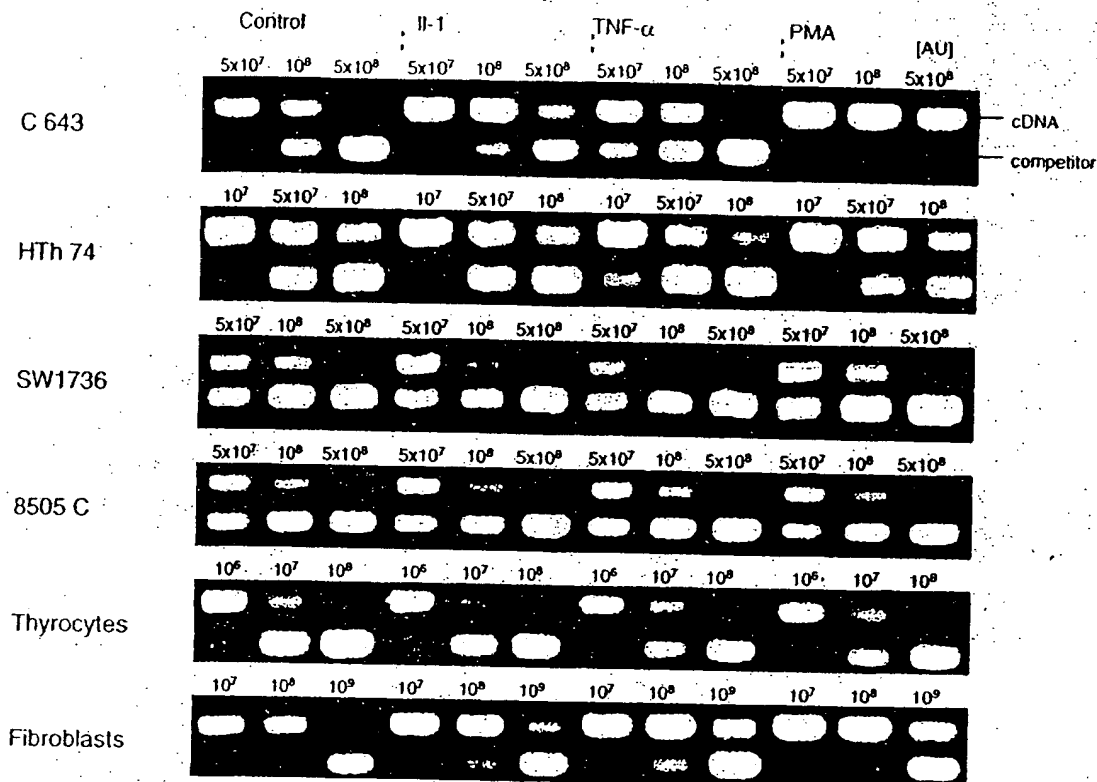


FIG. 4. Competitive TIMP-1 mRNA RT-PCR yielding a 351-bp (cDNA) and a 274-bp (competitor) PCR product. For further details see Figure 3.

study. However, the missing expression of MMP-1 by normal thyrocytes and the spontaneous secretion of this protein by highly malignant thyroid carcinoma cell lines, as demonstrated in our study, indicate the involvement of MMP-1 secretion of transformed thyrocytes in aggressive thyroid tumors.

Although all cell lines analyzed in our study spontaneously secreted MMP-1, we observed marked differences in the basal secretion capacity. The highest MMP-1 levels were determined in cultures of 8505 C cells. Only 8505 C cells expressed TPO and Tg mRNA that may be put down to residual differentiated components in the cell line (see *Materials*). However, none of the analyzed cell lines expressed TSH-R mRNA. The cell population doubling times were less than 40 hours. All cell lines had accumulations of multiple genetic events. These facts indicate the undifferentiated pathology of the studied lines. It is well known that anaplastic carcinoma cell lines well retain the malignant characteristics of their parental tumors (38–40).

Furthermore, we found a distorted proportion between MMP-1 and TIMP-1 mRNA/protein for carcinoma cell lines but not for normal thyroid-derived fibroblasts. The most disadvantageous constellation between MMP-1 and TIMP-1 was found in 8505 C cells. Similar to other studies (41), these results suggest the influence of an altered MMP/TIMP relation on tumor progression. However, it

should be mentioned that most studies, including the present one, do not take into consideration that a number of inhibitors distinct from TIMP-1 may regulate MMP-1 activity. Taking into account that the balance of active enzyme and TIMP-1 concentration strongly influence the extent of local matrix degradation, a number of studies showed unexpectedly high levels of TIMP-1 in malignant neoplasms (9,42,43). There is a great discussion as to whether the overall expression of MMP-1 and TIMP-1 or the amount of noncomplexed MMP-1 could be critical in aggressive tumor development. This fact underlines the nature of tissue breakdown, reflecting the complicated network of selective and coordinated production of individual proteinases and inhibitors under normal and pathophysiological conditions. Thus, the invasive and metastatic potential of thyroid tumors depends on the local net level of active MMPs.

The synthesis of MMP-1 and TIMP-1 is influenced by a variety of biochemical stimuli. The recent findings on MMP-1 and TIMP-1 gene promoters are useful in understanding the complex mechanisms implied in the regulation of MMP synthesis modulated by cytokines and tumor promoters (34,44,45). The promoter regions contain tumor promoter responsive elements (TRE) and binding motifs for the transcription factor PEA-3, which are recognized by proto-oncogenic transcription factors, such as the

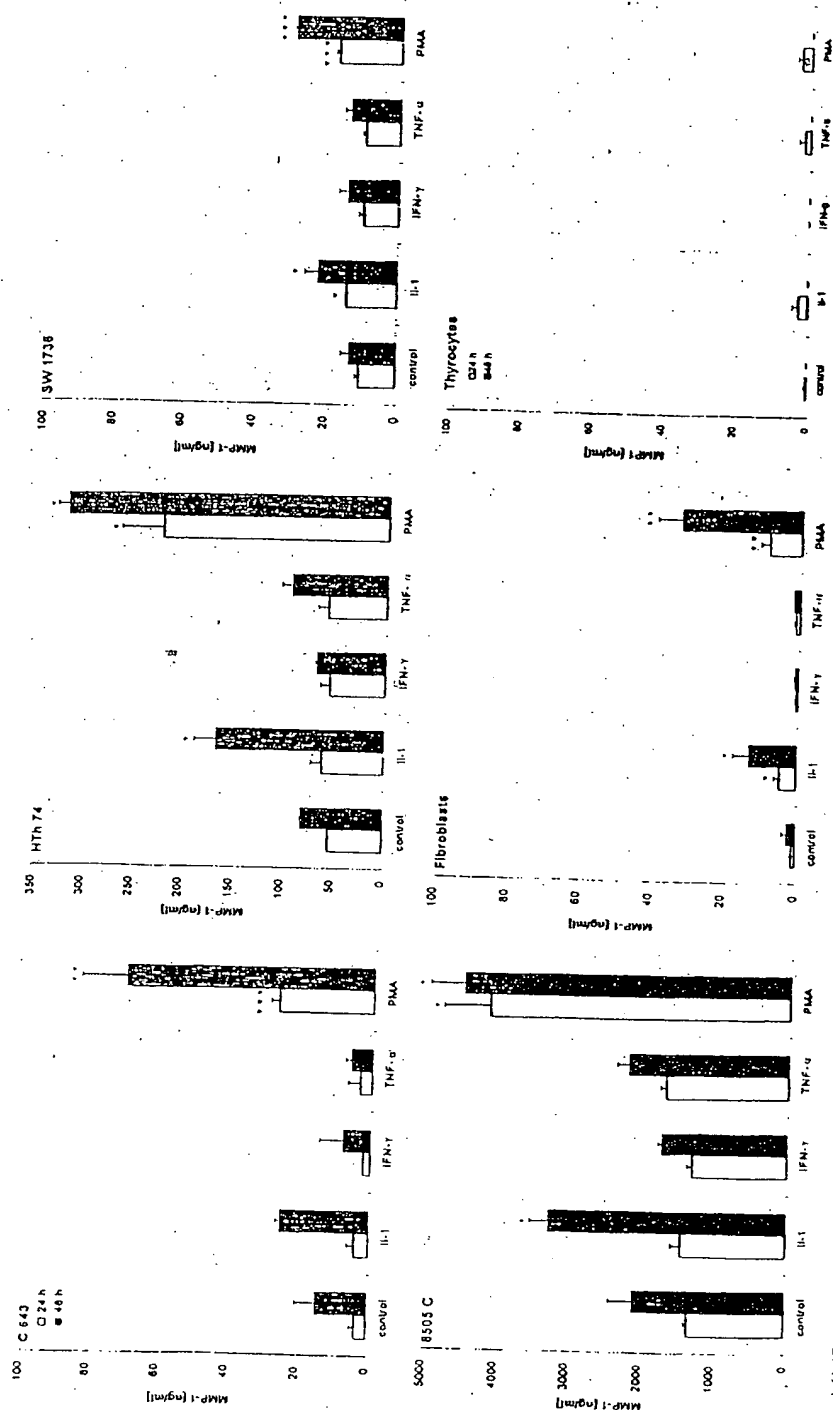


FIG. 5. MMP-1 protein levels (mean \pm SEM) in supernatants of unstimulated and stimulated cultures of thyrocytes ($n = 3$), thyroid-derived fibroblasts ($n = 4$) and the thyroid carcinoma cell lines 8305 C, SW 1736, C 643, HTh 74 ($n = 3$) detected by MMP-1 ELISA, which recognizes total MMP-1, ie, free MMP-1 and that complexed with inhibitors such as TIMP-1, but not α_2 -macroglobulin. Cells were stimulated with 10 U/mL IL-1 α , 100 U/mL TNF- α , 500 U/mL IFN- γ , or 10 ng/mL PMA for 24 and 48 hours. For fibroblasts, each point represents the mean \pm SEM of four different donors, each experiment performed in triplicate. For cell lines, each point represents the mean \pm SEM of three separate experiments each performed in triplicate. Significant differences between the basal and stimulated MMP-1 levels are indicated by asterisks (* $p < .05$; ** $p < .01$; *** $p < .005$). Please note the differences in scale between 8305 C, HTh 74, and the other cell types.

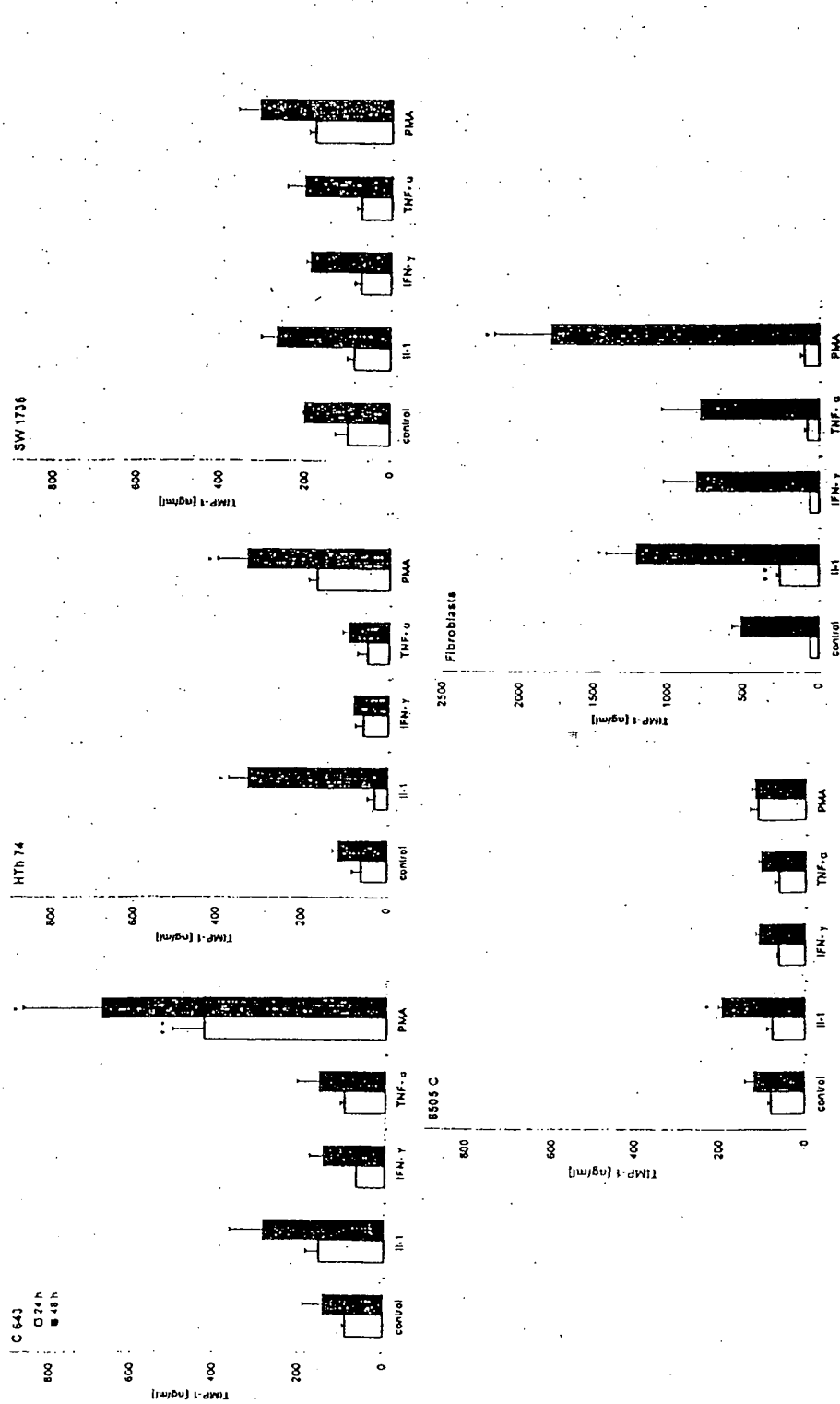


FIG. 6. ELISA detection of free and MMP-complexed TIMP-1 (mean \pm SEM). Asterisks indicate significant differences between the basal and stimulated TIMP-1 levels (* $p < .05$; ** $p < .01$; *** $p < .005$). For further details see Figure 5. Please note the differences in scale between fibroblasts and the other cell types.

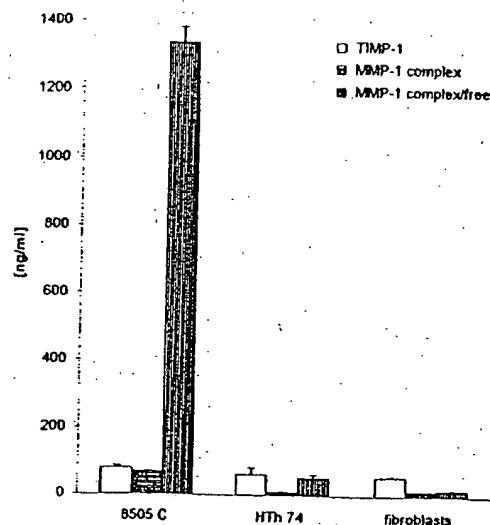


FIG. 7. Comparison between (i) free/complex and (ii) TIMP-1 complexed MMP-1 levels, and (iii) TIMP-1 levels in supernatants of unstimulated 8505 C and HTh 74 cells, and thyroid-derived fibroblasts after 24 hours using a (i) MMP-1 ELISA that recognizes total MMP-1 (see Figure 5). The (ii) MMP-1/TIMP-1 assay recognizes MMP-1/TIMP-1 complexes, ie, activated MMP-1 that has subsequently been complexed with the specific MMP inhibitor TIMP-1. The (iii) TIMP-1 ELISA recognizes total TIMP-1, ie, free TIMP-1 and that complexed with MMPs.

fos and *jun* family (45-47). IL-1, TNF- α , and PMA up-regulate proto-oncogenes like *fos* and *jun*, resulting in the stimulation of MMP-1 and TIMP-1 (45,48). The action of the cytokines is mediated by their specific receptors. In our study, IL-1R (type I and type II), TNF- α R (p75 and p55) and IFN- γ R mRNAs were demonstrated in all investigated cell types. PMA and IL-1 were shown to elevate MMP-1 and TIMP-1 in nearly all cell types investigated, thus confirming the results of several studies on other epithelial cells (reviewed in refs. 1,7,49). In the majority of experiments, we found a concordant expression of MMP-1 and TIMP-1 after stimulation, possibly achieved by the coordinated actions of the nuclear transcription factors, although MMP-1 and TIMP-1 expression can also be independently or even reciprocally regulated (1). The effect of TNF- α was not as distinct as in the case of PMA and IL-1, although several investigators found a pronounced effect of TNF- α particularly on TIMP-1 secretion (4,34). In contrast to studies performed with other cell types (863,864,819), IFN- γ did not influence MMP-1 and TIMP-1 expression in thyroid carcinoma cell lines. In summary, the involvement of the intrathyroidal physiological and pathological cytokine microenvironment in the regulation of MMP-1 and TIMP-1 induction activation and inhibition is strongly suggested.

Furthermore, the data demonstrate that regular human thyrocytes did not produce MMP-1, even after powerful stimulation with PMA. Investigating other mammalian epithelial cells, only one study revealed the production of

MMP-1 by rabbit corneal cells (21). It is yet not clear whether the MMP-1 mRNA detected in thyrocytes is due to a low level of constitutive transcription of the MMP-1 gene (illegitimate transcription), an existing pool of stable MMP-1 mRNA, or *in vitro* induction of MMP-1 mRNA. But it seems more likely that residual fibroblasts contained in the purified thyrocyte preparation (<0.2%) are responsible for the slightly positive RT-PCR results. Another explanation could be that thyrocytes are indeed MMP-1 producers, but the ELISA detection system used was not sensitive enough to measure extremely low MMP-1 secretion levels. Furthermore, the discrepancy between elevated TIMP-1 mRNA levels of thyrocytes and the extremely low TIMP-1 protein secretion by these cells is difficult to explain. Post-transcriptional regulatory events may be responsible for this confounding result.

Taken together, the present study suggests that the intrathyroidal cytokine microenvironment is involved in the regulation of MMP-1 and its inhibitor TIMP-1 in the thyroid, and that both proteins may be secreted by dedifferentiated thyroid carcinoma cells and involved in aggressive thyroid tumors *in vivo*.

REFERENCES

1. Ries C, Petrides PE 1995 Cytokine regulation of matrix metalloproteinase activity and its regulatory dysfunction in disease. *Biol Chem Hoppe Seyler* 376:345-355.
2. Pierce RA, Sandefur S, Doyle GA, Welgus HG 1996 Monocytic cell type-specific transcriptional induction of collagenase. *J Clin Invest* 97:1890-1899.
3. Pan L, Eckhoff C, Brinckerhoff CE 1995 Suppression of collagenase gene expression by all-trans and 9-cis retinoic acid is ligand dependent and requires both RARs and RXRs. *J Cell Biochem* 57:575-589.
4. Shingu M, Nagai Y, Isayama T, Naono T, Nobunaga M 1993 The effects of cytokines on metalloproteinase inhibitors (TIMP) and collagenase production by human chondrocytes and timp production by synovial cells and endothelial cells. *Clin Exp Immunol* 94:145-149.
5. Goldberg GL, Wilhelm SM, Kronberger A, Bauer EA, Grant GA, Eisen AZ 1986 Human fibroblast collagenase. Complete primary structure and homology to an oncogene transformation-induced rat protein. *J Biol Chem* 261:6600-6605.
6. Docherty AJ, Lyons A, Smith BJ, Wright EM, Stephens PE, Harris TJ, Murphy G, Reynolds JJ 1985 Sequence of human tissue inhibitor of metalloproteinases and its identity to erythroid-potentiating activity. *Nature* 318:66-69.
7. Mauviel A 1993 Cytokine regulation of metalloproteinase gene expression. *J Cell Biochem* 53:288-295.
8. Murphy G 1995 Matrix metalloproteinases and their inhibitors. *Acta Orthop Scand Suppl* 266:55-60.
9. Nomura H, Fujimoto N, Seiki M, Mai M, Okada Y 1996 Enhanced production of matrix metalloproteinases and activation of matrix metalloproteinase 2 (gelatinase A) in human gastric carcinomas. *Int J Cancer* 69:9-16.
10. Murray GI, Duncan ME, O'Neil P, Melvin WT, Fothergill JE 1996 Matrix metalloproteinase-1 is associated with poor prognosis in colorectal cancer. *Nat Med* 2:461-462.
11. Onisto M, Garbisa S, Caenazzo C, Freda MP, Di Francesco C, Nitti D, Liora LA, Stetler-Stevenson WG 1993 Reverse transcription-polymerase chain reaction phenotyping of met-

- allopoteinases and inhibitors involved in tumor matrix invasion. *Diagn Mol Pathol* 2:74-80.
12. Kameyama K 1996 Expression of MMP-1 in the capsule of thyroid cancer—Relationship with invasiveness. *Pathol Res Pract* 192:20-26.
 13. Campo E, Merino MJ, Liotta L, Neumann R, Stetler-Stevenson W 1992 Distribution of the 72-kd type IV collagenase in nonneoplastic and neoplastic thyroid tissue. *Hum Pathol* 23:1395-1401.
 14. Demeure MJ, Damsky CH, Elfman F, Goretzki PE, Wong MG, Clark O 1992 Invasion by cultured human follicular thyroid cancer correlates with increased beta 1 integrins and production of proteases. *World J Surg* 16:770-776.
 15. Nakano T, Kusunoki T, Funasaka K, Murata K, Nishida S, Tomura T 1995 Study of type I and IV collagenase activity in human thyroid diseases. *Nippon Jibiinkoka Gakkai Kaiho* 98:937-941.
 16. Zedenius J, Stahle-Backdahl M, Enberg U, Grimelius L, Larsson C, Wallin G, Backdahl M 1996 Stromal fibroblasts adjacent to invasive thyroid tumors: expression of gelatinase A but not stromelysin 3 mRNA. *World J Surg* 20:101-106.
 17. Arai M, Niiooka M, Maruyama K, Wada N, Fujimoto N, Nomiyama T, Tanaka S, Okazaki I 1996 Changes in serum levels of metalloproteinases and their inhibitors by treatment of chronic hepatitis C with interferon. *Dig Dis Sci* 41:995-1000.
 18. Nikkari ST, O'Brien KD, Ferguson M, Hatsukami T, Welgus HG, Alpers CE, Clowes AW 1995 Interstitial collagenase (MMP-1) expression in human carotid atherosclerosis. *Circulation* 92:1393-1398.
 19. Knowlden J, Martin J, Davies M, Williams JD 1995 Metalloproteinase generation by human glomerular epithelial cells. *Kidney Int* 47:1682-1689.
 20. Buisson AC, Zahm JM, Polette M, Pierron D, Bellon G, Puchelle E, Birembaut P, Tournier JM 1996 Gelatinase B is involved in the in vitro wound repair of human respiratory epithelium. *J Cell Physiol* 166:413-426.
 21. Tao Y, Bazan HE, Bazan NG 1995 Platelet-activating factor induces the expression of metalloproteinases-1 and -9, but not -2 or -3, in the corneal epithelium. *Invest Ophthalmol Vis Sci* 36:345-354.
 22. Aust G, Heuer M, Laue S, Lehmann I, Hofmann A, Heldin N-E, Scherbaum WA 1996 Expression of TNA-alpha mRNA and protein in pathological thyroid tissue and carcinoma cell lines. *Clin Exp Immunol* 105:148-154.
 23. Mark J, Ekedahl C, Dahlfors R, Westermark B 1987 Cytogenetical observations in five human anaplastic thyroid carcinomas. *Hereditas* 107:163-174.
 24. Heldin NE, Cvejic D, Smeds S, Westermark B 1991 Coexpression of functionally active receptors for thyrotropin and platelet-derived growth factor in human thyroid carcinoma cells. *Endocrinology* 129:2187-2193.
 25. Ito T, Seyama T, Hayashi Y, Hayashi T, Dohi K, Mizuno T, Iwamoto KS, Tsuyama N, Nakamura N, Akiyama M 1994 Establishment of two human thyroid carcinoma cell lines (8305C, 8505C) bearing p53 gene mutations. *International Journal of Oncology* 4:583-586.
 26. Wallin G, Backdahl M, Tallroth-Ekman E, Lundell G, Auer G, Lowhagen T 1989 Co-existent anaplastic and well differentiated thyroid carcinomas: a nuclear DNA study. *Eur J Surg Oncol* 15:43-48.
 27. Heuer M, Aust G, Ode-Hakim S, Scherbaum WA 1996 Different cytokine mRNA profiles in Graves' disease, Hashimoto's thyroiditis and non-autoimmune thyroid disorders determined by quantitative reverse transcriptase chain reaction (RT-PCR). *Thyroid* 6:97-106.
 28. Celi FS, Zenilman ME, Shuldiner AR 1993 A rapid and versatile method to synthesize internal standards for competitive PCR. *Nucleic Acids Res* 21:1047.
 29. Platzer C, Ode-Hakim S, Reinke P, Docke WD, Ewert R, Volk HD 1994 Quantitative PCR analysis of cytokine transcription patterns in peripheral mononuclear cells after anti-CD3 rejection therapy using two novel multispecific competitor fragments. *Transplantation* 58:264-268.
 30. Watson PF, Pickerill AP, Davies R, Weetman AP 1994 Analysis of cytokine gene expression in Graves' disease and multinodular goiter. *J Clin Endocrinol Metab* 79:355-360.
 31. Tada M, Diserens AC, Desbaillets J, de Tribolet N 1994 Analysis of cytokine receptor messenger RNA expression in human glioblastoma cells and normal astrocytes by reverse-transcription polymerase chain reaction. *J Neurosurg* 80:1063-1073.
 32. Nakano A, Tani E, Miyazaki K, Yamamoto Y, Furuyama J 1995 Matrix metalloproteinases and tissue inhibitors of metalloproteinases in human gliomas. *J Neurosurg* 83:298-307.
 33. Whitelock JM, O'Grady RL, Gibbins JR 1991 Interstitial collagenase (matrix metalloproteinase 1) associated with the plasma membrane of both neoplastic and nonneoplastic cells. *Invasion Metastasis* 11:139-148.
 34. Mackay AR, Ballin M, Pelina MD, Farina AR, Nason AM, Hartzler JL, Thorgeirsson UP 1992 Effect of phorbol ester and cytokines on matrix metalloproteinase and tissue inhibitor of metalloproteinase expression in tumor and normal cell lines. *Invasion Metastasis* 12:168-184.
 35. Urbanski SJ, Edwards DR, Maitland A, Leco KJ, Watson A, Kossakowska AE 1992 Expression of metalloproteinases and their inhibitors in primary pulmonary carcinomas. *Br J Cancer* 66:1188-1194.
 36. Polette M, Clavel C, Muller D, Abecassis J, Binnering I, Birembaut P 1991 Detection of mRNAs encoding collagenase 1 and stromelysin 2 in carcinomas of the head and neck by in situ hybridization. *Invasion Metastasis* 11:76-83.
 37. Clavel C, Polette M, Doco M, Binnering I, Birembaut P 1992 Immunolocalization of matrix metalloproteinases and their tissue inhibitor in human mammary pathology. *Bull Cancer (Paris)* 79:261-270.
 38. Boghaert ER, Ain K, Taylor K, Greenberg VL, Fowler C, Zimmer SG 1996 Quantitative and qualitative differences in growth, invasion and lung colonization of an anaplastic and a papillary human thyroid cancer cell line in vitro and in vivo. *Clin Exp Metastasis* 14:440-450.
 39. Asakawa H, Kobayashi T, Komoike Y, Yamagawa T, Takahashi M, Wakasugi E, Maruyama H, Tamaki Y, Matsuzawa Y, Monden M 1996 Establishment of anaplastic thyroid carcinoma cell lines useful for analysis of chemosensitivity and carcinogenesis. *J Clin Endocrinol Metab* 81:3547-3552.
 40. Viglietto G, Maglione D, Rambaldi M, Ceruni J, Romano A, Trapasso F, Fedele M, Ippolito P, Chiappetta G, Bortì G, et al 1995 Upregulation of vascular endothelial growth factor (VEGF) and downregulation of placenta growth factor (PIGF) associated with malignancy in human thyroid tumors and cell lines. *Oncogene* 11:1569-1579.
 41. Nuovo GJ, MacConnell PB, Simsir A, Valea F, French DL 1995 Correlation of the in situ detection of polymerase chain reaction-amplified metalloproteinase complementary DNAs and their inhibitors with prognosis in cervical carcinoma. *Cancer Res* 55:267-275.
 42. Naruo S, Kanayama H, Takigawa H, Kagawa S, Yamashita K, Hayakawa T 1994 Serum levels of a tissue inhibitor of

- metalloproteinases-1 (TIMP-1) in bladder cancer patients. *Int J Urol* 1:228-231.
43. Kossakowska AE, Urbanski SJ, Watson A, Hayden LJ, Edwards DR 1993 Patterns of expression of metalloproteinases and their inhibitors in human malignant lymphomas. *Oncol Res* 5:19-28.
44. Edwards DR, Rocheleau H, Sharma RR, Wills AJ, Cowie A, Hassell JA, Heath JK 1992 Involvement of AP1 and PEA3 binding sites in the regulation of murine tissue inhibitor of metalloproteinases-1 (TIMP-1) transcription. *Biochim Biophys Acta* 1171:41-55.
45. Schonthal A, Herrlich P, Rahmsdorf HJ, Ponta H 1988 Requirement for fos gene expression in the transcriptional activation of collagenase by other oncogenes and phorbol esters. *Cell* 54:325-334.
46. Gutman A, Wasylyk B 1990 The collagenase gene promoter contains a TPA and oncogene responsive unit encompassing the PEA3 and AP-1 binding sites. *EMBO J* 9:2241-2246.
47. Wasylyk C, Gutman A, Nicholson R, Wasylyk B 1991 The c-Ets oncoprotein activates the stromelysin promoter through the same elements as several non-nuclear oncoproteins. *EMBO J* 10:1127-1134.
48. Brenner DA, O'Hara M, Angel P, Chojkier M, Karin M 1989 Prolonged activation of jun and collagenase genes by tumour necrosis factor-alpha. *Nature* 337:661-663.
49. Opdenakker G, Van Damme J 1992 Cytokines and proteases in invasive processes: molecular similarities between inflammation and cancer. *Cytokine* 4:251-258.

Address reprint requests to:
Dr. Gabriela Aust
Institute of Anatomy
University of Leipzig
Liebigstr. 13
Leipzig, D-04103, Germany



**This Page is Inserted by IFW Indexing and Scanning
Operations and is not part of the Official Record**

BEST AVAILABLE IMAGES

Defective images within this document are accurate representations of the original documents submitted by the applicant.

Defects in the images include but are not limited to the items checked:

☒ **BLACK BORDERS**

☐ **IMAGE CUT OFF AT TOP, BOTTOM OR SIDES**

☐ **FADED TEXT OR DRAWING**

☐ **BLURRED OR ILLEGIBLE TEXT OR DRAWING**

☐ **SKEWED/SLANTED IMAGES**

☐ **COLOR OR BLACK AND WHITE PHOTOGRAPHS**

☐ **GRAY SCALE DOCUMENTS**

☒ **LINES OR MARKS ON ORIGINAL DOCUMENT**

☒ **REFERENCE(S) OR EXHIBIT(S) SUBMITTED ARE POOR QUALITY**

☒ **OTHER:** _____

IMAGES ARE BEST AVAILABLE COPY.

As rescanning these documents will not correct the image problems checked, please do not report these problems to the IFW Image Problem Mailbox.